23 Apr 1982

Performance evaluation of brick veneer with steel stud backup

Joseph O. Arumala

Russell H. Brown

F/ 1201-442

PERFORMANCE EVALUATION OF BRICK VENEER WITH STEEL STUD BACKUP

CONDUCTED BY

CLEMSON UNIVERSITY
College of Engineering
DEPARTMENT OF CIVIL ENGINEERING
110 LOWRY HALL • CLEMSON, SOUTH CAROLINA 29631

COSPONSORED BY

Brick Institute of America
1750 Old Meadow Road • McLean, VA 22102

Metal Lath/Steel Framing Association
221 North LaSalle Street, Chicago, IL 60601

CCFSS LIBRARY Joseph O. Arumala, Russell H.
24 oo * 561 Brown PERFORMANCE EVALUATION OF
1982 BRICK VENEER WITH STEEL STUD
BACKUP

FINAL REPORT

PERFORMANCE EVALUATION OF BRICK VENEER WITH STEEL STUD BACKUP

BY

JOSEPH O. ARUMALA

AND

RUSSELL H. BROWN

DEPARTMENT OF CIVIL ENGINEERING

CLEMSON UNIVERSITY

FOR

BRICK INSTITUTE OF AMERICA

AND

METAL LATH/STEEL FRAMING ASSOCIATION

APRIL 23, 1982

ABSTRACT

Experimental and analytical investigations were carried out to determine the behavior of laterally loaded walls constructed of brick veneer with metal stud backup.

The experimental investigation consisted of two phases: The first phase involved the testing of two different types of metal ties, corrugated and drywall adjustable (DW 10) ties, for axial stiffnesses. These ties are used to connect brick veneer to metal stud backup walls. The tests showed that the stiffer corrugated wall ties were comparable to the adjustable ties in axial stiffnesses. However, there is some variability in axial stiffnesses of the corrugated ties depending upon the point at which they are bent. Based on its performance in the tie test, a 14 gage DW 10 tie was chosen for use in connecting the brick veneer to the metal stud backup wall in the next phase.

The second phase involved the testing of six simple span brick veneer walls with metal stud backup to measure their deflection characteristics under lateral load. The purpose of Phase Two was to establish approximately the performance of walls designed in accordance with metal stud industry standards. In the current design procedure, the metal studs are designed to resist the full lateral load without exceeding a midspan deflection limit of L/360, where L is the stud height. Additionally, the maximum allowable stress in the metal stud may not be exceeded. The walls were tested in two batches: three under positive lateral load and three under negative lateral load to levels of design load, twice design load and three times design load. The walls were also tested for water penetration before and after loading using a modified version of ASTM E514.

The analytical aspect included the development of models to simulate the behavior of the wall system under wind pressures and for different boundary conditions and tie stiffnesses.

The results of the lateral load tests show that brick veneer walls supported on shelf angles with steel stud backup are capable of withstanding without flexural failure of the brick veneer, two times the load for which the wall system is designed. Also, the results of the analytical study show that the wall system's performance depends on such factors as the support conditions of the brick veneer, tie stiffness, composite action between the studs and the gypsum boards and the relative stiffnesses of the brick veneer and the backup wall.

Water permeance, measured using a modified version of ASTM E514, did not correlate closely with the level of load to which the wall was previously subjected. There was no significant increase or decrease in water permeance after the walls were subjected to twice design load.

ACKNOWLEDGEMENTS

The authors acknowledge the support of the Brick Institute of America and the Metal Lath/Steel Framing Association who jointly provided the funds to make this work possible. The financial support of the Department of Civil Engineering in the form of a graduate assistantship to the author during his stay in Clemson is hereby acknowledged.

Sincere gratitude goes to Mr. Milford Ward and Mr. Milton Lore, of the Civil Engineering Workshop and Mr. Larry Denmark of the Rural Housing Research Unit of USDA, for their technical assistance throughout the test. Also the assistance of the following Clemson students was much appreciated: Rhett Whetlock, Barry Palm, Tommy Cousins, John Murden, Babafemi Adesanya, Kenneth Holsberg, and Joel Baker. Special thanks go to Ralph Bryan, for his invaluable assistance in the construction work and in the conduction of the tests.

TABLE OF CONTENTS

Table of Contents (cont'd.)

LIST OF TABLES

List of Tables (Cont'd.)

LIST OF FIGURES

List of Figures (Cont'd.)

List of Figures (Cont'd.)

List of Figures (Cont'd.)

List of Figures (Cont'd.)

List of Figures (Cont'd.)

List of Figures (Cont'd.)

List of Figures (Cont'd.)

CHAPTER I

INTRODUCTION

Recently, the use of exterior brick-masonry veneer with cold-formed steel stud backup wall systems has become increasingly popular.

A veneered wall is by definition a wall having a facing of masonry units or other weather-resisting non-combustible materials securely attached to the backup, but not bonded or attached so as to exert common action under axial load (1)[a]. A brick veneered wall consists of an exterior wythe of brick isolated from the backup by an airspace and attached to the backup with corrosion resistant metal ties (Fig. 1). The outer brick wythe gives the appearance of traditional masonry construction, while the steel stud backup system may be erected with more speed and economy than a backup wythe of masonry. The steel stud system is lighter in weight than masonry backup systems, and may be easily insulated for thermal and sound control (1).

One area of concern of the steel stud and the brick veneer wall system is the apparent difference in flexural stiffness between the steel stud and the brick veneer wall it supports. Although the steel has sufficient strength to carry lateral wind loads, it may not do so without deflecting more than the attached veneer can tolerate. Simple beam theory shows that the stiffer brick veneer which is tied to the steel stud with metal ties, carries substantial lateral load until flexural tensile cracks form. Only after flexural failure of the brick wythe has occurred can the steel stud backup serve its intended purpose according

[a] Numbers in parenthesis refer to the Bibliography section.

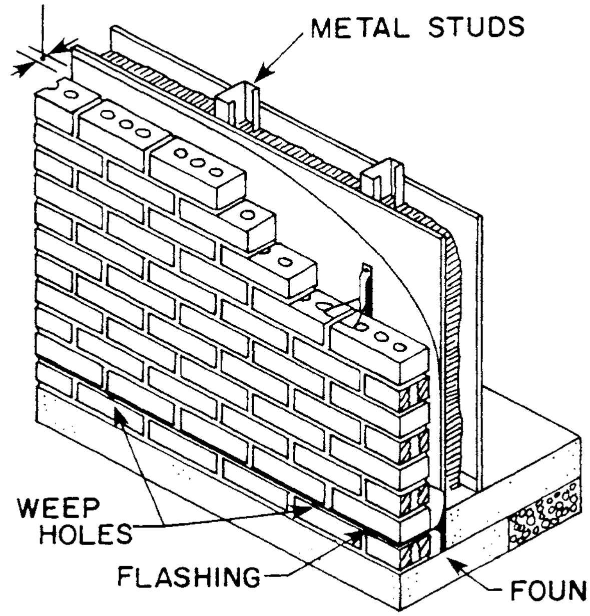

Figure 1. Typical Brick Veneer Wall

to simple beam theory. Even though flexural cracking of the brick veneer does not cause catastrophic structural failure, water permeance may be likely.

In order to tie the brick veneer to the steel stud backup, corrosion resistant metal ties are attached to the steel studs with self-drilling, self-tapping screws. Corrugated ties used for this detail are usually flexible, both axially and laterally (Fig. 2 a). The result of using such flexible ties is an increase in the lateral load resisted by the brick veneer. The Brick Institute of America (BIA) (1), recommends adjustable wire ties (Fig. 2 b), which have high axial stiffness, and tolerance to vertical movements. This is an adjustable Dry Wall (DW 10) tie.

The thicker corrugated ties, though stiffer than the lighter ones, have to be pre-bent because they cannot easily be bent at the building site. This poses some construction problems. The metal stud contractors install these ties and the masons encounter difficulties in laying the bricks with these ties sticking out. Moreover, the pre-bent ties may be difficult to line up with the mortar joints. The corrugated ties are not designed to accommodate vertical movements of the brick wall. The DW 10 ties are adjustable and can move laterally and vertically. The DW 10 ties are especially good for continuous wall construction where large relative vertical movements of the brick wall can be expected.

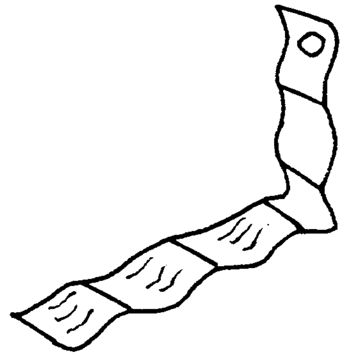

(a) Corrugated Wall Ties Fabricated From Galvanized Steel

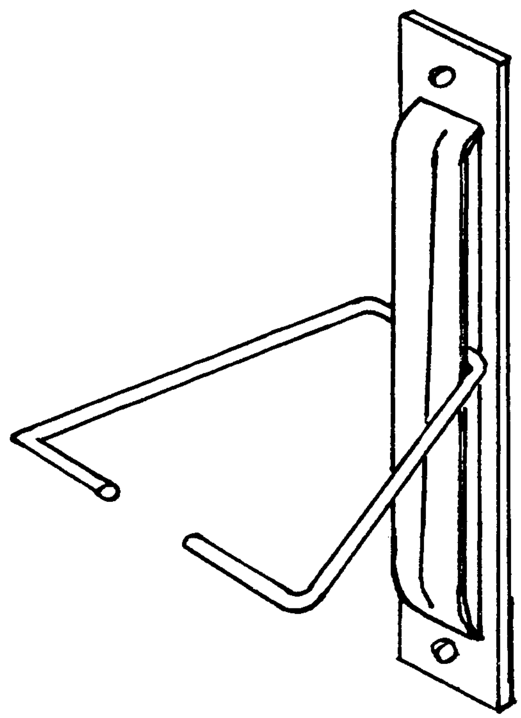

(b) Adjustable Wall Tie Consisting of 3/16 in. Wire with Galvanized Steel Backing

Figure 2. Two Types of Wall Ties Presently Used in Brick Veneer Steel Stud Construction

Present Design Criteria

In the current design procedure for the wall systems, the metal studs are designed to resist the full lateral load without exceeding a mid-span deflection limit of L/360, where L is the height of the wall. Another criterion which is used concurrently with the deflection limitation is a maximum stress limitation in the metal stud wall under full design wind load.

The Brick Institute of America (BIA) suggests that the design criteria presently used in producing most metal stud design tables are not adequate. In particular, the BIA contends that the imposition of a deflection limit of L/360 on the metal studs alone under full design wind load does not assure sufficient stiffness of the wall system to prevent cracking and distress of the brick veneer. The Metal Lath/Steel Framing Association, on the other hand, claims that such design criteria will result in wall assemblies with deflections that will not cause the cracking of the brick wall. They contend that the wall assembly as designed will remain elastic and functional.

Statement of Problem

Although this method of construction is gaining popularity, there are a number of questions to be answered regarding the current design methods. In the design of wall systems under lateral loads, it is usually assumed that the exterior wall must initially resist the lateral load and then transfer it to the building frame and eventually to the foundation. However it is hypothesized (1,2) that the metal studs carry appreciable load only after the veneer wall has failed structurally. The transfer of load in the wall system is therefore not fully known.

Also for proper load distribution, the brick veneer must be connected to the backup with metal ties, in sufficient numbers and of sufficient stiffness that under lateral loading both the brick veneer and the steel stud backup wall deflect nearly equally. Presently there is little information on the load carrying and deflection capacities of the metal ties. The axial stiffnesses of the metal ties for efficient and economic performance of the wall system are not published. It is therefore difficult to select the right type of ties for use in the wall system.

There is lack of established data on the question of relative rigidities of brick veneer facing and metal stud backup, therefore, the recommended limitations on deflection are based on engineering judgement. Full-scale experimental tests need to be performed to yield information necessary to understand the performance of the wall system.

Another area of concern involves the problems of water penetration. The majority of these problems occur because there are no standard accepted details available for this type of construction. Improperly designed flashing, weepholes, movement joints, ties and anchors, and projections of floor slabs to the outside face of the veneer, all may lead to water penetration problems. Water penetration may also be aggravated by lateral wind loads.

In addition to these problems, different support conditions, and inelastic behavior of the wall system need to be investigated. These will yield the necessary information required to better understand the behavior of the brick wall and the metal stud backup wall system.

Goal of Investigation

The objective of this investigation is to provide pertinent answers to some of the controversial questions concerning this method of building construction. This investigation will provide preliminary data necessary to establish new, or confirm existing guidelines for the systematic analysis and design criteria for this wall system.

The performance of the wall system resulting from current design procedures and construction techniques has raised questions as to the adequacy of these procedures and techniques. In order to determine the validity of the current design procedures, six full-scale walls will be designed and built according to these procedures. These walls will be subjected to lateral wind loads and deflections along their lengths measured. These full-scale lateral load tests will establish whether or not this is an acceptable method of design subject to certain limitations.

The axial stiffnesses of the corrugated and drywall adjustable ties used in this wall system are not published. This makes it difficult to recommend a tie for use in the wall system. Therefore, a tie test will be designed to obtain the axial stiffnesses of these two types of ties and a tie selected and recommended for use based on its performance in the tie test. The axial performance characteristics of all ties tested will be reported.

Another area of concern involves the problems of water penetration. Water permeance tests will be designed and performed on the walls before each lateral load test in order to determine their water permeance characteristics. Although each water permeance test will be for a duration of 3 hours, the tests will yield useful information about the water absorption characteristics of the walls.

In addition to these tests, mathematical models will be designed to investigate different support conditions, tie stiffnesses, relative wall stiffnesses and inelastic behavior of the wall system. The models coupled with the results of the experimental data will allow judgements concerning variations in the system to be made on a sound engineering basis.

Sequence of Investigation

Analytical and experimental investigations were undertaken to determine the interaction characteristics of the steel stud backup system used with brick veneer.

The experimental tests were in two phases. The first experimental phase included the determination of the axial load deformation characteristics of two types of wall ties, corrugated and drywall (DW 10) ties. Four kinds of corrugated ties with different thicknesses and two different kinds of DW 10 ties were tested. A 14 ga DW 10 tie was selected based on its performance in this test. The tie chosen was used in the construction of the full-scale walls in the second experimental phase.

The second experimental phase included the determination of lateral load versus deflection characteristics of six full-scale brick veneer walls with steel stud backup. Three walls were tested under positive lateral load and the other three, under negative lateral load. Each wall was subjected to a maximum of three times its design load. Also water permeance tests were performed on the walls before each loading.

The tests evaluated the resistance of this wall system to lateral forces and simulated wind driven rain.

The analytical investigation included developing mathematical models to study the effect of different support conditions of the brick veneer and the inelastic behavior and composite behavior of the wall system. Parametric studies were done on tie stiffness and relative stiffness of the brick veneer and the steel stud backup.

CHAPTER II

TEST PROGRAM

Phase One: Experimental Evaluation of Wall Ties

Purpose

Different types of wall ties are on the market today for use in many types of construction including brick veneer with steel stud backup walls. The axial characteristic behavior of these wall ties is not available. The objective of these tests was to determine the axial characteristic behavior of some of the wall ties that are commonly used today.

In mathematical models for this wall system, the metal ties are represented as linear springs. The tests showed that the corrugated wall ties behaved non-linearly. The thicker drywall adjustable ties showed linear behavior. Axial wall tie stiffnesses were determined from the tests so that accurate mathematical models could be obtained.

Materials and Equipment

The materials used in the tie tests included bricks, portland cement, sand, gypsum sheathing, four corrugated ties: gages 22, 20, 18, 16, and two DW (Dry Wall) 10 ties: gages 14 and 12, and a steel plate (6 in. by 23 in.). The two types of ties tested are shown in Fig. 2.

The equipment used included a universal testing machine accurate to within 1 lb. with drum plotter accessories, one dial gage, one linear transducer and a double-acting hydraulic pump. A photo of the test set-up is shown in Fig. 3, and a schematic drawing in Fig. 4.

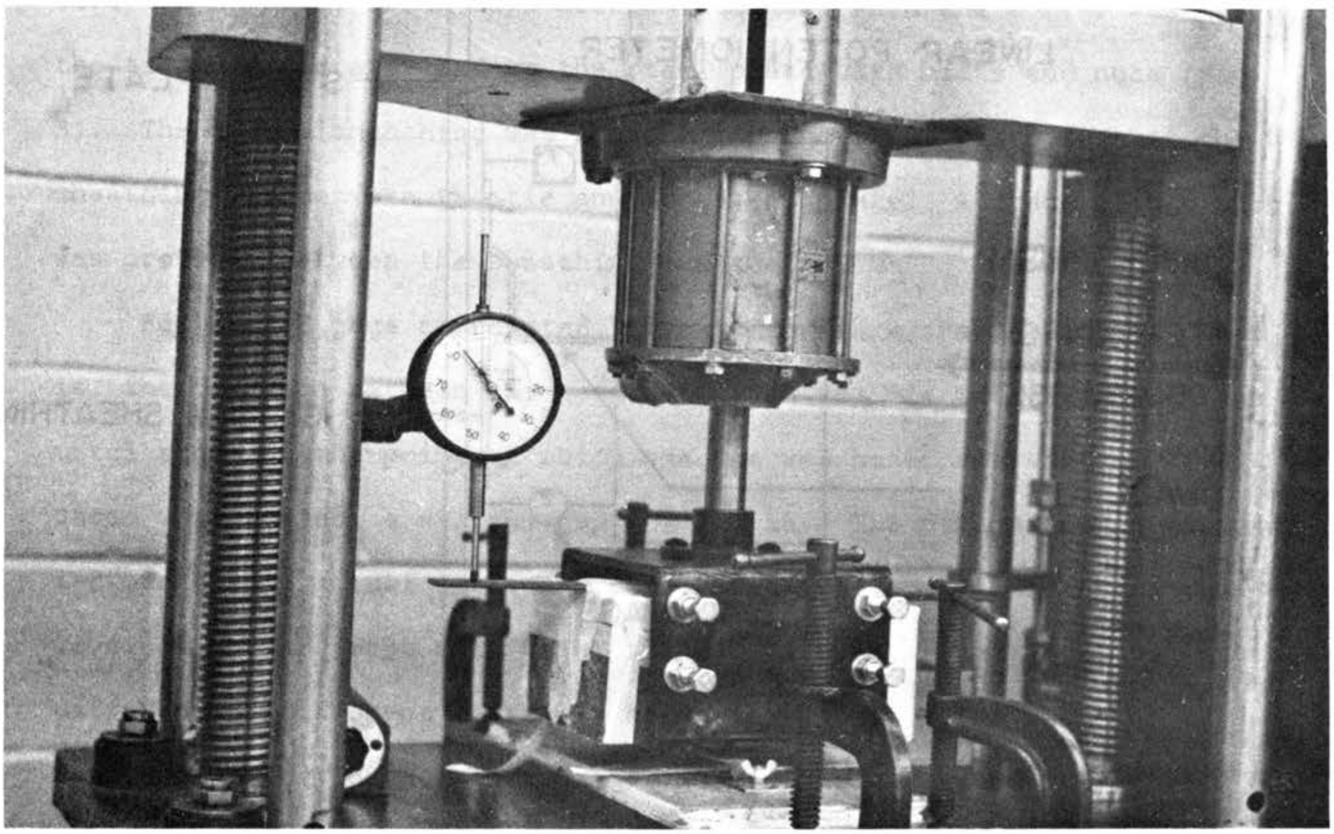

Figure 3. Wall Tie Test Set Up to Determine the Hysteretic Behavior of Wall Ties

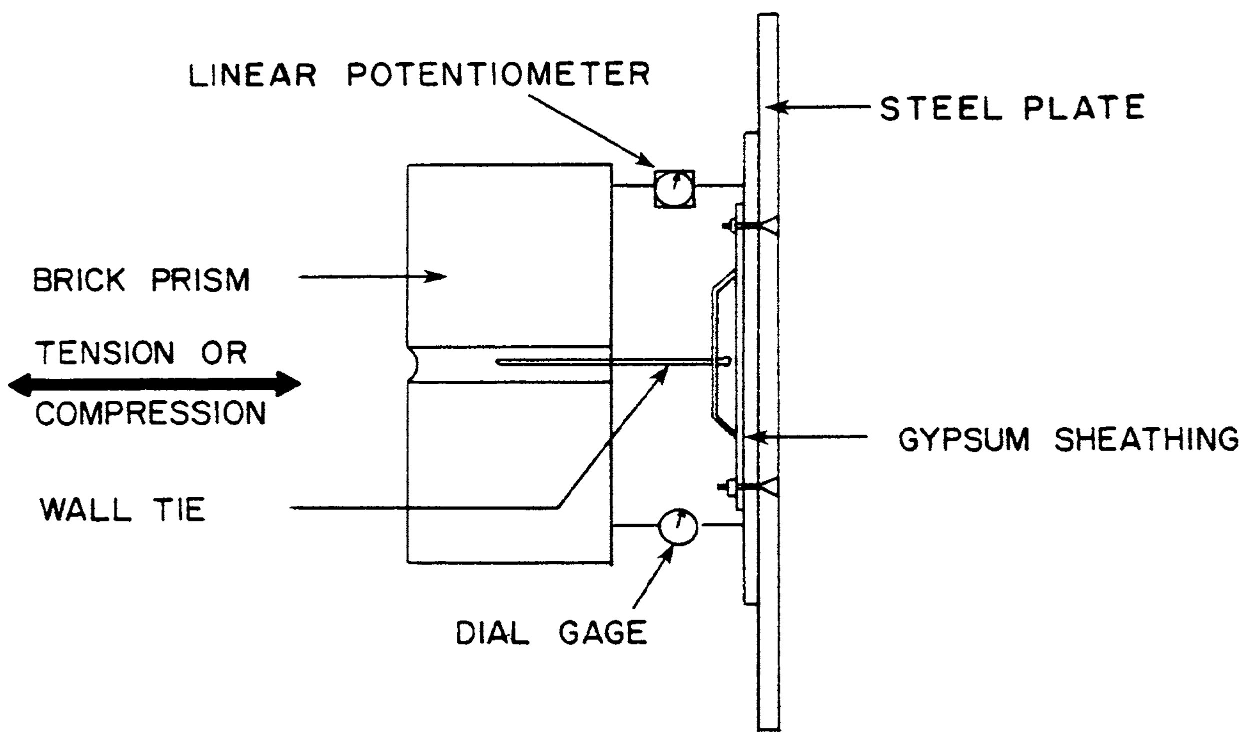

Figure 4. A Schematic Drawing of Tie Test Setup

Fabrication of Specimens

The mortar was made by taking one part by volume of portland cement, and three parts by volume of sand and mixing with a trowel in the basin. Water was added to the mix until it was plastic and workable.

Two bricks were laid on a flat surface one on top of the other, and leveled. The top brick was removed and mortar was applied to the lower brick. The tie was then embedded in the mortar and the top brick placed over the mortar, and leveled. Excess mortar was removed with the trowel. The mortar joint was made 3/8 in. thick. The brick prism was left to cure for at least seven days before testing. When the mortar was cured, the assembly was attached to the steel plate with bolts and nuts (Fig. 3). The gypsum sheathing was attached to the steel plate so that the sheathing was between the tie and the steel plate. A space of one inch was provided between the sheathing and the brick.

For the 18 gage corrugated tie, the distance, "a", (Fig. 5), that is, the distance between the point at which the tie was screwed to the metal stud and the point at which the tie was bent, was varied. Two cases were tested, a = 2 in. and a = 5/8 in. The dimension "a" was varied because in actual wall construction its value will depend on the level of mortar joint into which the tie is bent. Therefore, "a" may be different at different locations of mortar joints. The value of "a" was varied only for 18 gage corrugated ties. This was so because the 18 ga corrugated tie was the corrugated tie that had high axial stiffness with a = 5/8 in. from the tie tests. It can be bent by hand and has a high stiffness value with a = 5/8 in. In order to demonstrate the effect of "a" on the stiffness, a larger value of a = 2 in. was used in the test. With a = 2 in., the axial stiffness of the tie was reduced considerably.

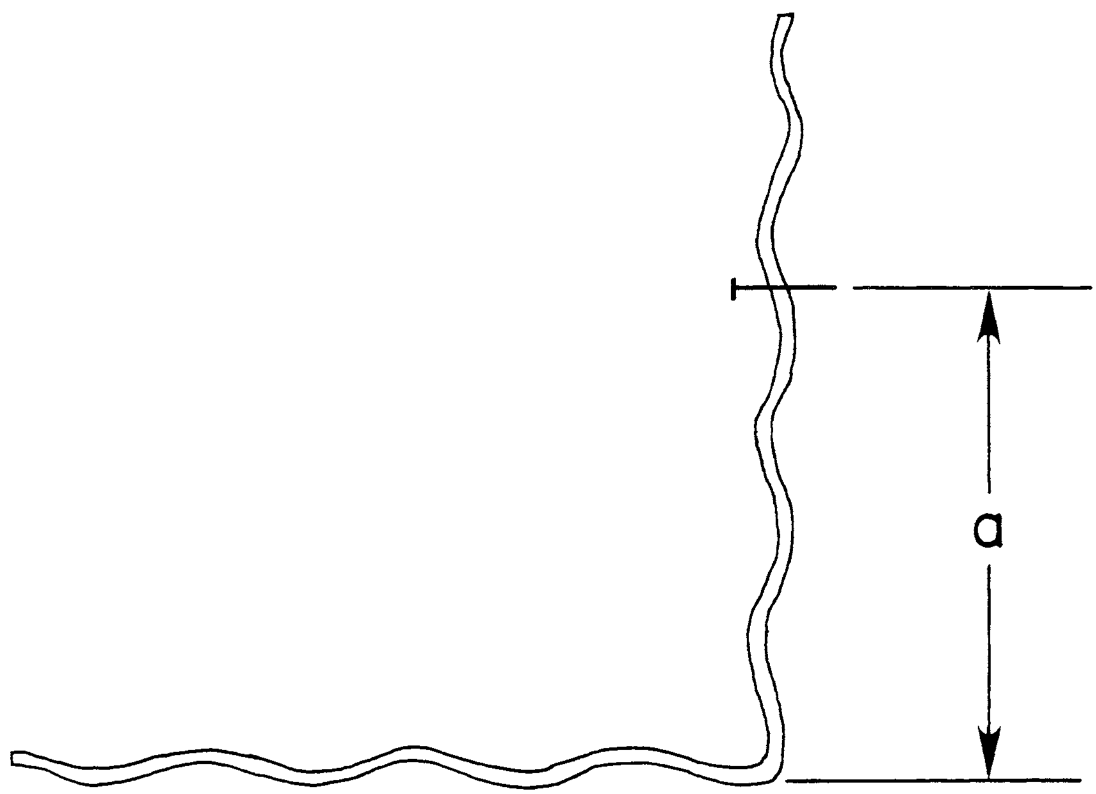

Figure 5. Measurement, a, of a Corrugated Tie

Test Procedure

The double-acting pump (Fig. 3) was attached to the head of the testing machine. To the pump was attached a clamp to hold the brick prism, (Fig. 6). The testing machine was pre-loaded with dead weights so that both compressive and tensile loads could be indicated by the testing machine. The test specimen was clamped to the base plate of the testing machine and the scale brought to the starting point. In the adjustable ties, the wires were centered, both horizontally and vertically, with respect to the backing (Fig. 4). It is expected that the minimum axial stiffness would result from such centering. The head of the testing machine was then lowered until the holding device encompassed the brick prism. The device was then screwed down to hold the brick prism firmly. The initial dial gage reading was noted and the pen on the plotter set at the starting point on the graph paper on the drum. The drum plotter was used to record the linear potentiometer output. Compressive and tensile loads were applied through a double acting actuator powered by a hand operated hydraulic pump.

Three peak loads were used, namely 50 lbs., 100 lbs., and 150 lbs, both in tension and compression. At any one level of loading, both the highest compressive load and the highest tensile load were numerically equal. At each load level the load was cycled five times. When the desired compressive load was attained, the load was reversed and brought back to zero. Tensile load was then applied until the desired tensile load was achieved. The load was reversed and brought back to zero. The process of loading from zero load to the desired compressive load and back to zero, then to the desired tensile load and back to zero, is

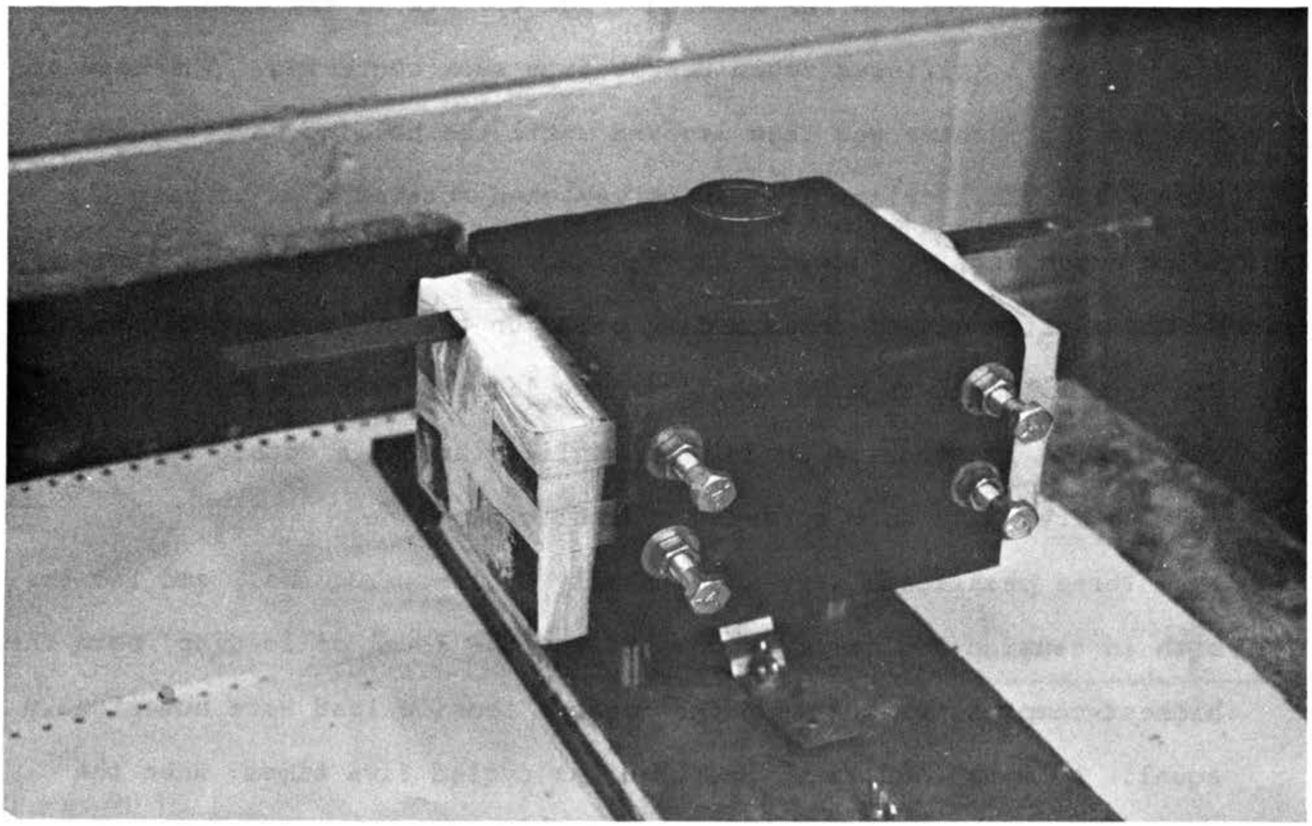

Figure 6. Clamping Device for Holding Brick Prism

called one cycle of loading. Each cycle required a time of approximately five minutes.

Phase Two: Lateral Load Testing of Full-Scale Panels

Purpose

The aim of this phase was to subject six full-scale wall panels to lateral loads and water permeance tests. Three of the walls were subjected to positive pressure and the other three to negative pressure. In the positive pressure test, the untooled mortar joints were in tension and in the negative pressure test, the tooled mortar joints were in tension. The tooled mortar joints have higher tensile strength than the untooled mortar joints.

Materials and Equipment

The materials used included the following: Bricks, Type S Portland cement/lime mortar, steel angles, neoprene strips, dial gauges, 3 5/8 in. wide 20 ga structural cee studs, 1 1/2 in. wide, 16 ga channel bridgings, 3 5/8 in. 20 ga runner tracks, 1/4 in. drilled expansion anchors, 1/2 in. gypsum wallboard, 1/2 in. gypsum sheathing, reglet and flashing, 14 ga DW 10 ties, 27 ft. circular rubber tube, weather stripping material, 1 in. No. 6-DG screws, epoxy, two 4 X 4 timber, 3/4 in. plywood, 1/4 in. plexiglass, glue, 2 X 4 timber, 1/2 in. screws, bolts and nuts. The physical and structural properties of the studs were: weight = 0.804 lb/ft, area = 0.208 in^2, I_{xx} = 0.540 in^4, S_x = 0.298 in^3, r_x = 1.450 in., I_{yy} = 0.076 in^4, r_y = 0.591 in., F_y = 33 ksi, allowable compression stress = 19,800 psi, resistance moment = 5,900 in-lb and E_s = 29500 ksi. The modulus of elasticity used for the gypsum sheathing was 245 ksi. All metal studs were galvanized.

The equipment used included the following: variable a-c voltage power supply (variac), water pump, plastic water tank, water hoses, flow meter, vacuum cleaner motor, 1/4 in. metal strips, clamps, pressure chamber, and water permeance chamber.

Fabrication of Supporting System and Pressure Chamber

The support system for the test specimens was a reinforced concrete frame. The frame was 18 ft. long and 10 ft. high. The bottom beam was rectangular and was 18 in. by 12 in., in section, Figs. 7 and 8. The top beam had an 'L' section with its long dimension equal to 12 in. (Fig. 8, Detail A). The two columns (Fig. 9), had a 12 in. square section. No. 6 rebars were used in the construction of the frame. The frame was designed and constructed to support the walls. The frame was cast horizontally, erected and braced with steel channels, Fig. 9. This type of construction was chosen to facilitate removal and storage of the concrete frame upon completion of the tests.

The pressure chamber was built using timber, 1/4 in. plexiglass, 3/4 in. plywood, 1 1/4 in. screws, glue, and bolts, Fig. 10. The sides of the chamber were made with the plexiglass. Two 12 in. by 12 in. plexiglass windows were built on the back of the chamber. The overall dimension of the chamber was 120 in. by 58 in. The inside dimension of the chamber was 113 3/4 in. by 49 in. and was 10 in. deep. A water manometer was attached to the back of the chamber.

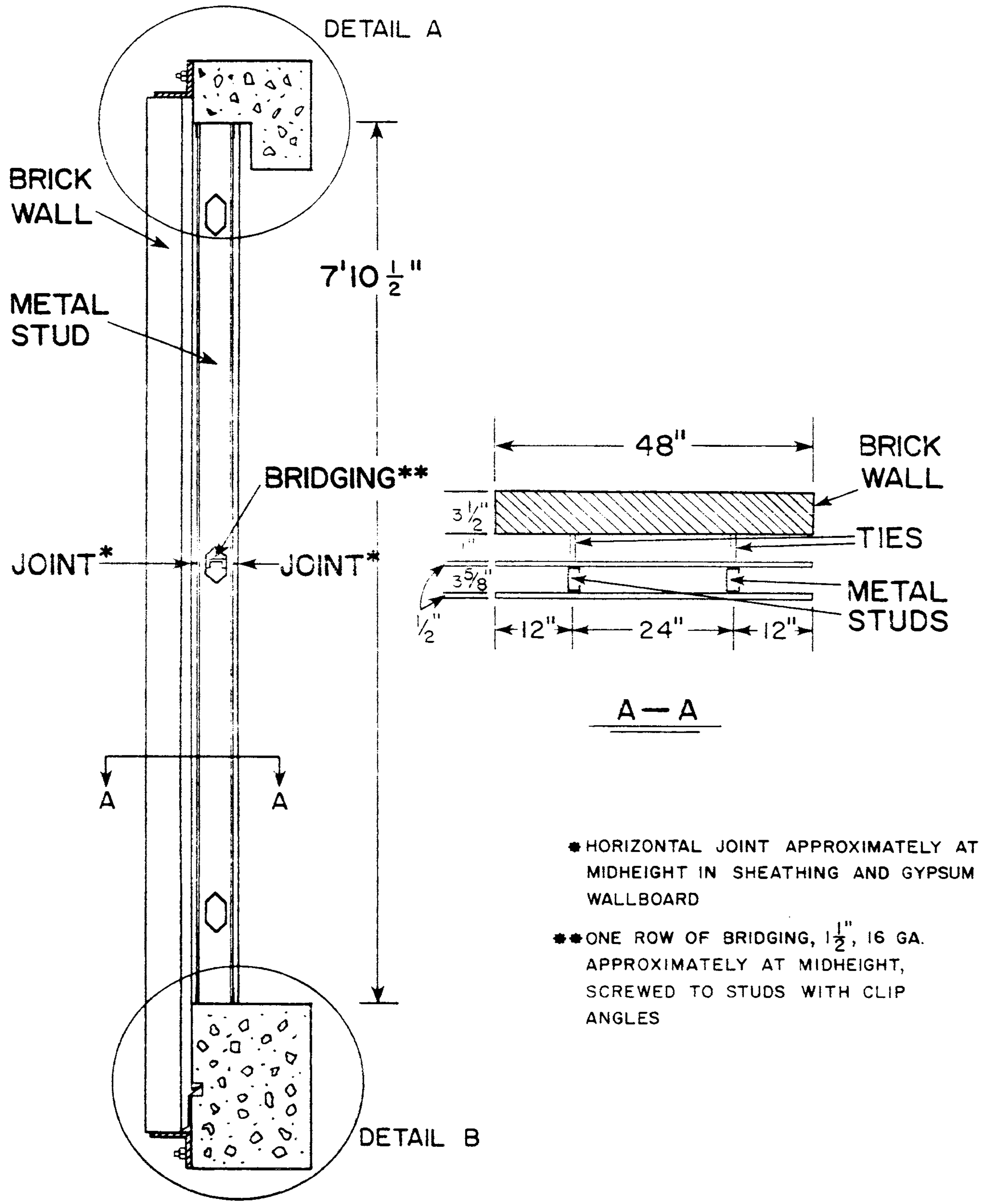

Figure 7. Typical Brick Veneer Steel Stud Wall Tested for Lateral Load Resistance and Water Permeance

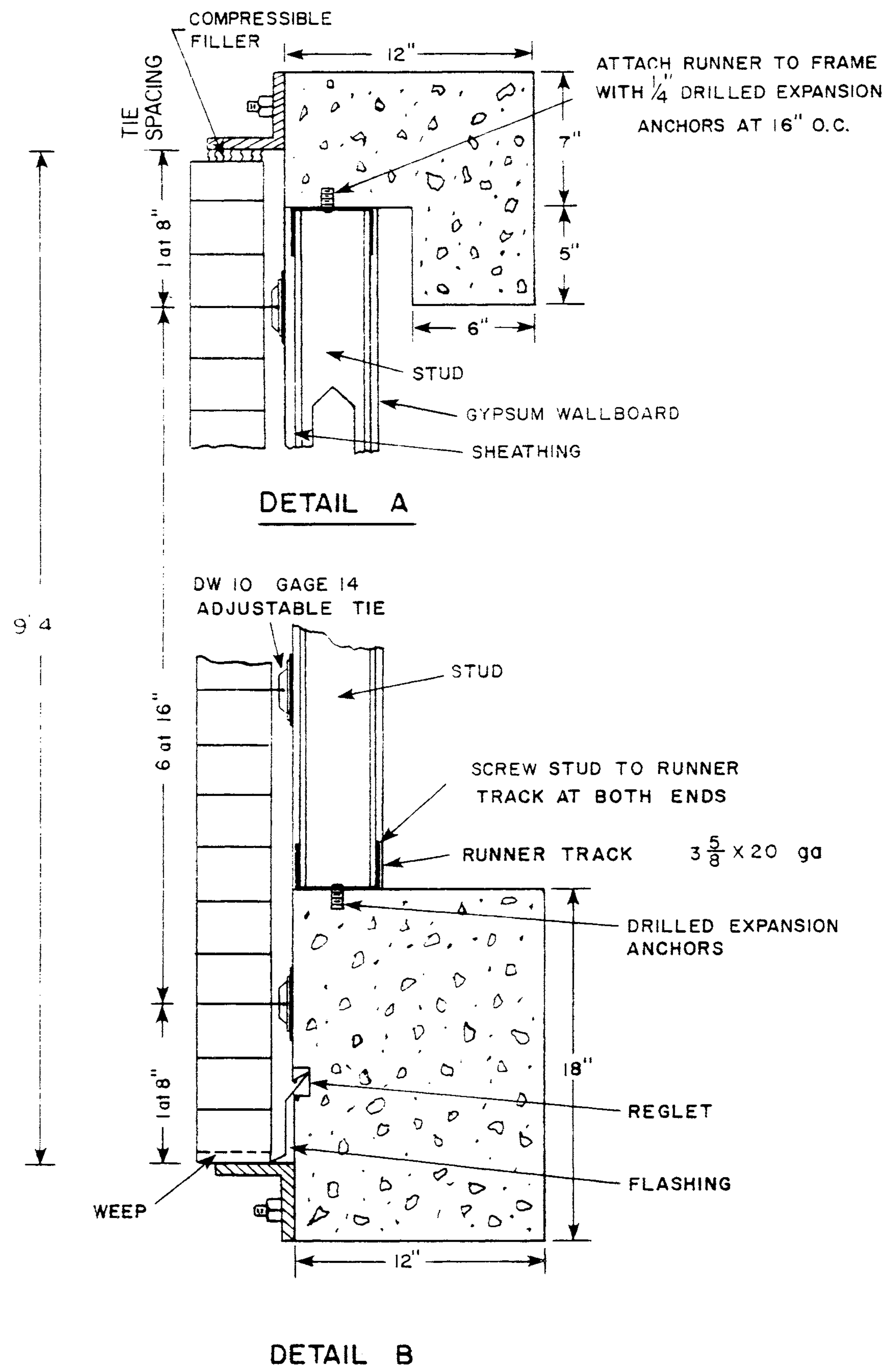

Figure 8. Details of Figure 7

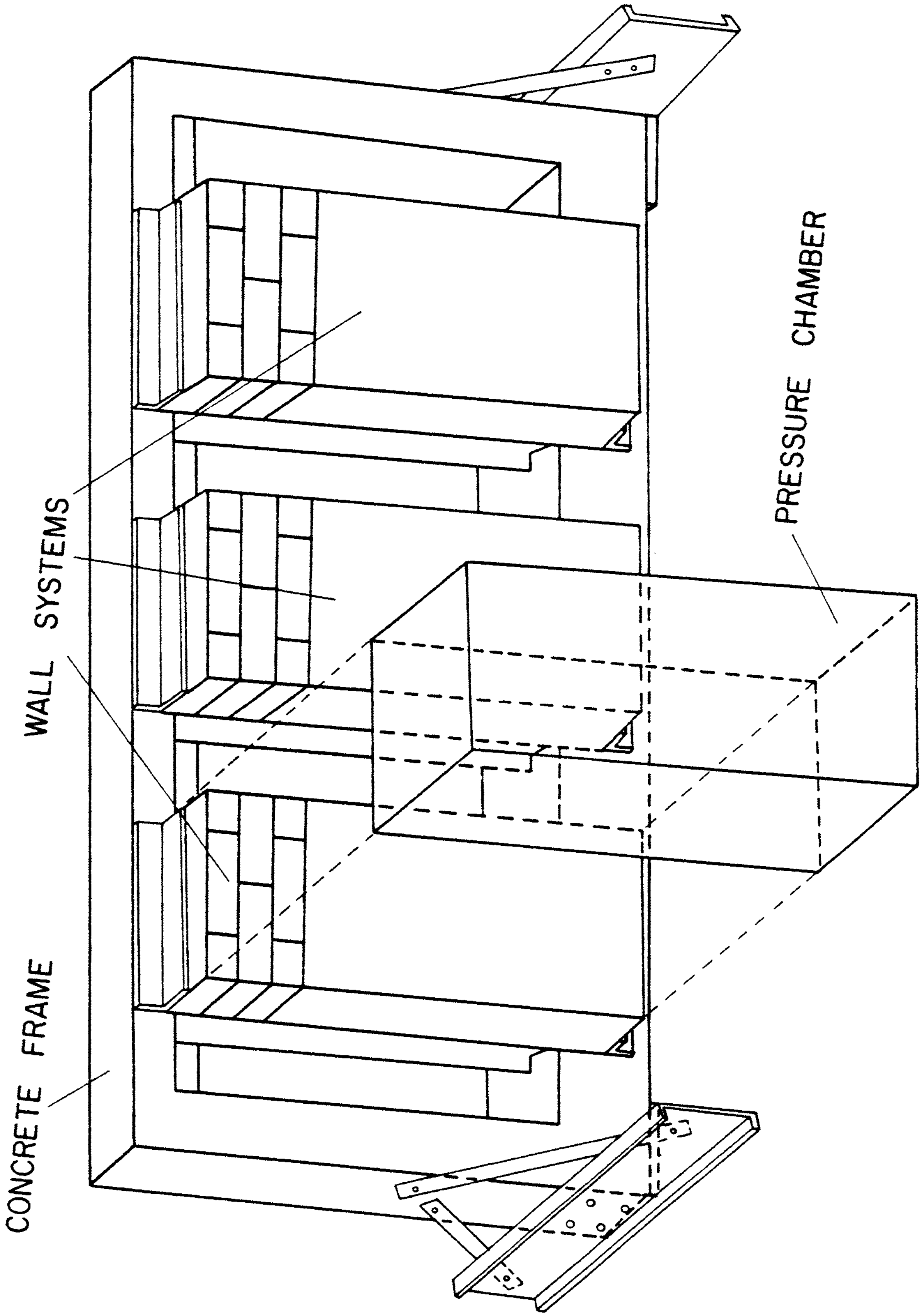

Figure 9. A Schematic Drawing of the Concrete Frame

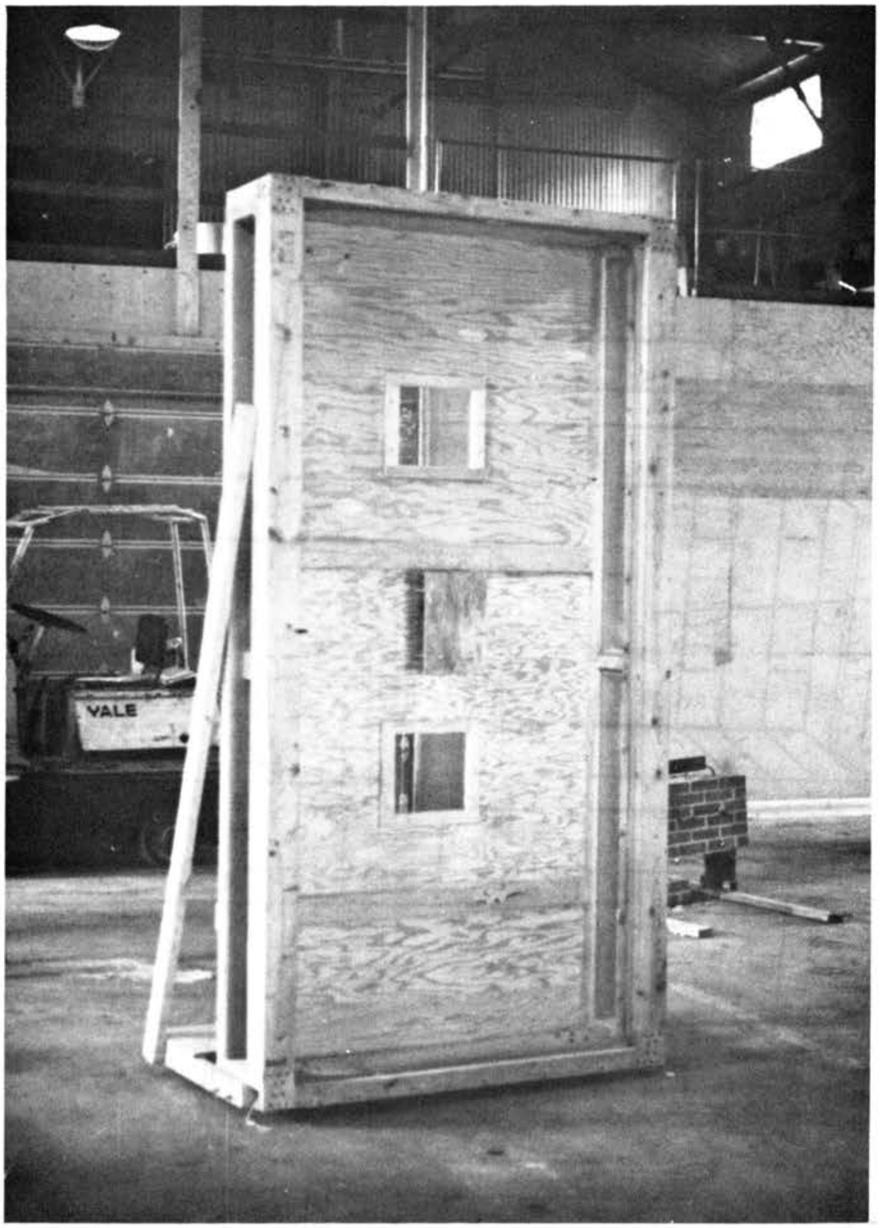

Figure 10. Pressure Chamber

A special feature of the pressure chamber was that it had a 1 in. by 1 1/2 in. groove around the inside periphery. In this groove was placed the long rubber inner tube. The tube was employed to seal the gap between the brick veneer and the chamber without restraining the wall's lateral movement. This meant that the sides of the walls were not restrained from moving during the lateral load tests. Prior to applying air pressure on the wall, the tube was placed in the groove. The chamber was then pushed to the wall and clamped to the two 4 by 4 timbers and the concrete frame (Fig. 11). The tube was then inflated to a pressure of 9 ± 0.5 psi and it expanded and pressed against the sides, top and bottom of the brick wall, thereby sealing the gap between the wall and the chamber. A cross section of the brick wall with the pressure chamber in place is shown in Fig. 12.

The chamber was mounted on four wheels so that it could be moved from wall to wall and also for easy storage. A hole was drilled at about the center of the chamber for applying the pressure with an industrial (vacuum cleaner) blower.

Design and Fabrication of Test Specimens

The wall panels were designed in such a way that the steel studs alone would experience a lateral deflection of L/360 under the design lateral wind load, where L is the height of the wall. For these tests, 20-gage, 3-5/8 inch channel studs at 24 inches on center, 7 feet 10 1/2 ins. in height were used to resist a 24.16 psf design wind load (Figs. 7 and 8). The physical and structural properties of the studs were: weight = 0.804 lb/ft, area = 0.208 in^2, I_{xx} = 0.540 in^4, S_x = 0.298 in^3, r_x = 1.450 in., I_{yy} = 0.076 in^4, r_y = 0.591 in, F_y = 33 ksi,

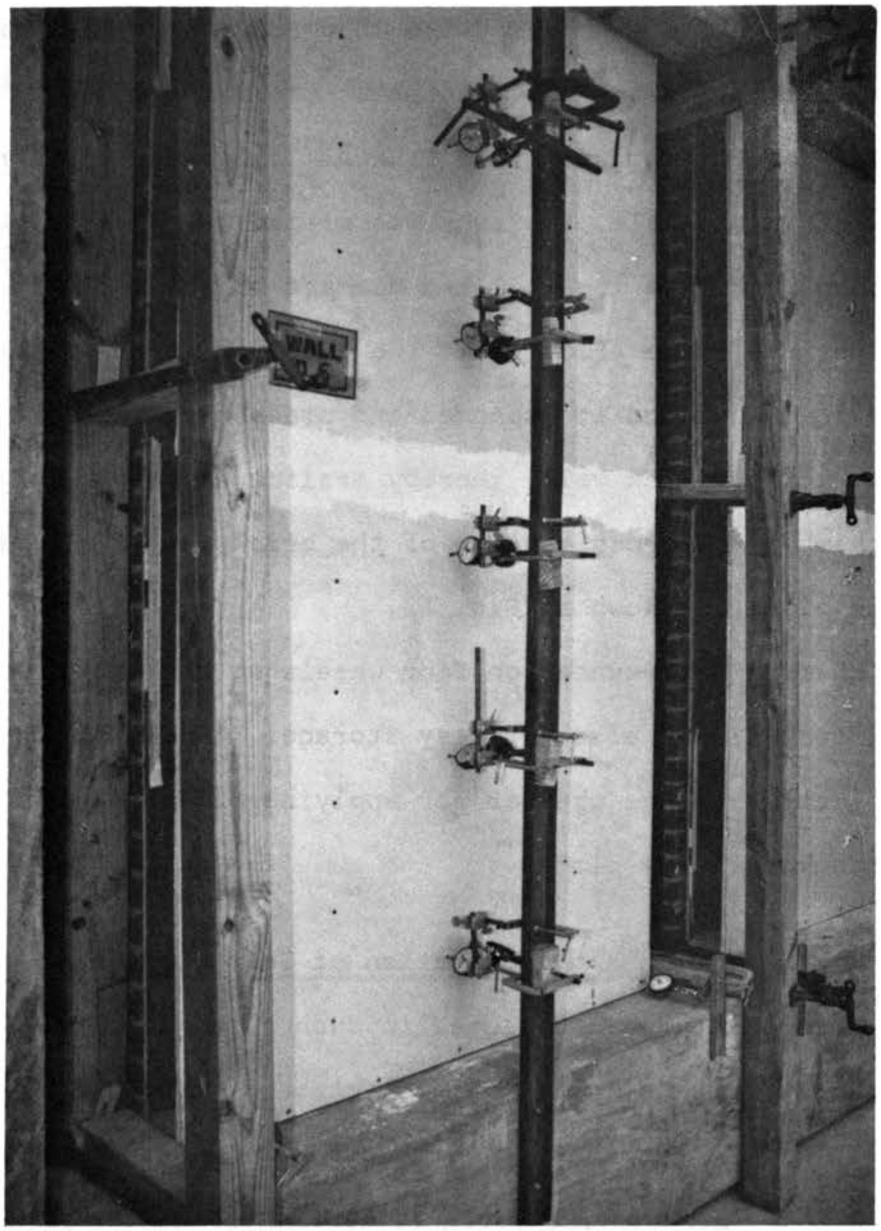

Figure 11. Location of Dial Gages at the Back of the Walls

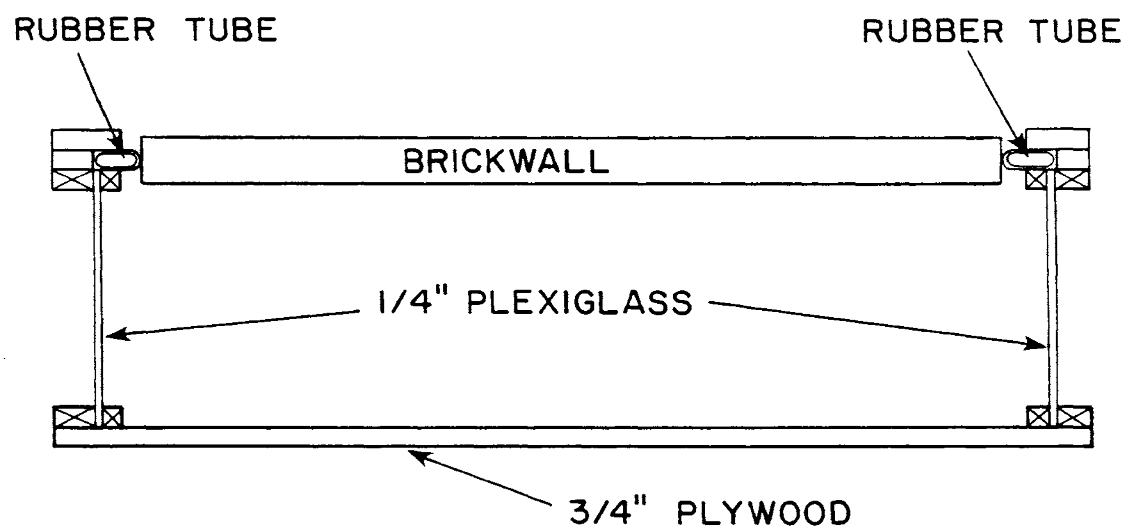

Figure 12. Cross Section Through Brick Wall and Lateral Loading Chamber Illustrating Inflatable Rubber Tube

allowable compression stress = 19,800 psi, resistance moment = 5,900 in-lb. The design load was obtained from the following formula:

$$\Delta = 5qL^4/384EI,$$

where E = 29,500 ksi, I = 0.540 in^4 and L = 94.5 in. The deflection was limited to $\Delta = L/360$. From these data, one obtains q = 4.026 lb/in.. Substituting into the formula for the load, Q, in psf = 144q/(stud spacing) with stud spacing = 24 in., the result is Q = 24.16 psf. Exterior gypsum sheathing, 1/2 in. thick and interior gypsum panel (1/2 in.) were attached to the studs using No. 6-DG screws, one inch in length. One row of 1 1/2 in., 16 ga bridging was provided at approximately mid-height of the studs. Horizontal joints were provided at approximately mid-height in the gypsum panel and at three different levels in the gypsum sheathing. The joints in the interior gypsum board were taped and floated. Runners were attached to the concrete frame with 1/4 in. diameter drilled expansion anchors (three anchors per runner). All the brick veneers were 4 in. walls.

Six full-scale wall panels, three of which are shown in Fig. 13, were constructed and tested for lateral load resistance and resistance to water permeance. The brick wall was supported on shelf-angles and the metal studs were attached to runners which were in turn attached to spandrel beams at top and bottom (Fig. 7).

A framing contractor was hired to construct the framing and a masonry contractor constructed the masonry. The masonry was constructed by journeyman bricklayers in its intended location on shelf angles attached to the concrete frames. Using this method of construction, no walls were moved after fabrication. The six brick walls were built in two

Figure 13. Three Walls Subjected to Lateral Load

batches, three walls in each batch. The mortar was mixed in a 2 1/2 ft paddle mixer according to the proportion method of ASTM C270, Type S.

The bed joints were lightly furrowed and tapered in order to minimize mortar droppings into the cavity. Head joints were completely filled with mortar. Joints were tooled with a concave joint tooler after the mortar was "thumbprint" hard.

The same backup walls were used throughout the tests. That is, the backup walls were reused with the second batch of brick walls.

The ties selected in Phase One (DW 10, 14 ga adjustable), were spaced at 16 in. on center vertically and 24 in. horizontally, according to the published recommendations of the Brick Institute of America (1).

Quality Control

Six full-scale walls were built and tested. The six walls were built in two batches with three walls built in each batch. In order to minimize variations in masonry quality from wall to wall, the masonry in each group of three walls was constructed in a single operation. In addition to the three prototype walls, nine prisms were fabricated; three for compressive tests (3), and six for flexural tests using the standard ASTM E518 (4) and the Bond Wrench (5) methods. Mortar was tested for air-content, flow, and cube strength (6). Prism and mortar test specimens were air cured in the environment in which the walls were stored. Brick was subjected to the following ASTM C67 (7) tests: compression, absorption (24 hr cold water and 5 hr boiling water), and initial rate of absorption. The walls were stored in controlled laboratory air for at least 28 days before testing (8). Attempts were made to insure a minimum of variation from specimen to specimen. All masonry work complied with inspected workmanship as defined by the Brick Institute of America (9).

Water Permeance Testing

A modified version of ASTM E514 - 79 (10) was used to evaluate the water permeance of the brick veneer before and after loading. It was necessary to modify the test procedure because of the difference in size between the prototype wall and the standard E514 wall specimen and because the back of the brick veneer was not accessible. In the tests conducted in this investigation there was a distance of approximately three feet below the bottom of the water permeance test chamber and flashing which collected leaking water (Fig. 14). The chamber was located here in order that the water permeance tests would be performed in the region of highest stress caused by lateral load. The large volume of masonry in the three foot height absorbed water that would ordinarily be caught in the flashing in a standard E514 test. In order to overcome this drawback, the water permeance test was performed using a closed-loop water supply. That is, the water permeance test began with a certain volume of water. At the end of the 3 hour test period, the amount of water remaining in the closed-loop system was subtracted from the original amount. The difference represented the amount of water which passed through the wall and was collected on the flashing as well as the amount of water absorbed by the brick. Fig. 15 shows the test set-up on one of the walls. Before the walls were subjected to lateral loads, they were subjected to a 24 hour preconditioning period as described in ASTM E514 (10).

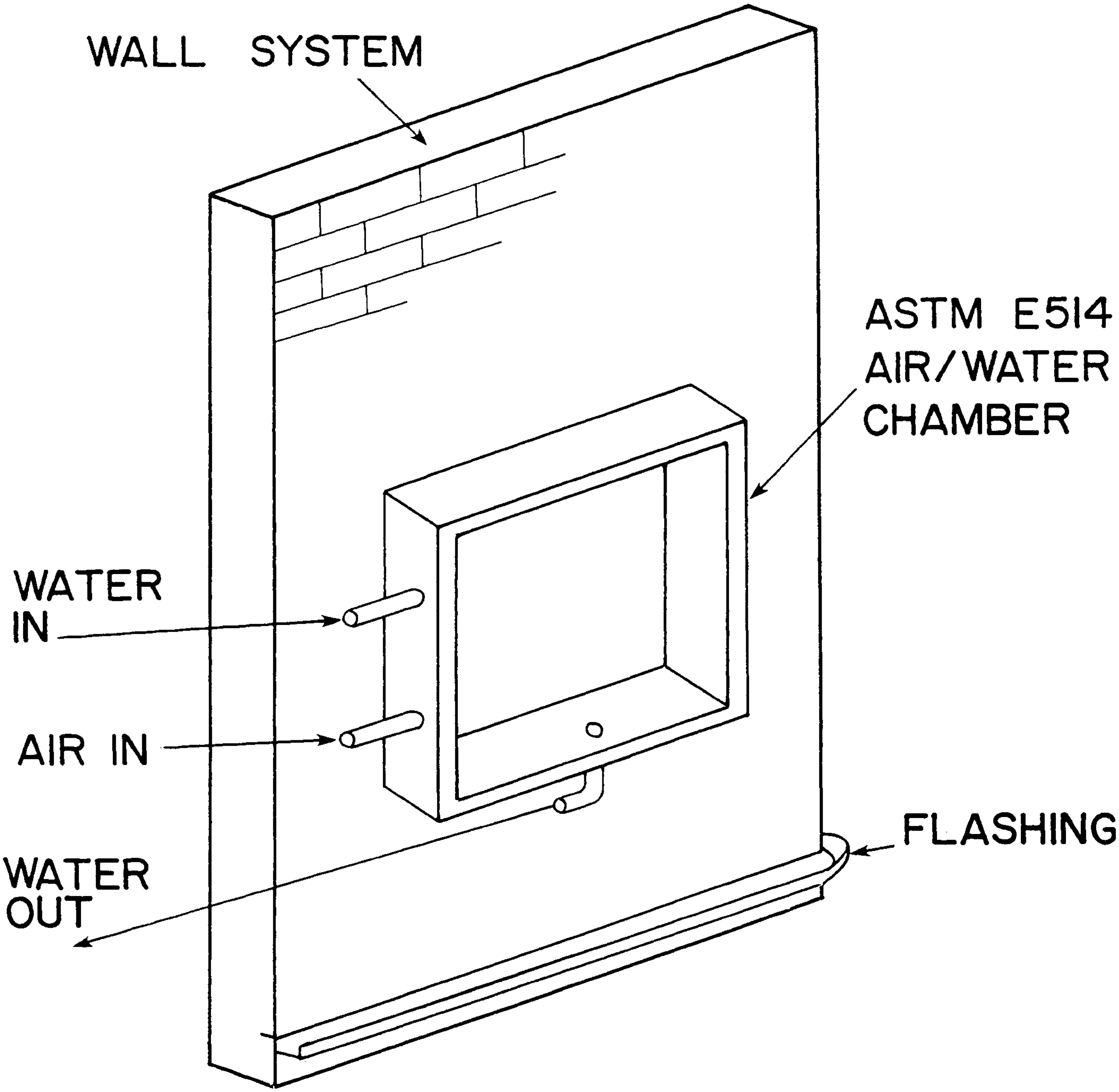

Figure 14. Drawing Illustrating the Apparatus to Perform the Modified E514 Water Permeance Tests

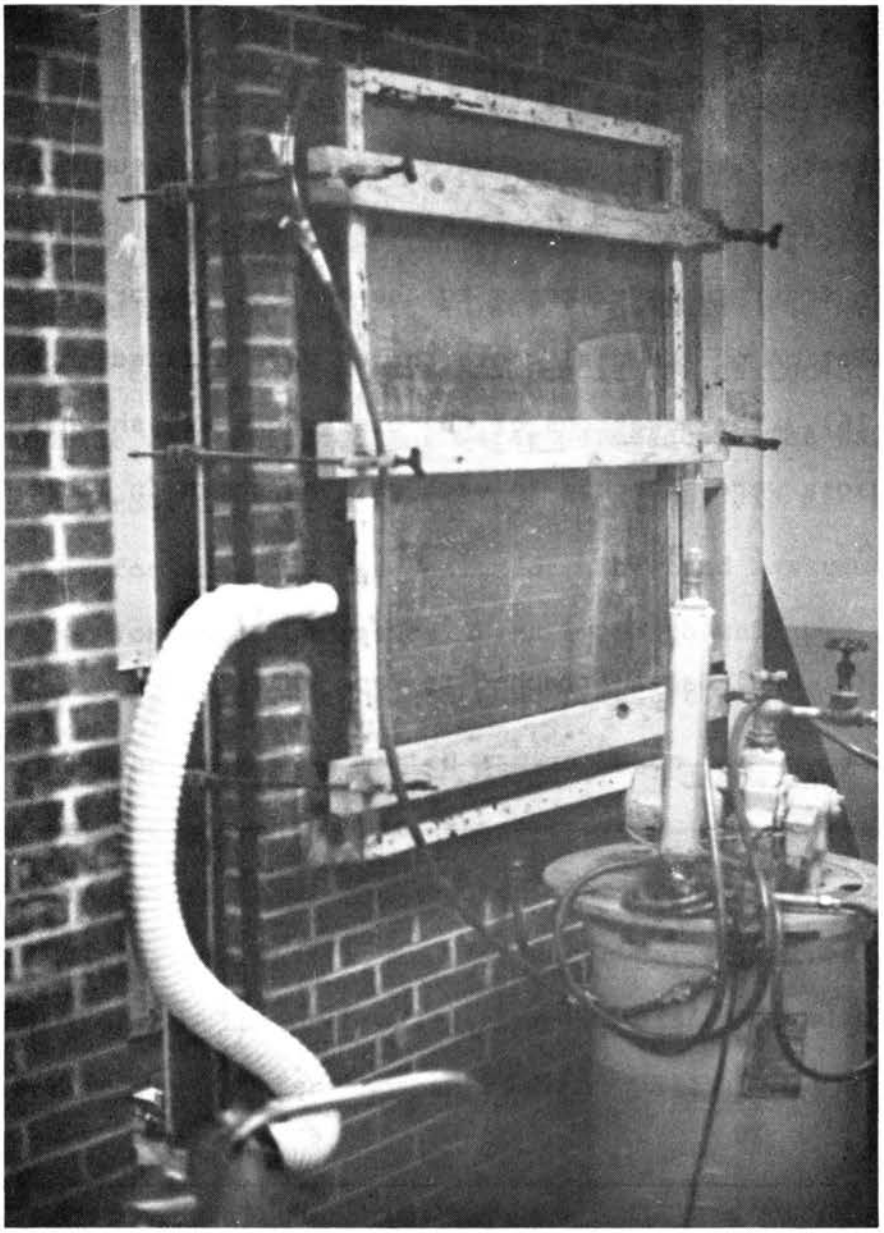

Figure 15. Water Permeance Test-set Up on One of the Walls

Instrumentation

In the lateral load testing, both the brick veneer and the metal stud backup were instrumented with dial gages to measure lateral deflection. Ten dial gages were used on the brick veneer in order to obtain the deflection profile of the brick wall before and after the formation of a crack. Ten dial gages were used on the gypsum board and stud assembly for lateral deflection measurement (Fig. 11).

In order to have access to the back of the brick wall for the installation of the dial gages, holes were drilled through the drywall (Fig. 16). The locations of the dial gages are shown in Fig. 17. The dial gages were attached to each wall as shown in Table I.

Table I. Dial Gages Attached to Each Wall

BRICKWALL	DRYWALL
1	3
2	4
6	5
8	7
10	9
12	11
14	13
16	15
19	17
20	18

a _____ See Fig. 17 for schematic drawing of dial gage locations.

Test Procedure for Wall Panels

Six full-scale wall panels were constructed and tested for lateral load resistance and resistance to water permeance. Three of the wall panels (Wall Nos. 1, 2, and 3), were tested for positive wind pressure, and the other three (Wall Nos. 4, 5, and 6), for negative (vacuum) wind pressure. All six panels were first preconditioned and tested for water permeance using a modified version of ASTM E514 - 79 (10). Next each wall was loaded incrementally to a lateral positive (or negative) air pressure equal to the intensity for which it was designed. The load was removed and the wall retested for water permeance. The wall was loaded incrementally to a lateral positive (or negative) air pressure of twice the intensity for which it was designed. The load was removed and the wall retested for water permeance. Finally, each wall was loaded incrementally to three times the design wind pressure.

The tests on each wall lasted 5 days. When the walls had been cured for at least 28 days, the tests were carried out as follows: The dial gages were installed in place, and the tests started by subjecting the wall to a 24 hour preconditioning for water permeance. At the end of the 24 hour period, the preconditioning was discontinued and the wall was allowed to dry-out for another 24 hours. This was the second day of test.

On the morning of the third day, the wall was subjected to a 3 hour water permeance test. At the end of the three hours, the water permeance chamber was removed from the wall. The lateral load pressure chamber was positioned so that the rubber tube in the chamber (Fig. 12) contacted the sides, top and bottom of the brick wall providing a seal

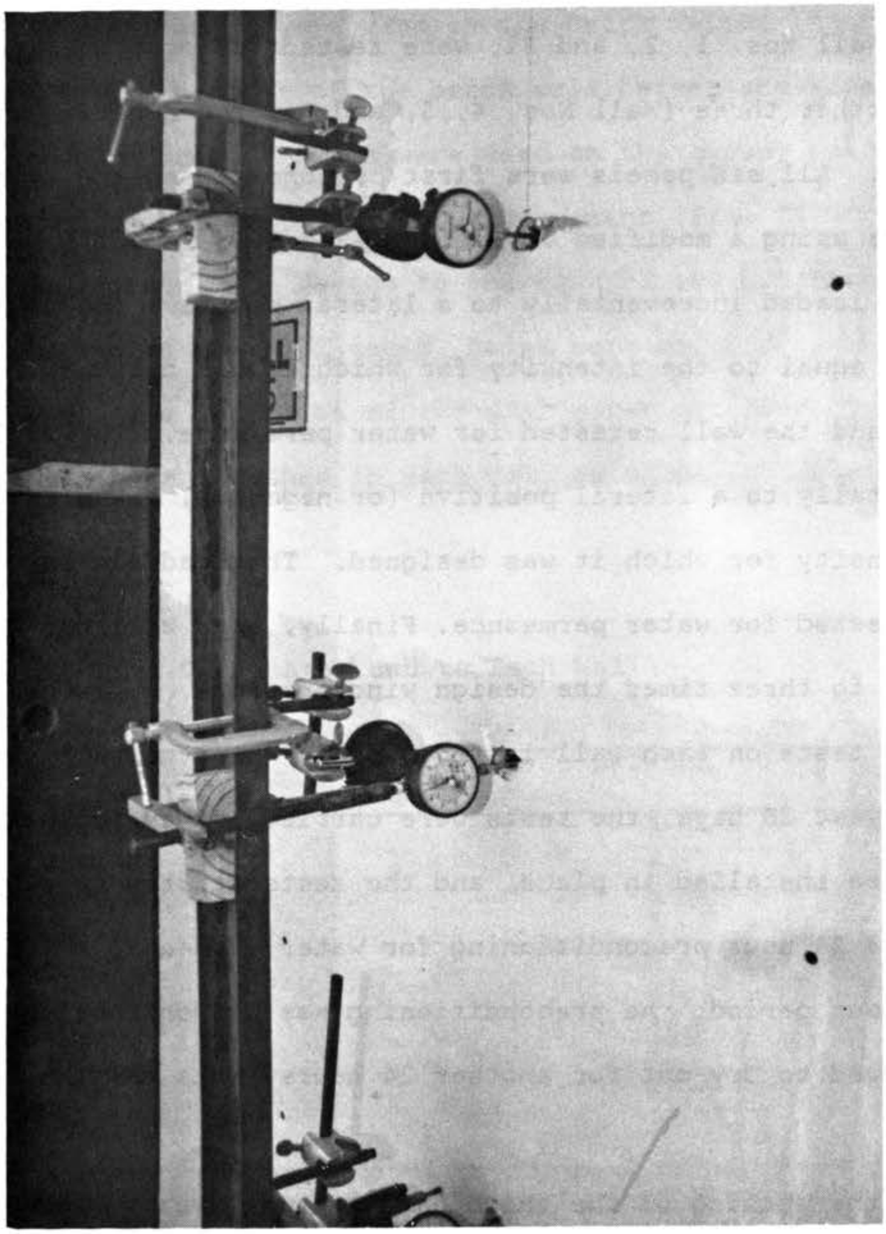

Figure 16. Close View of Dial Gages Attached to the Brickwall

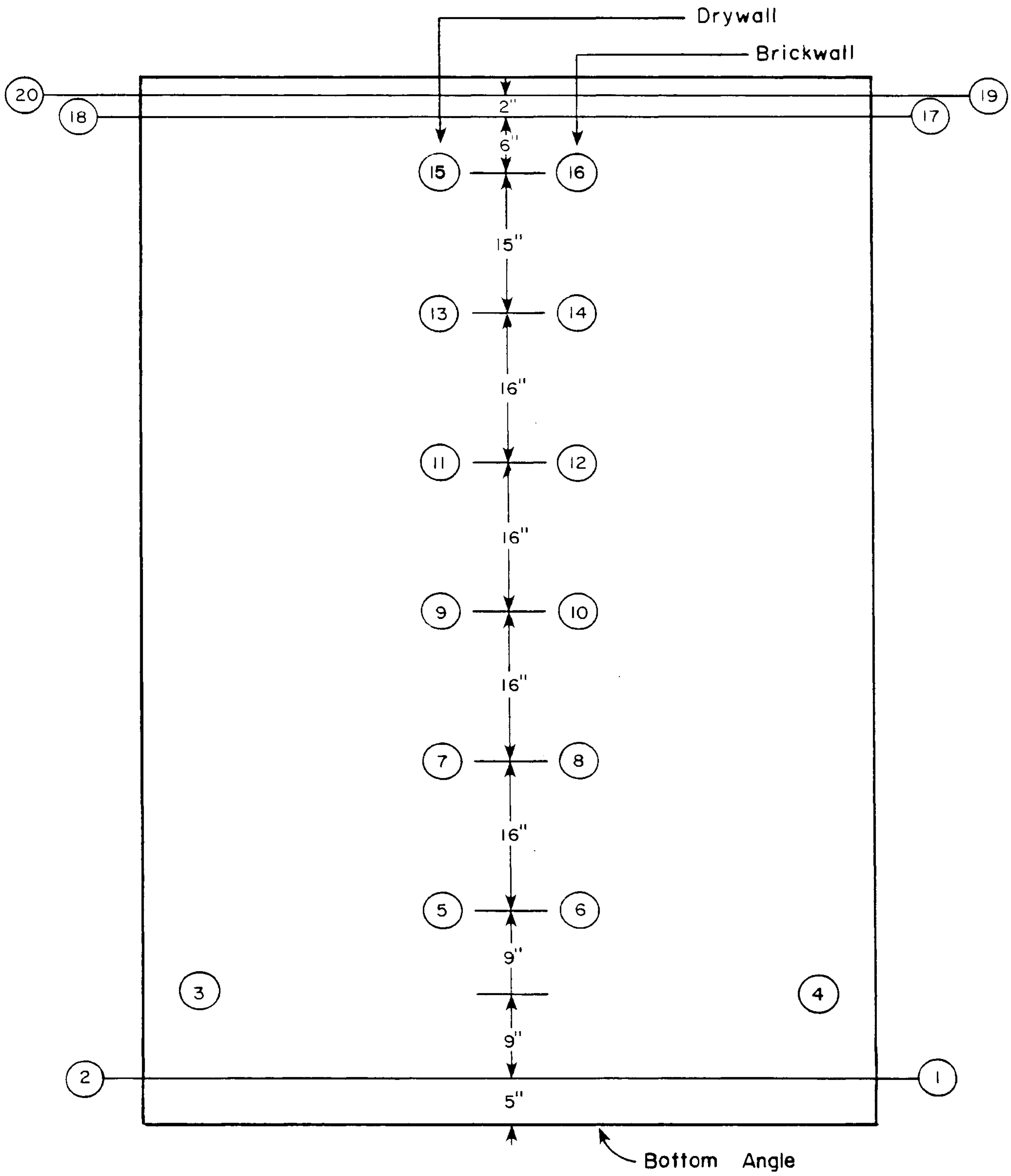

Figure 17. Dial Gage Locations

against air leakage around the wall's perimeter. The chamber was clamped to the concrete frame through a pair of 4 X 4 timbers (Fig. 11). At this point, the initial dial gage readings were taken. The tube was inflated to about 9 psi and the dial gages read again. The air pressure was applied to the wall in small increments until the design load was reached, the dial gages being read at each load increment. When the design load was achieved, the pressure was reduced incrementally, the dial gages being read at each load decrement. When the air pressure was brought to zero, the tube was deflated and the last dial gage readings were taken. The pressure chamber was then removed and the wall was prepared for another water permeance test.

On the fourth day of test, the wall was again subjected to a 3 hour water permeance test. The pressure chamber was clamped to the concrete frame. Initial dial gage readings were taken. The tube was inflated to 9 psi and another set of dial gage readings taken. The wall was loaded incrementally to twice the design load, dial gage readings being taken at each load increment. The pressure was reduced to zero incrementally, the dial gages being read at each load decrement. The tube was deflated and the last dial gage readings taken. The pressure chamber was unclamped and wheeled off and the wall prepared for the last water permeance test.

On the fifth day of test, the wall was again subjected to a 3 hour water permeance test. At the end of this period, the pressure chamber was reinstalled, dial gage readings were taken as before, and the wall was loaded incrementally to three times the design load. The pressure was then reduced to zero in equal increments. Dial gages were read at each load decrement.

This concluded the tests on the wall. The procedure was the same for both positive and negative pressures. The pressure on the wall was read on a water manometer attached to the back of the pressure chamber. The time required for each load increment was about ten minutes. In Fig. 13, Wall No. 6 is shown ready to be tested for lateral load.

CHAPTER III

TEST RESULTS

Tie Test Results

The results of the tie tests are shown in Appendix A. The test results for each tie, obtained from both the transducer and the dial gages, show that the ties travel through approximately the same path after the first cycle of loading. Therefore hysteretic behavior of the ties is approximately the same after the application of the first cycle of loading. For this reason, only the fifth cycle of load at each load level is given.

Corrugated Tie, Gage 22 With a = 1.75 in

Fig. A-1 shows the hysteresis loop for a 22 ga corrugated tie, for a load level of 50 lbs. The area of the hysteresis loop is large. The slope to the hysteresis loop at any point is small therefore the tie is very flexible. The tie's behavior becomes non-linear for large loads (over 50 lbs.). The tie is so flexible that it collapsed when a load of 150 lbs. was applied in compression.

Corrugated Tie, Gage 20 With a = 5/8 in

Figs. A-2, A-3 and A-4 show the hysteresis loops for 20 ga corrugated ties for load levels 50 lbs., 100 lbs., and 150 lbs., respectively. The areas of the hysteresis loops increase as the load level increases. The loops tend to flatten out about the zero load point as the load increases. At any given load level the slope at any given load is less as the load increases. This behavior indicates the loss of stiffness in the tie as the load increases.

Corrugated Tie, Gage 18 With a = 5/8 in

Figs. A-5, A-6 and A-7, show the hysteresis loops for an 18 ga corrugated tie with a = 5/8 in., for load levels 50 lbs., 100 lbs., and 150 lbs., respectively. The areas of the hysteresis loops increase as the load level increases. The area of the hysteresis loop for load level 150 lbs., is much larger than for lower maximum load levels.

Corrugated Tie, Gage 18 With a = 2 in

Figs. A-8, A-9, and A-10, show the hysteresis loops for an 18 ga corrugated tie with a = 2 in., for load levels 50 lbs., 100 lbs., and 150 lbs., respectively. The area of the hysteresis loops increased greatly by comparison to the same tie with a = 5/8 in. and the tie is much more flexible. As the load level increased, the loading and unloading portions of the loops became steeper.

Fig. A-10 shows that the hysteresis loop became steeper as the applied load was increased. This implies that the tie became stiffer with increased load. Owing to the large value of "a", in tension the tie resisted the applied load initially by bending about the point at which it is screwed to the steel plate. The tie is eventually pulled up into a smooth curve as the load increased. At this point the tie resists the load axially and hence the hysteresis loop becomes steeper than before indicating an increase in stiffness. In compression, the tie is pushed back until it comes in contact with the gypsum board. When the tie is fully in contact with the gypsum board, it again resists the load axially and the hysteresis loop becomes steeper.

Corrugated Tie, Gage 16 With a = 5/8 in

Figs. A-11, A-12, and A-13, show the hysteresis loops for a 16 gage corrugated tie, for load levels 50 lbs., 100 lbs., and 150 lbs., respectively. The area of the loops are small, the slope at any point on the loops is steep and therefore the tie is very stiff.

DW 10, Tie Gage 14

Two different diameter wires (links) were used in testing this DW 10 tie. The diameters of the wires used were 0.188 and 0.172 in., respectively. For the tie with wire diameter of 0.172 in, the tie backing was also thinner than 14 gage.

Figs. A-14, A-15, and A-16, show the hysteresis loops for a 14 ga DW 10 tie with wire diameter equal to 0.188 in. and Figs. A-17, A-18, and A-19, show the hysteresis loops for a 14 ga DW 10 tie with wire diameter equal to 0.172 in., for load levels 50 lbs., 100 lbs., and 150 lbs., respectively. The loops and their areas are small. At the 100 lb. load level, there is a permanent deformation of the tie backing. Consequently, in going through a cycle of loading, there are two times when the wire moves through the gap created by this permanent set. The wire goes through this gap at zero load. This phenomenon is seen in Figs. A-18 and A-19, at zero load. This behavior of the DW 10 ties was prominent in ties with thinner wire diameter and backing. Although designated 14 ga DW 10, it was observed that some of these ties varied in backing thickness and wire diameter. The standard dimensions for this tie are a backing of gage 14 and a wire diameter of 3/16 in. The ties with these dimensions displayed very little of this phenomenon, (Figs. A-14, A-15 and A-16).

DW 10 Tie, Gage 12

Figs. A-20, A-21 and A-22, show the hysteresis loops for a 12 ga DW 10 tie, for load levels 50 lbs., 100 lbs., and 150 lbs., respectively. The loops and their areas are small and the tie is stiff. No permanent set was observed at the load levels used.

Quality Control Test Results

The quality control test results for Brick, Mortar and Prisms are shown in Appendix B. Included in this section are tension (splitting) test results on mortar cubes and cylinders. These tests were performed by splitting the cubes along a diagonal and the cylinders along a diameter as described by Davis, et al. (11).

Also included in this section is the flexural test result on a piece of brick prism 32 in. by 8 in. that was sawed from Wall No. 1 during the demolition process. The prism was simply supported at the ends 30.1 in. apart and loaded at two points 8.425 in. from the supports. Fig. 18 shows the plot for the test. The modulus of rupture was found to be 114.0 psi and the modulus of elasticity, to be equal to 875,000.0 psi.

The formula used for calculating the modulus of elasticity is given as

$$EI\Delta = Pa(3L^2 - 4a^2)/48,$$

where

a = distance from the supports to the point of application of the loads,

I = moment of inertia of an 8 in by 3.5 in. prism section,

L = length of prism,

$P/2$ = load applied at "a" from each support,

Δ = mid-point deflection.

Solving the equation for modulus of elasticity yields

$$E_m = (P/\Delta)a(3L^2 - 4a^2)/(48I).$$

Substituting a = 8.425 in, L = 30.1 in, P/Δ = 114/.0019 and I = 28.53 in and evaluating the equation for E_m yields 875,000 psi. Subsequent tests of similar prisms cut from Walls 1, 2 and 3 have been performed resulting in measured values of E_m of 3,890,000 psi, 1,680,000 psi and 2,990,000 psi.

Brick, Brick Prisms and Mortar

The compressive strength and absorption properties of the bricks used in this investigation are shown in Table B-I. Table B-II contains the ultimate loads and stresses in compression and bending of stack bond brick prisms made from mortar used for Wall Nos. 1, 2 and 3. Tables B-III and B-IV show the maximum stresses of mortar cubes and cylinders for Wall Nos. 1, 2 and 3. Table B-V shows the mortar flow and air content for Wall Nos. 1, 2 and 3. Table B-VI shows the ultimate stresses in compression and bending of stack bond brick prisms for Wall Nos. 4, 5 and 6. Tables B-VII and B-VIII show the maximum stresses of mortar cubes and cylinders for Wall Nos. 4, 5 and 6. Table B-IX shows the mortar flow and air content for Wall Nos. 4, 5 and 6. Tables B-X and B-XI show the ultimate stresses for joint failure using the Bond Wrench (5) and ASTM E518 methods for wall prisms made from motars used for Wall Nos. 1, 2 and 3 and Wall Nos. 4, 5 and 6, respectively. Table B-XII shows mean values, standard deviations, coefficient of variations of

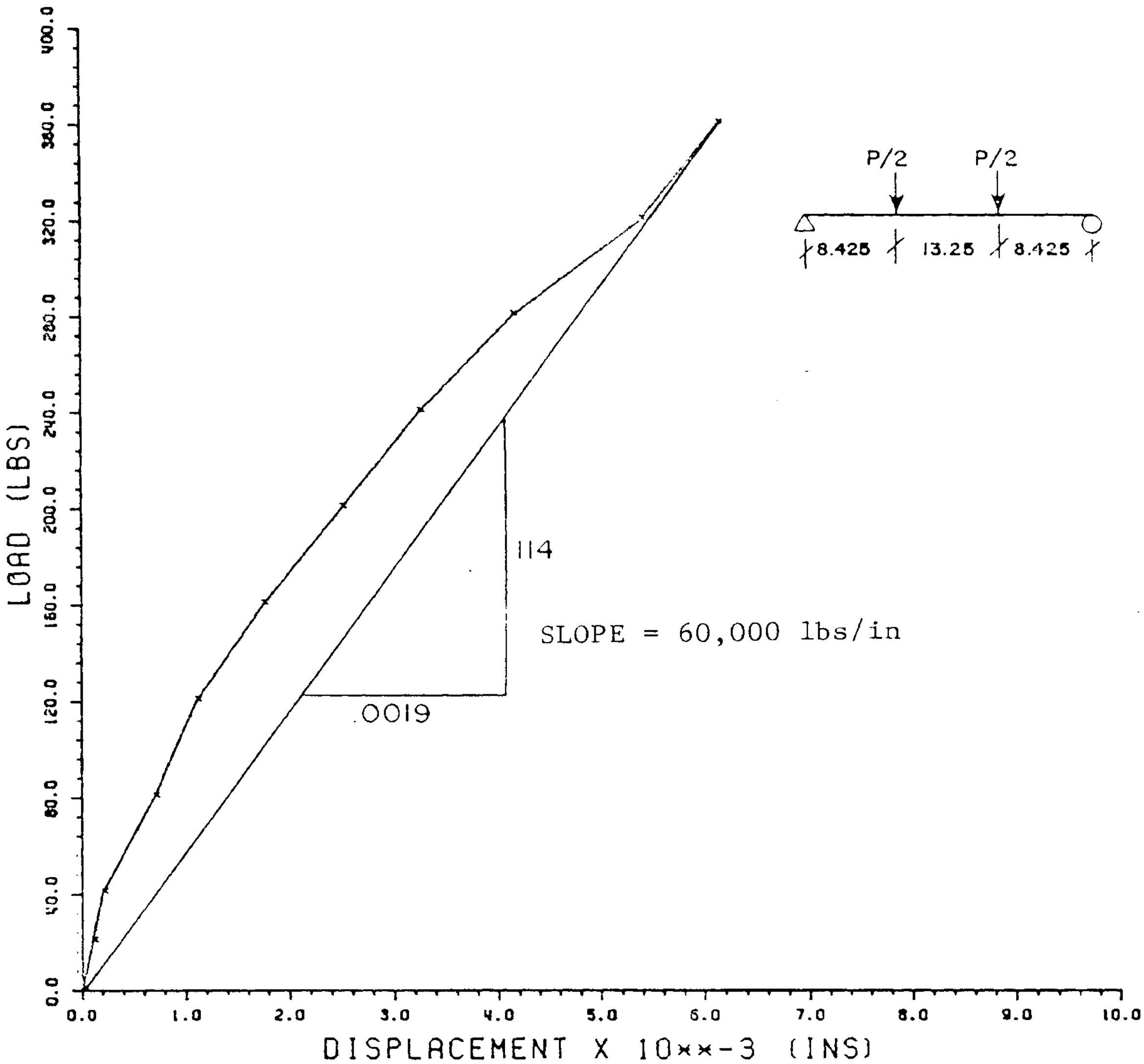

Figure 18. Flexural Test Result on Brick Prism Saved From Wall No. 1

brick prisms flexural test results using both the Bond Wrench and the ASTM E518 methods.

From Tables B-II and B-VI, the average moduli of rupture for prisms made from the mortar batches for Wall Nos. 1, 2, and 3, and Wall Nos. 4, 5, and 6, are 89 psi and 147 psi, respectively, by the ASTM E518 method and 107 psi and 169 psi, respectively, by the Bond Wrench method. Also the average prism compressive strength for Wall Nos. 1, 2 and 3 is 4035 psi, Table B-II, and for Wall Nos. 4, 5, and 6 is 5170 psi, Table B-VI. The average mortar cube strength for Wall Nos. 1, 2 and 3 (batch no. 6) is 3016 psi (Table B-III) and for batch no. 8, 3167 psi (Table B-IV). The average mortar cube strength for Wall Nos. 4, 5 and 6 (batch no. 3) is 1757 psi (Table B-VII) and for batch no. 7, 2230 psi (Table B-VIII). The mortar used for Wall Nos. 4, 5 and 6 had lower compressive strength which implies that it may have contained a larger water content. This may have led to high bond strength in spite of reduced compressive strength. The superior performance of Wall Nos. 4, 5, and 6 during the lateral loading tests may be attributable, in part, to superior flexural bond strength.

Water Permeance Tests

The water permeance test results for the six walls are given in Table II. For Wall No. 1, streaks of water were visible at the back of the brick wall throughout the three days of tests. On the third day of the water permeance test, the weep holes were wet after about 2 1/2 hours of the test; however no water was collected at the flashing.

On Wall No. 2, water was initially visible on the flashing after about 1 1/2 hours on the first day of test. The volume of water collected from the flashing on the first day of the water permeance test was 280 ml. On the second and third days of water permeance tests, 570 ml and 16 ml volume of water was collected, respectively. Streaks of water were visible at the back of the brick wall throughout the three days of tests. Water was observed to drip across mortar droppings to the gypsum sheathing at some points. Some of the metal ties were observed to be moist from these movements of water between the brick veneer and the exterior sheathing across the mortar droppings. On the second day of water permeance testing on Wall No. 2, there was profuse leakage of water around the periphery of the water permeance chamber which proved difficult to stop.

On Wall No. 3, streaks of water were observed at the back of the brick wall throughout the three days of the water permeance test; however, no water was collected at the flashing.

The back of the brick wall of Wall No. 4, was dry throughout the first day of the water permeance test. On the second and third days of tests, streaks of water were observed at the back of the wall after 60 min. and 40 min., respectively. No water was collected at the flashing.

On Wall No. 5, there was much flow of water through the weep holes throughout the three days of water permeance tests. On the first, second and third days of the tests, 660 ml, 148 ml and 1230 ml volume of water were collected at the flashing, respectively. The back of the brick wall was wet throughout the periods of the water permeance tests. There was profuse leakage of water from a tooled joint on the periphery of the water permeance chamber throughout the third day of the water permeance test.

On Wall No. 6, the back of the brick wall was dry throughout the three days of water permeance tests. No water was collected at the flashing.

In general, it was difficult to provide a watertight seal around the periphery of the water permeance chamber because of the tooled joints. Also there were occassional minor leaks around the chamber which were sealed as quickly as possible. It was found that once the brick wall was wet it was difficult to get the caulking compound used to adhere to it. This made the sealing of leaks difficult.

A water absorption test on a portion of Wall No. 1 showed that in 3 hours, a fully submerged prism absorbed 3% of its weight of water. In 24 hours, the absorption was 4.6% of its weight. Since the wall weighed 42 psf and the water permeance chamber had an area of 12 ft^2, a weight of 14.12 lb of water is required to fully saturate the masonry behind the chamber. In no case did such large quantity of water penetrate the wall.

The weights of water absorbed by the brick walls when the walls were subjected to a 3 hour water permeance test are shown in Table II.

Results of Lateral Load Tests

Appendix C shows the deflection plots of the six walls subjected to the lateral load tests at the design load, two times the design load, and three times the design load, respectively. Wall Nos. 1, 2 and 3, were subjected to positive pressure and Wall Nos. 4, 5 and 6, to negative pressure. The design load for these walls was 24.16 psf.

Table II. Weight of Water Absorbed by the Brickwall When Subjected to a 3 Hour Water Permeance Test

WALL NO.	BEFORE LOADING LB/3 HR	LITERS/HR	AFTER DESIGN LOAD LB/3 HR	LITERS/HR	AFTER 2 X DESIGN LOAD LB/3 HR	LITERS/HR
1	2.75	0.416	3.50	0.530	4.50	0.681
2	5.00	0.757	8.70 [a]	1.317[a]	4.25	0.643
3	2.25	0.341	2.25	0.341	1.50	0.227
4	1.00	0.151	1.75	0.265	2.00	0.303
5	4.00	0.605	4.50	0.681	6.50 [a]	0.981[a]
6	1.00	0.151	1.00	0.151	1.00	0.151

a ______________ Leaks Occurred During Test

Wall No. 1

Figs. C-1, C-2 and C-3 show the deflection plots for the brick wall under positive pressure for load levels design load, twice design load, and three times design load, respectively. Figs. C-1 and C-2, show that the wall behaved elastically. In Fig. C-3, the wall is seen to crack at between 10 and 11 inches of water (52-57 psf). The top of the brick wall remained in the same position just before the crack developed even when more load was applied after it cracked. The compressible filler material may have restricted the tendency of the top of the brick wall to move backwards after the crack.

Figs. C-4, C-5, and C-6 show the deflection plots for the drywall under positive pressure for load levels design load, twice design load, and three times design load, respectively. The increase in the deflection of the drywall is proportional to the applied load. Fig. C-6, shows that the drywall's deflection became much larger after the brick wall cracked. This indicated that the stud wall resisted substantially more load after the brick wall cracked.

Fig. C-7 shows the residual deflections of the brick wall, for the three levels of loading and Fig. C-8, the residual deflections of the drywall after unloading, for the three levels of loading.

It should be noted that the dial gage readings before each test were taken as the zero readings. Therefore the absolute residual deflection at any point in the brick wall, after three times design load has been applied to the wall, is equal to the sum of the residual deflections shown in Fig. C-7. Furthermore the maximum absolute deflection of Wall No. 1, for example, is equal to the sum of the maximum deflection from Fig. C-3 (0.370 in.) plus the residual deflection at that level from the two previous loadings from Fig. C-7 (0.025 + 0.080). Thus, the maximum absolute deflection is 0.475 in.

Wall No. 2

Figs. C-9, C-10, and C-11 show the deflection plots for the brick wall under positive pressure for load levels design load, twice design load and three times design load, respectively. Fig. C-9 shows that the brick wall deflection was proportional to the applied load. In Fig. C-10 the wall is seen to crack at between 5 and 6 inches of water (26-31 psf). Wall No. 2 was the only wall to experience cracking at a load less than twice design load.

Figs. C-12, C-13, and C-14 show the deflection plots for the drywall under positive pressure for load levels design load, twice design load, and three times design load, respectively. The increase in the deflection of the drywall is proportional to the applied load. Figs. C-13 and C-14 show that the drywall's deflection became much larger after the brick wall cracked

Fig. C-15 shows the residual deflections of the brick wall, for the three levels of loading and Fig. C-16, the residual deflections of the drywall after unloading, for the three levels of loading.

Wall No. 3

Figs. C-17, C-18, and C-19 show the deflection plots for the brick wall under positive pressure for load levels design load, twice design load, and three times design load, respectively. Fig. C-19 shows the wall cracked at between 10 and 11 inches of water (52-57 psf). The deflections are much larger after the crack.

Figs. C-20, C-21, and C-22 show the deflection plots for the drywall under positive pressure for load levels design load, twice design load, and three times design load, respectively. The increase in the deflection of the drywall is proportional to the applied load. Fig. C-22 shows that the drywall's deflection became much larger after the brick wall cracked Fig. C-23 shows the residual deflections of the brick wall, for the three levels of loading and Fig. C-24, the residual deflections of the drywall after unloading, for the three levels of loading.

Wall No. 4

Figs. C-25, C-26, and C-27 show the deflection plots for the brick wall under negative pressure for load levels design load, twice design load, and three times design load, respectively. Figs. C-25 and C-26 show that the brick wall's deflection is a combination of elastic deflection and a rigid body rotation about the base of the wall. Fig. C-27 shows that the deflection of the wall was a combination of rigid body rotation about the base of the wall and bending. It is apparent from Fig. C-27 that the wall did not crack at a load of 73 psf.

Figs. C-28, C-29 and C-30 show the deflection plots for the drywall under negative pressure for load levels design load, twice design load, and three times design load, respectively. The increase in the deflection of the drywall is proportional to the applied load.

Fig. C-31 shows the residual deflections of the brick wall, for the three levels of loading and Fig. C-32, the residual deflections of the drywall after unloading, for the three levels of loading.

Wall No. 5

Figs. C-33, C-34 and C-35 show the deflection plots for the brick wall under negative pressure for load levels design load, twice design load, and three times design load, respectively. Figs. C-33 and C-34 show that the brick wall's deflection is a combination of elastic deflection and a rigid body rotation about the base of the wall. There is much movement at the top of the wall. Fig. C-35 shows that the brick wall cracked at between 11 and 12 in. of water (57-62 psf). After the crack, the lateral movement of the top of the wall was reduced considerably compared to that of Wall No. 4. However, there was much lateral movement near the crack zone.

Figs. C-36, C-37 and C-38 show the deflection plots for the drywall under negative pressure for load levels design load, twice design load, and three times design load, respectively. The increase in the deflection of the drywall is proportional to the applied load. Fig. C-38 shows that the drywall's deflection became much larger after the brick wall cracked

Fig. C-39 shows the residual deflections of the brick wall, for the three levels of loading and Fig. C-40, the residual deflections of the drywall after unloading, for the three levels of loading.

This is the only wall that cracked under negative pressure.

<u>Wall No. 6</u>

Figs. C-41, C-42, and C-43 show the deflection plots for the brick wall under negative pressure for load levels design load, twice design load, and three times design load, respectively. Figs. C-41 and C-42 show that the brick wall's deflection is a combination of elastic deflection and a rigid body rotation about the base of the wall. All the figures show that there was a lot of movement at the top of the brick wall. Fig. C-43 shows that the deflection of the wall was a combination of rigid body rotation about the base of the wall and little bending. The wall did not crack at 3 times design load.

Figs. C-44, C-45 and C-46 show the deflection plots for the drywall under negative pressure for load levels design load, twice design load, and three times design load, respectively. The overall deflections of the drywall were very large, especially at three times design load.

Fig. C-47 shows the residual deflections of the brick wall, for the three levels of loading and Fig. C-48, the residual deflections of the drywall after unloading, for the three load levels.

Summary of Lateral Load Tests

The maximum deflections of the walls are shown in Tables III and IV.

Table III. Maximum Experimental Brick Veneer Deflections in Inches

WALL NO.	DESIGN LOAD	2 X DESIGN LOAD	3 X DESIGN LOAD
1	0.048	0.100	0.360
2	0.050	0.315	0.475
3	0.048	0.100	0.320
4	0.060	0.200	0.520
5	0.075	0.240	0.700
6	0.150	0.350	0.860

Table IV. Maximum Experimental Backup Wall Deflections in Inches

WALL NO.	DESIGN LOAD	2 X DESIGN LOAD	3 X DESIGN LOAD
1	0.050	0.090	0.280
2	0.060	0.270	0.380
3	0.030	0.080	0.240
4	0.060	0.140	0.310
5	0.060	0.140	0.500
6	0.080	0.180	0.400

The values of the deflections shown in Tables III and IV differ for all the walls largely due to the indeterminate restraining force at the top of the brick veneer caused by the compressible filler material.

In all the walls that cracked during the lateral load tests, the top of the brick wall was observed to stay in the same position after the brick wall cracked. In the analytical model in which the top of the brick wall was free, the top of the brick wall moved backwards in the opposite direction to its movement after a crack was introduced (Fig. 41). Therefore the top of the brick wall moves in while the point of the crack moves out. In the walls tested, the friction between the top of the brick wall and the compressible filler material may have been sufficient to prevent this inward movement causing the top of the wall to remain nearly stationary after the crack developed. In all the figures in Appendix C, the brick veneer deflected more than the metal stud backup at every point at all load levels. The summary of the test results is given in Table V.

Positive Versus Negative Load Test Results

The test results of Wall Nos. 1, 2 and 3 (Figs C-1 to C-24) and Wall Nos. 4, 5 and 6 (Figs. C-25 to C-48) show that Wall Nos. 4, 5 and 6 subjected to negative loads exhibited superior performance during the tests. This superior performance of these walls may be attributed to the following reasons:

1. Wall Nos. 4, 5 and 6 had superior flexural strength.

2. In the negative load tests the tooled mortar joints were in tension whereas in the positive load tests the untooled joints were in tension. The tooled mortar joints are stronger in tension than the untooled mortar joints.

3. In the positive load tests, the interior face of the brick veneer is in tension, causing it to elongate . Since the veneer is restrained by the shelf angle at the bottom and the neoprene at the top, this elongation causes a binding effect at the neoprene at the top. Thus, for positive loads, slightly greater lateral restraint is provided by the neoprene at the top of the brick wall than would be expected for suction loads. For suction loads, the outer face of the veneer is in

tension. Since the outer face is not in contact with the shelf angle at the bottom or the neoprene at the top, the elongation of the outer fibers does not result in lateral restraint of the wall. This phenomenon may explain the difference in behavior of the walls under positive and negative loads.

Table V. Summary of Lateral Load Test Results

WALL NO.	MAX. DEFL (IN.) DRYWALL	MAX DEFL (IN.) BRICKWALL	CRACKING LOAD[c] (PSF) (BRICKWALL)
1.	0.280	0.360[a]	52.0-57.0
2.	0.380	0.475[a]	26.0-31.0
3.	0.240	0.320[a]	52.0-57.0
4.	0.310	0.520[b]	no crack at 73.0
5.	0.500	0.700[a]	57.0-62.0
6.	0.400	0.860[b]	no crack at 73.0

a ____________ maximum deflection occurred at crack

b ____________ maximum deflection occurred at the top of the brick wall. These walls did not crack.

c ____________ cracking occurred within the range of load shown.

CHAPTER IV

DEVELOPMENT OF MATHEMATICAL MODELS

Mathematical models were developed for the DW 10 ga 14 tie and the wall system. In the model for the tie, the axial stiffnesses of the tie in tension and compression were obtained. For the wall system, a mathematical model was used in which the brick veneer and the studs were treated as parallel beams connected at regular intervals with ties. A section of the wall 2 feet wide with a single steel stud at the center was used in this analysis. The ties were represented as linear springs with the appropriate tie stiffnesses. The analytical computer model developed is capable of accommodating different boundary conditions of both the brick veneer and steel stud. Size and spacing of stud, wall thickness, tie stiffness, and tie spacing were systematically varied in a parametric study. The models are presented below.

Mathematical Model for the Tie Used in the Tests

Tie Stiffness Mathematical Model for DW 10 Gage 14 Tie, with Wire Diameter = 0.188 in.

From the load versus displacement plots, mathematical models of axial tie stiffness can be developed. The load versus displacement plots of DW 10 gage 14 ties for the three load levels are shown in Figs. A-14, A-15, and A-16. The loading portions of these plots are shown in Fig. 19. The Figure shows the compression load versus displacement plots for the three load levels 50 lbs., 100 lbs., and 150 lbs., respectively and also shows the tension load versus displacement plots for the three load levels.

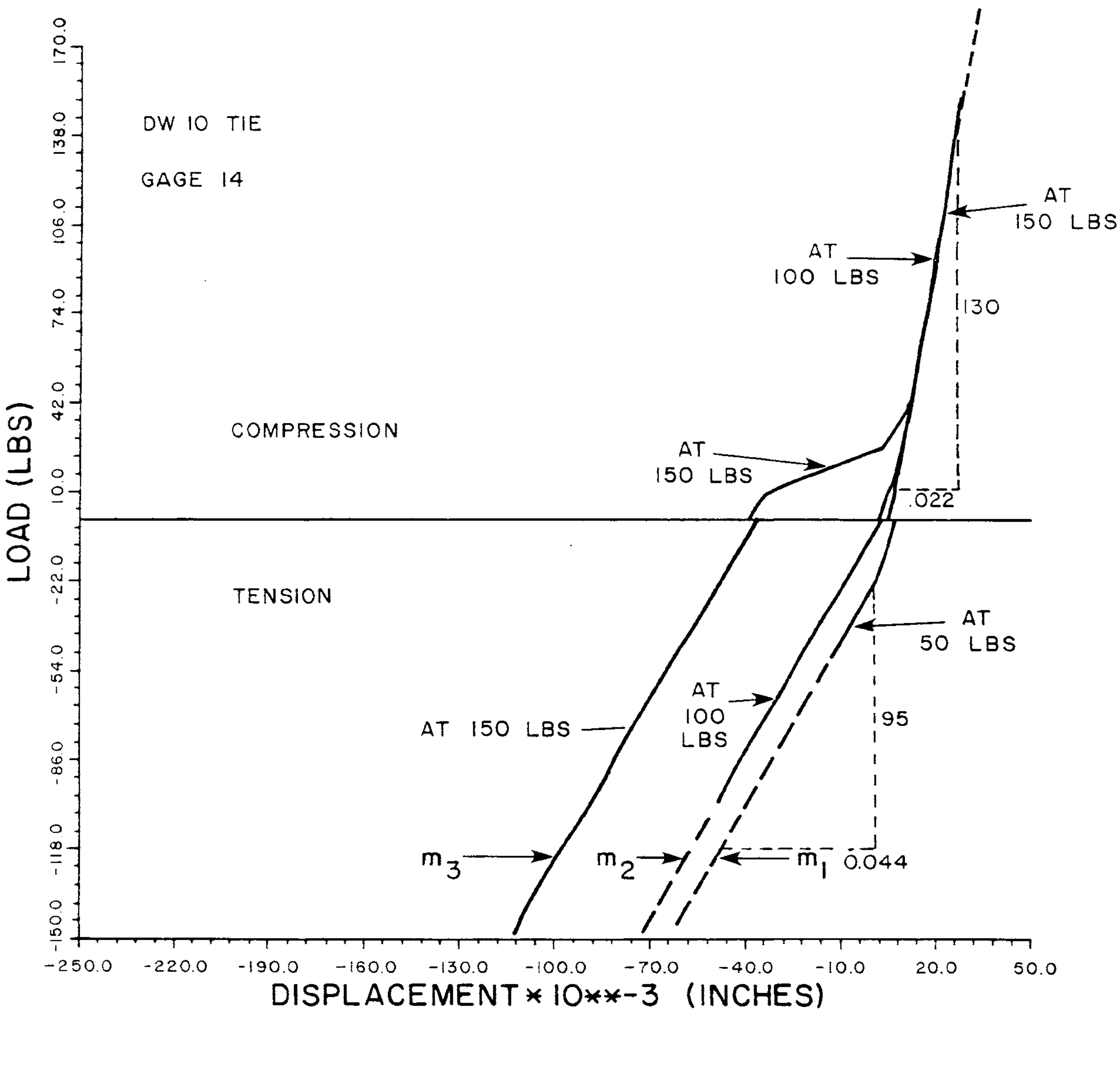

Figure 19. Load Versus Displacement Plot for DW 10 Gage 14 Tie with Wire Diameter = 0.188 in.

From these plots, the behavior of the tie is seen to be different in tension and compression. In compression, the tie's behavior remains relatively the same from about 30 lbs. upwards (Fig. 19), for all three levels of loading. Between 0 and 30 lbs., the plots for the 50 lbs. and 100 lbs. load levels are close. But between 100 lbs. and 150 lbs. load levels, the difference is very large. Between 50 lbs and 100 lbs., the tie seems to behave linearly. However, between 100 lbs. and 150 lbs., the tie backing is permanently deformed in tension so that in subsequent cycles, the tie wire (link) goes through free displacement. The free displacement is responsible for the shape of the plot at 150 lbs. This shape will alter considerably until the tie fails.

In developing a mathematical model for the DW 10 gage 14 tie, it is assumed that the tie behaves linearly. In compression, a line (dotted) as shown in Fig. 19, is used to model the load versus displacement plot. The slope of the dotted line which is the tie stiffness is therefore equal to:

$$m = 130/.022 = 5900 \text{ lb./in.}$$

From Fig. 19, it is seen that the tie load versus displacement plots for the 50 lbs., 100 lbs., and 150 lbs., load levels are approximately parallel, when acting in tension. Assuming that the tie behaves linearly between 0 and 100 lbs., the tie stiffness in tension which is the slope of the dotted line, is equal to:

$$m = 95/.044 = 2160 \text{ lb./in.}$$

This is then the stiffness of the tie in tension.

Tie Stiffness Mathematical Model for DW 10 Gage 14 Tie, with Wire Diameter = 0.172 in.

To determine the tie stiffness for this tie, the loading portions of the hysteresis loops as shown in Fig. 20 were used.

The stiffness of the tie was determined in compression and tension. In compression, the stiffness was computed for zero to 12.0 lbs and for 12.0 lbs. upwards. In tension, the average of the stiffnesses for the three levels of loading was taken as the stiffness of the tie in tension.

Compression

From 0 to 12 lbs, the tie stiffness was taken as the slope of the dotted line in this range as shown in Fig. 20,

$$m = 400 \text{ lbs/in..}$$

From 12 lbs. up, the tie stiffness was taken as the slope of the dotted line in this range. And

$$m = 142/.019 = 7440 \text{ lb/in..}$$

Tension

The slopes of the tension portion of Fig. 20 for the three levels of loading, m_1, m_2 and m_3, were as follows.

$$m_1 = 85/.07 = 1200 \text{ lb/in.} \quad \text{at } 50 \text{ lb,}$$

$$m_2 = 66/.047 = 1400 \text{ lb/in.} \quad \text{at } 100 \text{ lb,}$$

$$m_3 = 51/.026 = 2000 \text{ lb/in.} \quad \text{at } 150 \text{ lb.}$$

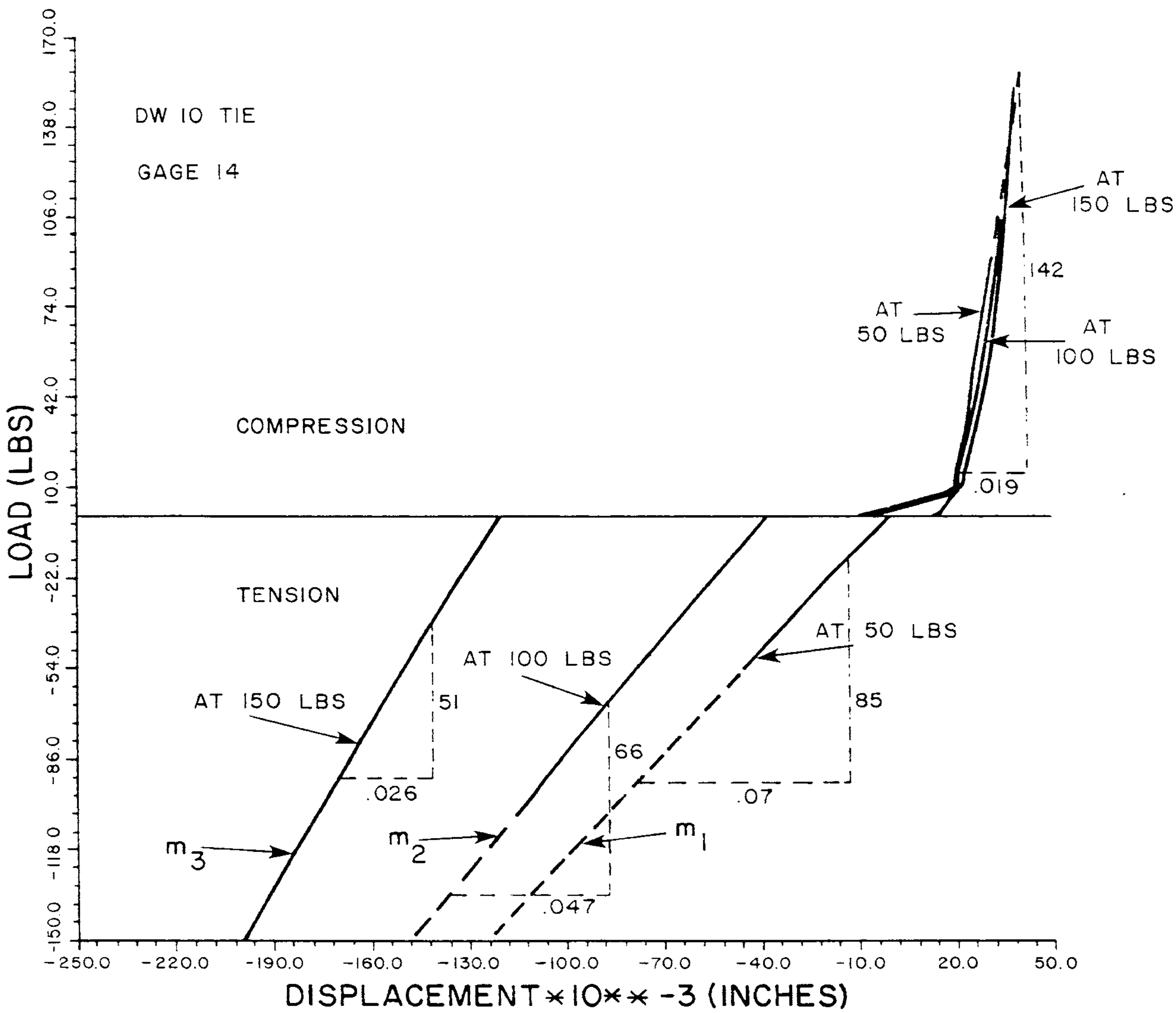

Figure 20. Load Versus Displacement Plot for DW 10 Gage 14 Tie with Wire Diameter = 0.172 in.

The mean value was

$$m = 1500 \text{ lb/in.}$$

This mean value of "m" was taken as the stiffness for this tie in tension.

Note that in tension, the tie stiffness increased as the load increased. This was probably due to the fact that as the load increased, the tie backing was pulled up along with the tie wire which produced membrane forces in the tie backing.

Mathematical Model for Wall System

A mathematical model was developed to determine the interaction of the brick veneer wall and the metal stud backup, interconnected by metal ties. The metal ties were represented by linear springs in the model. The model used in the analysis is shown in Fig. 21. The first tie was attached to the bottom concrete spandrel beam. I_1, the moment of inertia of the brick wall, was based on a 24 in width and 3.5 in. thickness. I_2, the strong axis moment of inertia of the stud, was taken from the tables (12) for a 3 5/8 in. wide, 20 ga thick, channel stud.

The analysis of the wall system interconnected by discrete springs was done using the displacement method. Variables considered were the stiffness of interior springs (K), relative stiffness of the brick veneer wall to that of the metal stud backup, $(EI)_1/(EI)_2$, and the relative stiffness of interior springs to end springs (K/K_e). The veneer brick wall was taken as pinned at the bottom. There was a compressible filler between the bottom of the top shelf angle and the top of the brick wall (Fig. 8, Detail A). In order to model the effect of this filler on the movement of the top of the wall, a linear spring that can

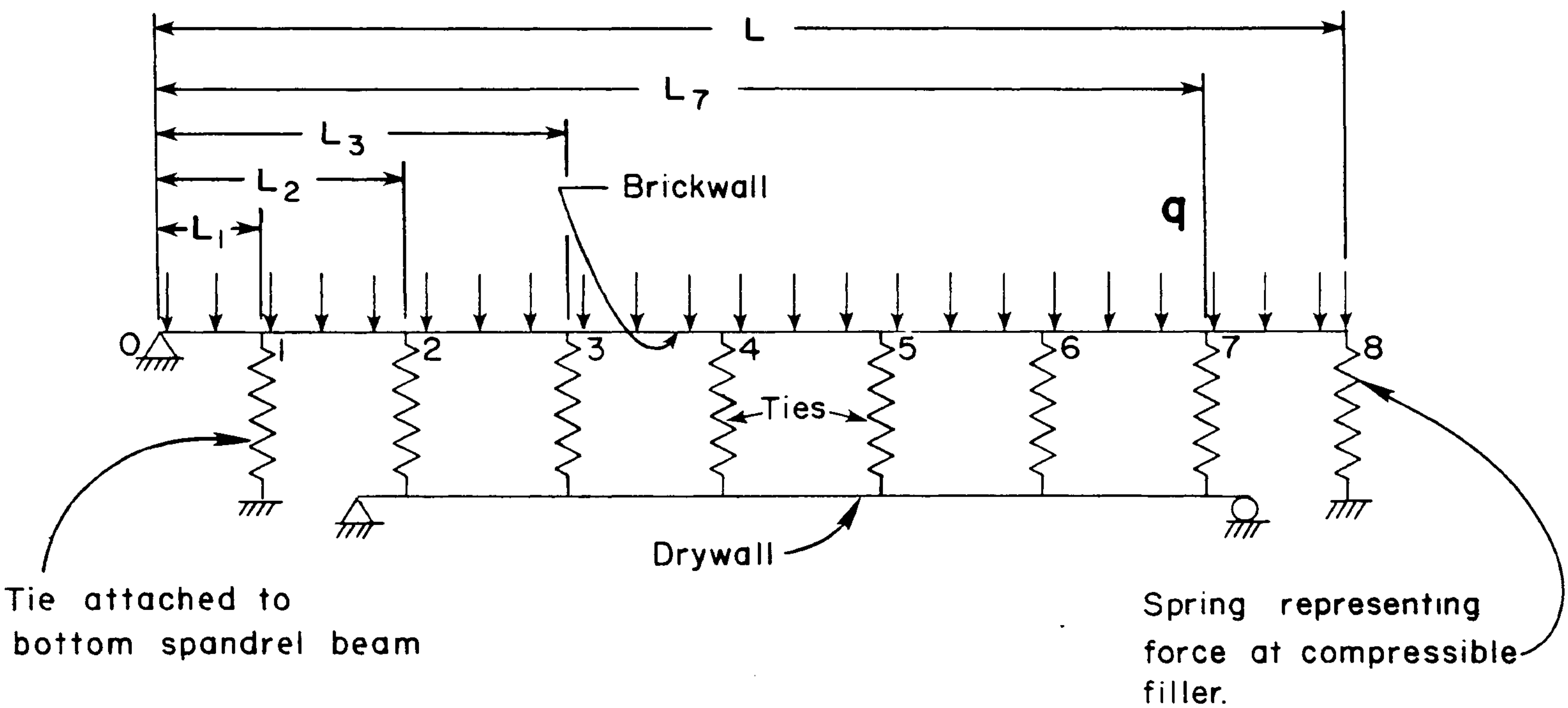

Figure 21. Mathematical Model for Wall System

be given different stiffnesses was located at the top of the wall, (Fig. 21). The metal stud backup was represented as pinned at top and bottom. Displacement at the upper end of the brick wall was permitted with non-zero values of K/K_e.

The formulation of the problem involved writing the deflection equations for the brick veneer wall at interior spring location, i, due to spring forces i,j,k,.....n, to the uniformly distributed lateral load and to end support settlement. The same was done for location, i, in the metal stud backup. The difference in the deflection between the brick veneer wall and the inner metal stud backup at location i, was related to the spring force P_i by the spring stiffness constant, K. Such equations were written for each interior spring. When i = 1, $\Delta_a = 0.0$, since this tie is attached to the bottom spandrel beam and not to the stud. These equations were then solved for the spring forces. For this case, there is produced a set of seven equations.

The formulation of the equations with seven interior springs was as follows:

$$\Delta_1 = \Delta'_1 + \Delta_e(L_1/L) + \delta_{11}P_1 + \delta_{12}P_2 + \delta_{13}P_3 + \delta_{14}P_4 + \delta_{15}P_5 + \delta_{16}P_6 + \delta_{17}P_7. \qquad (1)$$

$$\Delta_a = \Delta'_a + \delta_{ab}P_2 + \delta_{ac}P_3 + \delta_{ad}P_4 + \delta_{ae}P_5 + \delta_{af}P_6 + \delta_{ag}P_7.$$

$(\Delta_1 - \Delta_a)K = -P_1$, where

Δ_i = lateral deflection of either the veneer brick wall or the metal stud backup at location of interior spring i.

Numbered subscripts are for the brick veneer wall, and lettered notation for the metal stud backup.

Δ'_i = deflection of brick veneer due to the lateral load without interior springs or end settlement.

δ_{ij} = deflection of beam at i due to a unit load applied to the same beam at j.

P_i = interior spring force (compression positive)

P_e = exterior spring force

The deflection of the exterior spring is related to P_e by the end spring stiffness constant K_e. The force P_e in the end spring is related to the interior spring forces by equilibrium resulting in the equation:

$$\Delta_e = (qL - P_0 - P_1 - P_2 - P_3 - P_4 - P_5 - P_6 - P_7)/K_e, \qquad (2)$$

where q is the uniform wind load on the veneer brick wall and

P_0 = reaction at the base of the brick wall,

L = height of wall.

Deflection equations similar to Eq. 1 and Eq. 2 were written for the seven interior springs resulting in the following matrix:

$$\Delta'_1 - \Delta'_a + qL/K_e = (\delta_{11} \ +(1/K_e)(L_1/L) + 1/K)P_1 +$$

$$(\delta_{12} + 1/K_e(L_2/L))P_2 + (\delta_{13} + (1/K_e)(L_3/L))P_3 +$$

$(\delta_{14} + 1/K_e(L_4/L))P_4 + (\delta_{15} + (1/K_e)(L_5/L))P_5 +$

$(\delta_{16} + 1/K_e(L_6/L))P_6 + (\delta_{17} + (1/K_e)(L_7/L))P_7.$

$\Delta'_2 - \Delta'_b + qL/K_e = (\delta_{21} + (1/K_e)(L_1/L))P_1 +$

$(\delta_{22} - \delta_{bb} + (1/K_e)(L_2/L) + 1/K)\ (\delta_{23} - \delta_{bc} + (1/K_e)(L_3/L))P_3 +$

$(\delta_{24} - \delta_{bd} + (1/K_e)(L_4/L))P_4 + (\delta_{25} - \delta_{be} + (1/K_e)(L_5/L))P_5 +$

$(\delta_{26} - \delta_{bf} + (1/K_e)(L_6/L))P_6 + (\delta_{27} - \delta_{bg} + (1/K_e)(L_7/L))P_7.$

$\Delta'_3 - \Delta'_c + qL/K_e = (\delta_{31} + (1/K_e)(L_1/L))P_1 +$

$(\delta_{32} - \delta_{cb} + (1/K_e)(L_2/L))P_2 + (\delta_{33} - \delta_{cc} + (1/K_e)(L_3/L) + 1/K)P_3 +$

$(\delta_{34} - \delta_{cd} + (1/K_e)(L_4/L))P_4 + (\delta_{35} - \delta_{ce} + (1/K_e)(L_5/L))P_5 +$

$(\delta_{36} - \delta_{cf} + (1/K_e)(L_6/L))P_6 + (\delta_{37} - \delta_{cg} + (1/K_e)(L_7/L))P_7.$

$\Delta'_4 - \Delta'_d + qL/K_e = (\delta_{41} + (1/K_e)(L_1/L))P_1 +$

$(\delta_{42} - \delta_{db} + (1/K_e)(L_2/L))P_2 + (\delta_{43} - \delta_{dc} + (1/K_e)(L_3/L))P_3 +$

$(\delta_{44} - \delta_{dd} + (1/K_e)(L_4/L) + 1/K)P_4 + (\delta_{45} - \delta_{de} + (1/K_e)(L_5/L))P_5 +$

$(\delta_{46} - \delta_{df} + (1/K_e)(L_6/L))P_6 + (\delta_{47} - \delta_{dg} + (1/K_e)(L_7/L))P_7.$

$\Delta'_5 - \Delta'_e + qL/K_e = (\delta_{51} + (1/K_e)(L_1/L))P_1 +$

$(\delta_{52} - \delta_{eb} + (1/K_e)(L_2/L))P_2 + (\delta_{53} - \delta_{ec} + (1/K_e)(L_3/L))P_3 +$

$(\delta_{54} - \delta_{ed} + (1/K_e)(L_4/L))P_4 + (\delta_{55} - \delta_{ee} + (1/K_e)(L_5/L) + 1/K)P_5 +$

$$(\delta_{56} - \delta_{ef} + (1/K_e)(L_6/L))P_6 + (\delta_{57} - \delta_{eg} + (1/K_e)(L_7/L))P_7.$$

$$\Delta'_6 - \Delta'_f + qL/K_e = (\delta_{61} + (1/K_e)(L_1/L))P_1 +$$

$$(\delta_{62} - \delta_{fb} + (1/K_e)(L_2/L))P_2 + (\delta_{63} - \delta_{fc} + (1/K_e)(L_3/L))P_3 +$$

$$(\delta_{64} - \delta_{fd} + (1/K_e)(L_4/L))P_4 + (\delta_{65} - \delta_{fe} + (1/K_e)(L_5/L))P_5 +$$

$$(\delta_{66} - \delta_{ff} + (1/K_e)(L_6/L) + 1/K)P_6 + (\delta_{67} - \delta_{fg} + (1/K_e)(L_7/L))P_7.$$

$$\Delta'_7 - \Delta'_g + qL/K_e = (\delta_{71} + (1/K_e)(L_1/L))P_1 +$$

$$(\delta_{72} - \delta_{gb} + (1/K_e)(L_2/L))P_2 + (\delta_{73} - \delta_{gc} + (1/K_e)(L_3/L))P_3 +$$

$$(\delta_{74} - \delta_{gd} + (1/K_e)(L_4/L))P_4 + (\delta_{75} - \delta_{ge} + (1/K_e)(L_5/L))P_5 +$$

$$(\delta_{76} - \delta_{gf} + (1/K_e)(L_6/L))P_6 + (\delta_{77} - \delta_{gg} + (1/K_e)(L_7/L) + 1/K)P_7.$$

Values of Δ'_i were input and the matrix solved for P_i. The sum of the spring forces represent the load transferred to the backup wall. The results of the mathematical model are used for comparison to data and for predicting the effects of variation of other parameters in subsequent sections.

CHAPTER V

ANALYSIS OF TEST RESULTS

Tie Tests

The metal ties used in brick veneer with metal stud back up wall systems are designed to transmit load from the brick wall to the stud wall. The brick walls cannot carry high tensile stresses without developing cracks and the ties should be such that load can readily and adequately be transferred through them to the back up wall without excessive deflection of the brick wall. The tie therefore should be stiff; should be easily installed; should not be expensive; and should be non-corrosive. Ties generally can fail in the following ways: 1). the ties pulling out of the mortar, 2). the ties pulling out the screws and 3). the ties failing in tension, in compression or in bending.

Hysteresis

The term hysteresis is used to denote lost energy in a system. Applied to materials, it indicates the amount of strain energy per unit volume which is lost in a cycle of loading and unloading. The energy per unit volume may be determined from the stress-strain diagram as an area; the area between the loading and unloading stress-strain curves represents the hysteresis (13). The energy absorbed in a cycle of loading and unloading may be expended in many ways. It may be dissipated in the form of heat (excessive heating of the material may result in the deterioration of its mechanical properties), or may be utilized in producing permanent relative displacement of the particles of the materials, resulting in permanent set, or it may serve to alter the properties of the material.

Also the hysteresis may be used to determine the damping characteristics of materials. Damping in a vibrating system may be divided into external damping and internal damping (14). External damping is due to the loss of energy associated with the slippage of structural connections either between members or between the structure and the supports. Internal damping is associated with the response of the material itself to cyclic forces. The damping capacity of a material or internal damping may be defined as energy absorbed during a cycle of vibration. Therefore, it can be said that the damping capacities of the corrugated ties are more than those of the DW 10 ties.

Corrugated Ties

The loading and unloading portions of the hysteresis loops of the ties are far apart. This implies that the slopes of the hysteresis loops differ for loading and unloading portions, and therefore the ties behave inelastically. The stiffness of corrugated ties depends considerably on the distance from the point at which the screw is attached to the studs to the point at which the tie is bent up. The corrugated ties are 7/8 in. wide.

For the corrugated tie, gage 18, comparing the hysteresis loops for loads at which a = 2 in. and a = 5/8 in. (compare Figs. A-5, A-6 and A-7 and A-8, A-9 and A-10), it is seen that the tie is less stiff when the bent up portion is far away from the point at which the tie is screwed to the stud. For example, at the 50 lbs. load level, the average tie stiffness for the corrugated gage 18 tie is 5880 lbs./in. when a = 5/8 in. compared to the value 130 lbs./in when a = 2 in. Corrugated ties therefore, become less stiff as "a" gets large.

The corrugated ties vary in their characteristics depending on the gage of the steel used in making the tie. The lighter gage ties are so flexible that they bend and stretch excessively even at low load levels. In compression, these ties transfer load by bearing on the stud wall at the bend. The lighter gage ties, because they cannot withstand even small loads, tend to flatten out and the brick wall virtually moves in without restraint. In tension, the ties completely stretch out and the load is applied to the studs at the point at which the tie is screwed to the studs. Excessive stresses in the tie and the screw may build up at this point and the strength of the tie system may depend on the pull out strength of the screws. For light ties, there is the possibility of the ties being torn off at this point.

DW 10 Ties

The hysteresis loops for the DW 10 ties tested are narrow. This means that the loading and unloading portions are close and can be approximated by an average curve for mathematical models. That is, the same stiffness can be used for loading and unloading. The ties are elastic as they tend to return to their original shape after load has been removed.

One characteristic observed in the behavior of the DW 10 gage 14 tie is that at high loads (100 lbs. and above) in tension, the backing of the tie is pulled up and is permanently deformed. In subsequent cycles during the loading and unloading, the wire portion of the tie goes through some distance without contacting the tie backup. This behavior occurs at the zero load point as shown in Figs. A-18 and A-19. Fig. 22 shows the wire in the gap. This phenomenon has the effect of reducing the stiffness of the tie resulting in a reduced load transfer to the backup stud wall. This means that this phenomenon makes the metal stud backup system less effective.

Comparison of Tie Stiffnesses

The following notations are used in this section. The average stiffness values given here are over the tension and compression zones. That is, these stiffness values are based on the slopes of the lines connecting the highest and lowest points on the hysteresis loops.

K_1 = Average tie stiffness at 50 lbs. load level,

K_2 = Average tie stiffness at 100 lbs. load level,

K_3 = Average tie stiffness at 150 lbs. load level,

$K = (K_1 + K_2 + K_3)/3$.

See Table VI for stiffnesses of the ties calculated as indicated above. It should be noted that for all the ties tested, except for the 18 ga corrugated tie with a = 2 in., $K_1 > K_2 > K_3$. For the 18 ga corrugated tie with a = 2 in., the reverse is the case. That is $K_1 < K_2 < K_3$. This is so because the tie actually carries the applied load, after the slack caused by the large value of "a" has been removed by the application of large loads.

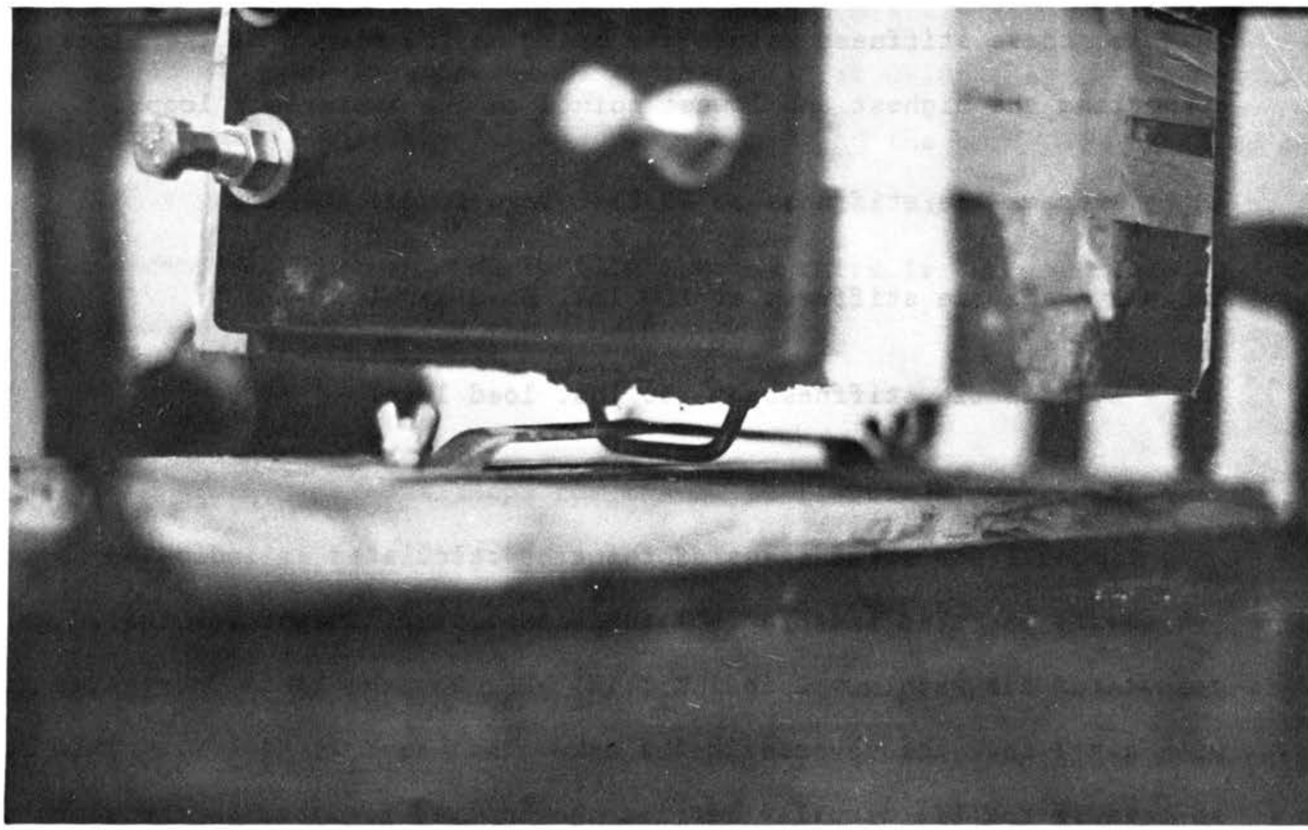

Figure 22. A DW 10 Gage 14 Tie Going Through the Gap

Table VI. Average Tie Stiffnesses (lb/in.)

Tie Type	ga	a	K_1	K_2	K_3	K
Corrugated	22	1.75	400	-	-	400
Corrugated	20	5/8	1390	740	570	900
Corrugated	18	5/8	5880	3330	1200	3470
Corrugated	18	2.0	130	170	220	170
Corrugated	16	5/8	16670	14290	11540	14160
DW 10 TP1	14		3850	2900	2130	2960
DW 10 TP2	14		1490	1380	1260	1380
DW 10 TP1	12		7143	6061	4615	5940

------- TP1 Wire diameter = 0.188 in.

-------- TP2 Wire Diameter = 0.172 in.

The stiffest tie tested was the 16 ga corrugated tie, with K = 14,160 lb/in. The 12 ga DW 10 tie with K = 5940 lb/in. was the tie with the second largest average stiffness. The 14 ga DW 10 tie had K = 2960 lb/in. with wire diameter equal to 0.188 in. and K = 1380 lb/in with wire diameter equal to 0.172 in. The 18 ga corrugated tie had K = 3470 lb/in with a = 5/8 in. and K = 170 lb/in with a = 2 in. The 20 ga corrugated tie had K = 900 lb/in. with a = 5/8 in. and the 22 ga corrugated tie had K_1 = 400 lb/in. with a = 1.75 in.

Water Permeance Tests

The water permeance tests revealed some very interesting trends. Wall No. 2 and Wall No. 5, absorbed higher percentages of water during the tests than the other walls. The brick veneer in these walls cracked at loads that did not crack the veneer in the other walls. During the positive pressure test, Wall No. 2, cracked at between 5 and 6 ins. of water while Walls Nos. 1 and 3 cracked at between 10 and 11 ins. of water. In the negative pressure test, Wall No. 5, cracked at between 11 and 12 ins of water while Wall Nos. 4 and 6, did not experience any crack. The water permeance tests therefore may somehow be related to which walls will develop early cracks.

Mortar droppings invariably accumulated in the air-space between the brick veneer and the drywall, usually around the ties. During the water permeance test, water seeped through the brick veneer and along the mortar droppings. In some cases, droplets of water were observed on the surface of the gypsum sheathing. The ties and screws became wet in some cases.

In Wall Nos. 2 and 5, water was collected at the flashing. Most of the mortar droppings accumulated at the base of the wall where the weep holes were located. Mortar droppings that fill the weep holes during construction need to be thoroughly cleaned out to make them useful.

Only Wall No. 2, was subjected to water permeance tests after a crack developed in the brick veneer. It cracked at about mid-height at between 5 and 6 ins. of water on the fourth day of test, and was subjected to the water permeance test on the fifth day of test. It was anticipated that after the crack, much water would be collected at the flashing. But this was not the case (see Table II). The crack tended to close up after unloading, because of the weight of masonry above the crack. However, in actual wall construction the cracks in the brick wall generally may not close.

Some practical problems were encountered while conducting the water permeance tests. The tooled joints made it difficult to obtain a water tight joint around the periphery of the water permeance chamber. Once a leak started, it was difficult to stop because the silicone caulking will not adhere to wet surfaces. It was also difficult to quantify the amount of water lost from the leaks, since a portion of it spilled on the ground and was lost and the rest collected at the flashing. This meant that water collected at the flashing was more than the amount of water that flowed through the wall in some cases. For example on Wall No. 2, the amount of water collected at the flashing on the second day of water permeance testing, was much higher than the other two days of tests, because there were leaks that were difficult to stop (see Table II). In view of these difficulties, the water permeance test results for those specimens in which leaks in the seals were observed are to be regarded with caution.

The results of the water permeance tests shown in Table II do not show any direct correlation between the amount of water passing through the brick wall and the magnitude of applied load.

Lateral Load Tests

Wall Nos. 1, 2 and 3, were subjected to positive pressure and Wall Nos. 4, 5 and 6, to negative pressure. In all three walls tested under positive pressure, the brick veneer cracked at about mid-height. Wall

Nos. 1 and 3, cracked at between 10 and 11 ins. of water (52-57 psf) on the fifth day of testing to three times design load. Wall No. 2, cracked at between 5 and 6 ins. of water (26-31 psf) on the fourth day of testing to two times design load. Only Wall No. 5 developed cracks in the brick veneer during the negative pressure test. It cracked at between 11 and 12 ins. of water (57-62 psf) on the fifth day of testing to three times design load. All six walls performed well at design load, none developing any cracks in the veneer at this load level. All six walls were tested to three times the design load. The deflections of the walls were proportional to the applied load until the brick veneer developed cracks.

There was substantial movement at the top of the brick veneer in all the walls, especially in the walls tested under negative pressure (e.g Fig. C-27). This movement decreased after the brick veneer cracked. After the wall cracked, the brick veneer rotated about the crack nearly as a rigid body. This is shown in the deflection plots Figs. C-3, C-11, C-19. Owing to the free movement at the top of the brick veneer, the deflection consisted of rotation about the base of the veneer and deflection due to bending. This was very prominent in the walls tested under negative pressure. In fact, Fig. C-43, shows that there was very little bending in the brick veneer. Almost all the deflection was due to the rigid body rotation of the veneer about the base of the wall.

The same drywalls (backup walls) were used throughout the test. That is, Wall Nos. 1 and 4, Wall Nos. 2 and 5, and Wall Nos. 3 and 6, had the same backup walls, respectively. The same tie backings were used; only the tie wires were changed. The drywall deflections were proportional to applied load; they became abruptly larger after the brick veneer cracked. The runner tracks at the top and bottom of the drywall appeared to be unaffected by the load testing. One screw that held the ties on Wall No. 2, was found loose at the end of the test under positive pressure. In the negative pressure tests, the tie backings were deformed especially the topmost ties in wall Nos. 4 and 6, in which there was considerable movement at the top of the brick veneer. None pulled out, however.

The residual deflections in the walls were large in some cases especially after the brick veneer cracked. Before the veneer walls cracked, the residual deflections were the rigid body movements of the walls (Figs. C-7, C-15 and C-23). However after the brick walls cracked, the residual deflections consisted of the rigid body movement and the rotation about the crack (Figs. C-3, C-11 and C-35).

As mentioned previously, the top of the brick veneer walls moved substantially under lateral load. This affected greatly the performance of the wall system. It is believed that if the top of the brick veneer is restrained from moving, the brick veneer will crack at much lower load levels. The top end boundary condition of the brick veneer is therefore a very important factor in the performance of this wall system.

CHAPTER VI

RESULTS OF ANALYTICAL STUDY

Parametric studies were done on the models described below for the walls tested, and for walls for one story and two story buildings with different boundary conditions. The results are shown below.

Notations

The following notations were used in this section and the plots.

$$B = (EI)_1/(EI)_2,$$

$$A = (EI)_1/KL^3,$$

$$K/K_e = \text{relative tie stiffness},$$

where

$(EI)_1$ = flexural rigidity of the brick wall, where E_1 ranges from 875 ksi to 3000 ksi and I_1 is the moment of inertia of a 24 in. wide by 3.5 in. thick brick prism, therefore I_1 = 85.75 in.^{4},

$(EI)_2$ = flexural rigidity of the drywall, where E_2 is 29500 ksi and I_2 is the moment of inertia of the metal stud wall including the contribution of the gypsum board in partial composite action,

K = axial stiffness of interior springs (Fig. 20) and

K_e = axial stiffness of exterior springs at supports.

Values of A and B shown on the figures represent a broad range of possible values. Typical values of A and B may be calculated as follows:

$$A = (EI)_1/KL^3 = (875)(85.75)/(7.440)(112)^3 = 0.0071, \text{ and}$$

$$B = (EI)_1/(EI)_2 = (875)(85.75)/(29500)(0.54) = 4.71.$$

Other assumptions regarding tie stiffness, masonry elastic modulus and composite action will produce a broad range of values for A and B.

Results of Mathematical Model

The effect of the boundary condition at the top of the brick wall and tie sizes on the performance of the wall system were evaluated in a parametric study. The values of A = 0.0246 and B = 16.15 were evaluated for the model when E_m was taken as 3000 ksi, according to the Brick Institute of America's recommendation. A = 0.0071 and B = 4.712 were obtained when E_m = 875 ksi as obtained from a prism flexure test was used. When full composite action between the studs and the gypsum boards was considered for E_m = 875 ksi, A = 0.0071 and B = 1.818 resulted. These values of A and B with different values of K_e were used in the parametric study. The results are shown in Figs. 23, 24 and 25.

Fig. 23 shows the effect of the movement at the top of the brick wall on the maximum moment in the brick wall. It should be observed that these movements reduced the maximum moments and therefore the brick wall will develop cracks at higher loads.

Fig. 24 shows the plot of the maximum moments in the brick wall versus the ratio of the tie stiffness to the end stiffness modeling the brick top end support condition. The maximum moments approached an asymptotic minimum value as the end stiffness approached zero. This shows that if the top of the wall were pinned, the peak moment in the

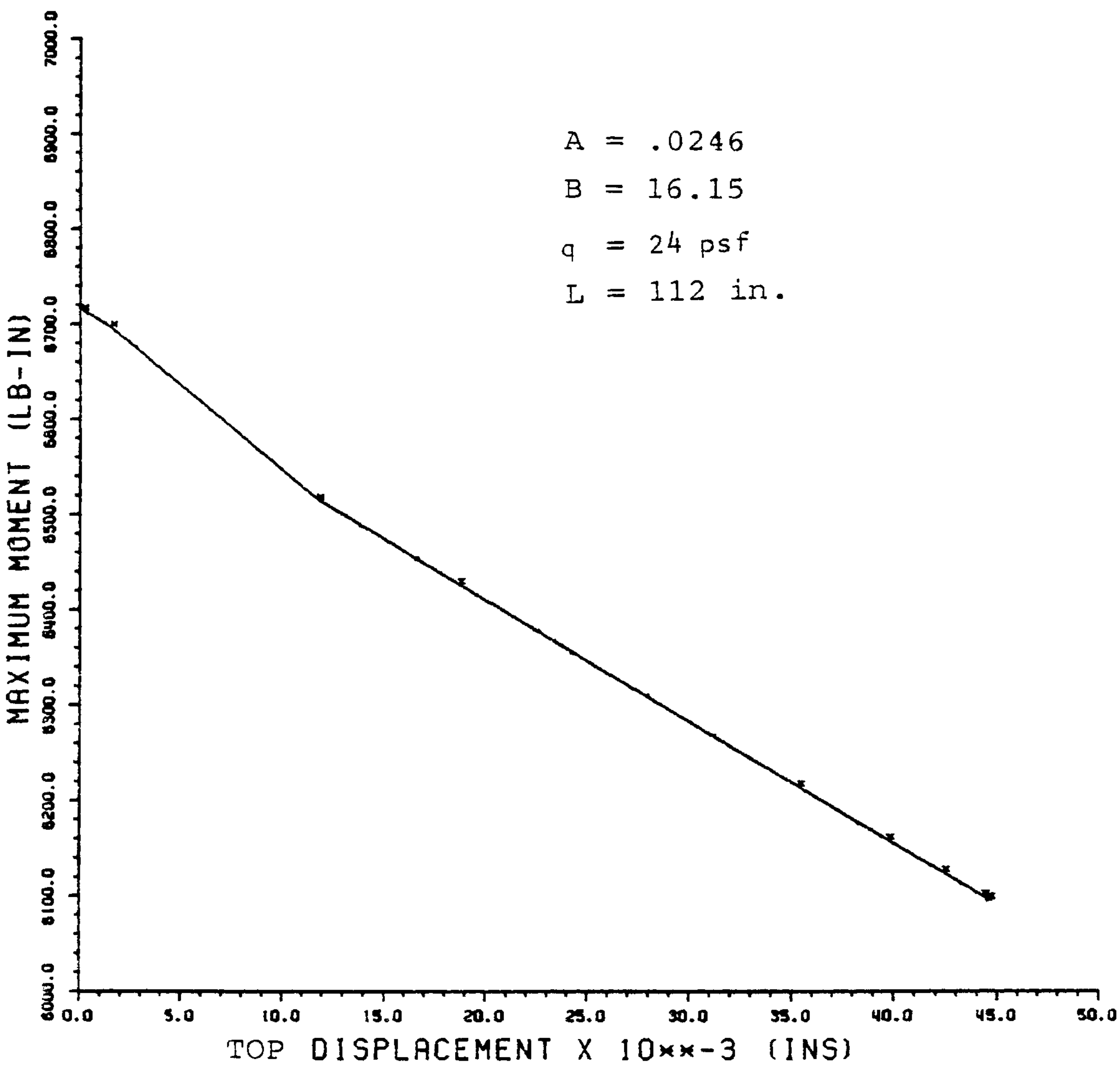

Figure 23. The Effect of Boundary Conditions on the Maximum Moments in the Brickwall

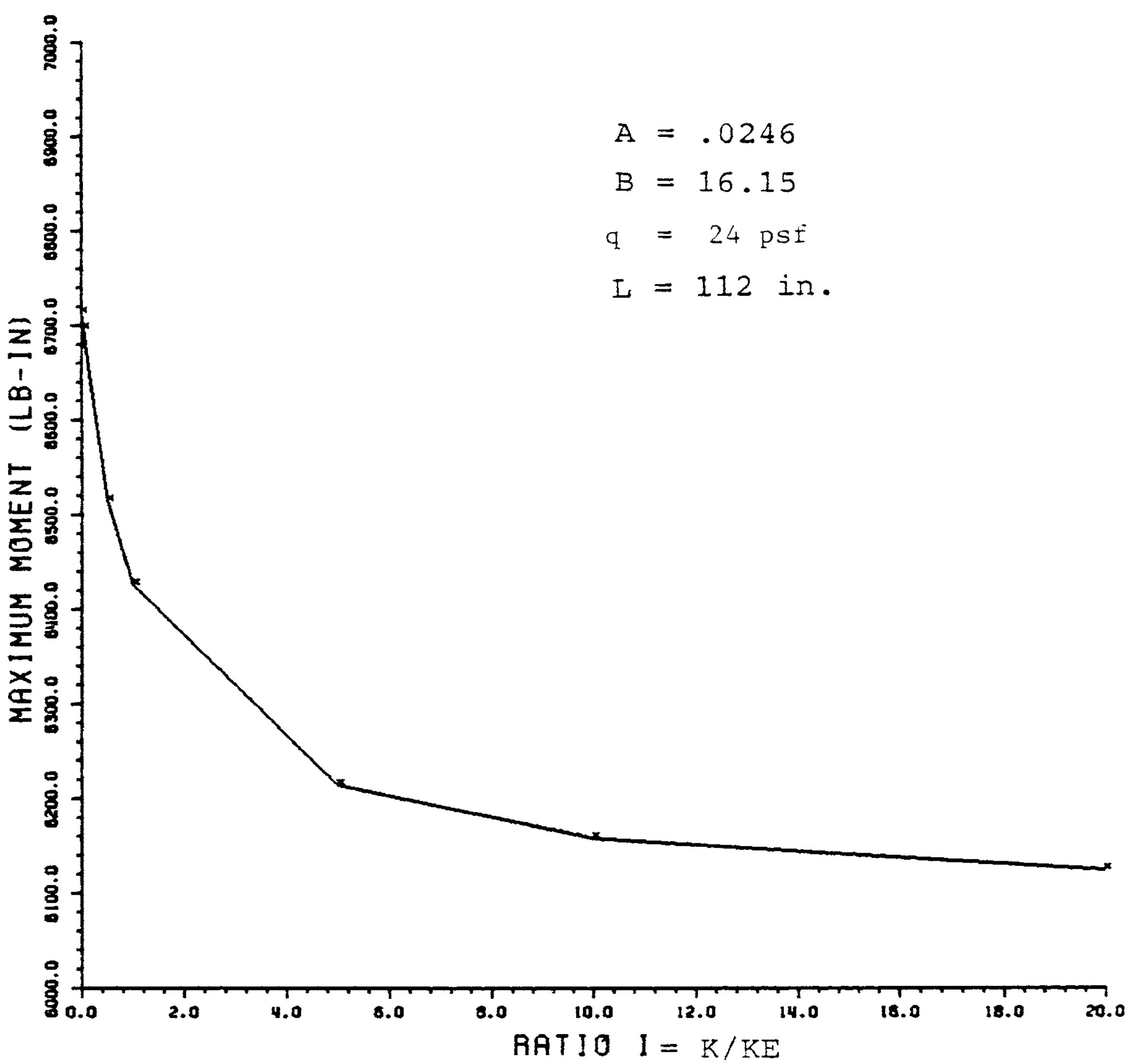

Figure 24. The Variation of Maximum Moments in the Brickwall with End Stiffness

brick wall will be larger than the peak moment if the top is free to move.

Fig. 25 shows the brick wall moment plots for two different tie stiffnesses. The stiffer ties restrain the movement of the wall and maximum moments are generated near the foot of the brick wall.

Figs. 26 and 27 show the moment variation in the brick wall with K/K_e at A = 0.005 and A = 0.20, respectively. As K/K_e increased (more flexible top support), the moments in the brick wall decreased especially in the upper half of the brick wall. This increase in the moment was more as A increased, Fig. 27.

Fig. 28 shows the moment in the brick wall with variation in B. The moment increased as B increased. Fig. 29 shows the moment in the brick wall with variation in A. As A increased the moment also increased.

Figs. 30 and 31 show the nondimensionalized forces in the ties in the wall model for A = 0.0246 and A = 0.20, respectively. The spring forces were nondimensionalized by dividing them by the applied load per unit length multiplied by the height of the wall. The forces in the ties are sometimes reversed. The large force in the tie that is attached to the bottom spandrel beam in Fig. 31 should be noted.

Discussion of Analytical Results for the Test Wall Model

The behavior of the wall system tested was complex and difficult to model. Probably the most meaningful way to evaluate the effectiveness of the wall system is to compare the bending moment in the brick veneer wall backed up by the metal stud system to that of the brick veneer wall

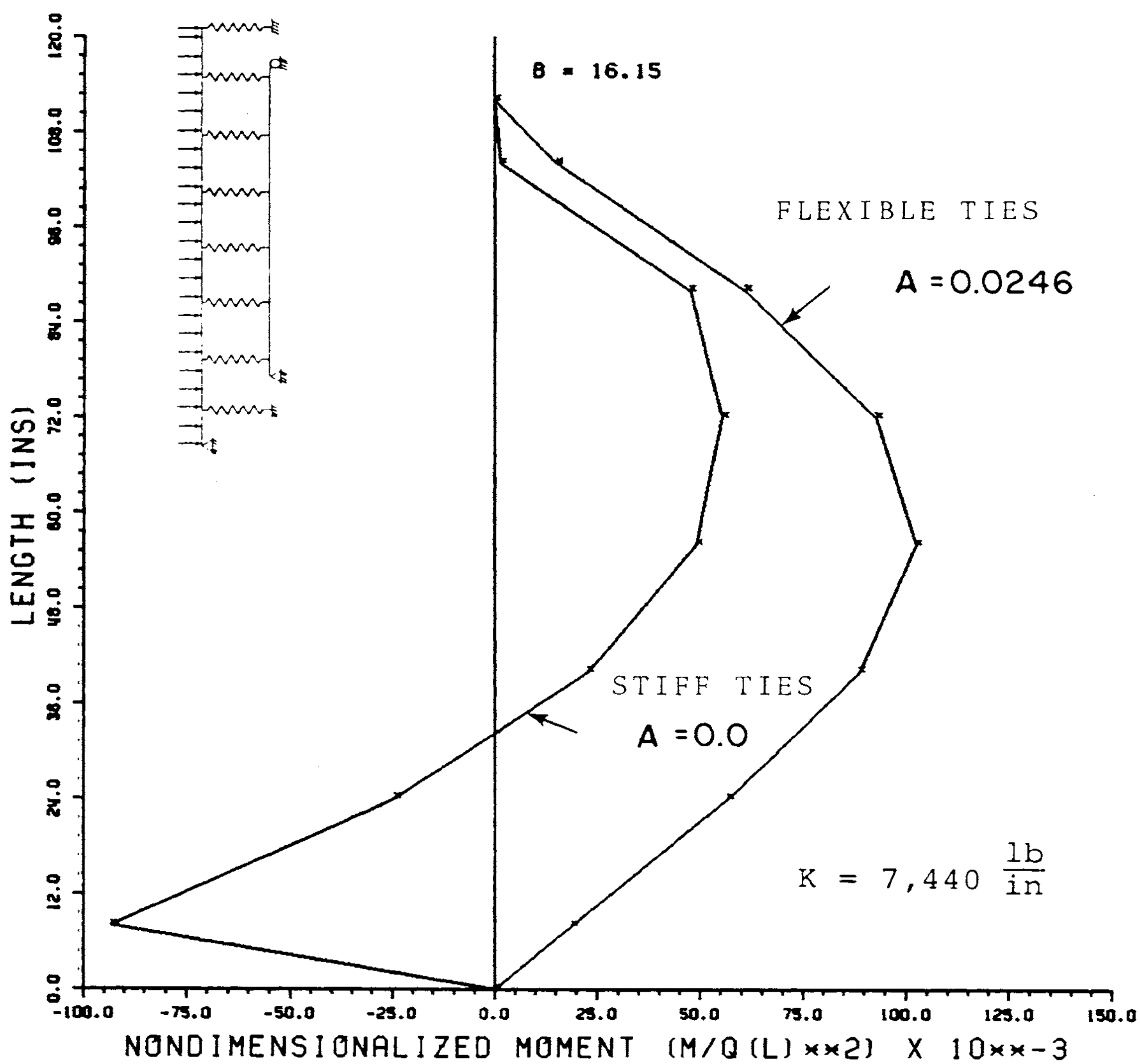

Figure 25. The Effect of Tie Stiffness on Maximum Moments in the Brick-wall

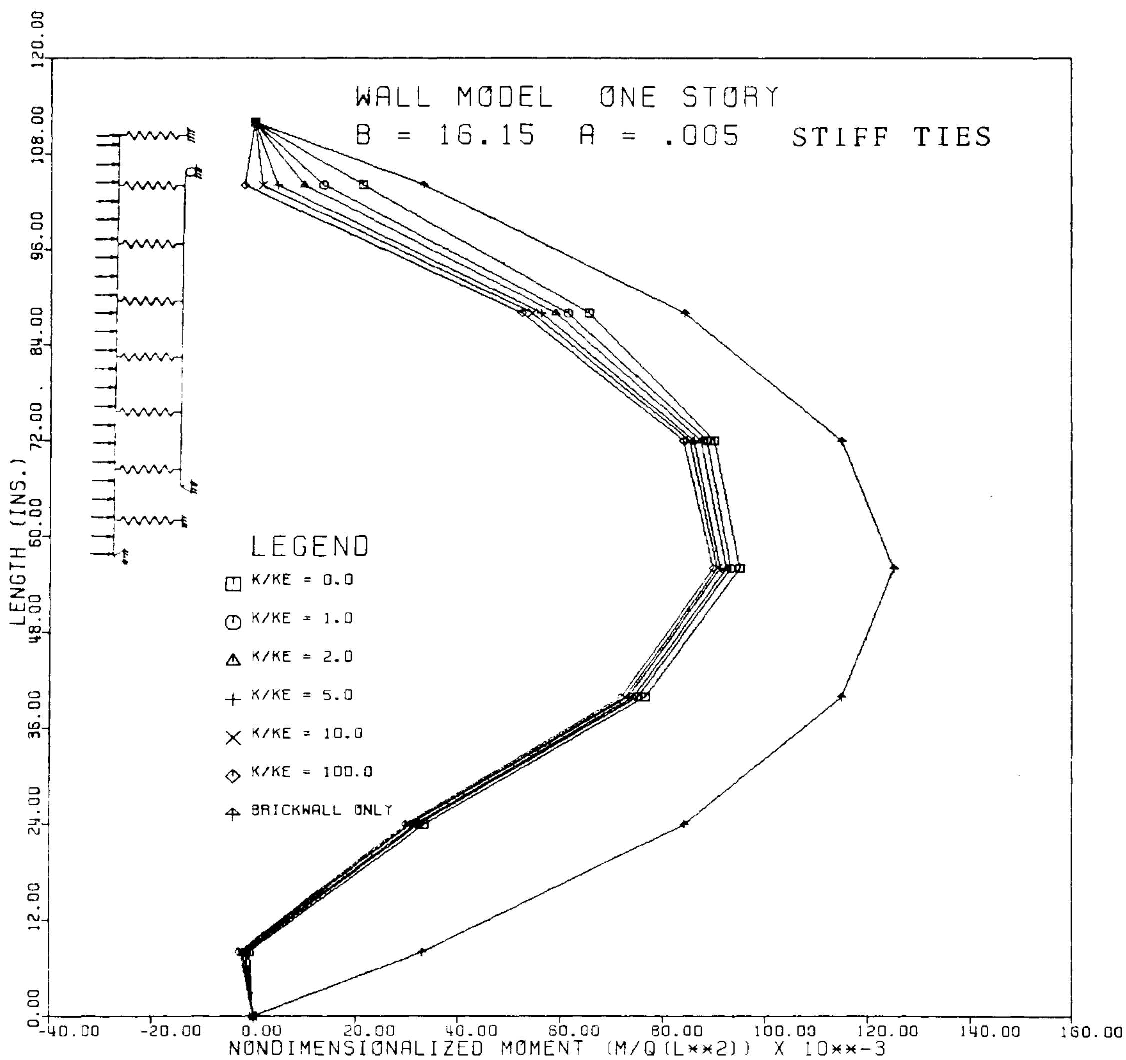

Figure 26. Moment Variation in the Brickwall with K/K_e for Wall Model at A = 0.005

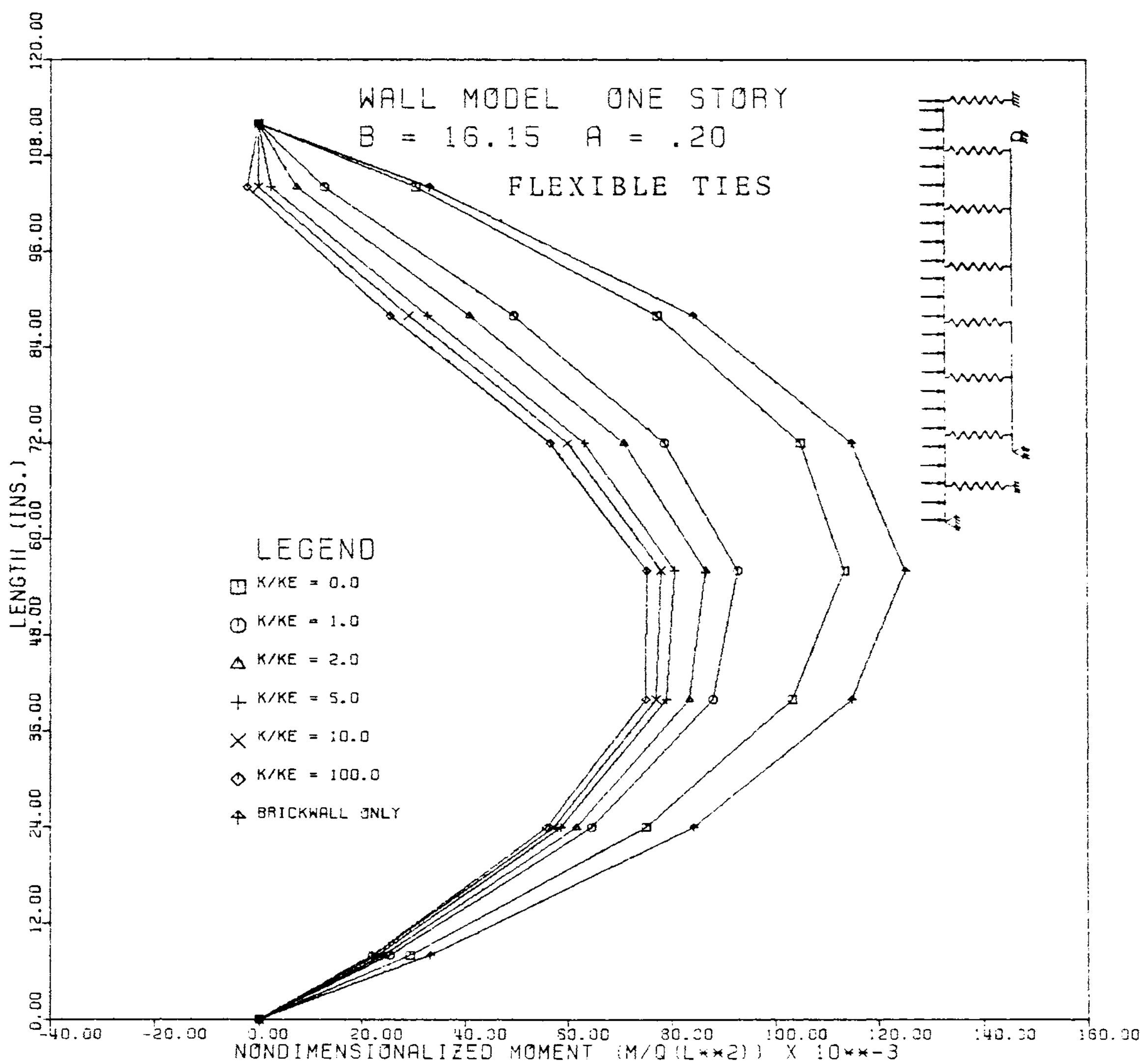

Figure 27. Moment Variation in the Brickwall with K/K_e for Wall Model at A = 0.20

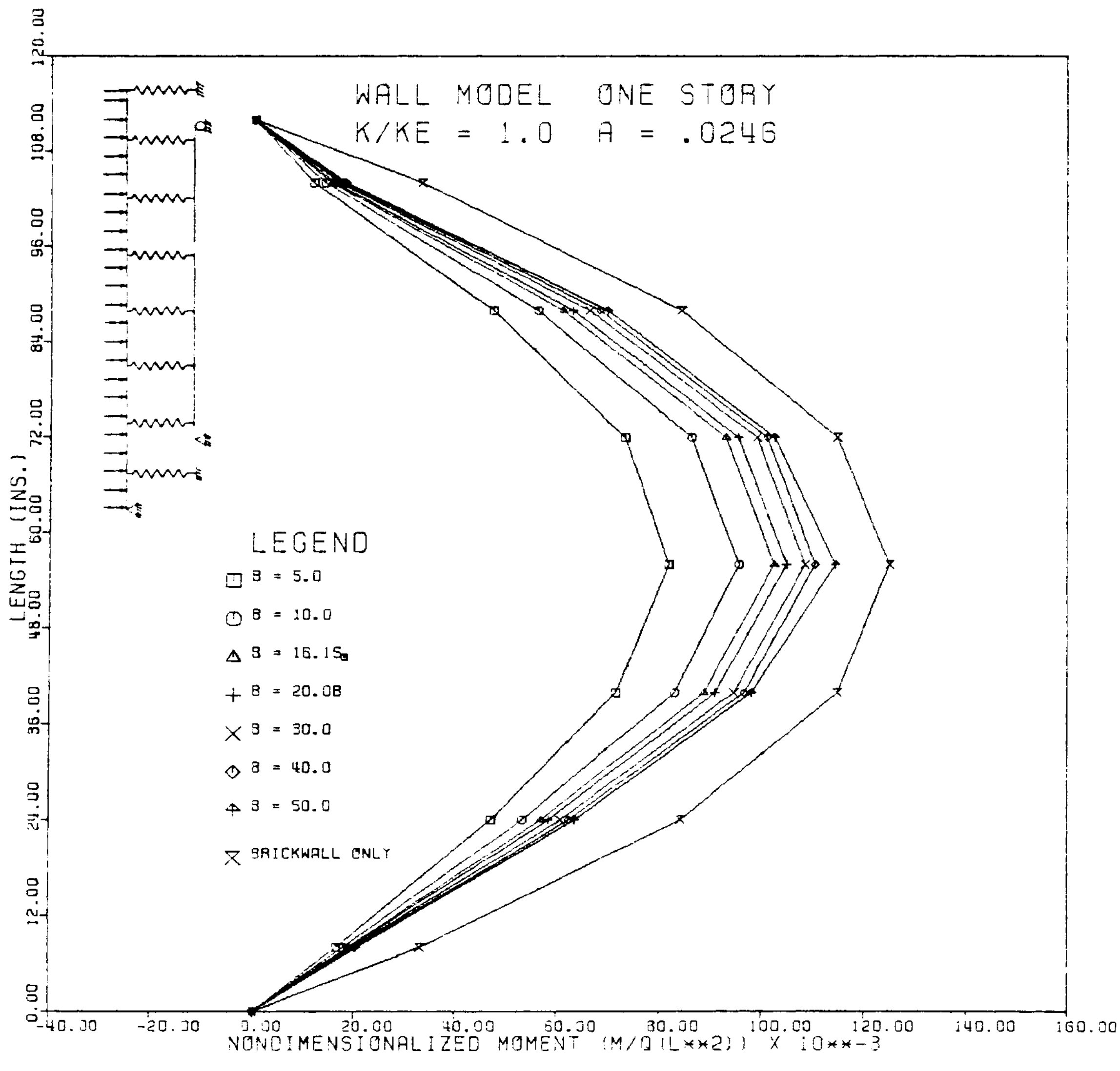

Figure 28. Moment Variation in the Brickwall with B for Wall Model

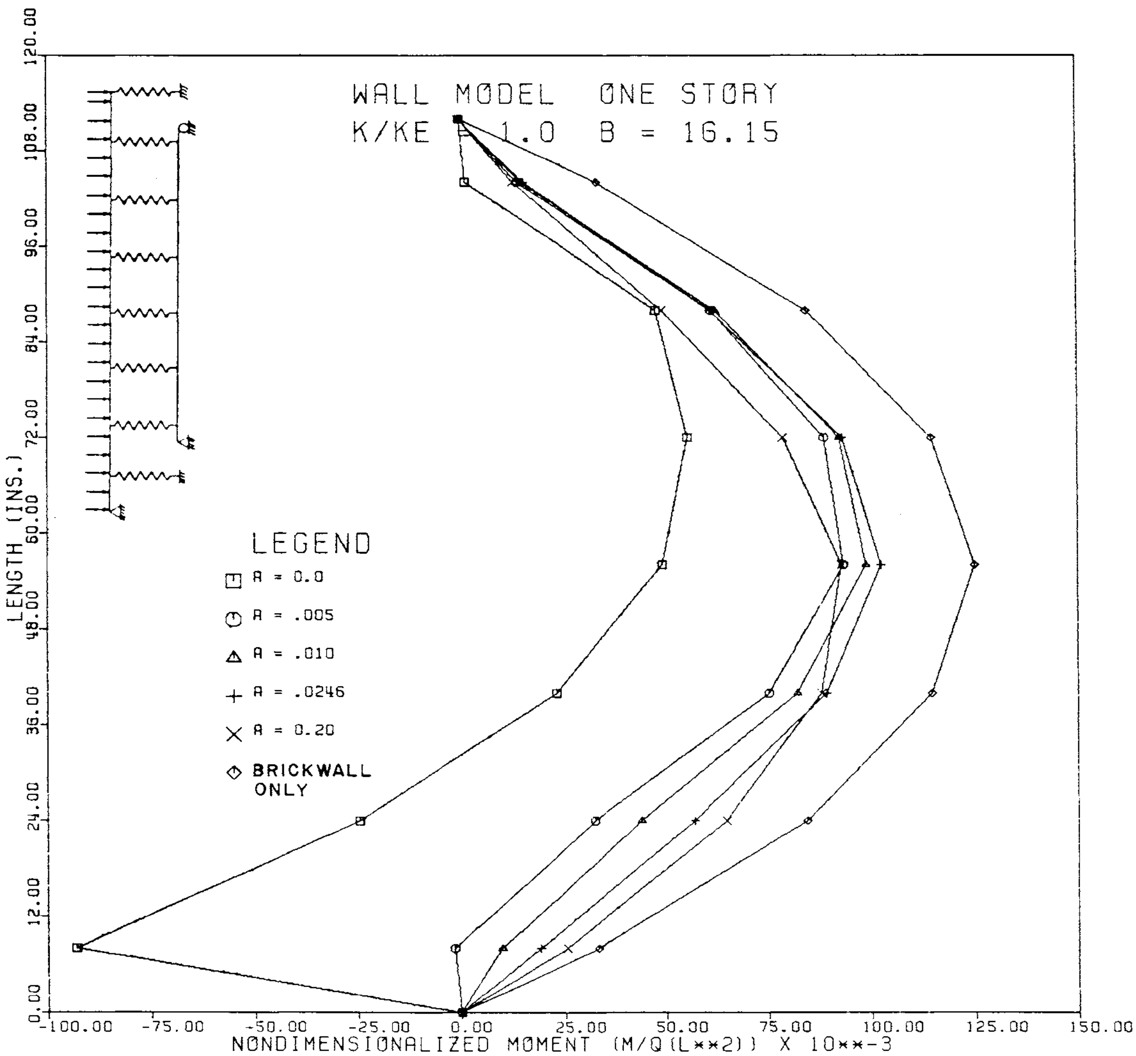

Figure 29. Moment Variation in the Brickwall with A for Wall Model

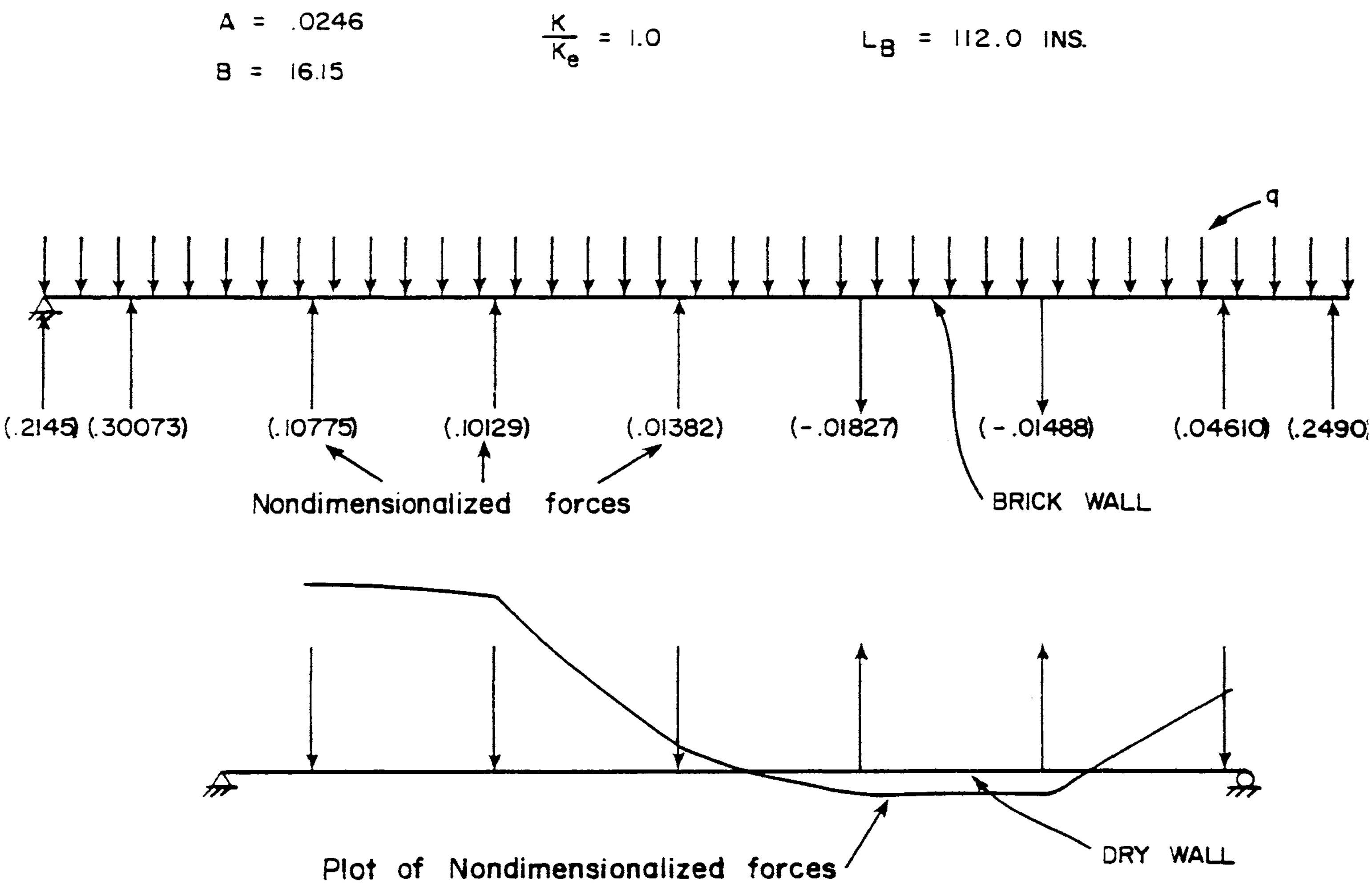

Figure 30. Nondimensionalized Forces in the Ties for Wall Model at A = 0.0246

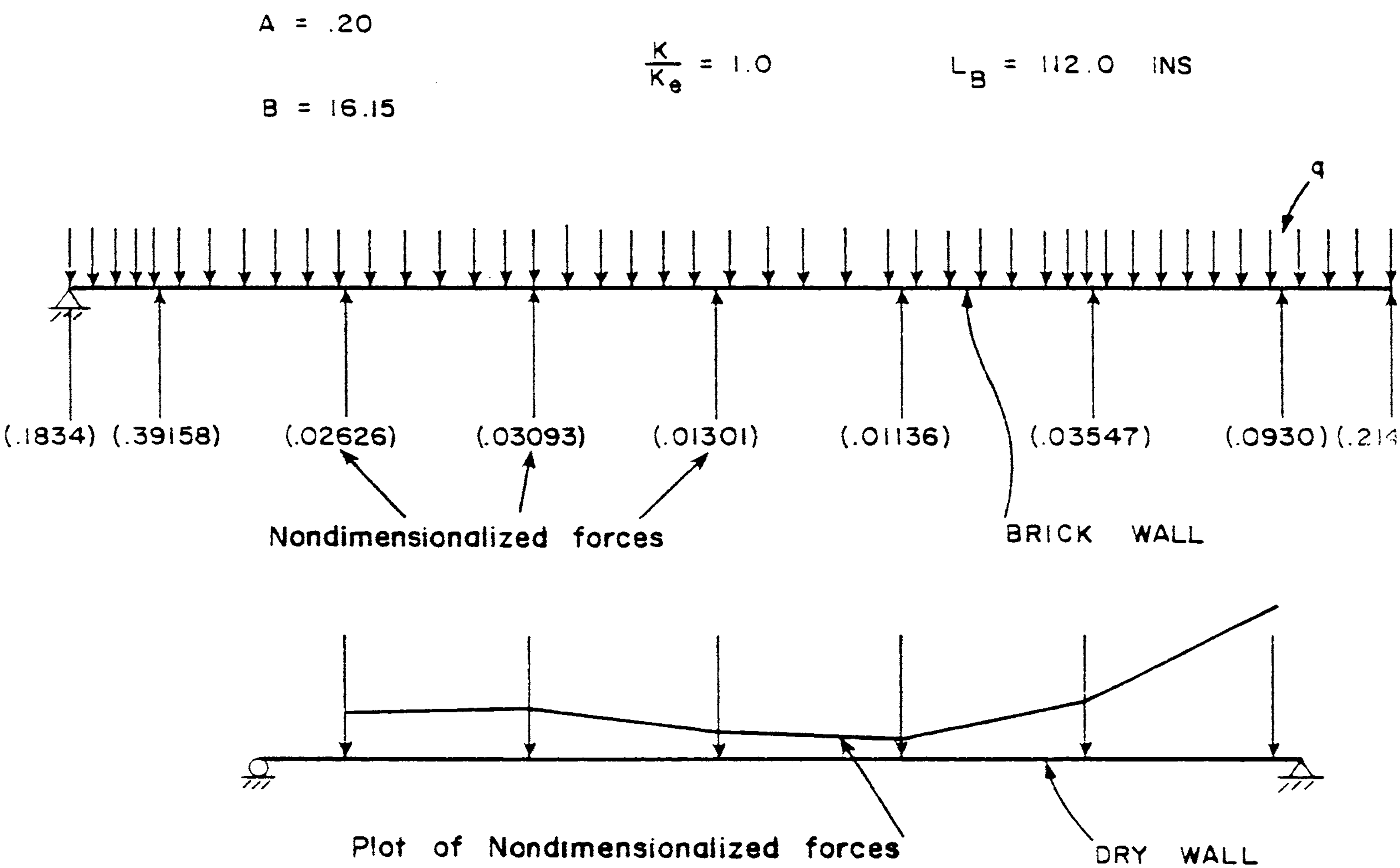

Figure 31. Nondimensionalized Forces in the Ties for Wall Model at A = 0.20

as if it resisted all lateral load alone. The difference in these bending moments represents the amount by which the backup system reduces the load carrying requirements of the brick veneer alone. Using the values of wall stiffness, end support stiffness, composite action of metal stud wall and boundary conditions, which best fit the mathematical model to the experimental data, the bending moments in the brick veneers were calculated (Figs. 32, 33, and 34). Lines which are identified "brick wall only" are plots of the moments in the brick wall without backup. An example of the usefulness of such a plot may be illustrated from Fig. 32. The maximum nondimensionalized moment, M/qL^2 for B = 4.712, A = 0.0071, K/KE = 0 is found from the graph to be 0.075. If the brick veneer resisted all of the load, the value would be 0.125. Therefore, according to the model, the bending stress of the "backed up" wall would be 60% of a wall which was not backed up.

The effect of the stiffness of the support at the top of the brick wall can be illustrated by Fig. 33. A wall having K/KE = 0, which corresponds to a rigid top spring, has nondimensionalized maximum moment of 0.103. The same wall having K/KE = 100, corresponding to an extremely flexible top spring, has a nondimensionalized moment of 0.050. The same wall without backup has a nondimensionalized moment of 0.125. Thus, a wall with stiff lateral support at the top would have 83% of the stress of a wall without backup. The same wall with very flexible top support would have only 40% as much flexural stress as a wall without backup. It is therefore expected that brick veneers supported by shelf angles with flexible support at the top can be expected to perform better than those which have stiffer top lateral support. The effect of K/KE is not

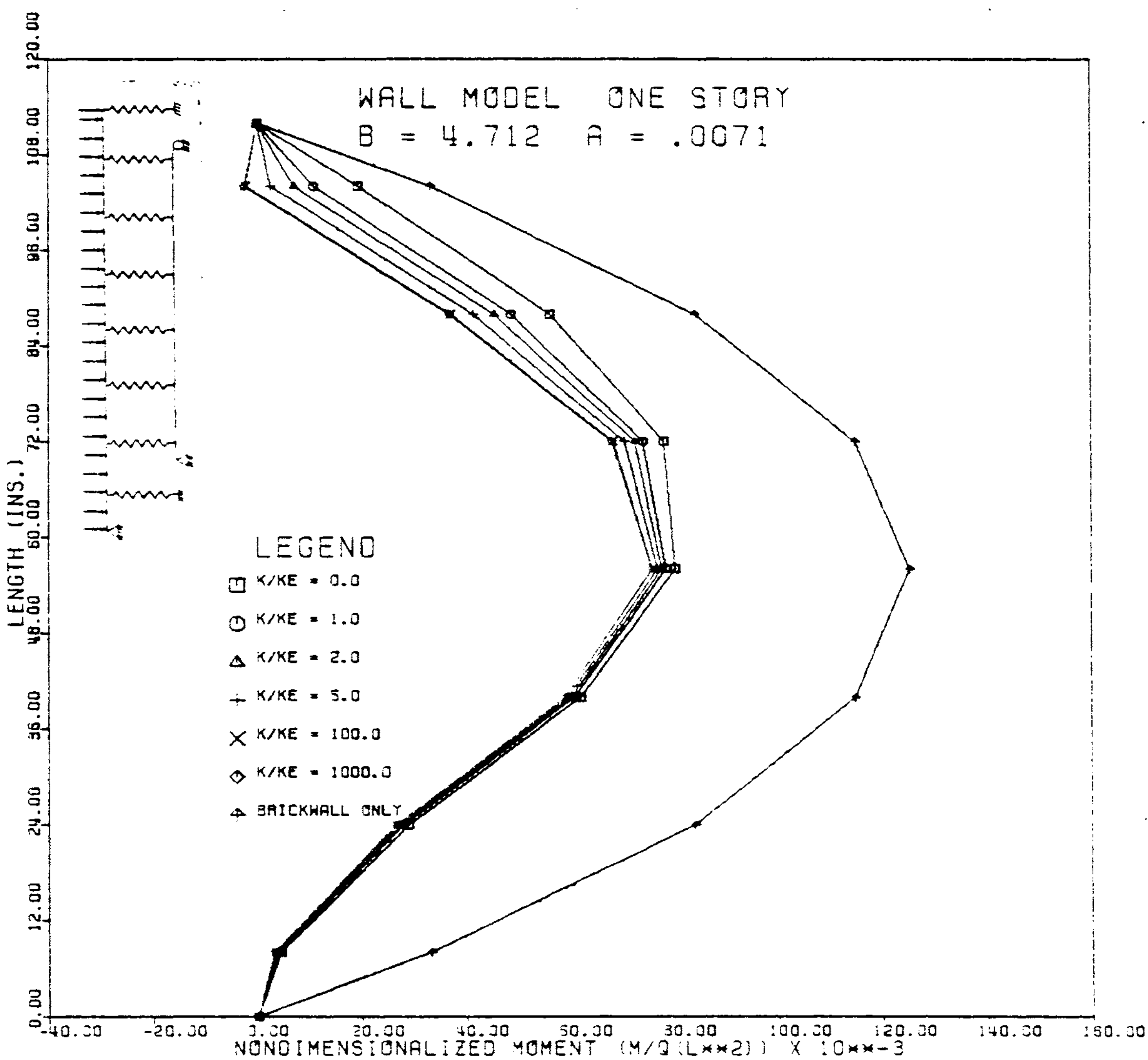

Figure 32. Moment Variation in the Brickwall with K/K_e for Wall Model at A = 0.0071 and B = 4.712

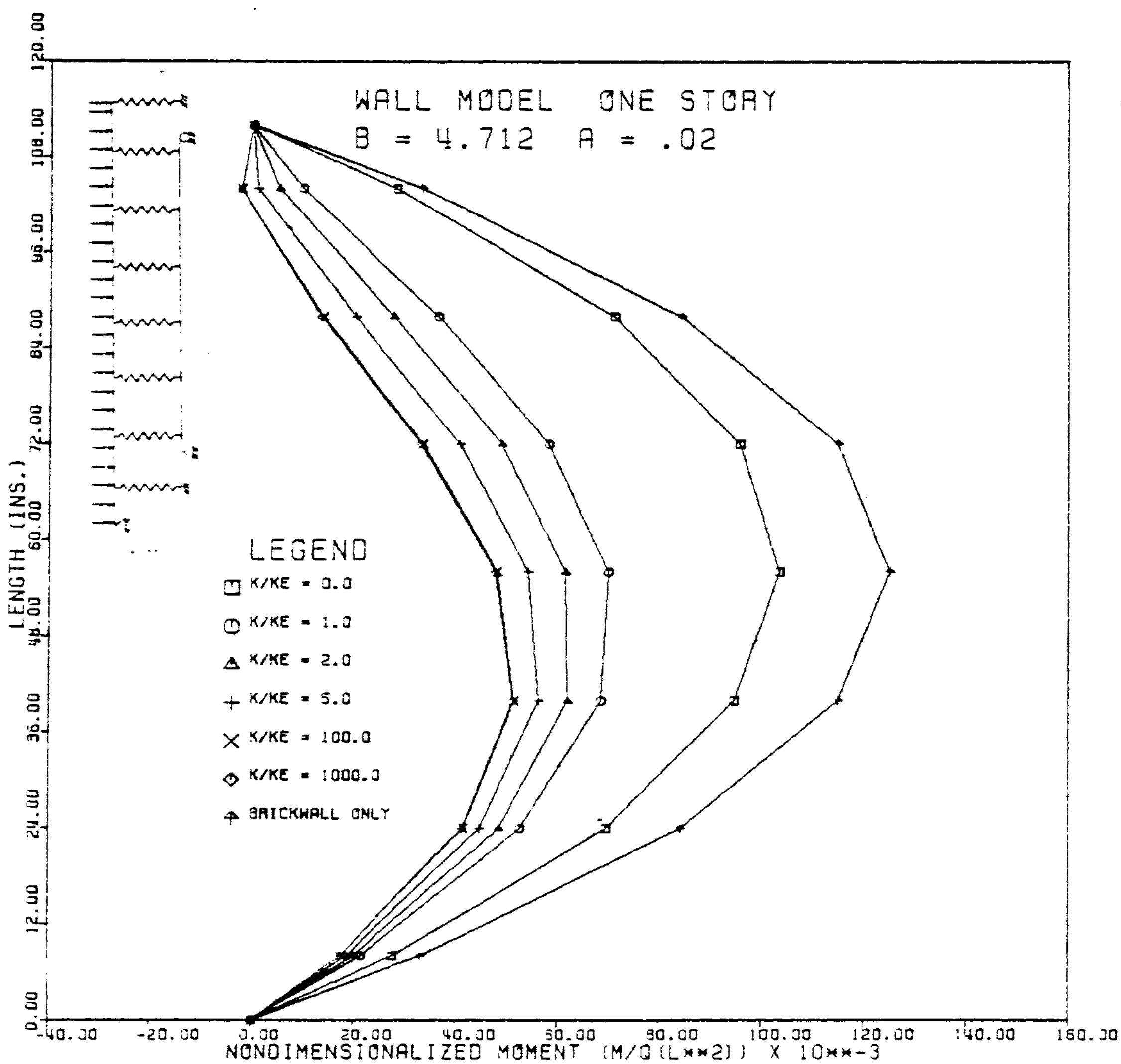

Figure 33. Moment Variation in the Brickwall with K/K_e for Wall Model at A = 0.20 and B = 4.712

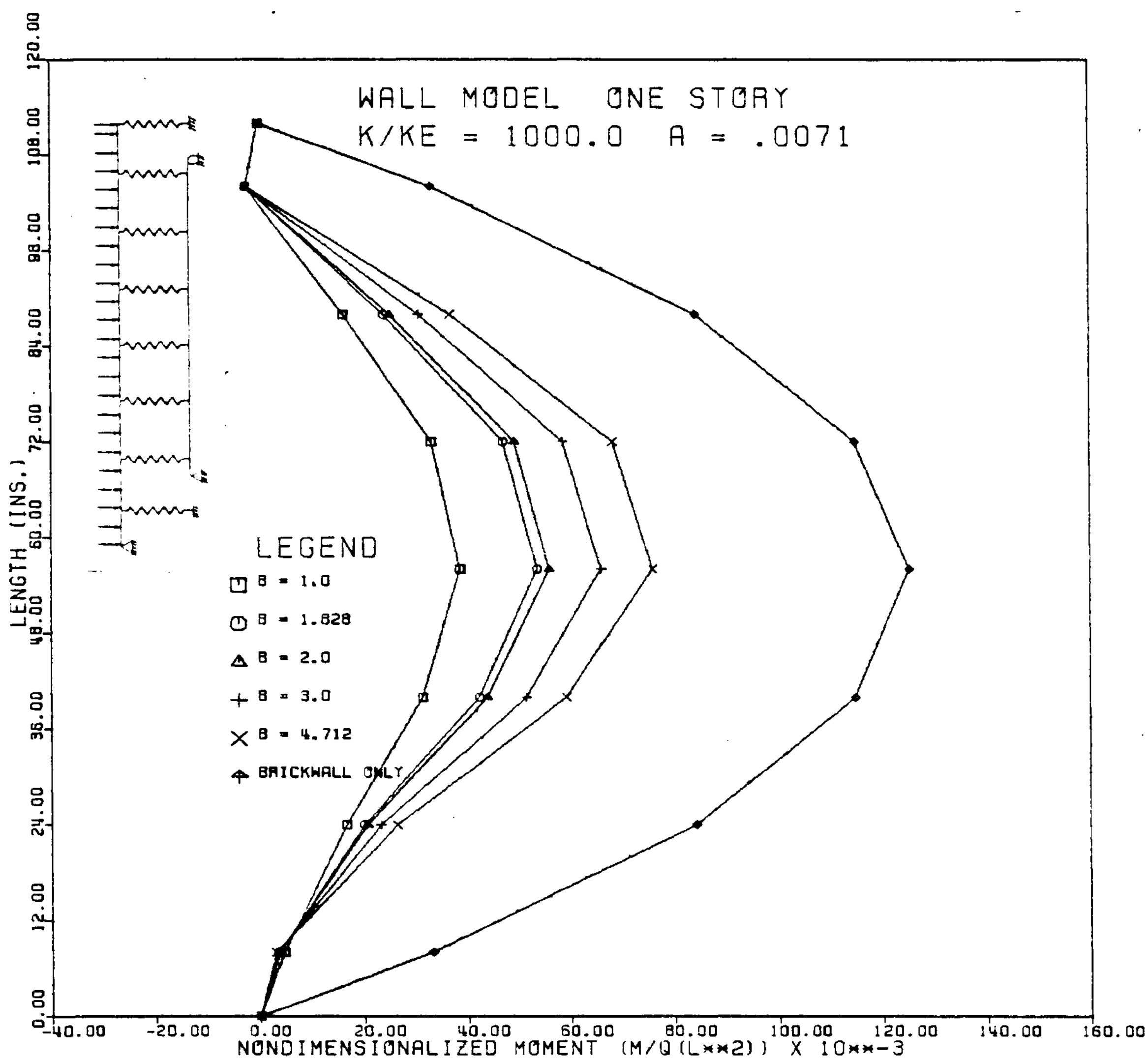

Figure 34. Moment Variation in the Brickwall with B for Wall Model at A = 0.0071

as great when the ties are stiffer, as shown in Fig. 32. Here there is little difference between values corresponding to K/KE = 0 and K/KE = 100, both values resulting in approximately 60% of the flexural stress as a wall without backup.

The effect of relative flexural rigidity is shown in Fig. 34. When the brick veneer is 4.712 times stiffer than the backup wall (no composite action), the nondimensionalized moment is 0.075, compared to 0.125 with no backup. When the relative flexural stiffness decreases to 1.828 (full composite action), the nondimensionalized moment decreases to 0.053. Thus, for B = 4.712, the veneer carries 60% as much bending moment as it would without backup. When B = 1.828, the percentage decreases to 42%. Since composite action is uncertain, the value of 60% is suggested.

Fig. 34 also illustrates that the use of relative stiffness (EI) as a means of distributing load to each wythe is not a good method of design. For example, a value of B = 1 would imply equal distribution of lateral load to each wythe, thus a 50% reduction in bending stress. However, Fig. 34 shows a 70% reduction for B = 1. Similar inaccuracies are observed for other values of B.

The forces in the wall ties were found to be non-uniform. In fact, analysis shows that ties can even have different signs depending upon boundary conditions at tie location. According to the computer model (Figs. 30 and 31), the forces in the ties ranged from 0 up to values as high as 20% of the total force on the entire wall. Thus, since there were a total of 14 ties in the wall, the practice of distributing load equally to all the ties would result in a maximum of only 7% of total load per tie. A second implication of unequal tie force distribution in the wall system is that the backup wythe is not uniformly loaded. In fact, the distribution of load on the backup wythe is much larger near the supports than it is near midspan. Since the backup wall is much stiffer in resisting lateral force near a support, it is logical that more force would be attracted to these locations.

CHAPTER VII

RESULTS OF PARAMETRIC STUDIES

In this section, the results of the parameters and other factors investigated are reported. These include tie stiffness, modulus of elasticity, composite action, height of metal stud wall, air space thickness, and inelastic behavior of the wall system.

Effect of Tie Stiffness

The effect of tie stiffness and relative tie stiffness K/K_e on the wall system was also investigated. The maximum moment in the brick wall for different conditions was compared to the moment M_0, the maximum moment in the brick wall if there were no backup stud wall. That is, M_0 is the maximum moment in the brick wall if it resisted the whole applied load. It was found that the extent to which the backup wall resists the applied load depends on factors such as end support conditions, the stiffness of the ties and the stiffness of the backup wall.

At low values of A (A = 0.005), that is for stiff ties, the maximum moment in the brick wall decreased from 76% to 72% of M_0 as K/K_e increased from 0.0 to 100.0 (Fig. 26). At high values of A (A = 0.20), that is for flexible ties, the maximum moment in the brick wall decreased from 74% to 60% of M_0 as K/K_e increased from 0.0 to 100.0 (Fig. 27).

At B = 16.15 and K/K_e = 1.0, the maximum moment in the brick wall increased to 82% of M_0 as A increased from 0.005 to 0.0246. At higher values of A, this percentage became smaller. At A = 0.20, the moment in the brick wall was 74% of M_0 (Fig. 29).

The results show that the stiffer ties are capable of attracting high loads. Therefore, more load is transferred to the backup wall when stiffer ties are used. That is, stiff ties are beneficial to the system as they relieve the stress in the veneer by transferring load to the backup. Since the transfer of the applied load to the backup wall is highly dependent on stiff ties, the tie stiffness is an important factor on the overall behavior of the wall system.

Effect of Smaller Modulus of Elasticity for Masonry

The Brick Institute of America's handbook on Engineered Brick Masonry (8), specifies that the modulus of elasticity of brick masonry should be taken as $E_m = 1000f'_m$ and not greater than 3000 ksi, where f'_m is the compressive strength of the brick prisms. The average compressive strengths of the brick prisms made during the construction of the test wall specimens are 4035 psi for Walls 1, 2 and 3 and 5170 psi for Walls 4, 5 and 6, respectively. By the BIA specification, E_m = 3000 ksi for these walls. However, from the flexure test performed on a 32 in by 8 in specimen taken from Wall No. 1 during the demolition process E_m, was found to be 875 ksi (Fig. 18). This reduced the value of B for the walls tested from 16.15 to 4.712. The maximum moment in the brick wall is thus reduced (see Figs. 32 and 40). This means that more load was transferred to the backup wall.

Effect of Airspace Thickness

The effect of the airspace thickness is equivalent to variations in A. If the airspace is increased from one inch to two inches, the effect is to increase A by a factor of two. In Fig. 29, the effect of increasing A from 0.005 to 0.01 on the moments in the brick wall is small. In Fig. 33, the effect of increasing A from 0.005 to 0.010 on the moments is also negligible. Therefore, an increase in the airspace has little effect on the load resisted by the brick wall.

Effect of Partial Base Fixity

In order for the brick veneer to rotate about its base, the moment caused by the self-weight of the veneer about the point of rotation has to be overcome by the applied load. Assuming that the veneer rotates about an edge, this moment can be calculated and is equal to 1372 in.-lb., using a strip of brick veneer two feet wide. It appears that the brick walls tested behaved as fixed at their bases until enough load was applied to overcome the resisting moments due to the self-weights of the veneers and the mortar droppings that accumulated at the bottom of the airspace. After these moments have been acheived, the brick veneers then bahaved as simply supported at their ends.

In discussing the end fixity of the brick wall, the wall model shown in Fig. 21 is used. The base of the veneer is fixed instead of pinned as shown in the figure. The applied load is 24.3 psf and the wall is 24 in. wide. In the wall model with the veneer base fixed, the maximum negative moment at the base is 5619.0 in.-lb., and the maximum positive moment slightly above mid-height of the wall is 2474.0 in.-lb.. Since the moment required to overcome the self-weight of the wall is 1372.0 in.-lb., the portion of the load resisted by the veneer behaving as fixed at its base is (1372/5619)24.3 = 5.93 psf. The remaining load, 18.37 psf is resisted with the veneer simply supported at its base. The maximum positive moment when the brick veneer is simply supported at its ends and loaded to 24.3 psf is 3866.0 in.-lb. which is 61% of the moment in the veneer without backup. If the positive moments are at nearly the same location on the veneer, superimposing the two positive moments gives the maximum positive moment to be

$$(5.93 \times 2474)/24.3 + (18.37 \times 3866)/24.3 = 3526.0 \text{ in.-lb.},$$

which is 56% of the moment in the veneer without backup. Therefore, the stresses in the veneer are reduced by about 44% compared to a veneer without backup, when partial end restraint of the base of the brick veneer is considered.

Composite Action

There are two types of potential composite action in the wall system. There is potential composite action between the brick wall and the backup, and there is potential composite action between the metal studs and the gypsum sheathings. These forms of composite action were investigated as follows:

Composite Action Between the Brick Veneer and the Stud Wall

When corrugated metal ties are used in the wall system, the ties may be able to withstand shear forces and moments at their ends. The degree to which this is done and the effect this has on the performance of the system is not known.

In order to study this effect, The Structural Design Language (STRUDL) (15), was used to analyse the model shown in Fig. 21 for three different types of corrugated ties as given below. The ties were made to carry only axial load by releasing the end moments of the ties. The result from this analysis was compared with the result obtained by allowing the ties to carry in addition to axial loads, shear forces and moments as shown in Fig. 35. Figs. 36, 37 and 38 show moments in the brick wall when composite action is expected in the interaction of the wall system with the ties and when no composite action is expected for three types of corrugated ties. They are corrugated ties gages 16, 18 and 20, respectively. They are 0.0598 in., 0.0478 in. and 0.0359 in. thick, respectively and are each 7/8 in. wide. From the plots it is clear that little composite action is obtained from the interaction of the corrugated wall ties with the wall system. The results obtained here can be said to be the upper bound on the composite behavior of these ties.

It should be noted that no composite action is obtained with the adjustable DW 10 ties because it can only withstand axial loads.

Composite Action Between the Metal Studs and the Sheathings

The gypsum sheathings are used to laterally brace the metal studs. One metal stud manufacturer (16) assumes that there is partial composite action between the studs and the sheathings. In trying to evaluate the contribution of the sheathings to the studs, the method of transformed sections has been used.

When the studs were assumed to act alone, that is, no composite action between the studs and sheathings, the cross sectional area of the stud was 0.208 $in.^2$ and the moment of inertia, was 0.540 in^4. Using E_m of 875 ksi, the resulting value of B was 4.712. When the gypsum sheathing was assumed to act fully in composite action with the metal studs, the transformed area was 0.4073 $in.^2$, and the transformed moment of inertia was 1.392 $in.^4$. The resulting value of B was 1.828. The maxi-

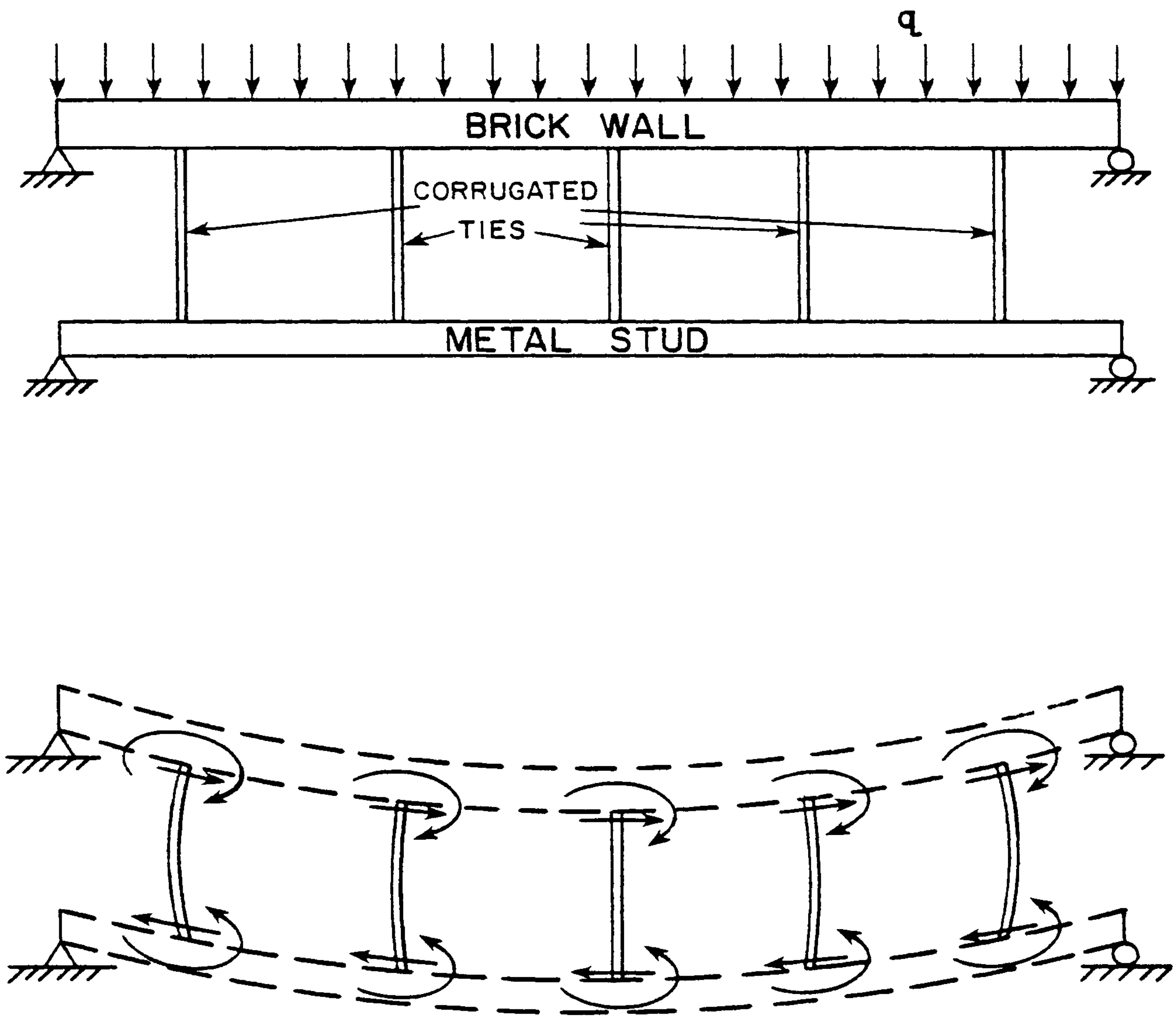

Figure 35. Composite Behavior

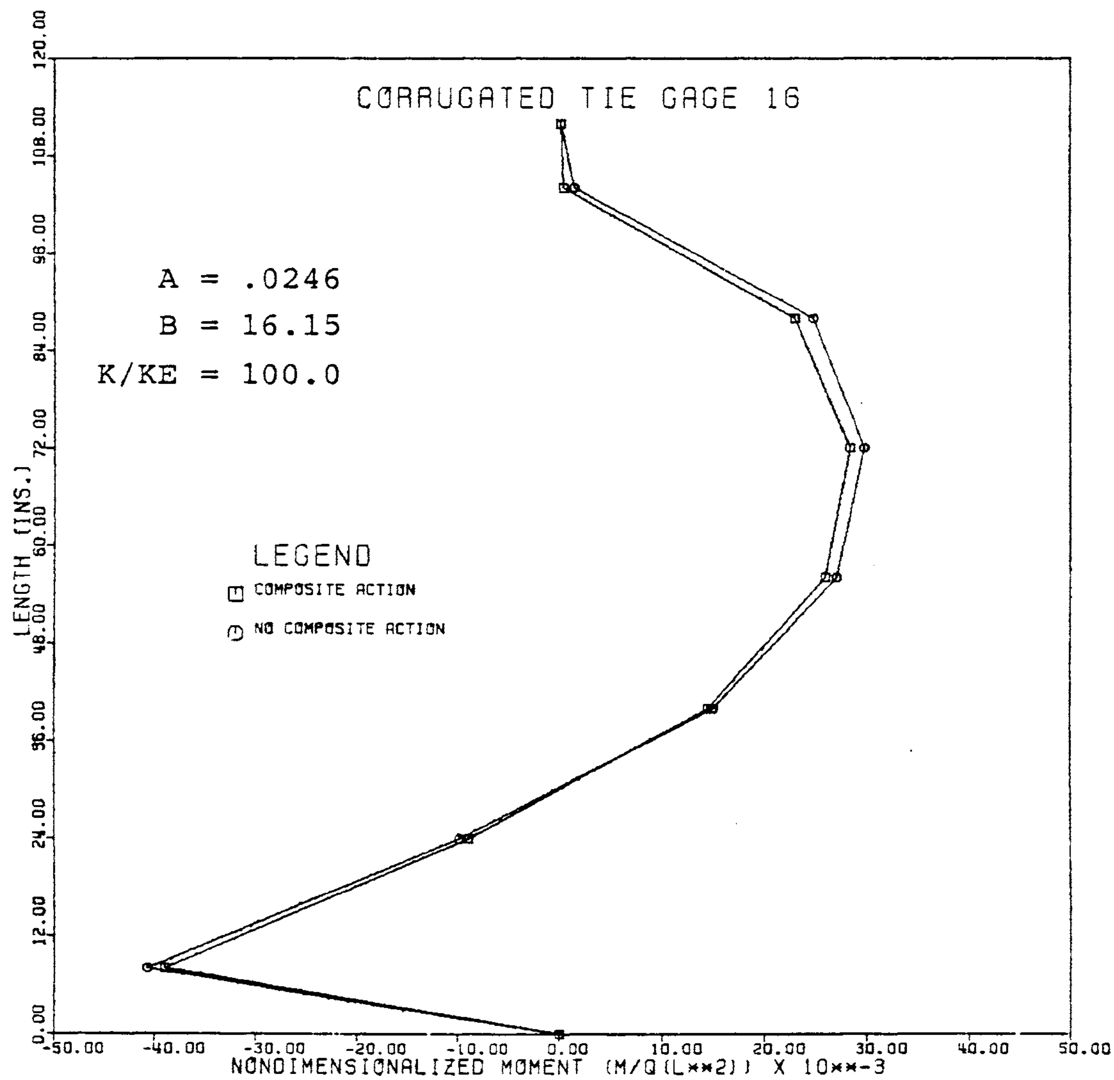

Figure 36. Brickwall Moment Plots for Corrugated Tie Gage 16 in Composite Behavior

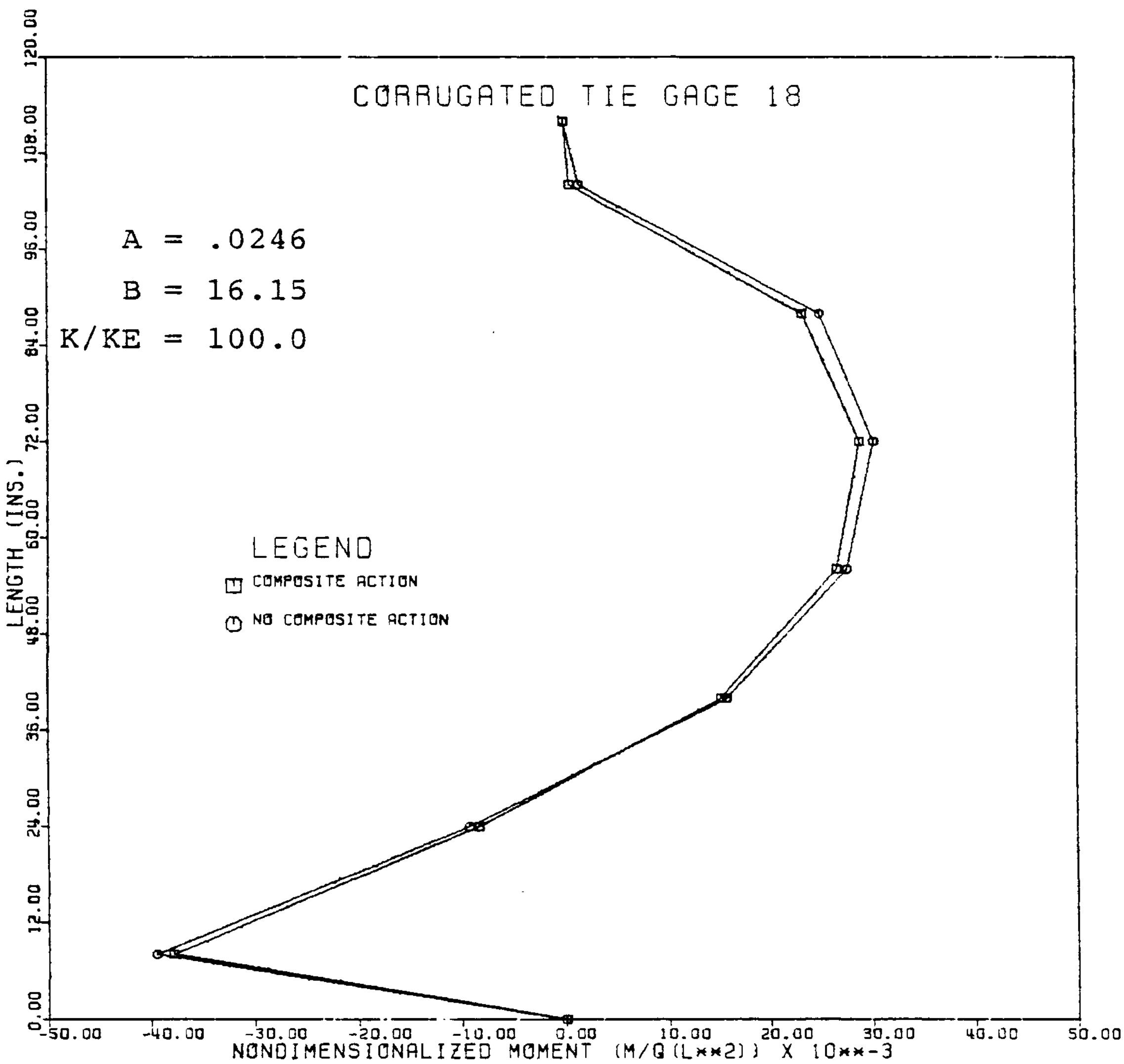

Figure 37. Brickwall Moment Plots for Corrugated Tie Gage 18 in Composite Behavior

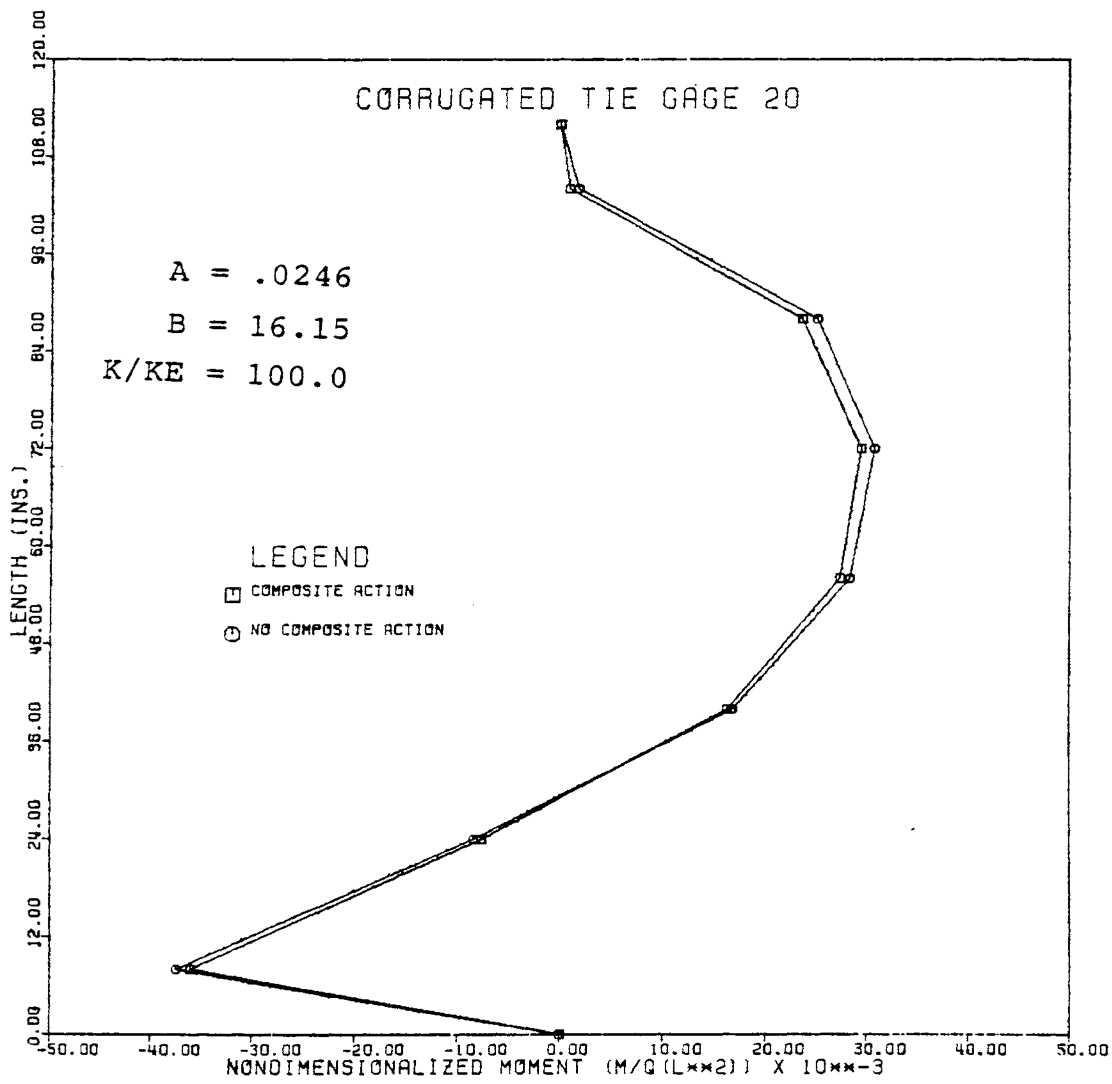

Figure 38. Brickwall Moment Plots for Corrugated Tie Gage 20 in Composite Behavior

mum nondimensionalized moments are 0.075 and 0.053, when B = 4.712 and B = 1.828, respectively. If the brick wall resisted all the load with no backup, the maximum nondimensionalized moment is 0.125. That is, if there is no composite action between the studs and the sheathings, the brick wall carries 60% as much bending moment as it would without backup. When there is full composite action, the brick wall carries 42% as much bending moment. It is believed that there is little partial composite action between the studs and the gypsum sheathings and the value of the portion of load resisted by the brick veneer is closer to 60% than to 40%.

Inelastic Behavior of the Wall System

In this analysis it was assumed that after the brick wall cracked, the wall system behaved in an inelastic manner. The model used to study the inelastic behavior of the wall system is shown in Fig. 39. The hinge in the model which simulated the crack was located at the point of maximum moment. It is assumed that after a crack forms, the brick veneer will develop a hinge, which cannot transfer moment, at the point of the crack.

After the brick wall cracked, it was assumed to rotate about the crack as a rigid body (see dotted lines in Fig. 39). Fig. 39 was used to study this effect employing STRUDL (15). Fig. 40 shows the deflection plots in the brick wall before and after a crack develops for $K/K_e = 0.5$ and Fig. 41, the deflection plots in the brick wall for K/K_e = infinity, that is, when the top of the brick wall is free. In Fig. 40, the deflections, D, were nondimensionalized by dividing them by DO, the maximum deflection in the brick veneer when it is simply supported and carries the total applied wind load. These agree with the shapes obtained from the lateral wall tests before and after the brick veneer cracked, see Fig. C-3.

Figure 42 shows the moment variation (at the same load) in the drywall before and after the crack was introduced. The maximum moment in the drywall after the crack was about three times the maximum moment before the crack.

Prediction of Cracking Load

An attempt was made to predict the load at which the brick wall will develop cracks using the calculated moments from the mathematical model with the value of the modulus of rupture obtained from the flexure test. From the plots the nondimensionalized moment factor, Z, can be obtained.

$$Z = M/qL^2. \tag{1}$$

The load at which the brick wall will crack can be calculated from the following equation:

$$Z(qL^2) = f'_r S, \tag{2}$$

where f'_r is the modulus of rupture from prism tests.

For example, when no composite action is considered between the stud and the sheathings and the drywall is considered pinned at both ends and the movement of the top of the wall is restrained (Fig. 29), the maximum nondimensionalized moment in the brick wall for A = .0246, $K/K_e = 1.0$ and B = 16.15 is equal to Z = 0.10246. Using a section modulus of S =

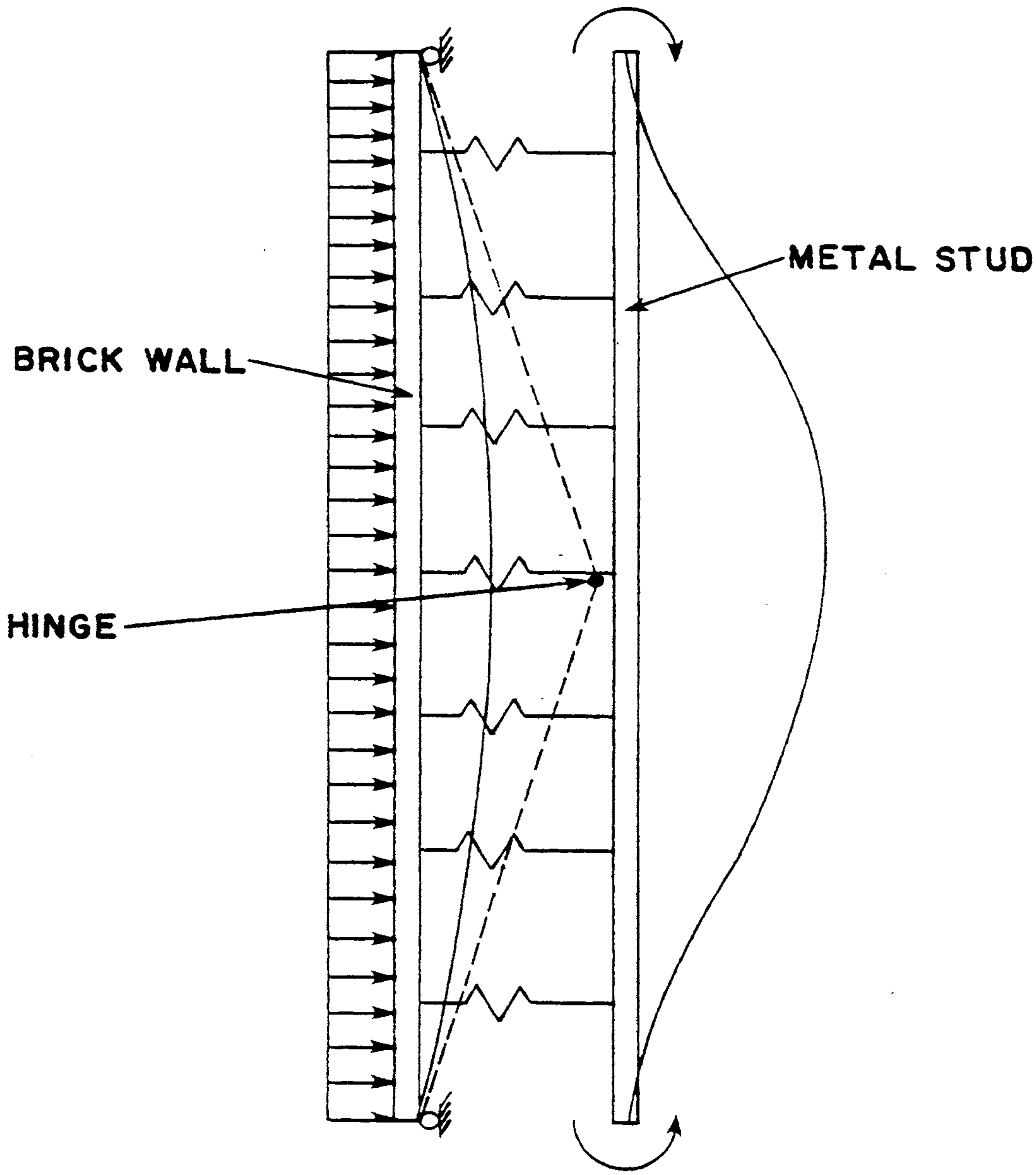

Figure 39. Inelastic Behavior

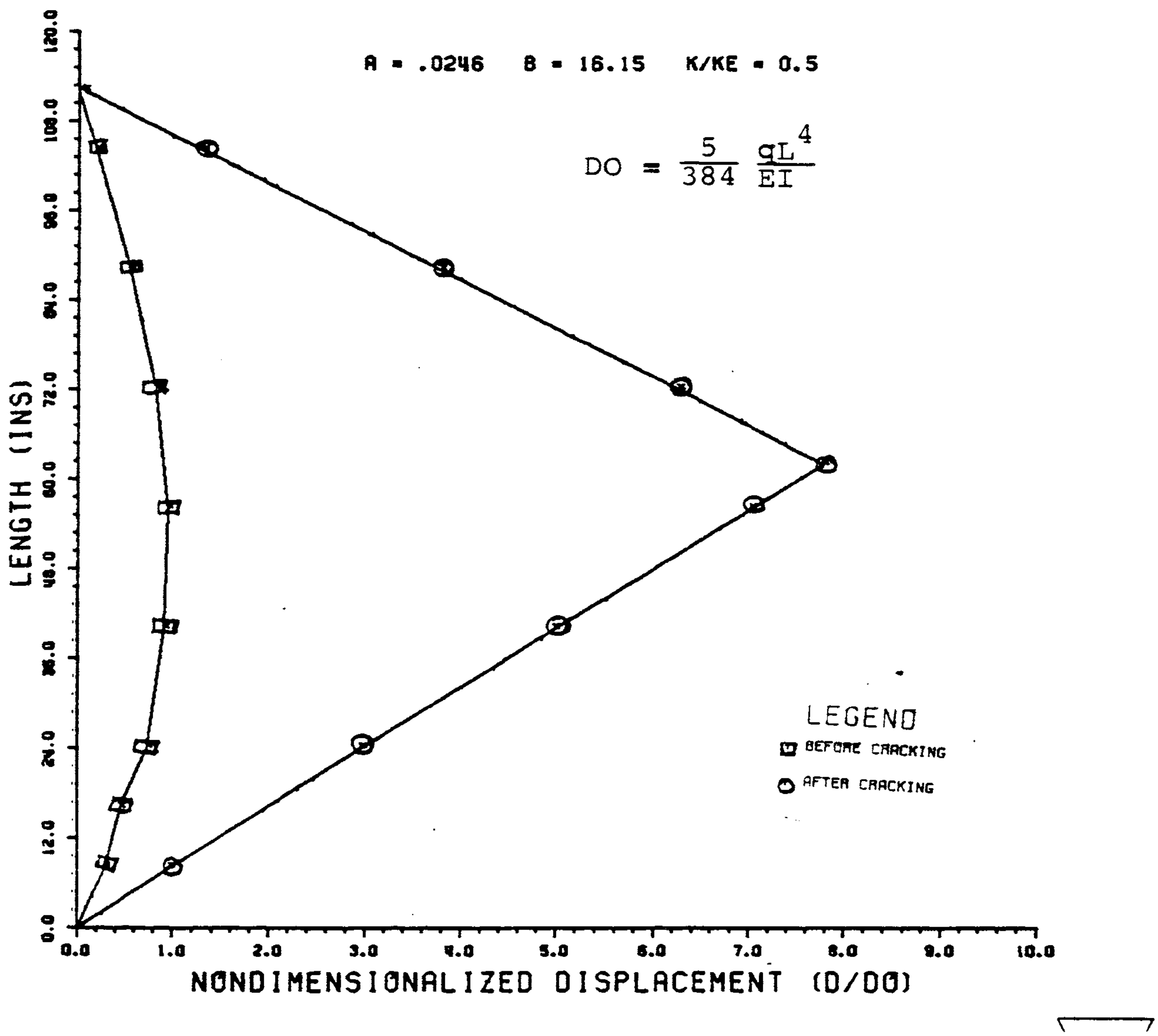

Figure 40. Theoretical Deflection Plots (Inelastic Behavior) for K/K_e = 0.5

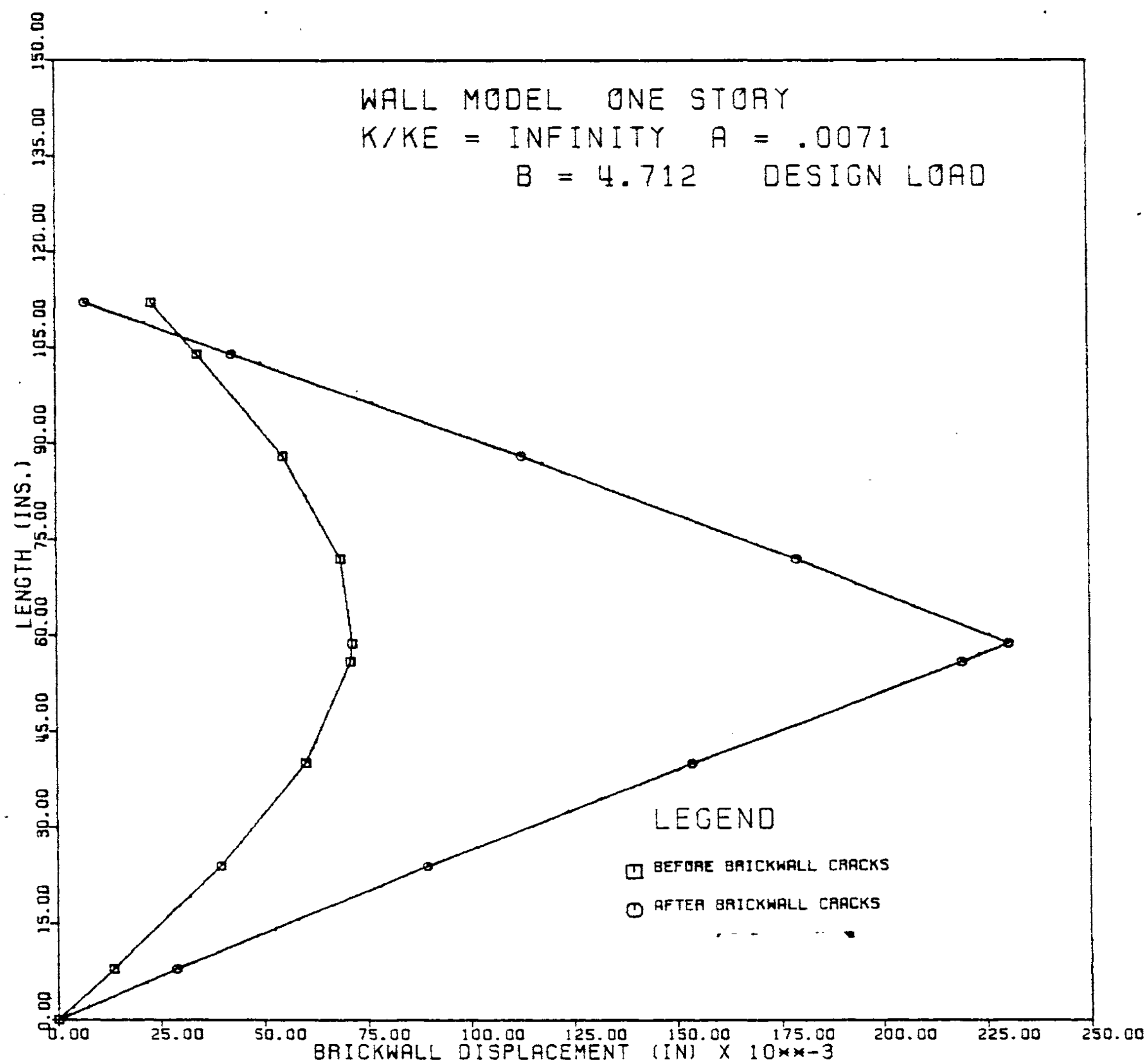

Figure 41. Theoretical Deflection Plots (Inelastic Behavior) for K/K_e = Infinity

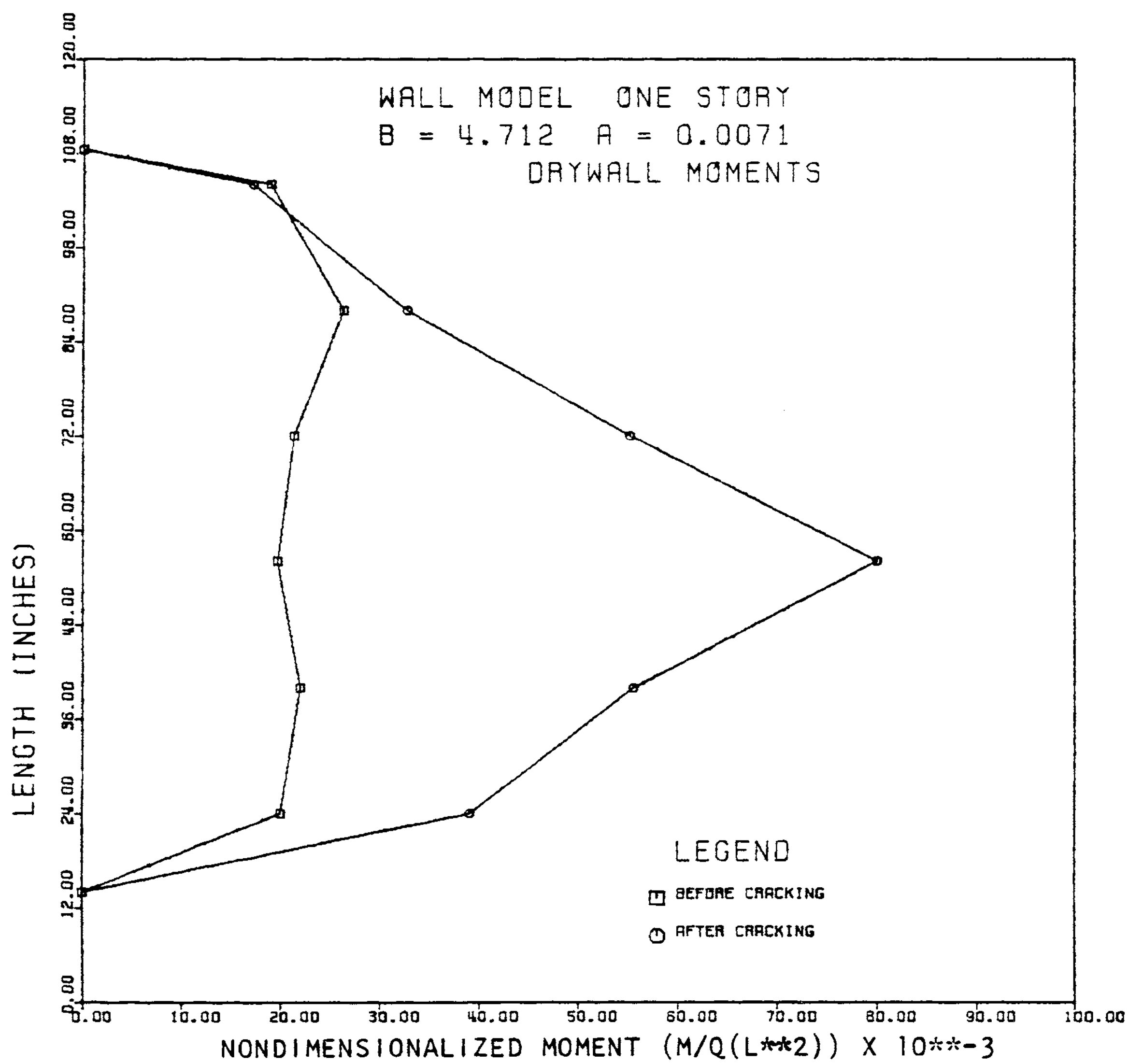

Figure 42. Theoretical Drywall Moment Plots

24.5 in^3 per ft and f_r' = 114 psi, the load at flexural cracking may be calculated from the equation

$$q = f'_r S/ZL^2$$

is found to be 26.0 psf. From Fig. 27, with K/K_e = 1.0, A = 0.20 and B = 16.15, a maximum value of Z = 0.0927 is obtained from which the calculated failure load is 29.0 psf.

These low calculated loads led the author to believe that there is partial composite action between the stud and the sheathings. Also the runners at the top and bottom of the studs cause the end conditions of the studs to be somewhere between complete fixity and pinned. Figs. 43 and 44 show the moment plots for the brick wall for full composite and no composite action between the stud and the sheathings and for the drywall completely fixed and pinned, respectively. When the top of the brick wall is unrestrained and for full composite action between the studs and the sheathings, the predicted failure load is 137.0 psf, when the ends of the drywall are fixed, and the predicted failure load is 50.0 psf, when the ends of the drywall are pinned. For the same brick wall end conditions, and no composite action between the stud and the sheathings, the predicted failure load is 77.0 psf, when the ends of the drywall are fixed and is 35.0 psf, when the ends of the drywall are pinned.

The experimentally measured failure load for two of the walls tested under positive pressure was between 52.0 and 57.0 psf. This falls within the range estimated above for the wall system for the extreme values obtained for the wall under the conditions the wall system functions. It can be observed that there is some composite action obtained from the interaction of the studs and sheathings. Also the end conditions of the drywall are observed to be between complete fixity and pinned, when the runners are screwed to the runners and the runners bolted to the support concrete frame as was done in this experiment.

Figs. 45 and 46 show the theoretical deflection plots at design load, for the different conditions mentioned above. Alongside the plots is the plot of the test data at design load for Wall No. 1. The deflection of the wall is seen to fall within the predicted range. Fig. 47 shows the brick wall deflection test data for Wall No. 1 at design load and the brick wall theoretical deflection data at design load for a model with the brick veneer fixed at the bottom and the drywall pinned at both ends and no composite action between the studs and the sheathings. Fig. 48 shows the backup wall deflection test data for Wall No. 1 at design load and the theoretical backup wall deflection data for a model with the brick wall fixed at the bottom and the backup wall pinned at both ends and no composite action between the studs and the sheathings. It can be seen that the theoretical data are close to the actual test data.

Evaluation of Current Design Method

In the current design method, the metal stud sizes are obtained by either the imposition of mid-point deflection limitation of L/360 on or the maximum stress limitation in, the metal stud alone under full design wind load. This method neglects the support conditions and the flexural stiffness of the brick veneer. The wind load is assumed uniformly distributed on the metal studs instead of the point loads on the studs at the point of attachment of the metal ties. The test results show that

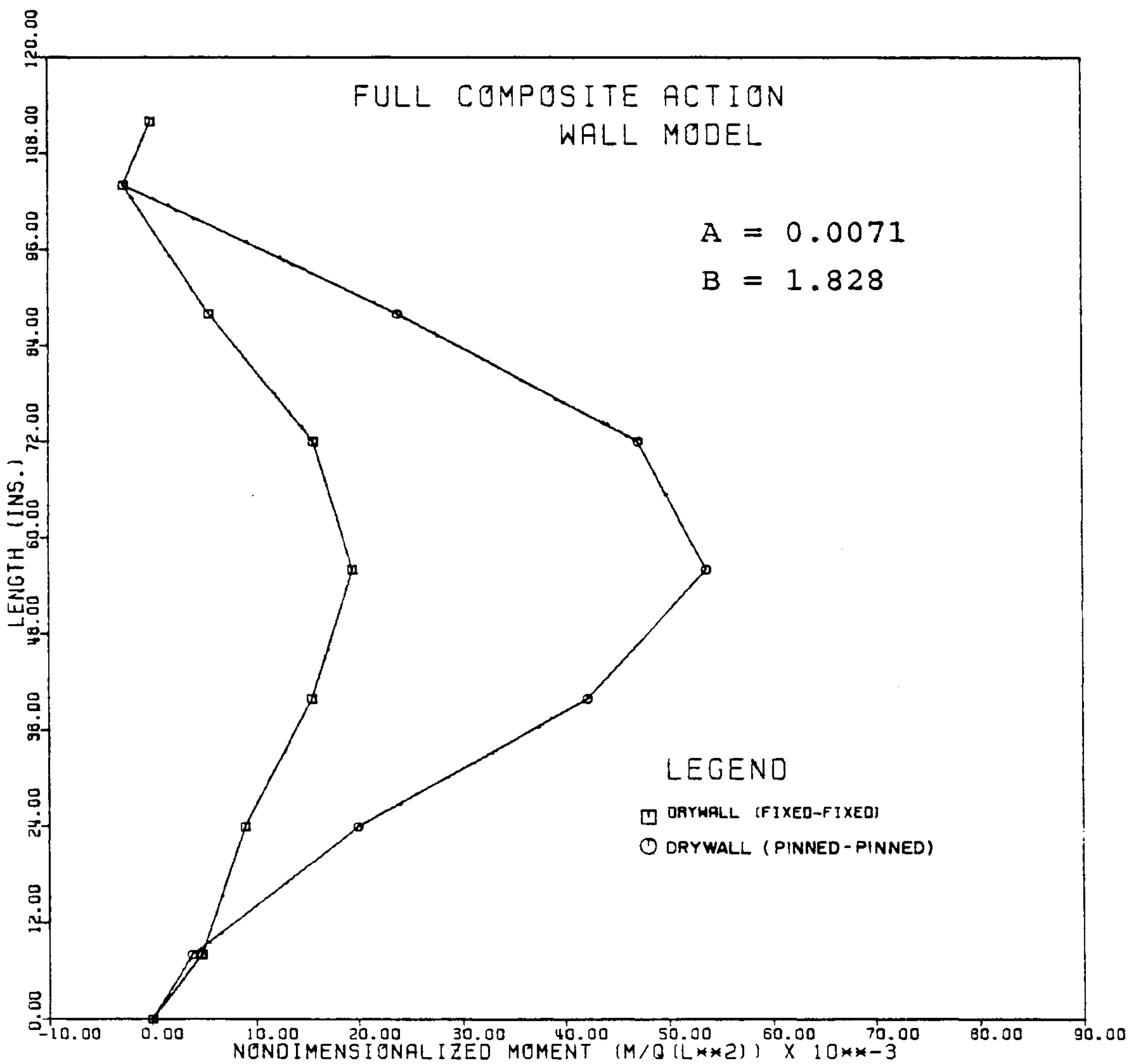

Figure 43. Theoretical Brickwall Moments at Full Composite Action

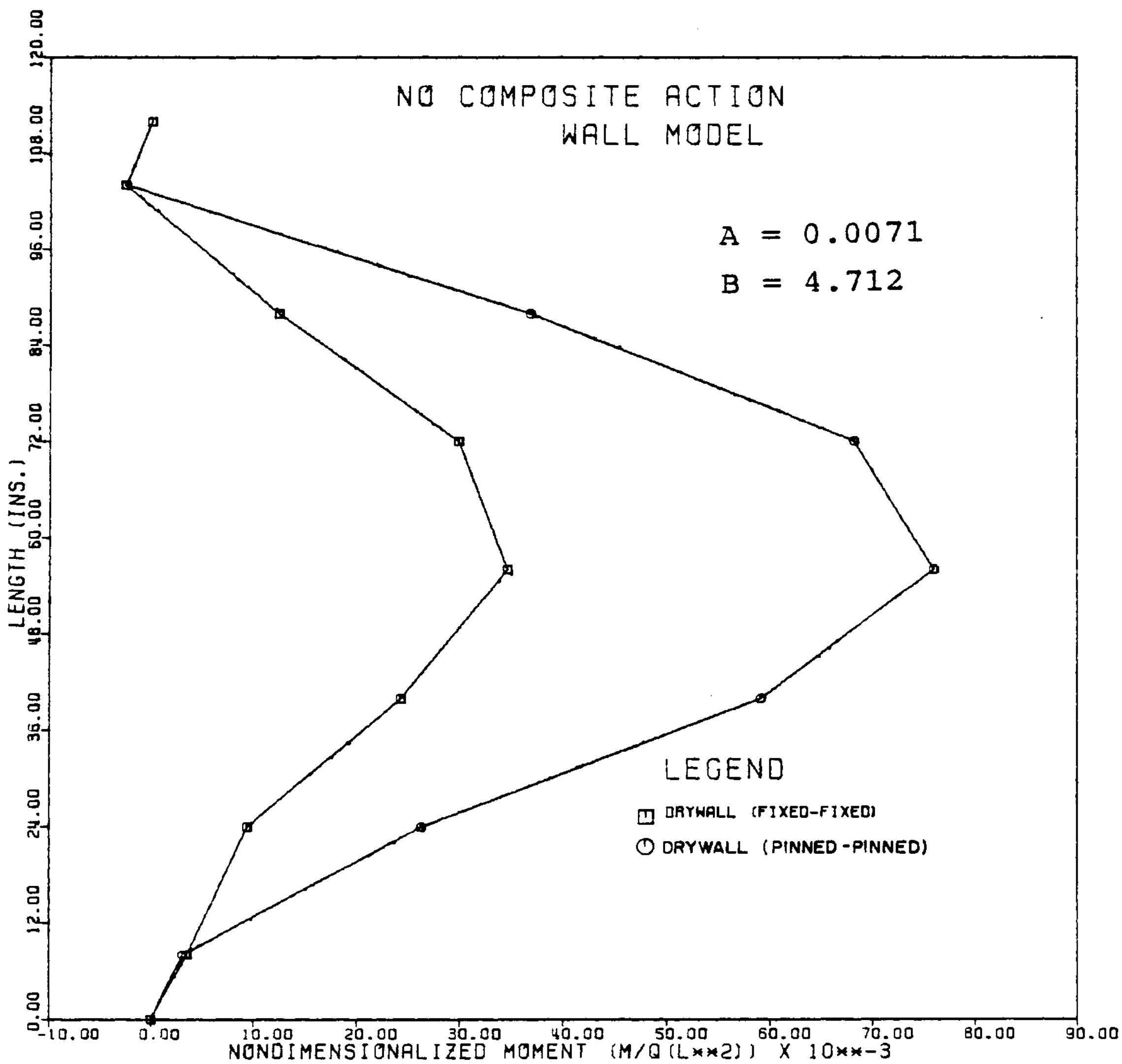

Figure 44. Theoretical Brickwall Moments at No Composite Action

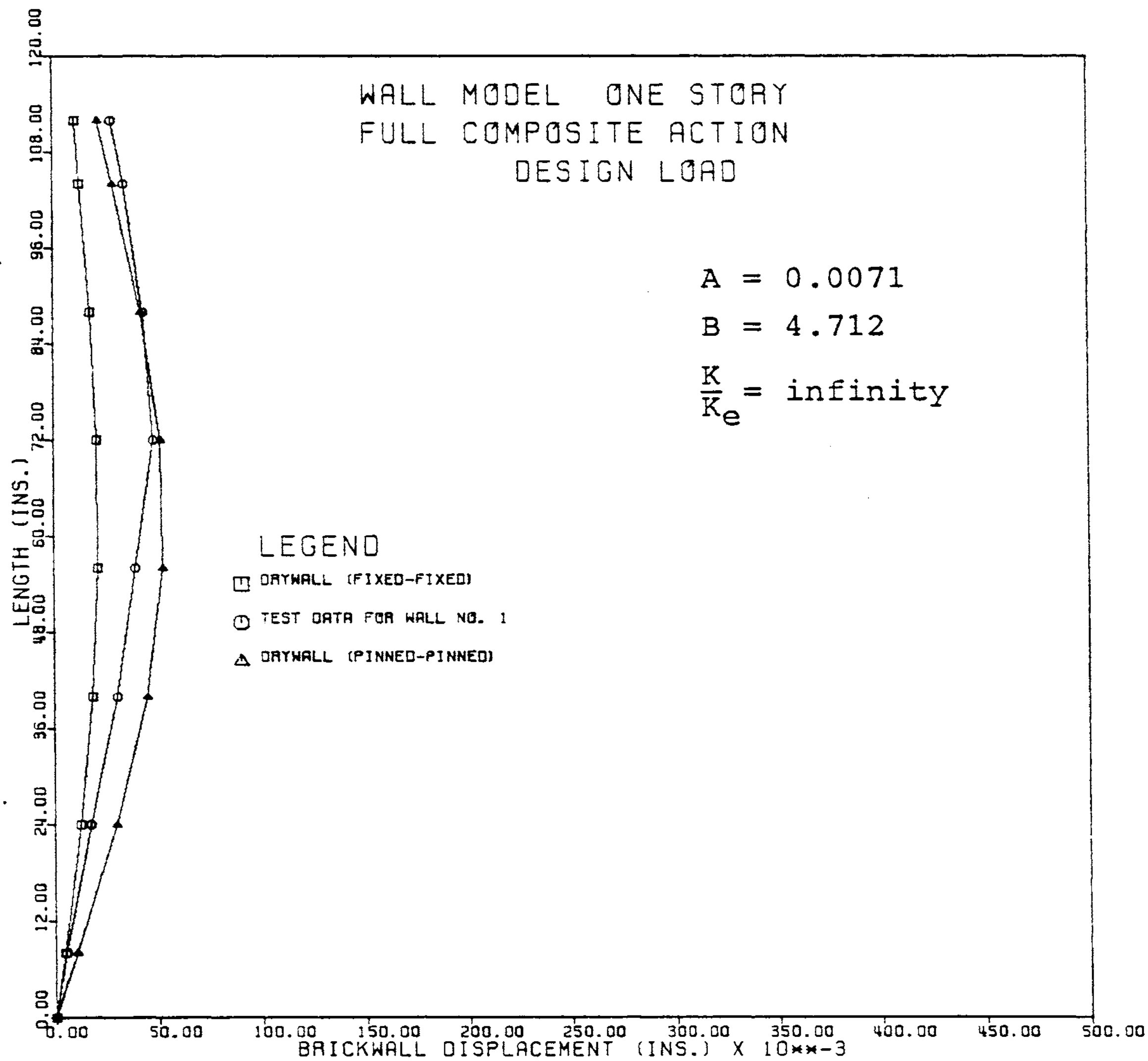

Figure 45. Comparison of Theoretical and Experimental Deflection Plots at Full Composite Action

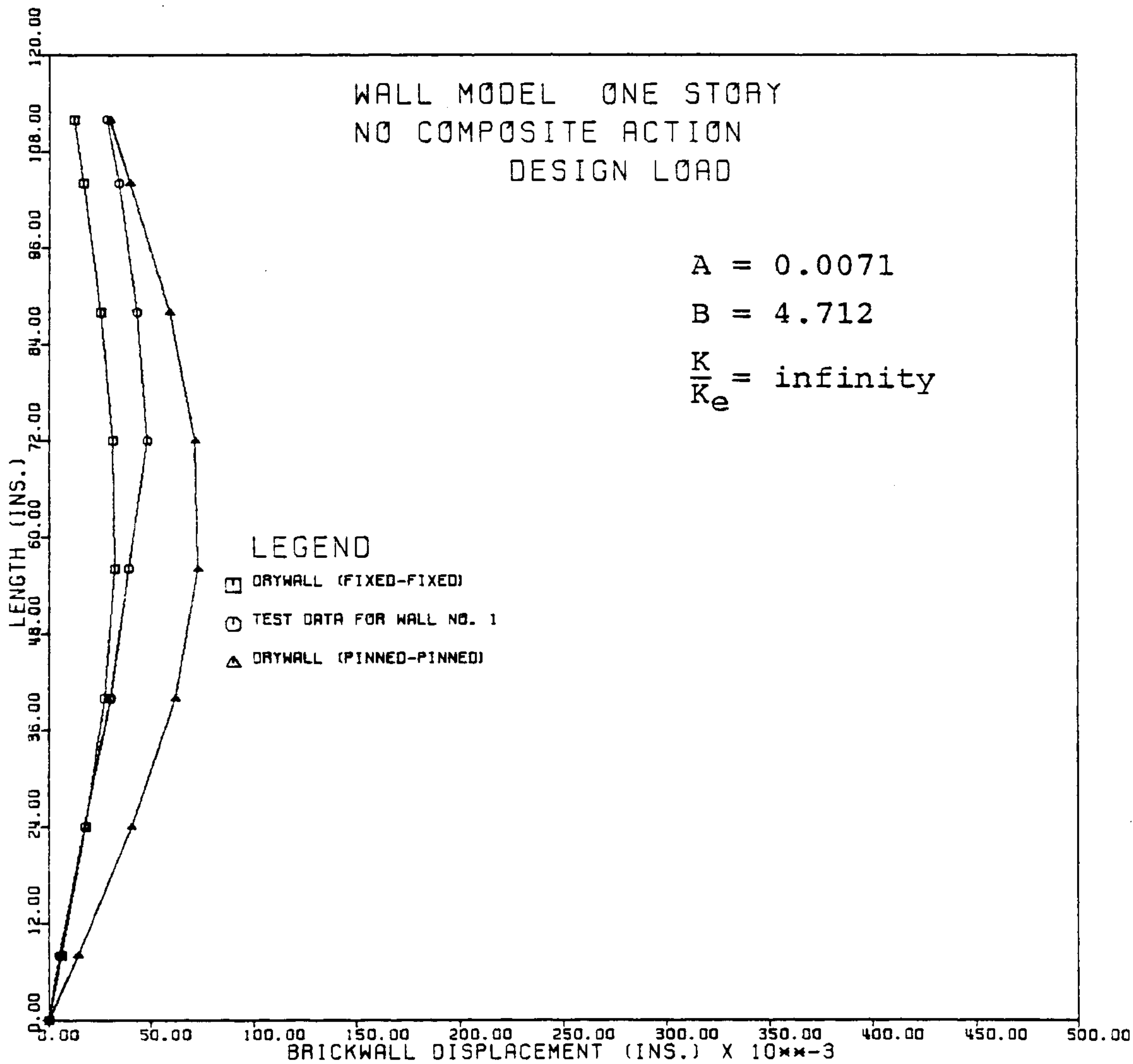

Figure 46. Comparison of Theoretical and Experimental Deflection Plots at No Composite Action

this method of design is adequate for brick veneer with compressible filler material at the top and which also is capable of lateral movement at the top.

The experimental and analytical results in this investigation show that the brick veneer is as critical to the performance of the wall system as the metal stud. Its end support conditions and flexural stiffness are very important to the overall performance of the wall system. If flexural cracking is to be avoided, the brick veneer should be taken into consideration in the design of the metal studs.

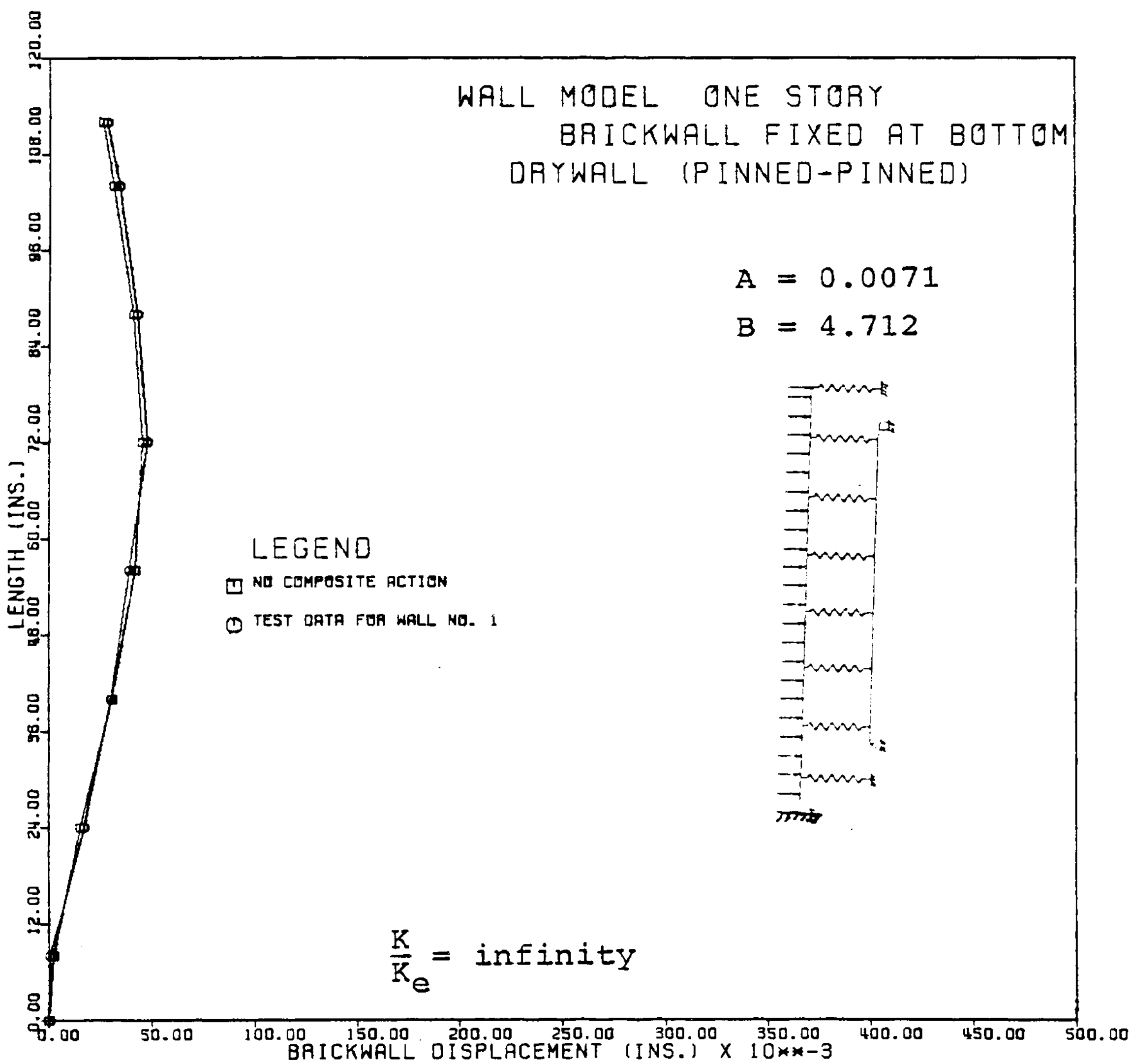

Figure 47. Brick Veneer Theoretical Versus Actual Deflection Plots for Wall No.1 with No Composite Action Between the Metal Studs and the Sheathings

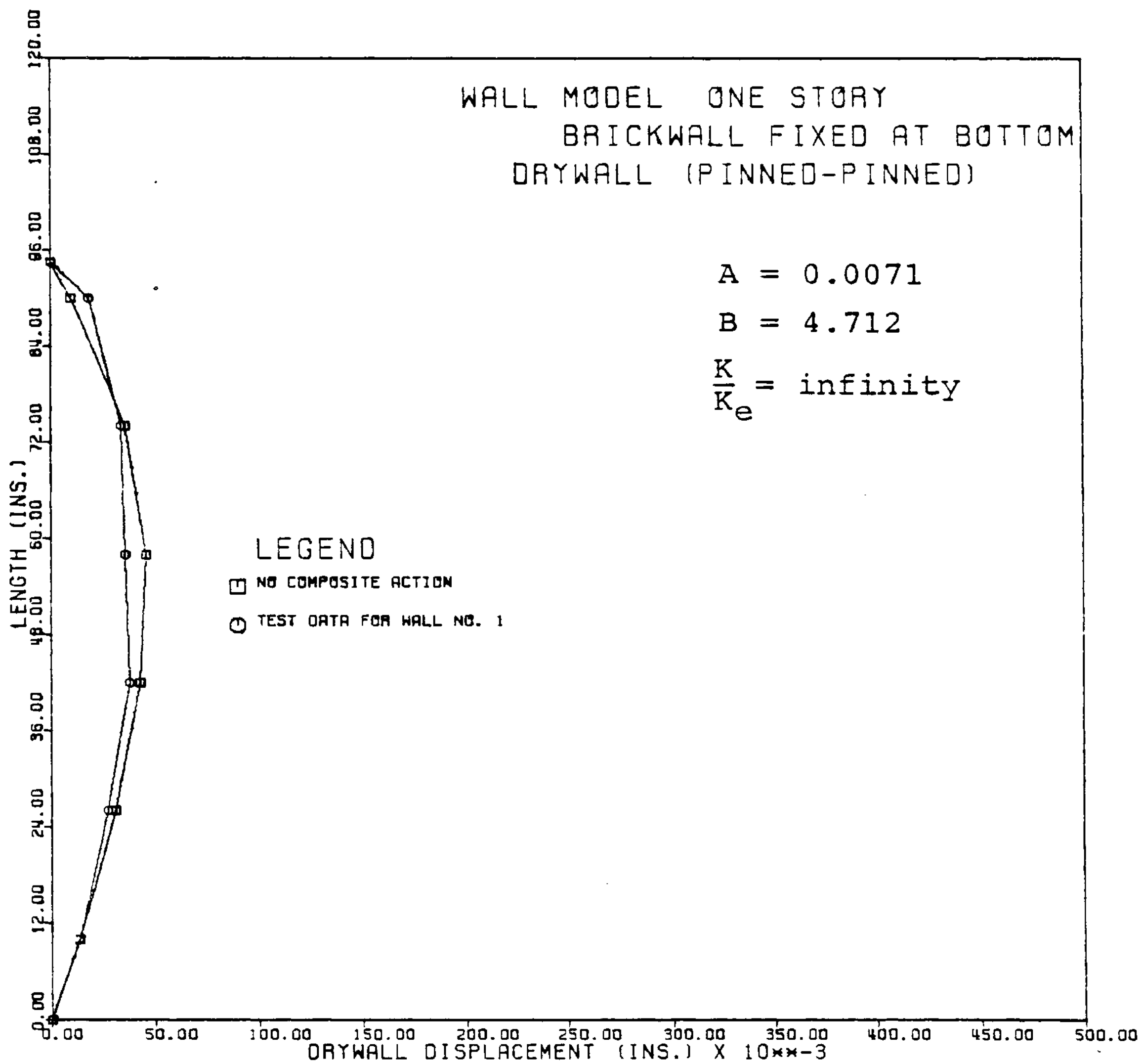

Figure 48. Backup Wall Theoretical Versus Actual Deflection Plots for Wall No.1 with No Composite Action Between the Metal Studs and the Sheathings

CHAPTER VIII

CONCLUSIONS

The walls tested were very complex in their behavior. Even with the substantial data obtained during the experimental program, the system remained difficult to explain. The loads carried by the system exceeded values predicted by conventional analysis.

Based on the experimental test results and the computer models, the following conlcusions were reached:

1. The 14 ga DW 10 adjustable tie used in the tests performed well and is therefore recommended for use in this wall system, especially in construction cases where lateral and vertical movements are expected. For large design loads it is recommended that a heavier backing (12 ga) be used.

2. The walls subjected to lateral loads were all capable of resisting their design lateral wind load without flexural cracking of the brick veneer; five of the six walls reached twice design load without flexural cracking; and two of the six walls reached three times design load without cracking. In the current design procedure, the metal studs are designed to resist the full lateral load without exceeding a midspan deflection limit of L/360, where L is the stud height. Additionally, the maximum allowable stress in the metal stud may not be exceeded.

3. The compressible filler material at the top of the brick veneer allowed appreciable movement of the top of the brick veneer. This movement relieved the stresses in the brick and enabled the system to resist

more load than it would have done without the movement. The load capacity of the walls during the tests is attributable, in part, to these brick veneer top movements. The analytical results show that if the top of the wall is not permitted to move laterally, the brick veneer will develop cracks at lower loads.

4. The mathematical model developed predicted failure loads to a good degree of accuracy. The brick veneer behaved as if it were restrained at the base and free at the top, and the drywall behaved as pinned at both ends. The composite action obtained between the stud and the gypsum wallboard did not appear to be significant.

5. In the walls tested, it appears that the metal stud backup reduced the flexural stresses on the brick veneer about 44% compared to that of a veneer without backup.

6. Forces in the wall ties are nonuniform, even when wind pressure is uniformly distributed. The practice of distributing force to ties uniformly in design appears to substantially underestimate maximum tie forces.

7. Composite action between the studs and gypsum sheathing and between the brick veneer and the studs when corrugated ties are used, though partially present, do not significantly alter the load which must be resisted by the brick veneer.

8. The use of flexural rigidity as measured by the value EI as a means to distribute lateral load to each wythe is inaccurate. Such factors as tie stiffness, span difference between the two wythes, and boundary conditions have as much effect as flexural rigidity on distribution of lateral load.

9. Water permeance, measured using a modified version of ASTM E514, did not correlate closely with the level of load to which the wall was previously subjected. There was no significant increase or decrease in water permeance after the walls were subjected to twice design load.

APPENDICES

Appendix A

Hysteresis Loops for Metal Ties

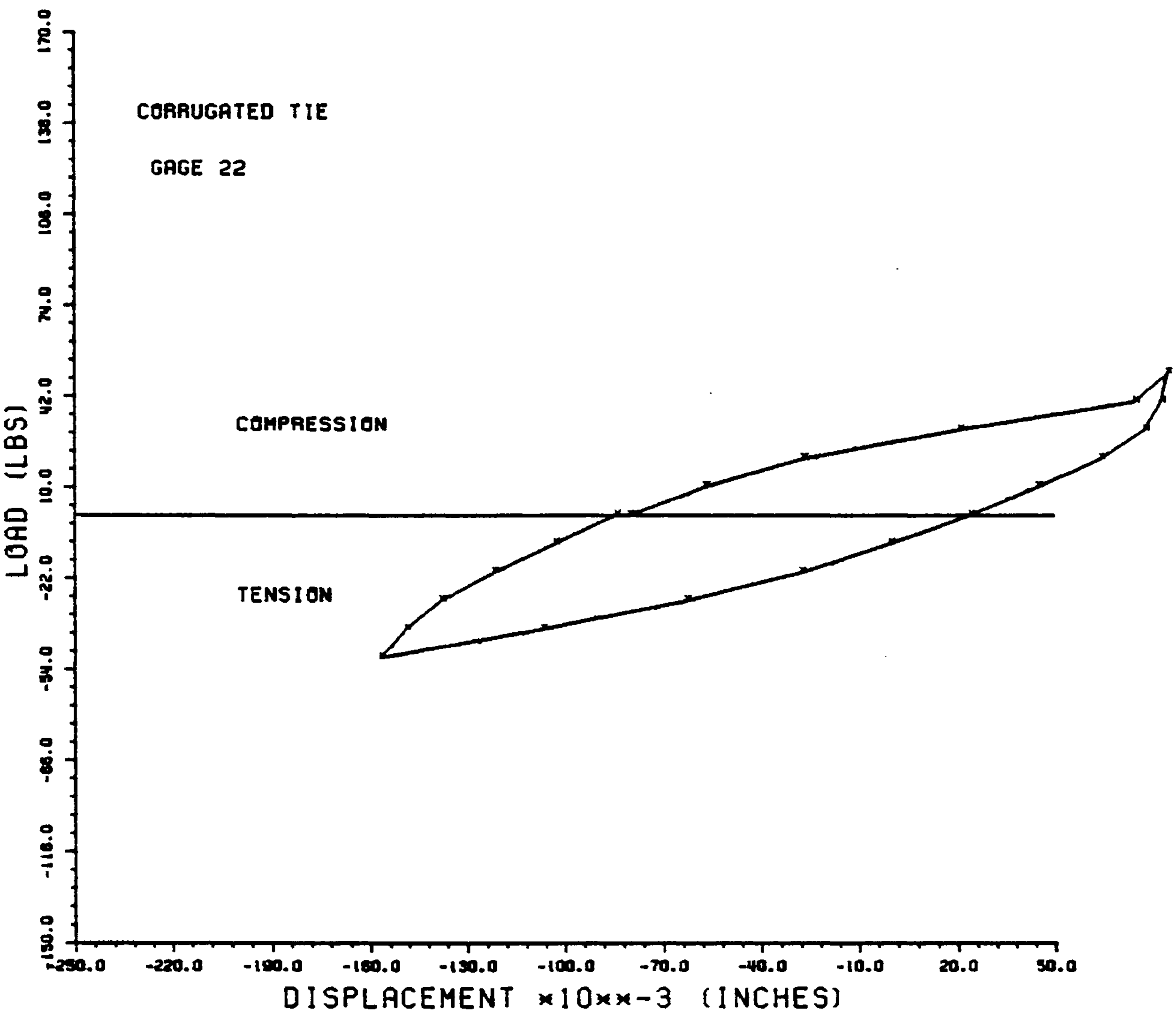

Figure A-1. Hysteresis Loop for Corrugated Tie ga 22 at 50 lbs

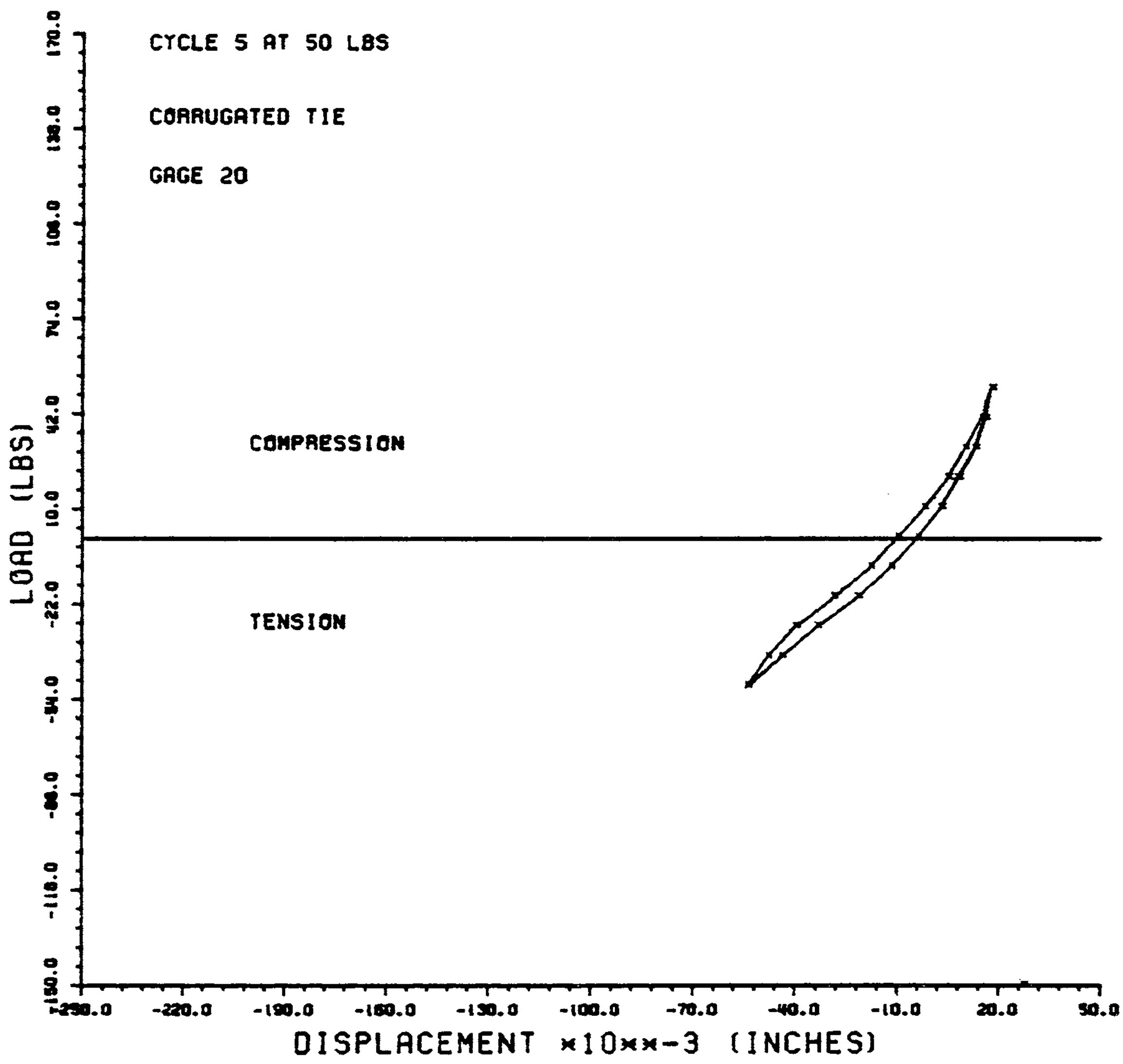

Figure A-2. Hysteresis Loop for Corrugated Tie ga 20 at 50 lbs

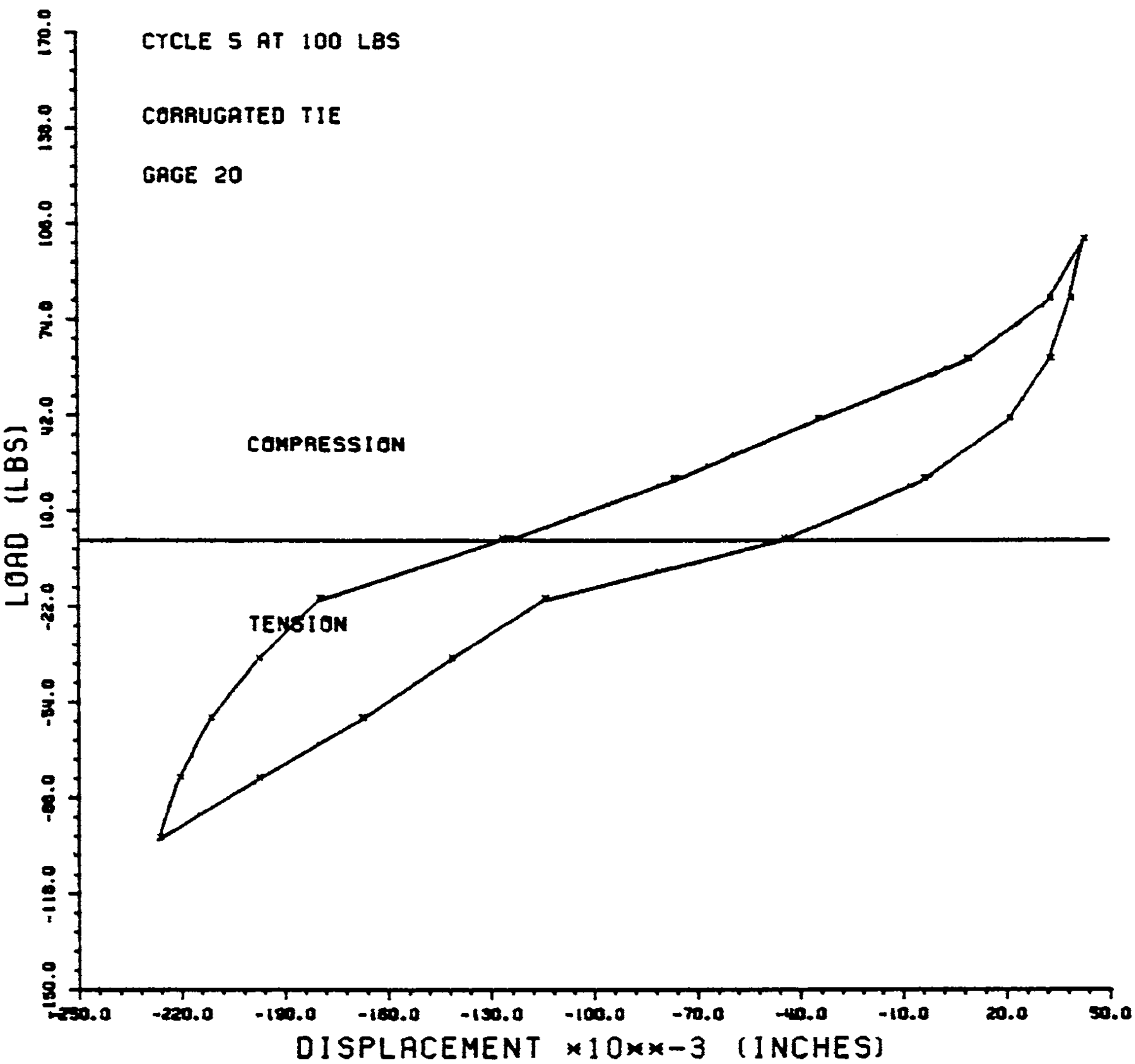

Figure A-3. Hysteresis Loop for Corrugated Tie ga 20 at 100 lbs.

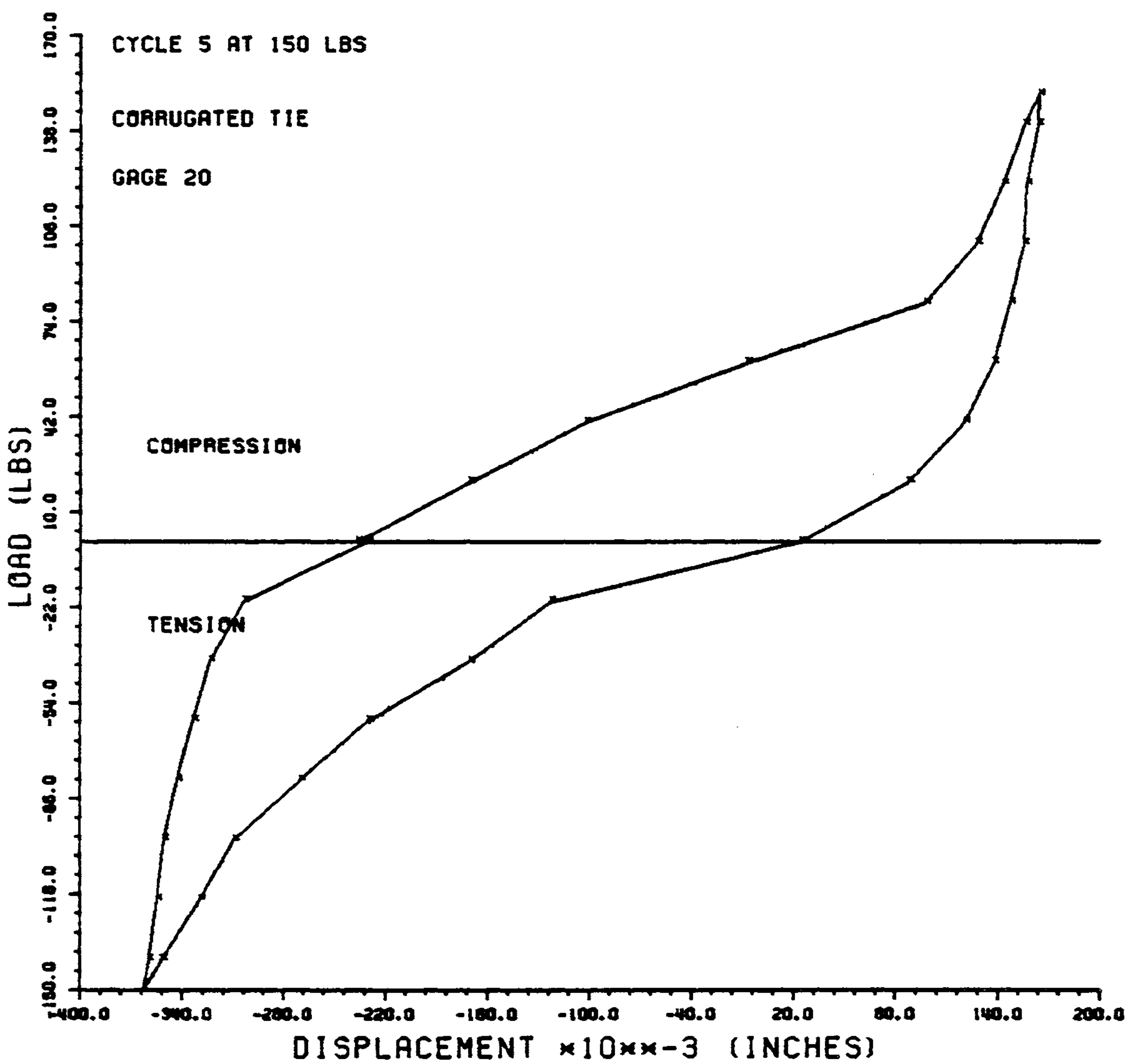

Figure A-4. Hysteresis Loop for Corrugated Tie ga 20 at 150 lbs.

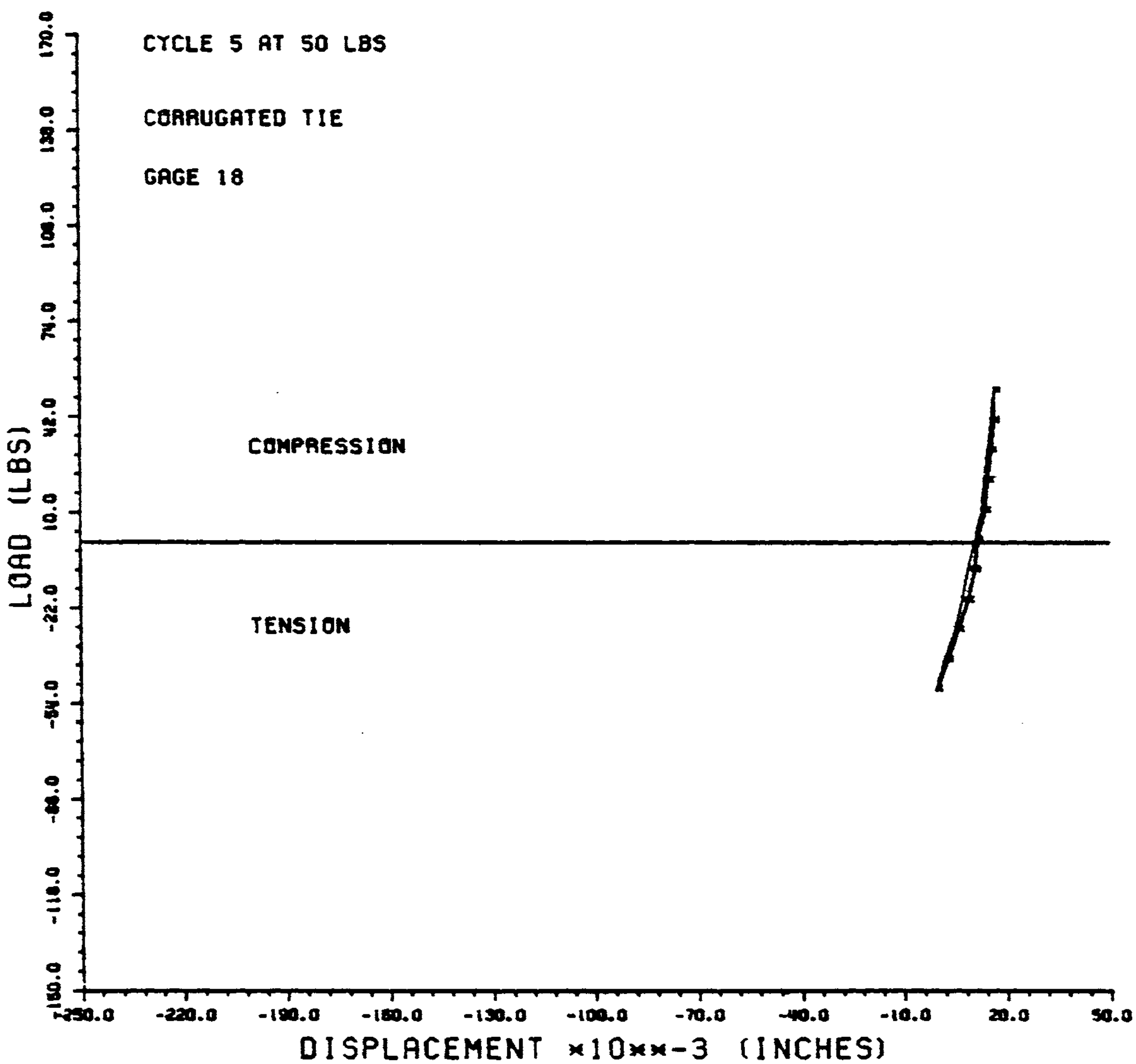

Figure A-5. Hysteresis Loop for Corrugated Tie Gage 18 at 50 lbs, with a = 5/8 in.

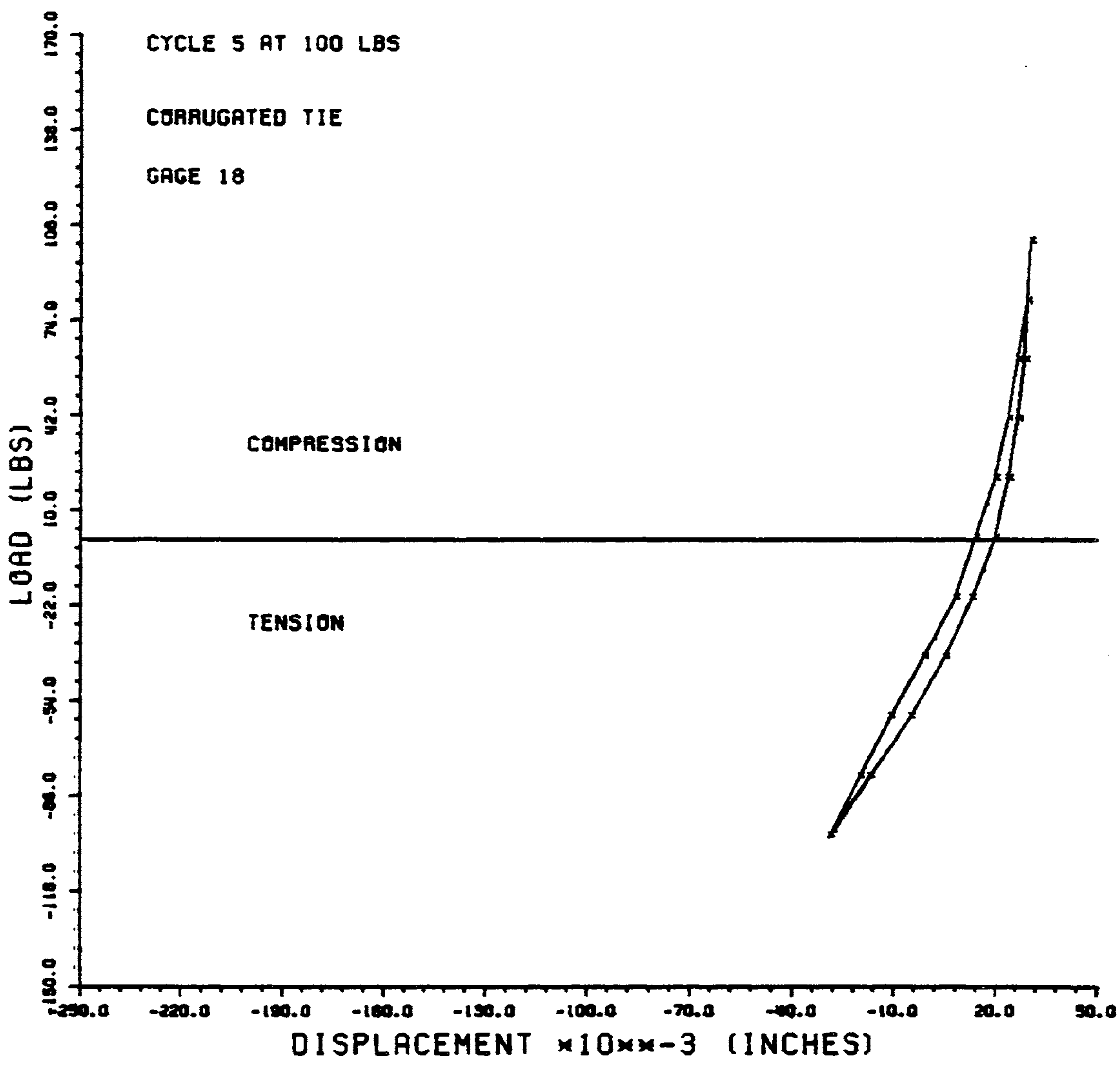

Figure A-6. Hysteresis Loop for Corrugated Tie Gage 18 at 100 lbs, with a = 5/8 in.

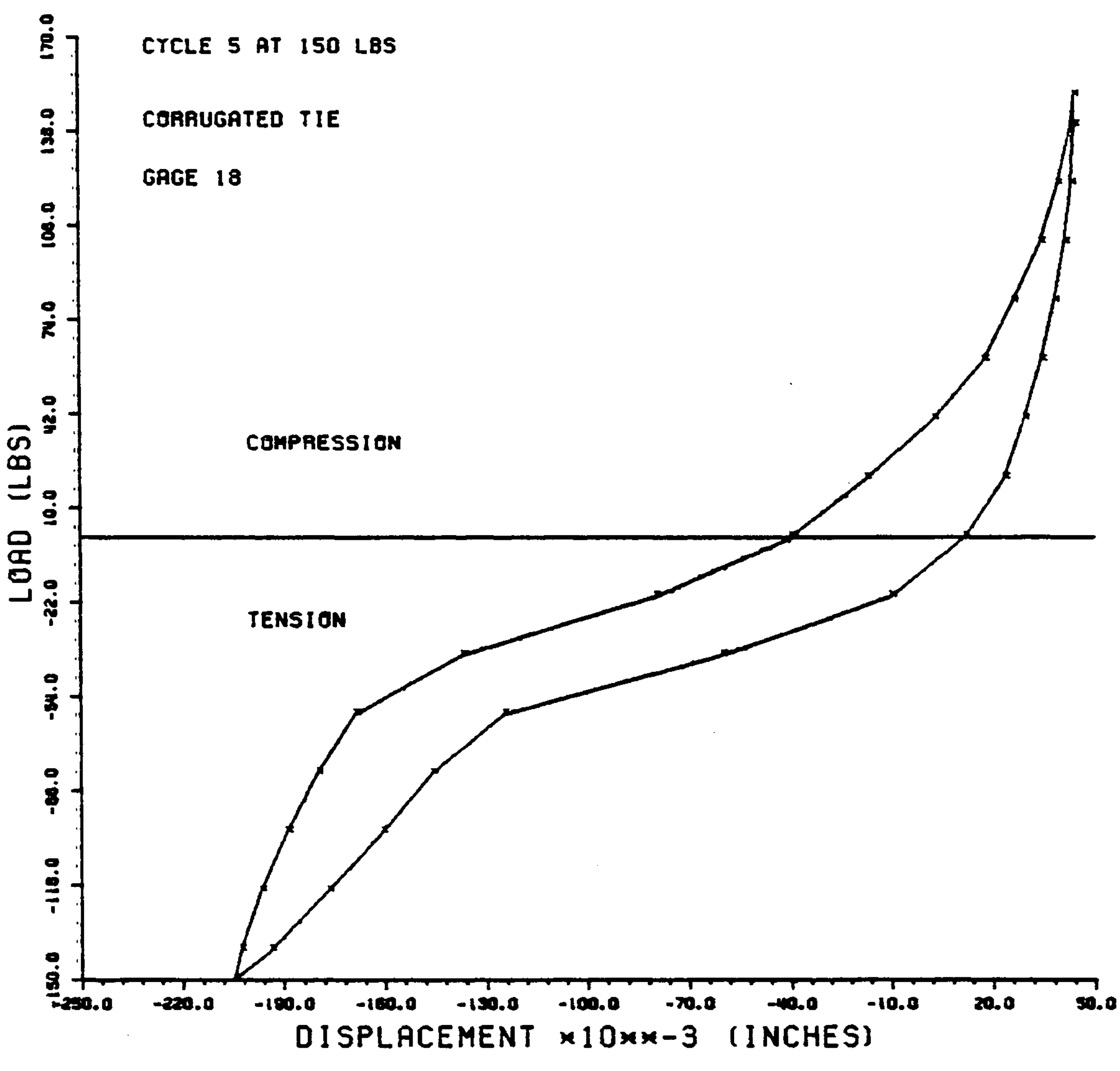

Figure A-7. Hysteresis Loop for Corrugated Tie Gage 18 at 150 lbs, with a = 5/8 in.

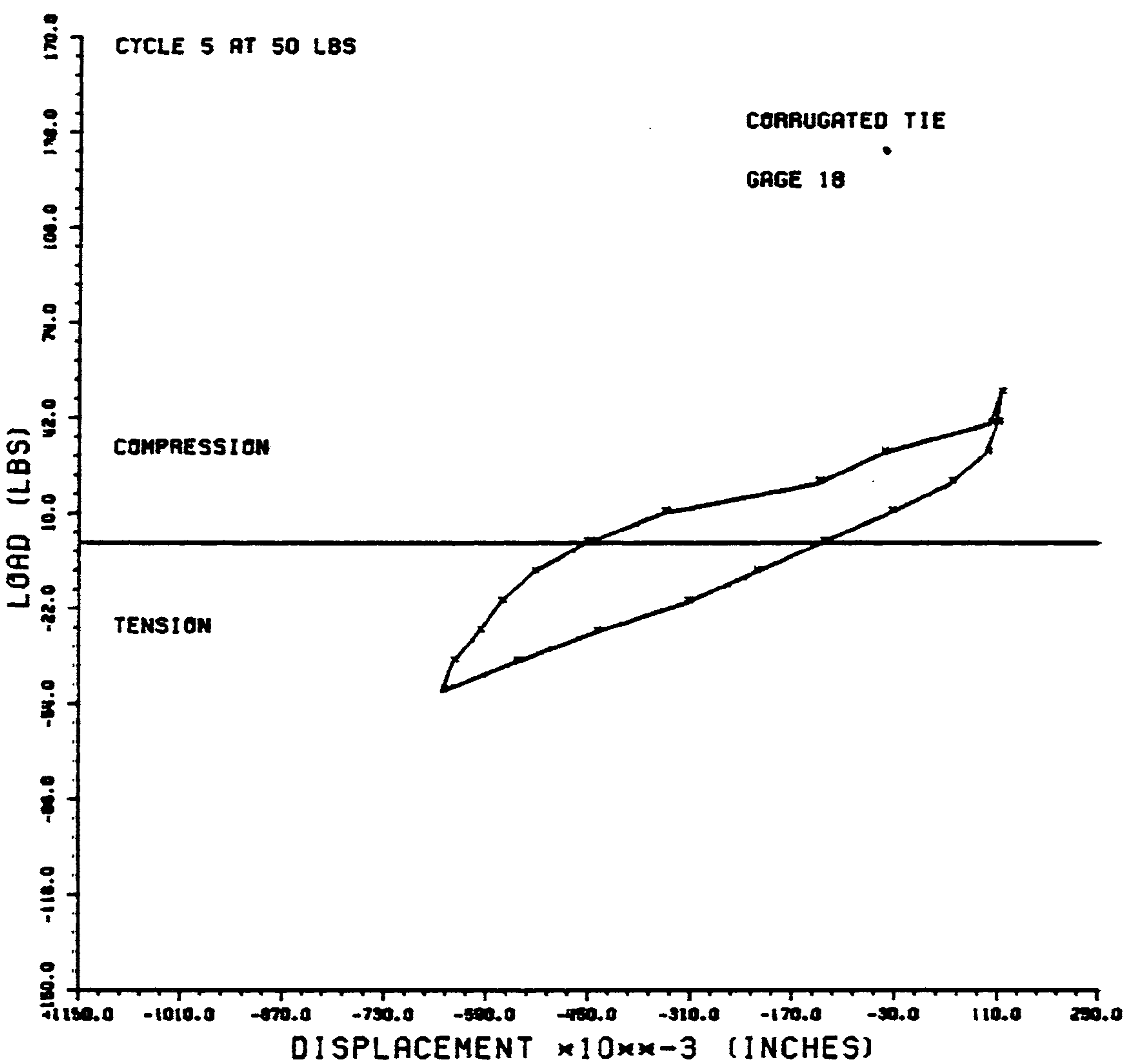

Figure A-8 Hysteresis Loop for Corrugated Tie Gage 18 at 50 lbs, with a = 2 in.

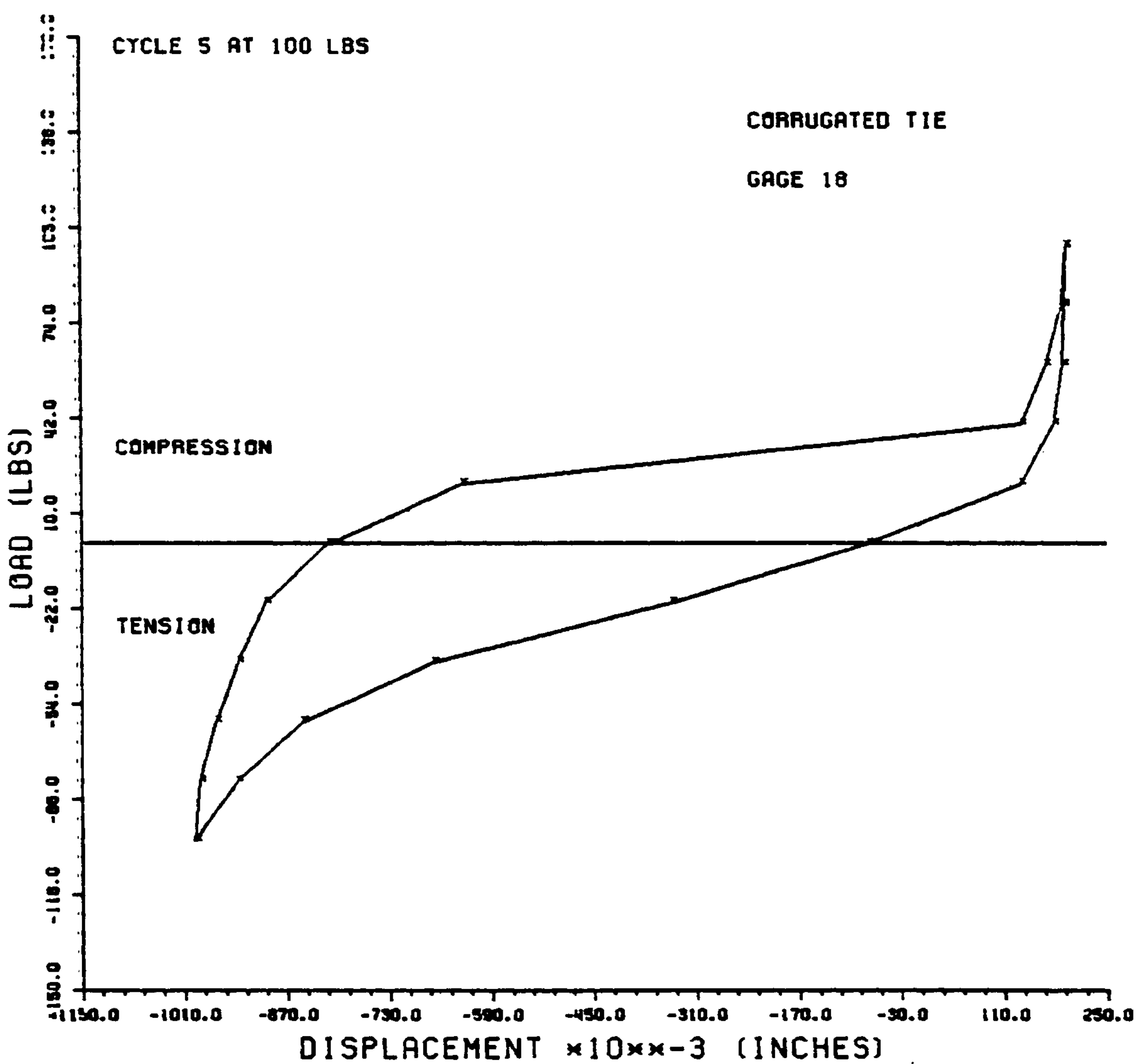

Figure A-9 Hysteresis Loop for Corrugated Tie Gage 18 at 100 lbs, with a = 2 in.

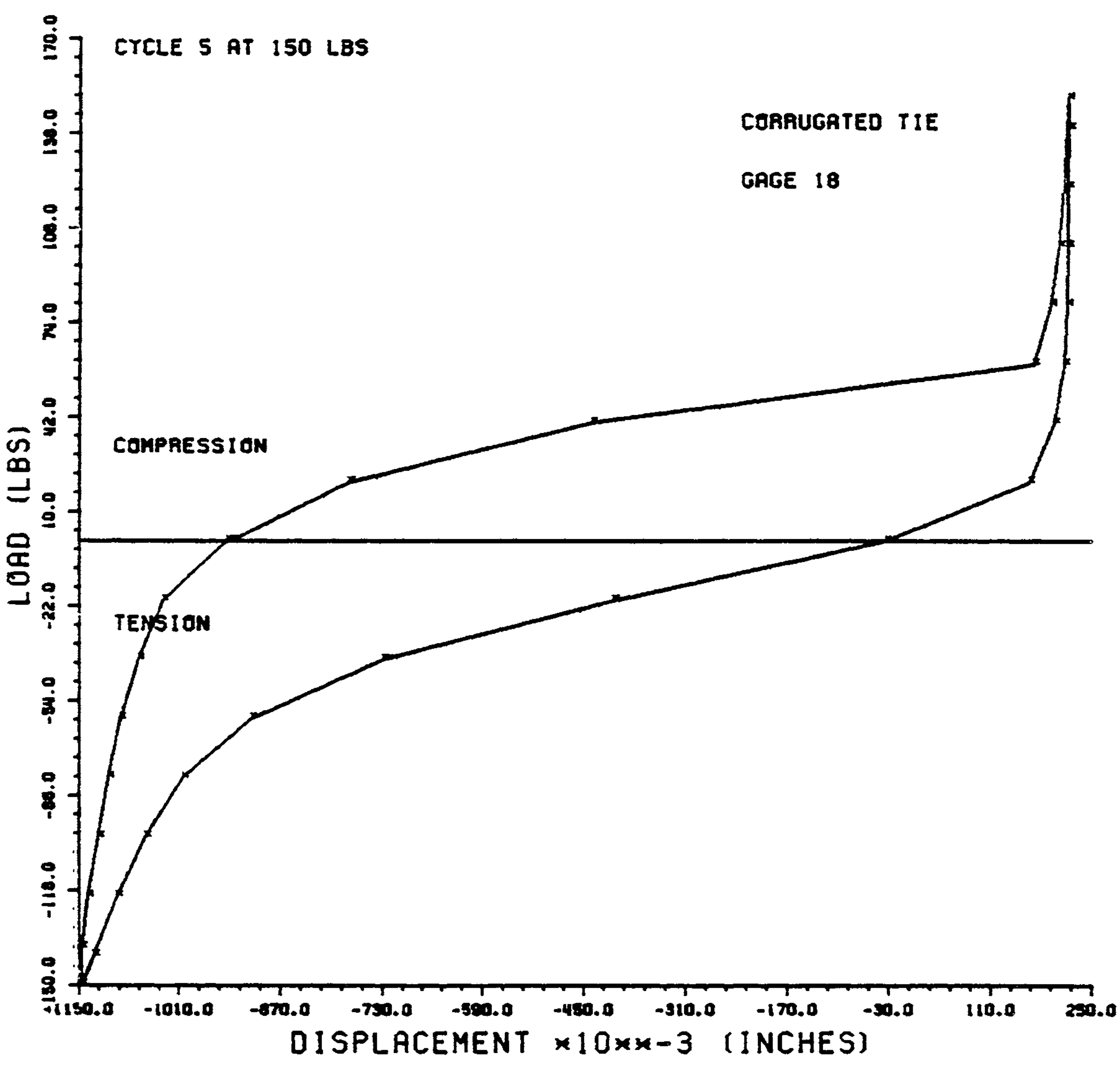

Figure A-10 Hysteresis Loop for Corrugated Tie Gage 18 at 150 lbs, with a = 2 in.

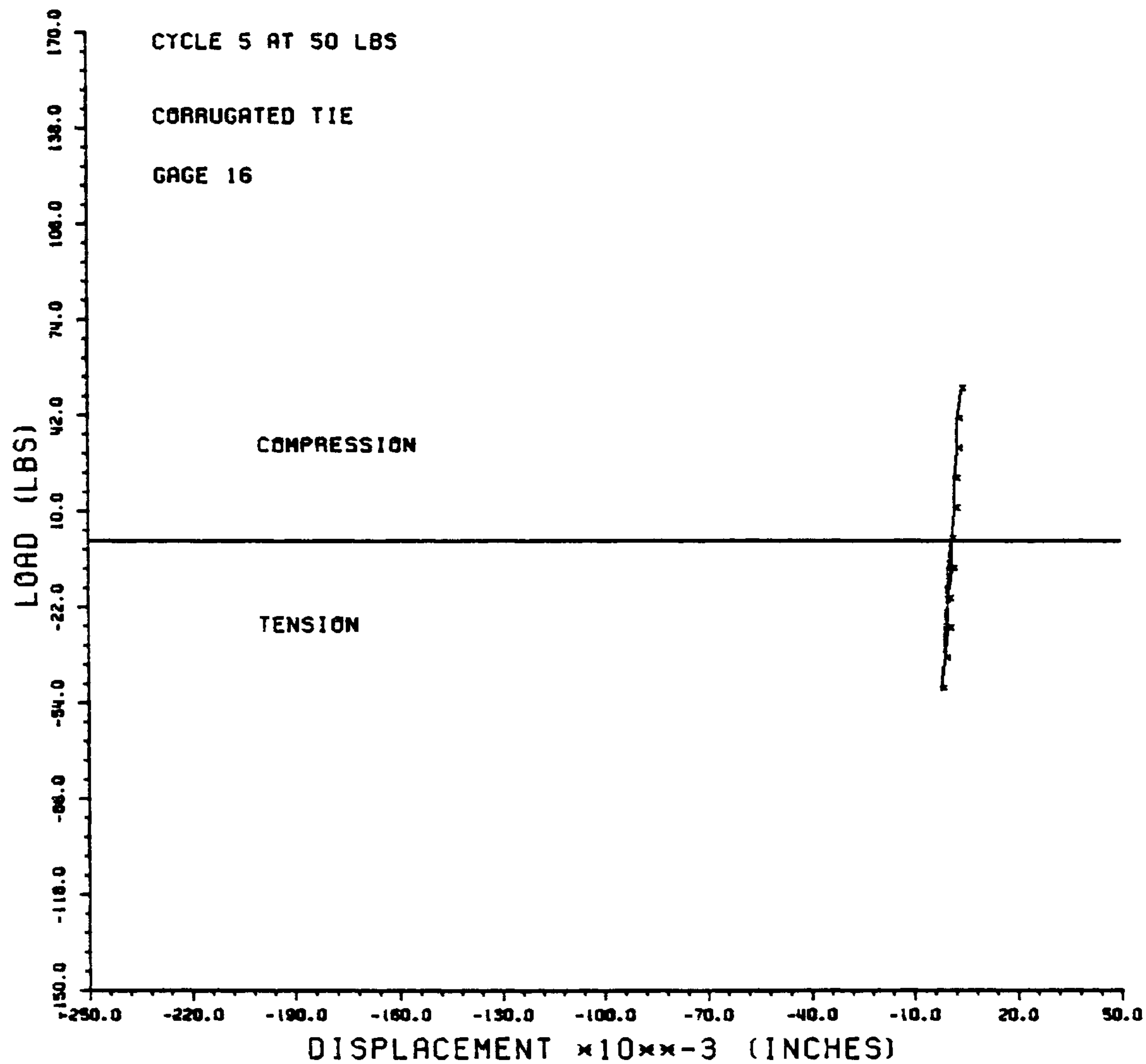

Figure A-11. Hysteresis Loop for Corrugated Tie ga 16 at 50 lbs.

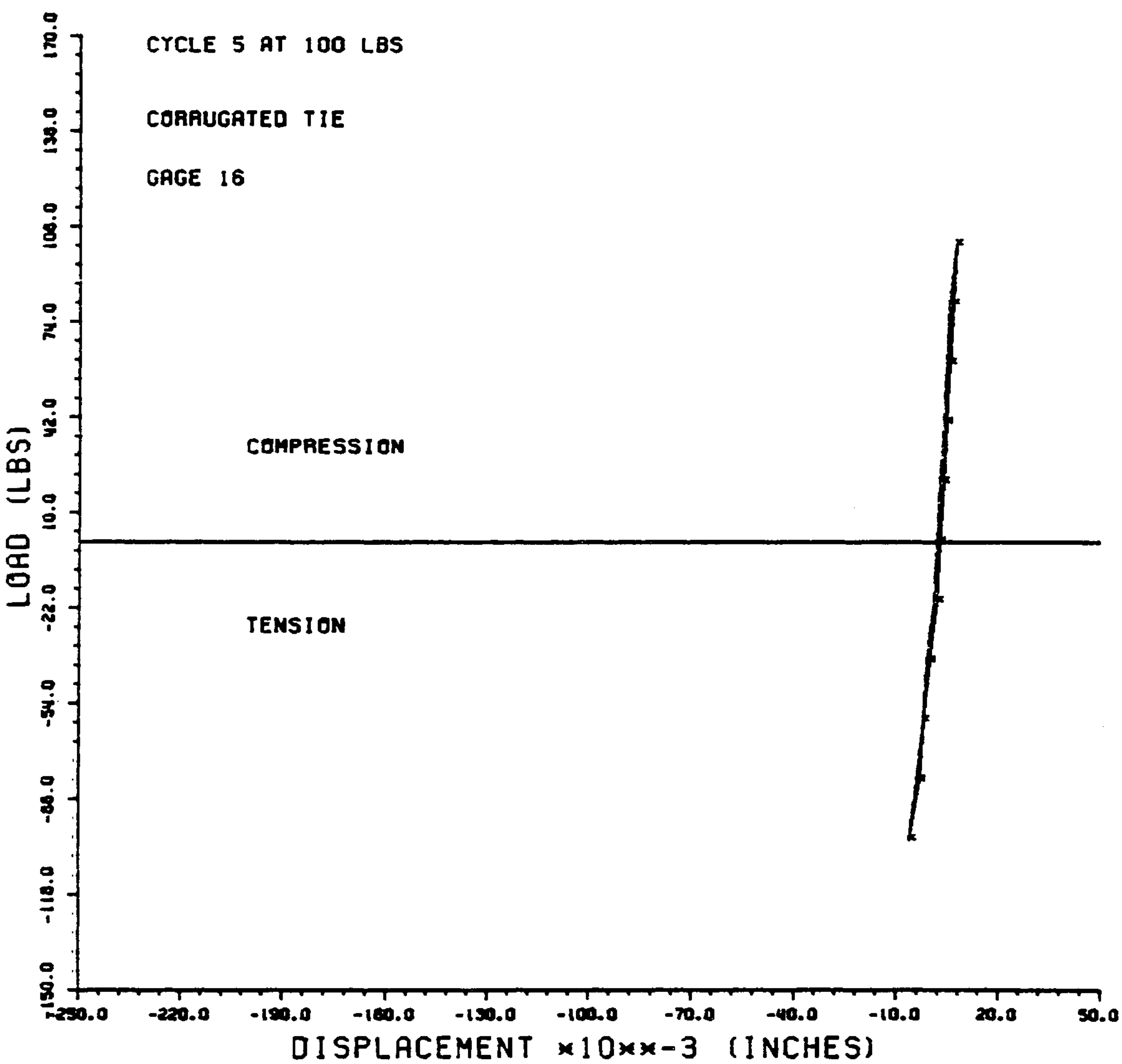

Figure A-12. Hysteresis Loop for Corrugated Tie ga 16 at 100 lbs.

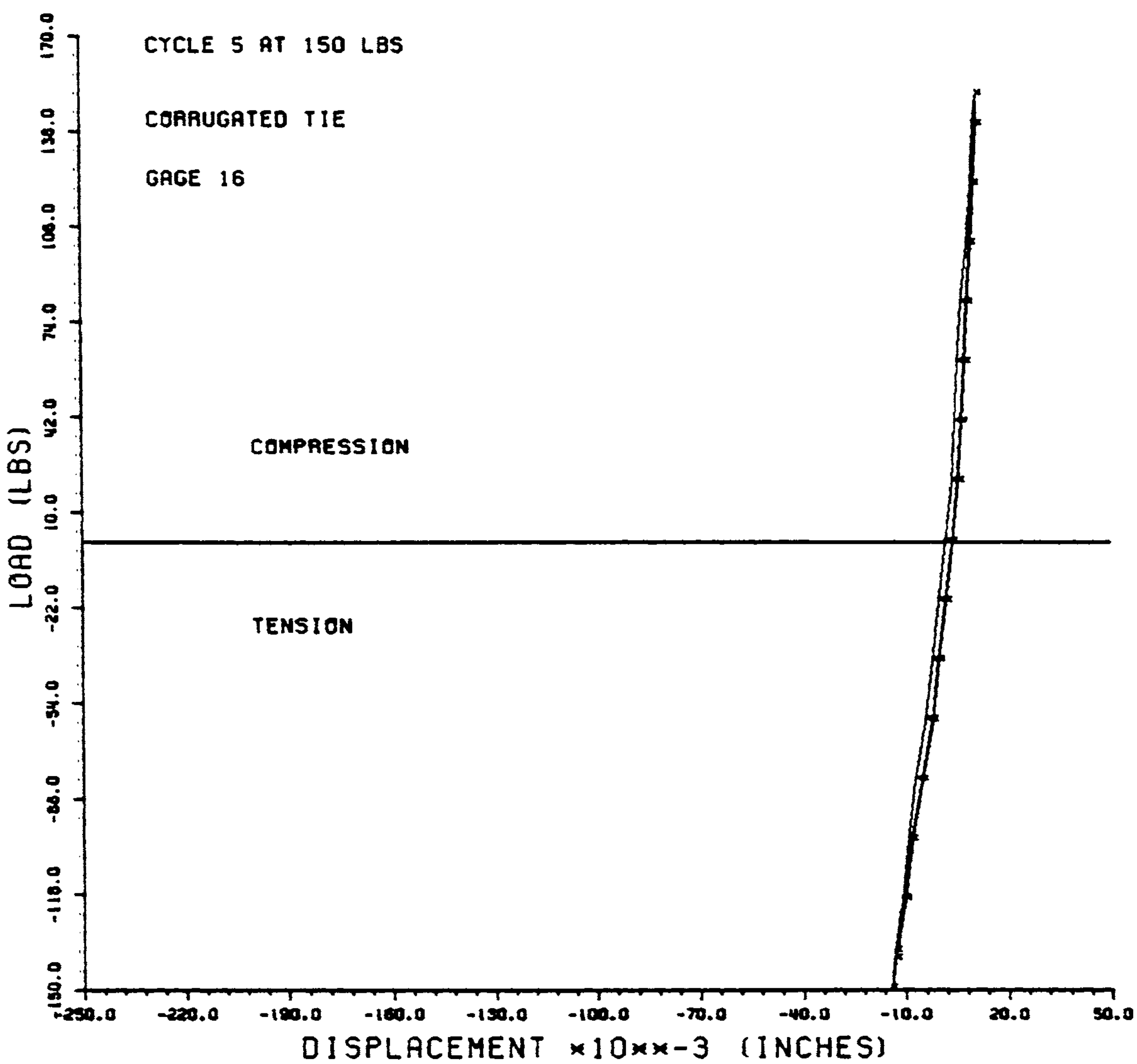

Figure A-13. Hysteresis Loop for Corrugated Tie ga 16 at 150 lbs.

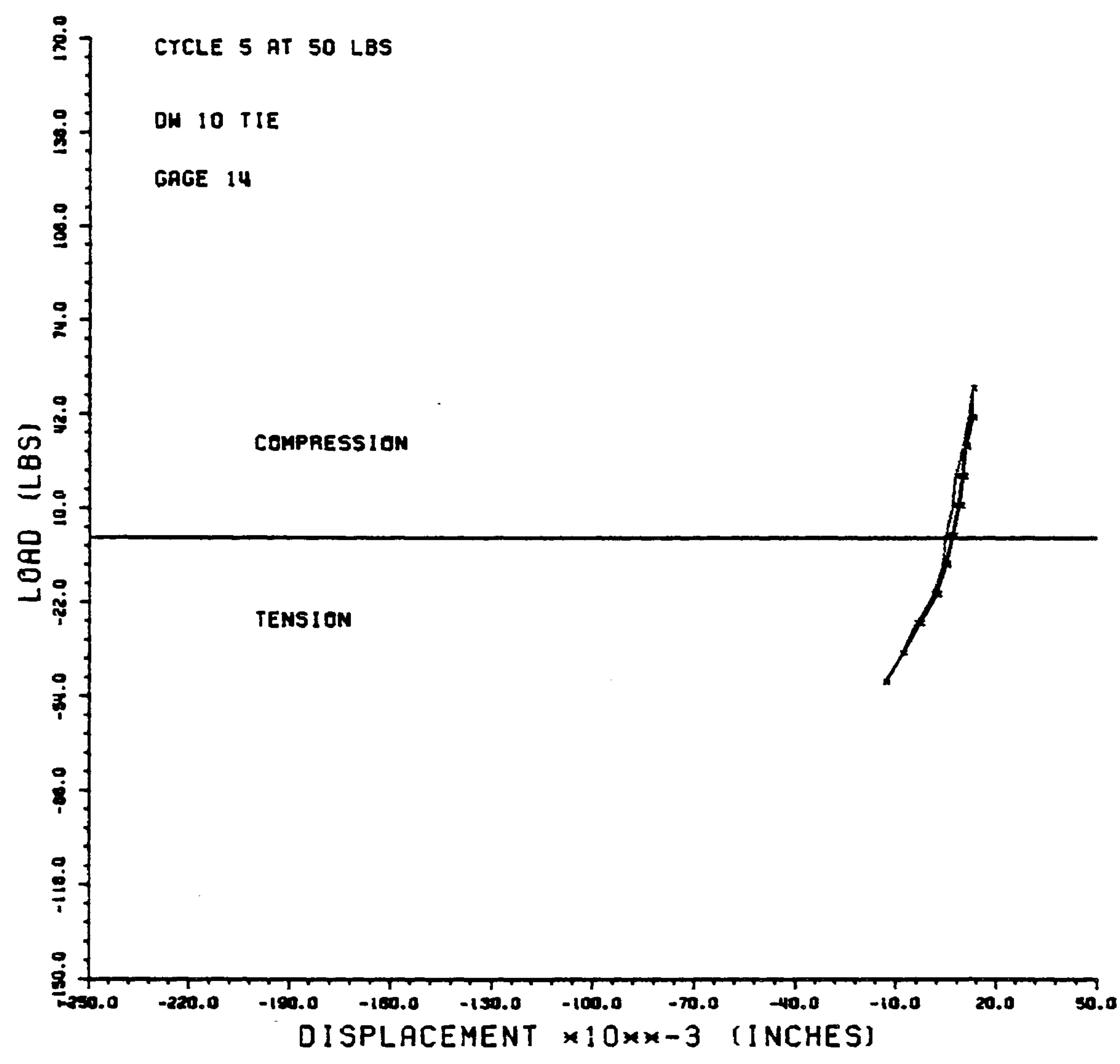

Figure A-14. Hysteresis Loop for DW 10 Tie Gage 14 at 50 lbs, with Wire Diameter = .188 in.

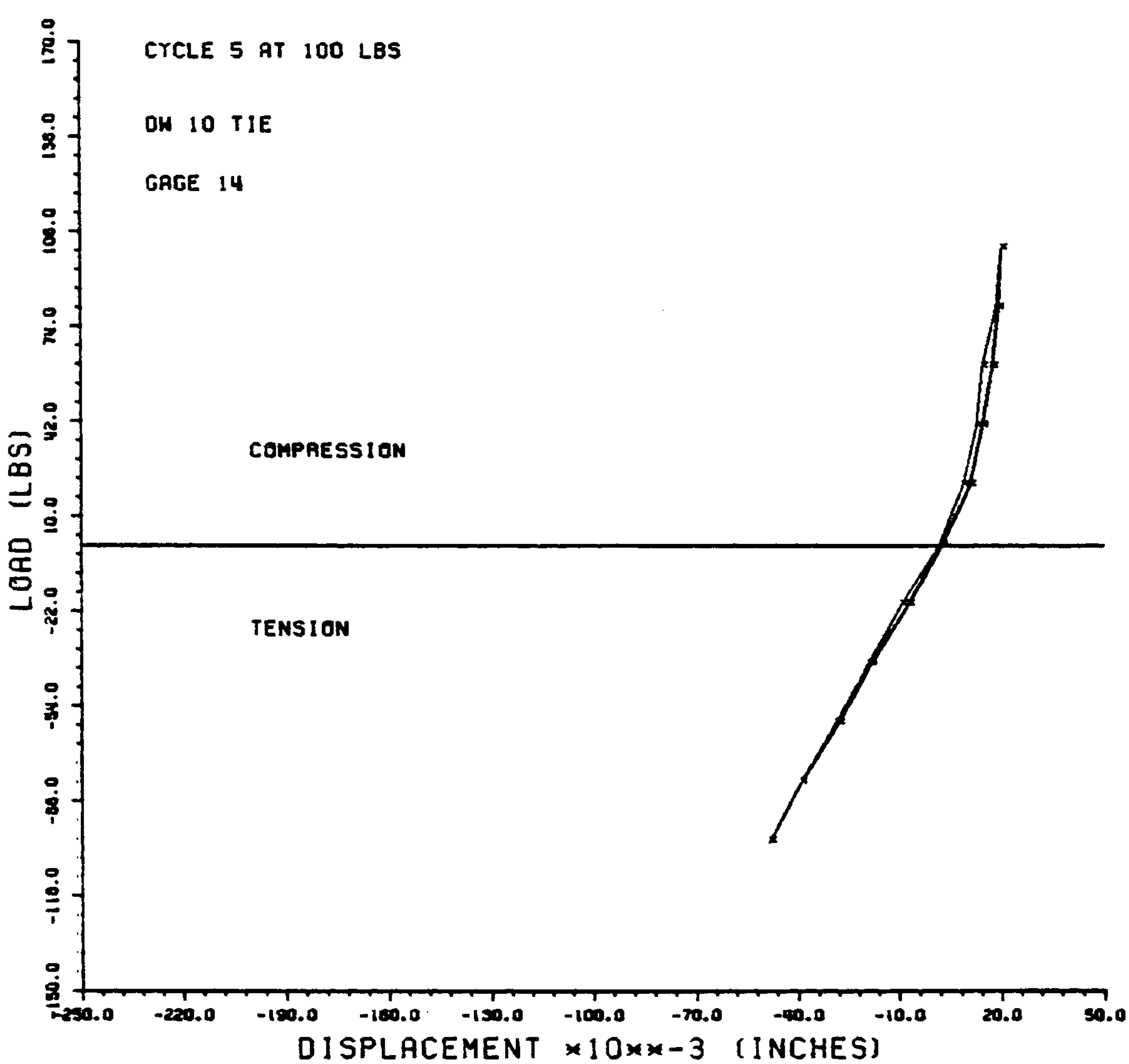

Figure A-15. Hysteresis Loop for DW 10 Tie Gage 14 at 100 lbs, with Wire Diameter = .188 in.

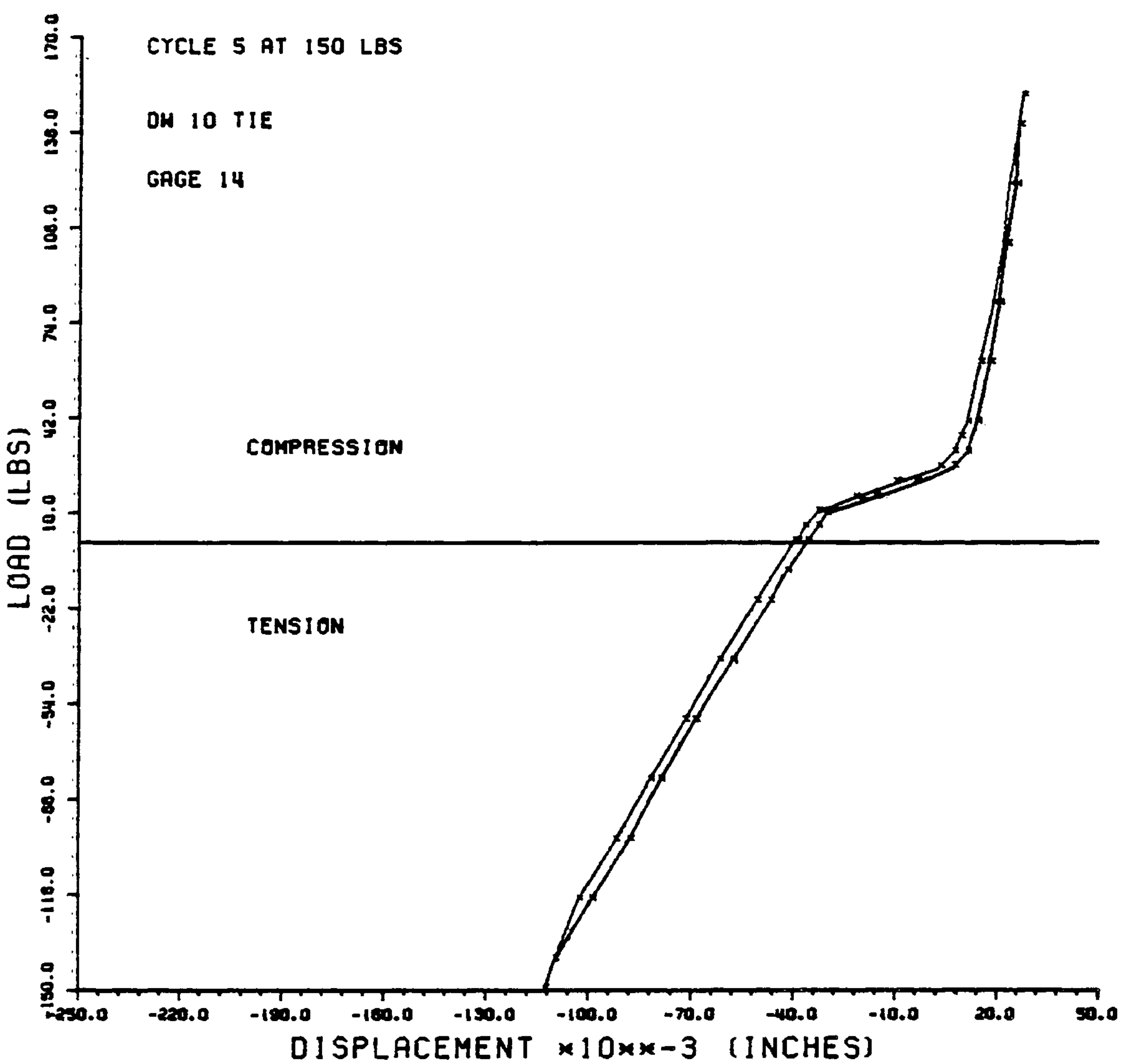

Figure A-16. Hysteresis Loop for DW 10 Tie Gage 14 at 150 lbs, with Wire Diameter = .188 in.

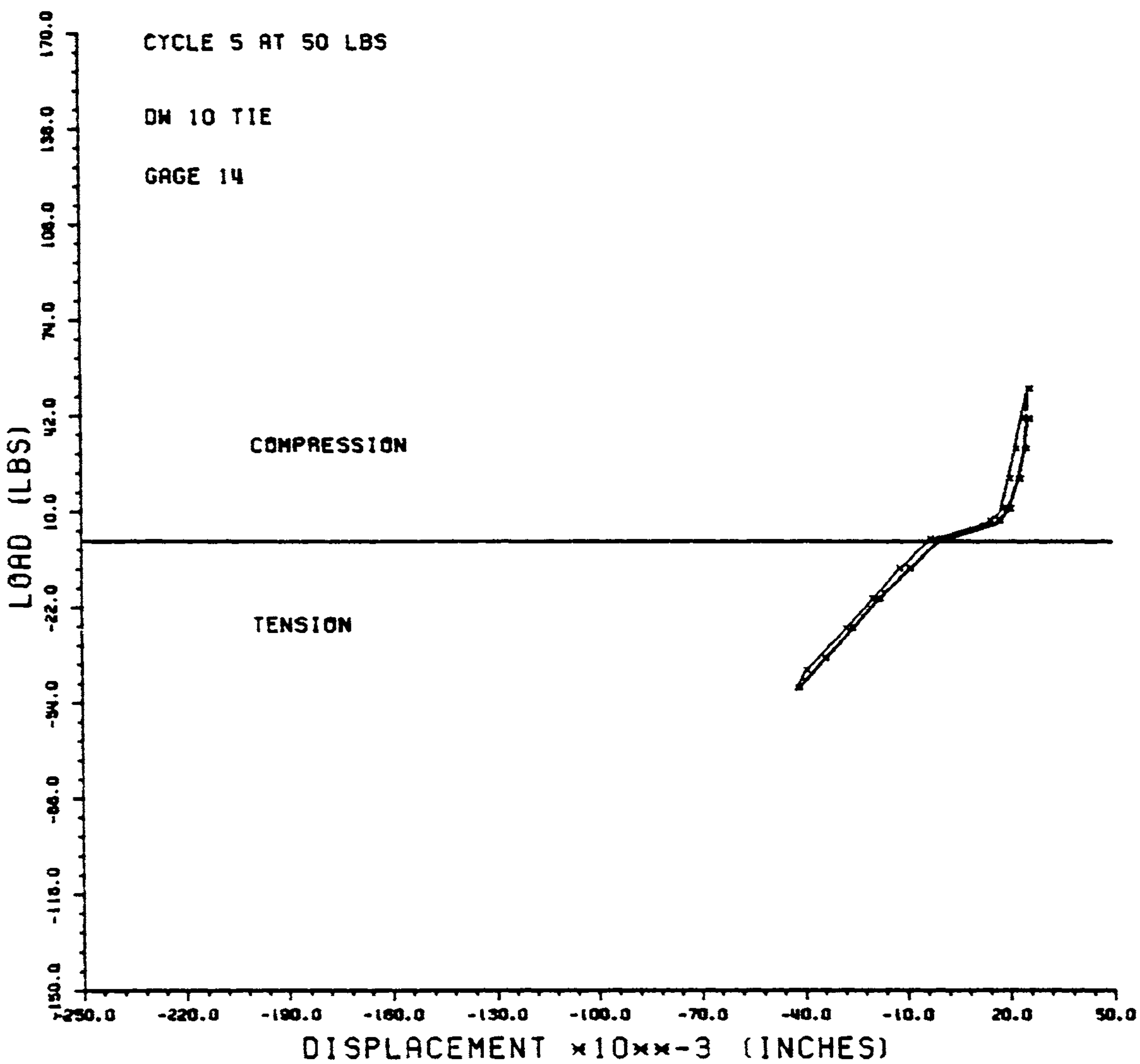

Figure A-17. Hysteresis Loop for DW 10 Tie Gage 14 at 50 lbs, with Wire Diameter = .172 in.

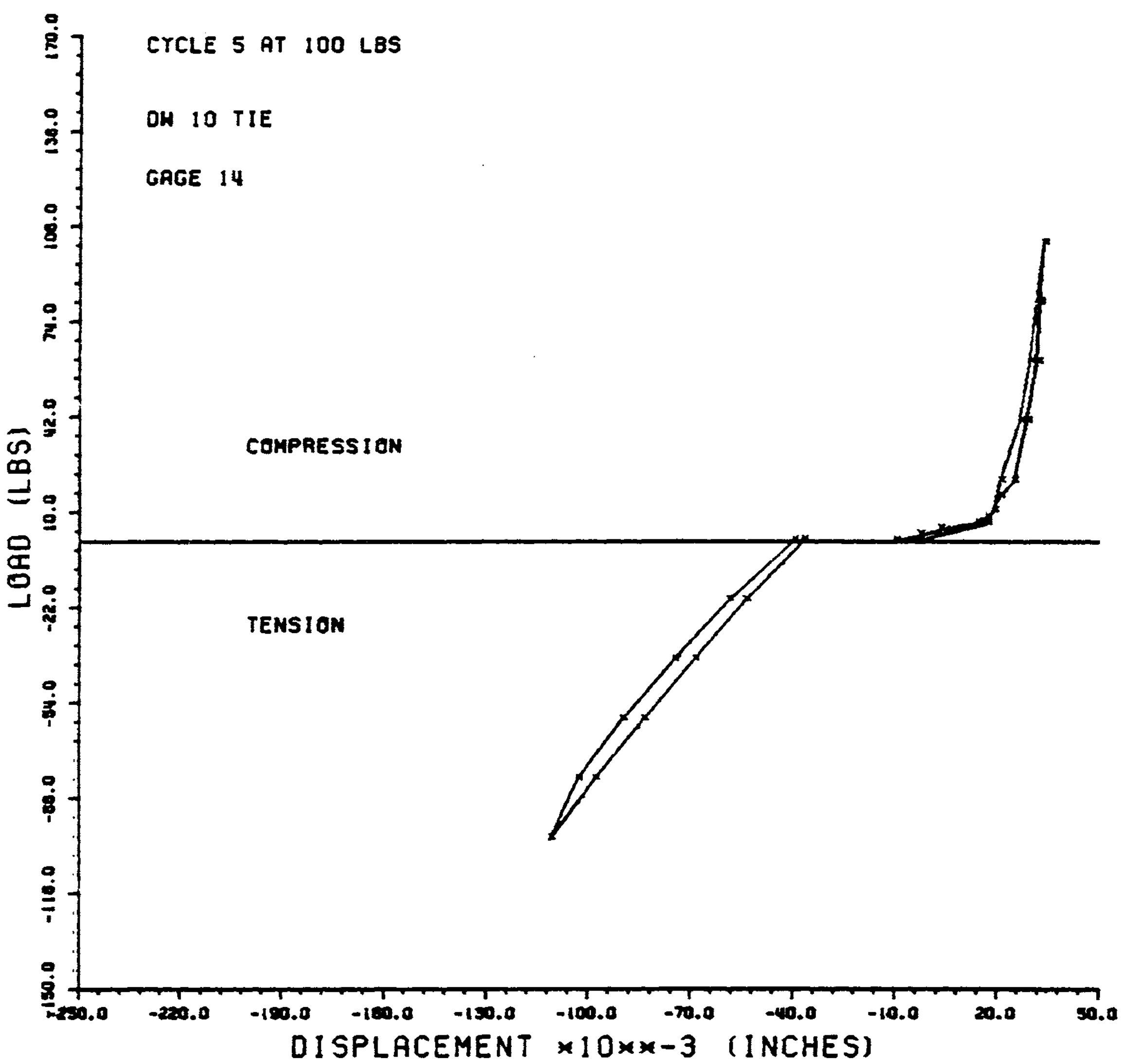

Figure A-18. Hysteresis Loop for DW 10 Tie Gage 14 at 100 lbs, with Wire Diameter = .172 in.

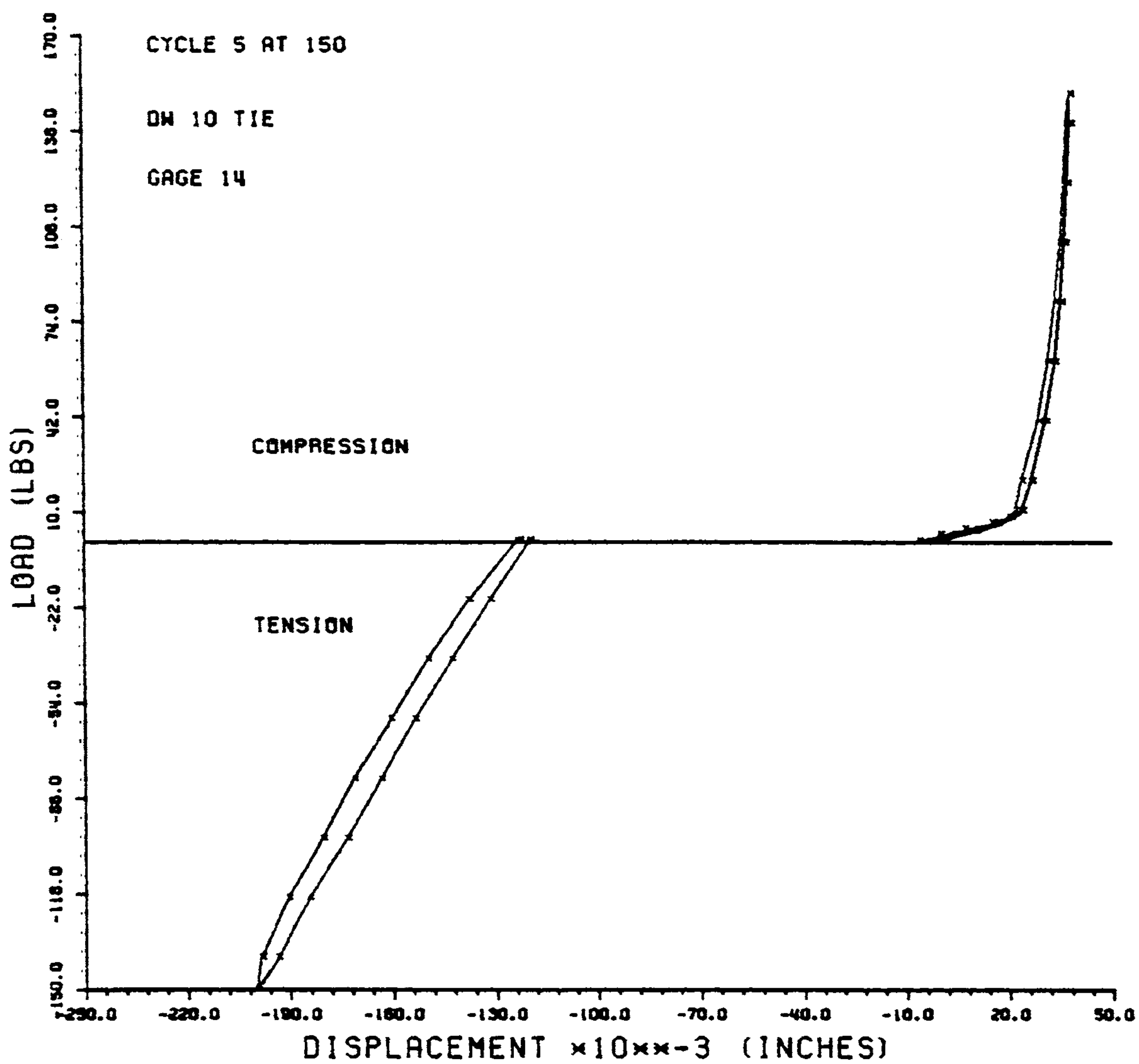

Figure A-19. Hysteresis Loop for DW 10 Tie Gage 14 at 150 lbs, with Wire Diameter = .172 in.

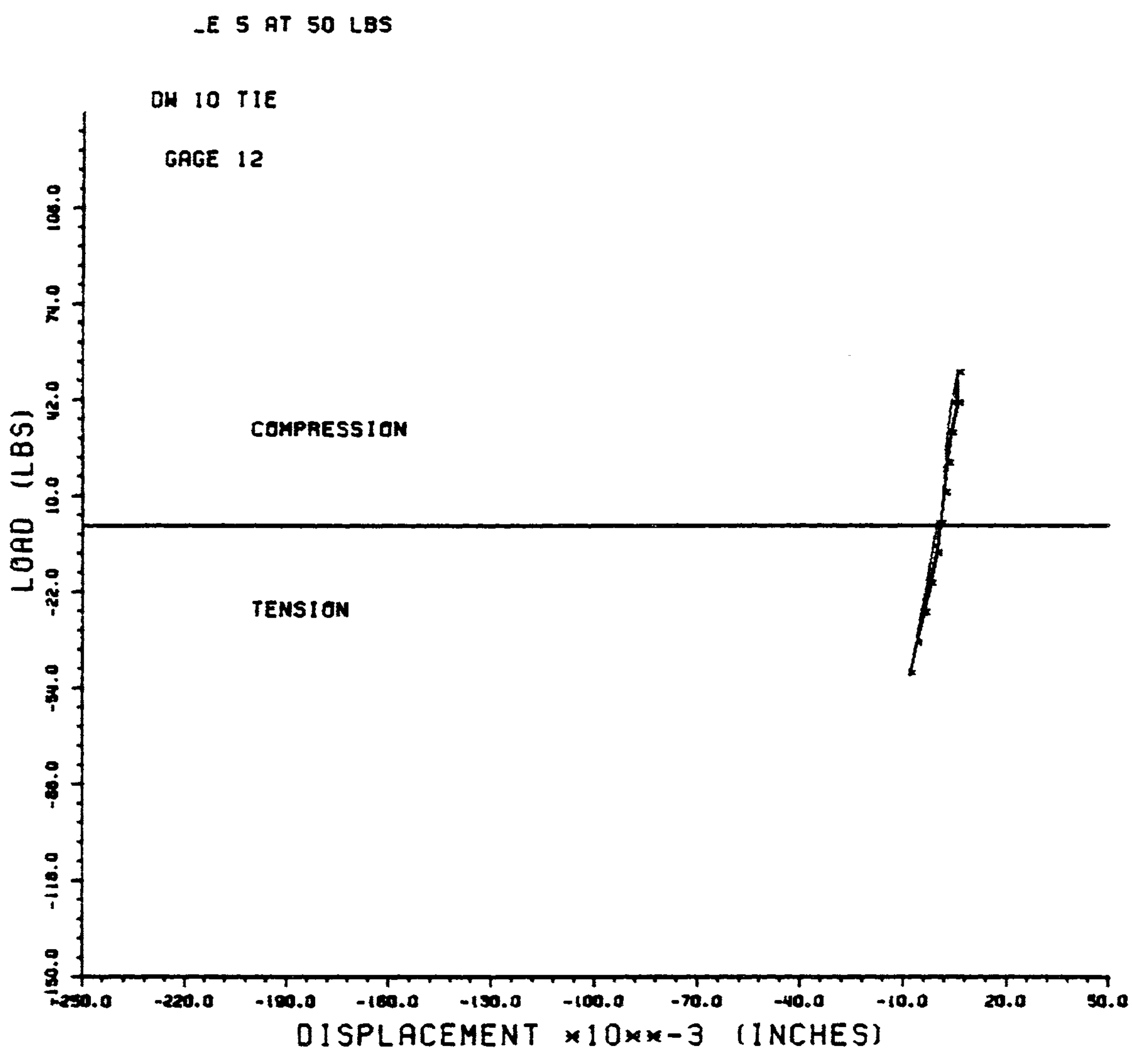

Figure A-20. Hysteresis Loop for DW 10 Tie ga 12 at 50 lbs.

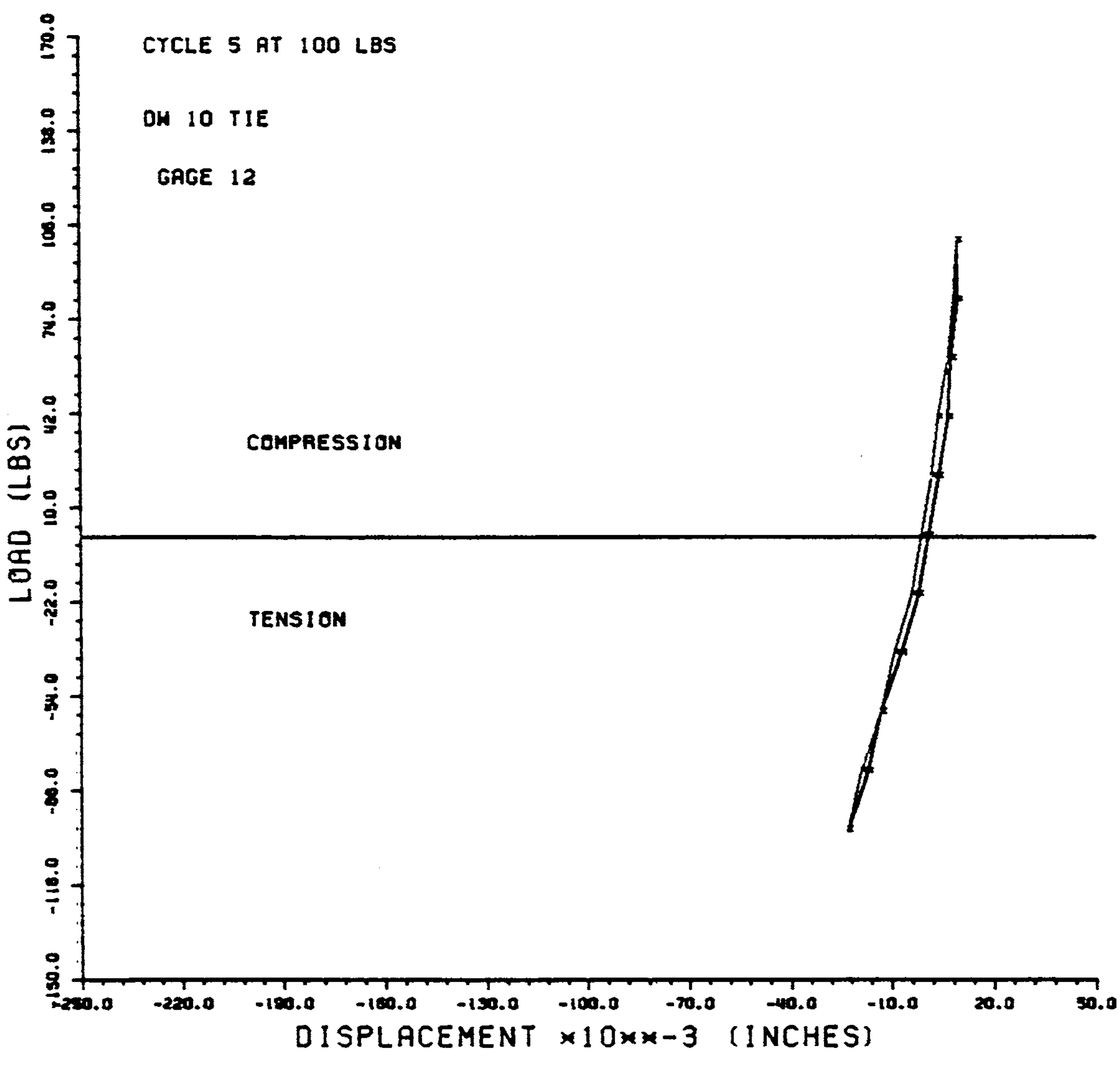

Figure A-21. Hysteresis Loop for DW 10 Tie ga 12 at 100 lbs.

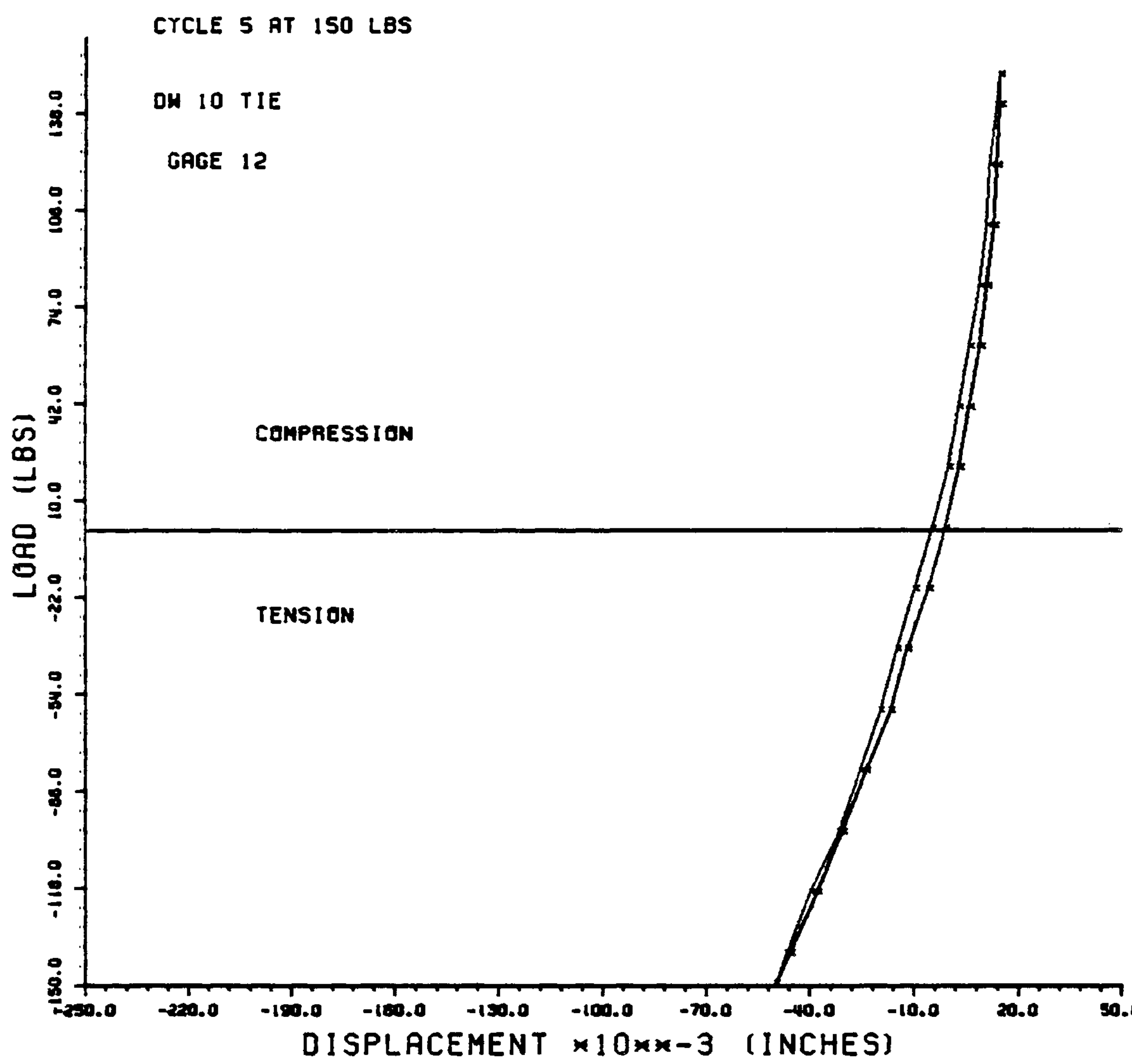

Figure A-22. Hysteresis Loop for DW 10 Tie ga 12 at 150 lbs.

Appendix B

Material Properties

Table B-I. Brick Properties

SAMPLE	COMPRESSIVE STRENGTH (PSI)	ABSORPTION (%) 5HR. COLD	24HR. COLD	5HR. BOIL	SATURATION COEFFICIENT	INITIAL RATE OF ABSORPTN. ($g/30in^2$)
1	16,920	5.28	5.33	7.35	.73	7.8
2	17,230	5.53	5.81	7.99	.73	13.5
3	18,720	5.57	5.80	7.95	.73	12.0
4	20,450	5.13	5.47	7.36	.74	9.5
5	20,110	5.02	5.28	7.27	.73	9.0
Average	18,680	5.30	5.54	7.58	.73	10.4

Table B-II. Stack Bond Prism Properties for Wall Nos. 1, 2 and 3.

	PRISM NO.	ULTIMATE LOAD (LBS)	STRESS ($LBS/IN.^2$)
	1	116,000	4,070
COMPRESSION	2	108,000	3,789
	3	121,000	4,246
	AVERAGE	114,990	4,035
	COEF. OF VAR.	5.7%	5.7%
	1	485	79
BENDING	2	487	79
	3	670	108
	AVERAGE	547	89
	COEF. OF VAR.	19.41%	18.53%

Table B-III. Mortar Properties for Wall Nos. 1, 2 and 3 (Batch No. 6).

MORTAR CUBES

	CUBE NO.	MAX. LOAD (LBS)	STRESS (LBS/IN.^{2})
	1	12,190	3,048
COMPRESSION	2	12,300	3,075
	3	11,700	2,925
	AVERAGE	12,063	3,016
	COEF. OF VAR.	2.6%	2.6%

Table B-IV. Mortar Properties for Wall Nos. 1, 2 and 3 (Batch No. 8).

MORTAR CUBES

	CUBE NO.	MAX. LOAD (LBS)	STRESS (LBS/IN^2)
	1	12,400	3,100
COMPRESSION	2	12,460	3,150
	3	13,000	3,250
	AVERAGE	12,667	3,167
	COEFF. OF VAR.	2.4%	2.4%
	4	1,600	180
TENSION	5	2,125	239
	6	1,450	163
	AVERAGE	1,725	194
	COEFF. OF VAR.	20.5%	20.5%

MORTAR CYLINDERS

	CYLINDER NO.	MAX. LOAD (LBS)	STRESS (LBS/IN.^{2})
	1	7,200	2,292
COMPRESSION	2	6,400	2,037
	3	6,900	2,196
	AVERAGE	6,833	2,175
	COEFF. OF VAR.	5.9%	5.9%
	4	3,800	302
TENSION	5	2,600	207
	6	4,100	326
	AVERAGE	3,500	278
	COEFF. OF VAR.	22.7%	22.7%

Table B-V. Mortar Air Content for Wall Nos. 1, 2 and 3.

BATCH NO.	INIT. FLOW (%)	FLOW AFTER SUCTION (%)	AIR CONTENT (%)
1	113.	89.8	(-)[a]
2	125.	83.0	(-)[a]
3	122.	79.0	4.4
4	113.	(-)[a]	(-)[a]
5	106.	(-)[a]	(-)[a]
6	119.	(-)[a]	6.0
7	119.	(-)[a]	(-)[a]
8	113.	(-)[a]	(-)[a]

a ___ indicates that the test was not performed

Table B-VI. Prism Properties for Wall Nos. 4, 5 and 6.

	PRISM NO.	INI. CRA. LOAD (LBS)	ULTIMATE LOAD (LBS)	STRESS (LBS/IN.^{2})
	1	90,000	158,000	5,544
COMPRESSION	2	-	146,000	5,123
	3	58,000	138,000	4,842
	AVERAGE		147,000	5,170
	COEFF. OF VAR.		6.83%	6.83%
	1	-	800	129.6
BENDING	4	-	1,120	151.9
	6	-	900	132.6
	AVERAGE	-	940	138.0
	COEFF. OF VAR.	-	17.42%	16.33%

Table B-VII. Mortar Properties for Wall Nos. 4, 5 and 6 (Batch No. 3).

MORTAR CUBES

	CUBE NO.	MAX. LOAD (LBS)	STRESS (LBS/IN.^{2})
	1	7,340	1,835
COMPRESSION	2	6,140	1,535
	3	7,600	1,900
	AVERAGE	7,027	1,757
	COEFF. OF VAR.	11.08%	11.08%
	4	1,950	219
TENSION	5	1,960	221
	6	1,400	158
	AVERAGE	1,770	199
	COEFF. OF VAR.	18.11%	18.11%

MORTAR CYLINDERS

	CYLINDER NO.	MAX. LOAD (LBS)	STRESS (LBS/IN.^{2})
	1	4,620	1,471
COMPRESSION	2	5,140	1,636
	3	5,040	1,604
	AVERAGE	4,933	1,570
	COEFF. OF VAR.	5.59%	5.59%
	4	3,710	295
TENSION	5	2,810	224
	6	3,620	288
	AVERAGE	3,380	269
	COEFF. OF VAR.	14.67%	14.67%

Table B-VIII. Mortar Properties for Wall Nos. 4, 5 and 6 (Batch No. 7).

MORTAR CUBES

	CUBE NO.	MAX. LOAD (LBS)	STRESS (LBS/IN.^{2})
	1	8,040	2,020
COMPRESSION	2	9,420	2,355
	3	9,300	2,325
	AVERAGE	8,920	2,230
	COEFF. OF VAR.	8.57%	8.57%
	4	2,045	230
TENSION	5	1,970	222
	6	1,900	214
	AVERAGE	1,972	222
	COEFF. OF VAR.	3.68%	3.68%

MORTAR CYLINDERS

	CYLINDER NO.	MAX. LOAD (LBS)	STRESS (LBS/IN.^{2})
	1	5,630	1,792
COMPRESSION	2	5,800	1,846
	3	5,360	1,706
	AVERAGE	5,597	1,781
	COEFF. OF VAR.	3.96%	3.96%
	4	4,235	337
TENSION	5	3,700	295
	6	2,435	197
	AVERAGE	3,457	275
	COEFF. OF VAR.	26.74%	26.74%

Table B-IX. Mortar Air Content for Wall Nos. 4, 5 and 6.

BATCH NO.	FLOW (%)	FLOW AFTER SUCTION (%)	AIR CONTENT (%)
1	106.	-	-
2	106.	-	-
3	110.	83.0	5.6
4	125.	-	-
5	113.	-	-
6	100.	-	-
7	107.	79.0	5.4

Table B-X. Tensile Stress at Failure Loads (psi) Using the Bond Wrench Method for Wall Nos. 1, 2 and 3

PRISM NO.	1	2	3	4	5	6
JOINT [c]						
1	120.2	117.8	112.6	90.0	80.0	148.8
2	122.2	125.4	136.7	183.4	169.3	98.5
3	85.2	75.5	112.2	108.9	152.8	127.1
4	(79.20)[a]	(79.50)[a]	(107.8)[a]	75.5	133.5	75.1
5	55.4	111.4	182.2	(-)[b]	118.2	76.3
6	26.0	67.5	117.4	113.4	48.2	70.3

a ____ Stress at failure load by ASTM E518

b ______ This joint failed while testing joint 4

c ______ Joint 1 refers to the top bed joint in a prism

Table B-XI. Tensile Stress at Failure Loads (psi) Using the Bond Wrench Method for Wall Nos. 4, 5 and 6

PRISM NO.	1	2	3	4	5	6
JOINT [c]						
1	119.8	161.7	190.7	230.9	201.1	179.0
2	(129.6)[a]	177.8	166.5	148.8	174.6	190.7
3	181.8	(-)[b]	160.9	(151.9)[a]	(-)[b]	(132.6)
4	144.0	146.4	176.2	205.9	244.6	157.6
5	184.2	131.9	125.8	148.0	140.7	158.5

a ____ Stress at failure load by ASTM E518

b ______ This joint failed while testing joint 4

c ______ Joint 1 refers to the top bed joint in a prism

Table B-XII. The Bond Wrench and ASTM E518 Methods on Wall 1,2 and 3.

(a). BOND WRENCH METHOD: STATISTICAL CALCULATIONS PER PRISM.

PRISM	n	MEAN (LBS)	STANDARD DEVIATION (LBS)	COEFFICIENT OF VARIATION (%)
1	5	101.8	51.70	50.8
2	5	124.3	32.00	25.7
3	5	164.4	36.88	22.4
4	5	142.1	51.58	36.3
5	6	145.5	56.66	38.9
6	6	123.6	39.95	32.3

(b). BOND WRENCH METHOD: STATISTICAL CALCULATIONS PER JOINT.

JOINT [c]	n	MEAN (LBS)	STANDARD DEVIATION (LBS)	COEFFICIENT OF VARIATION (%)
1	6	138.75	30.24	21.8
2	6	173.16	39.29	22.7
3	6	137.58	34.23	24.9
4	3	117.83	41.71	35.4
5	5	135.20	60.18	44.5
6	6	91.83	44.64	48.6

c ______ Joint 1 refers to the top bed joint in a prism

Appendix C

Lateral Deflection Plots for the Walls Tested.

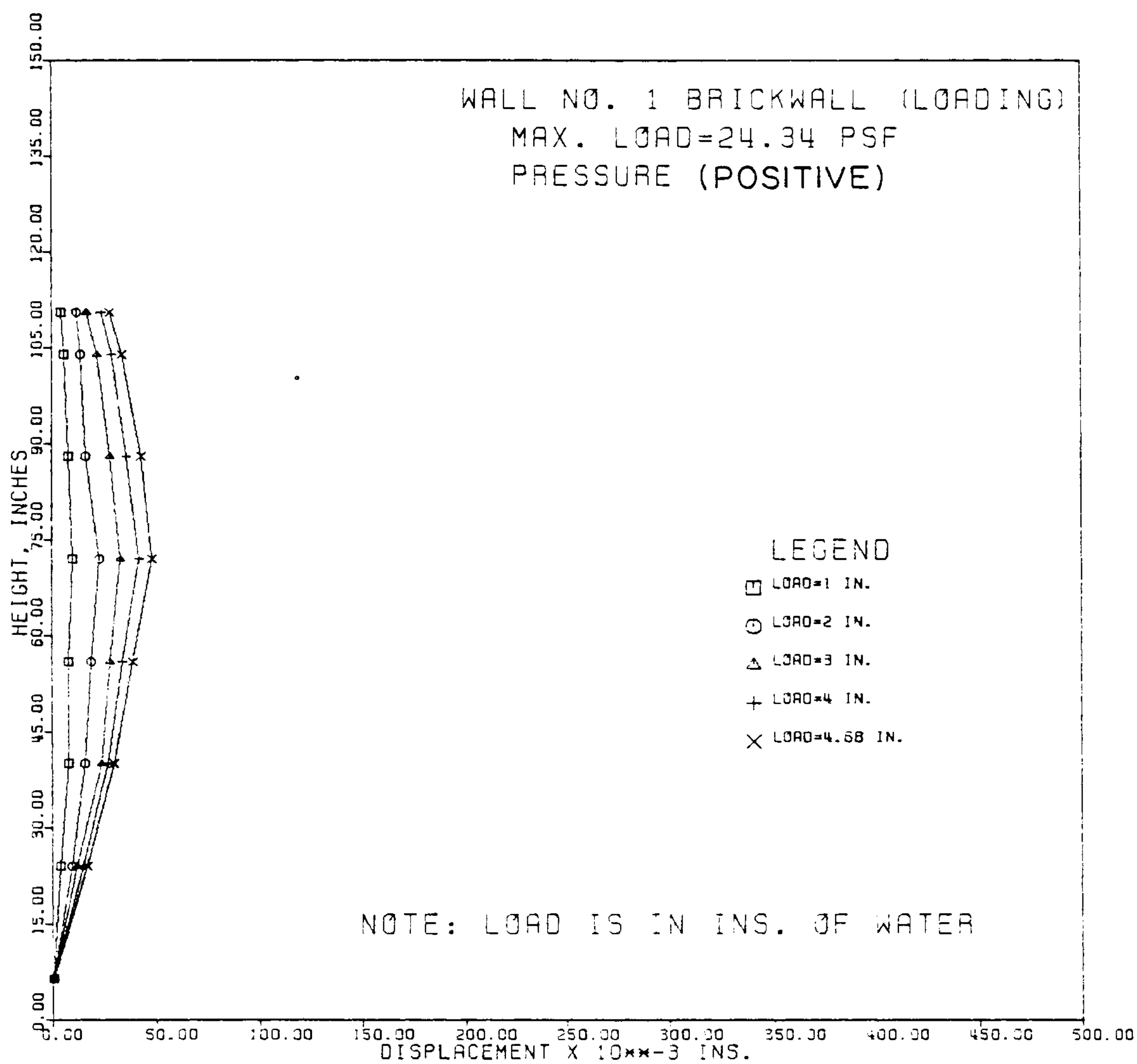

Figure C-1. Brickwall Lateral Deflection for Wall No. 1 at Design Load.

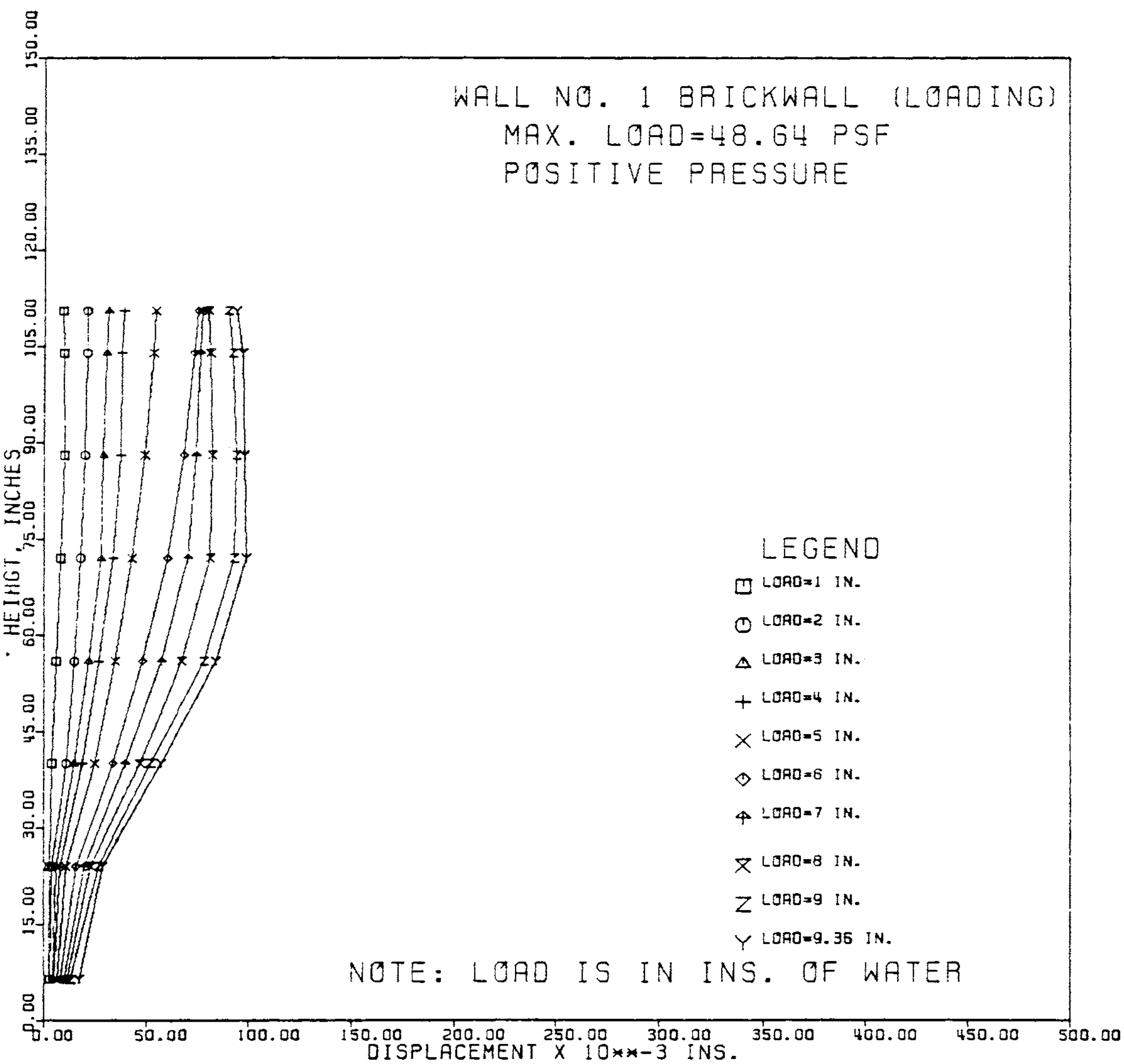

Figure C-2. Brickwall Lateral Deflection for Wall No. 1 at Twice Design Load.

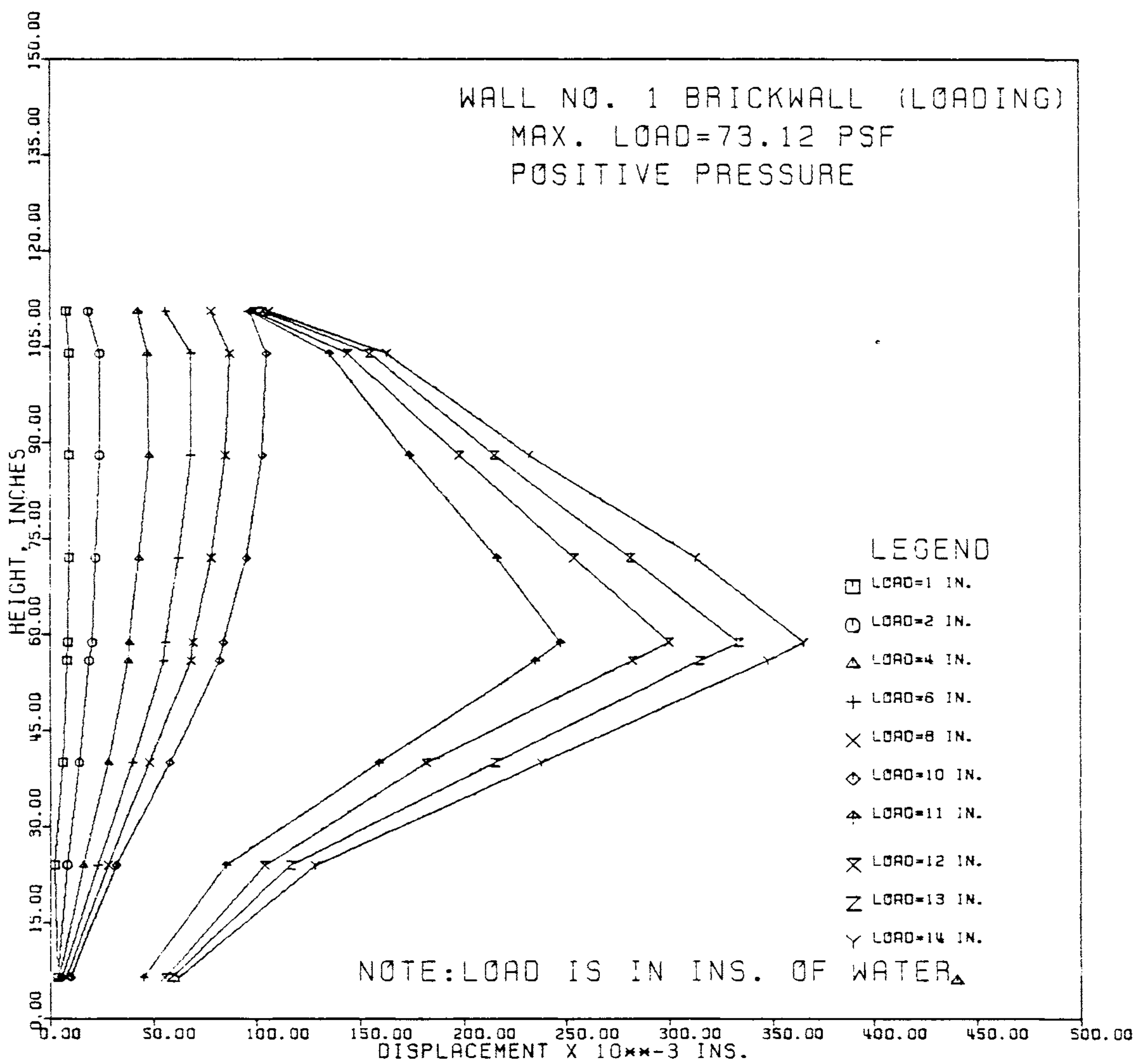

Figure C-3. Brickwall Lateral Deflection for Wall No. 1 at Three Times Design Load.

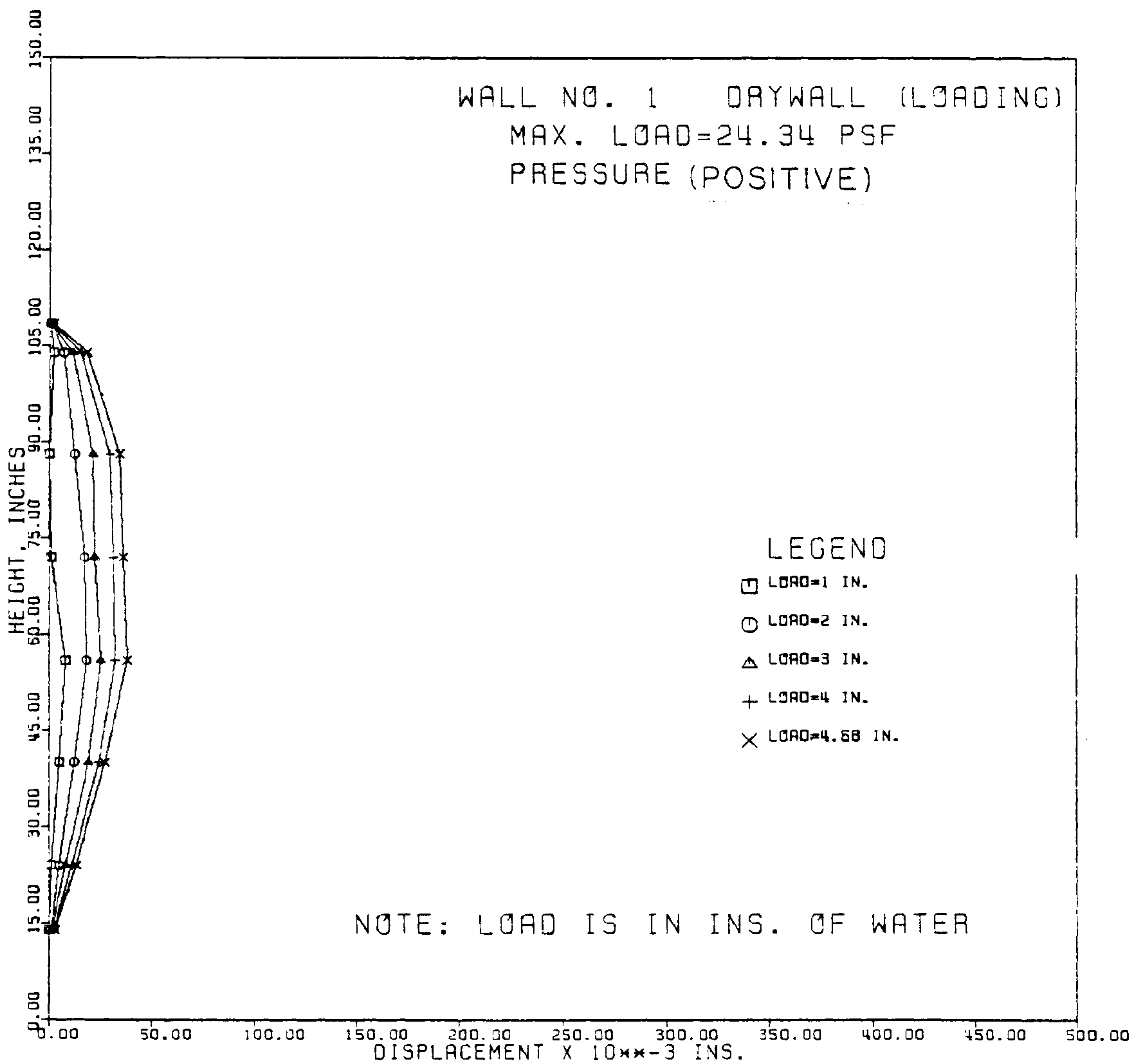

Figure C-4. Drywall Lateral Deflection for Wall No. 1 at Design Load.

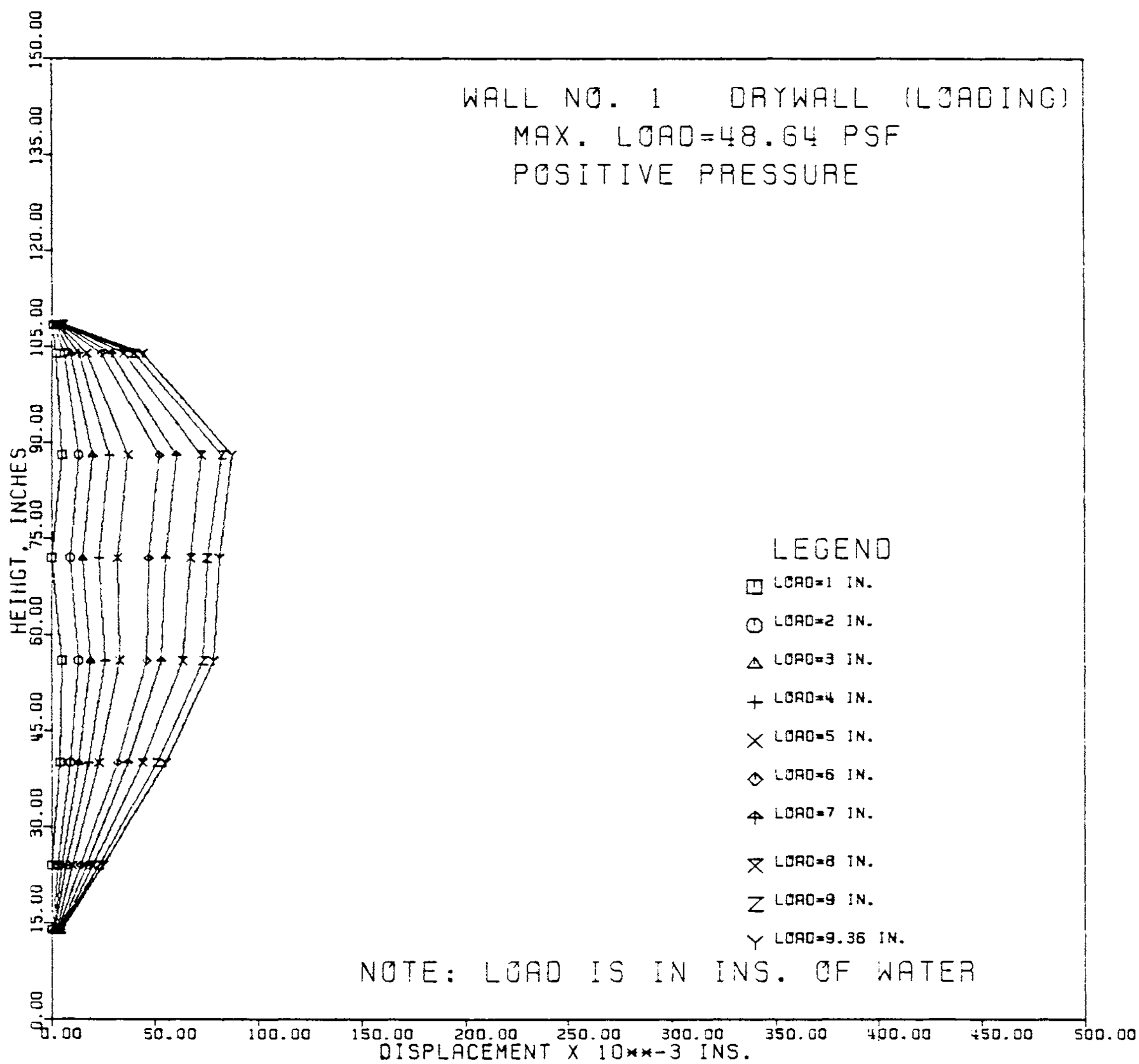

Figure C-5. Drywall Lateral Deflection for Wall No. 1 at Twice Design Load.

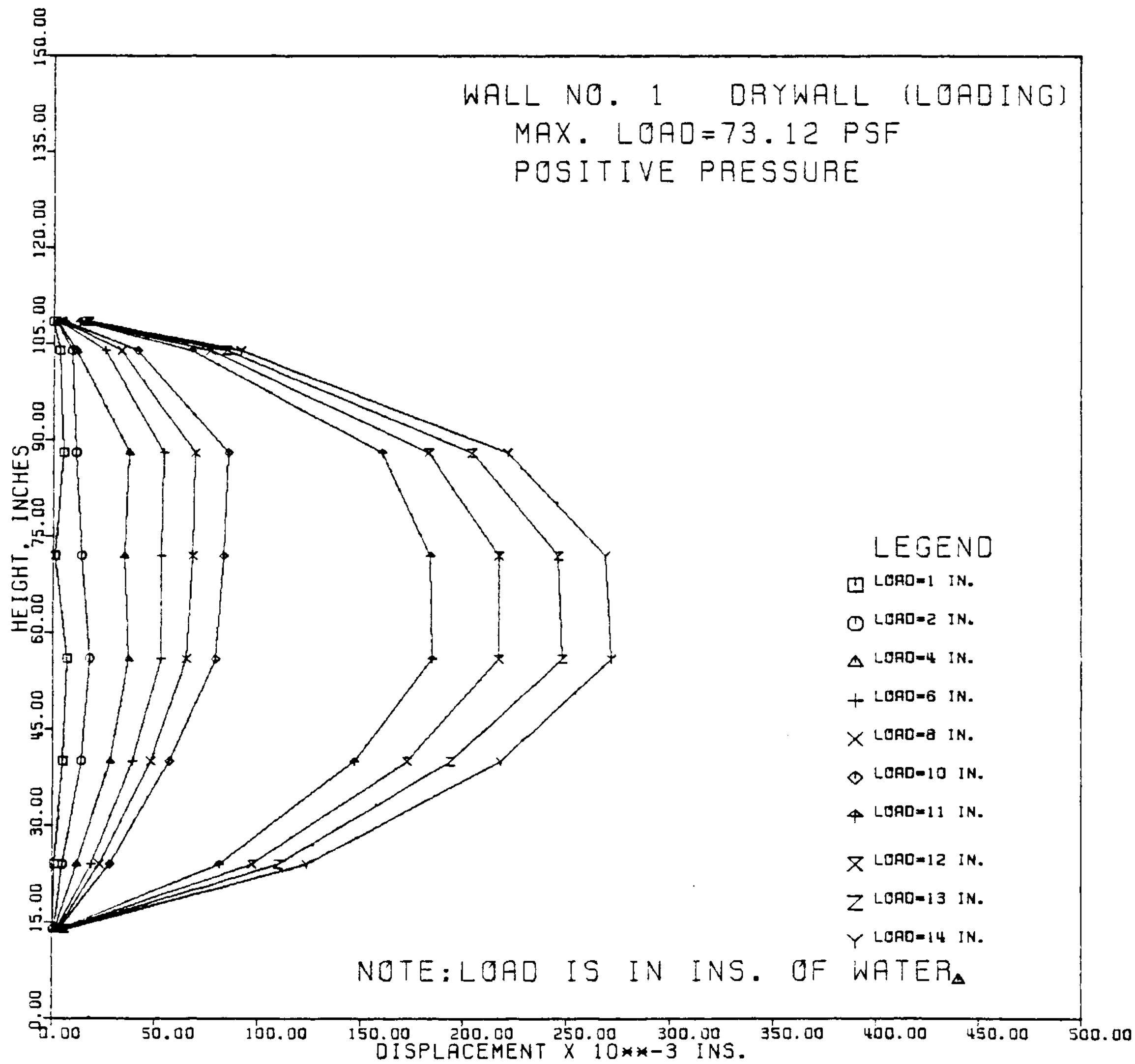

Figure C-6. Drywall Lateral Deflection for Wall No. 1 at Three Times Design Load.

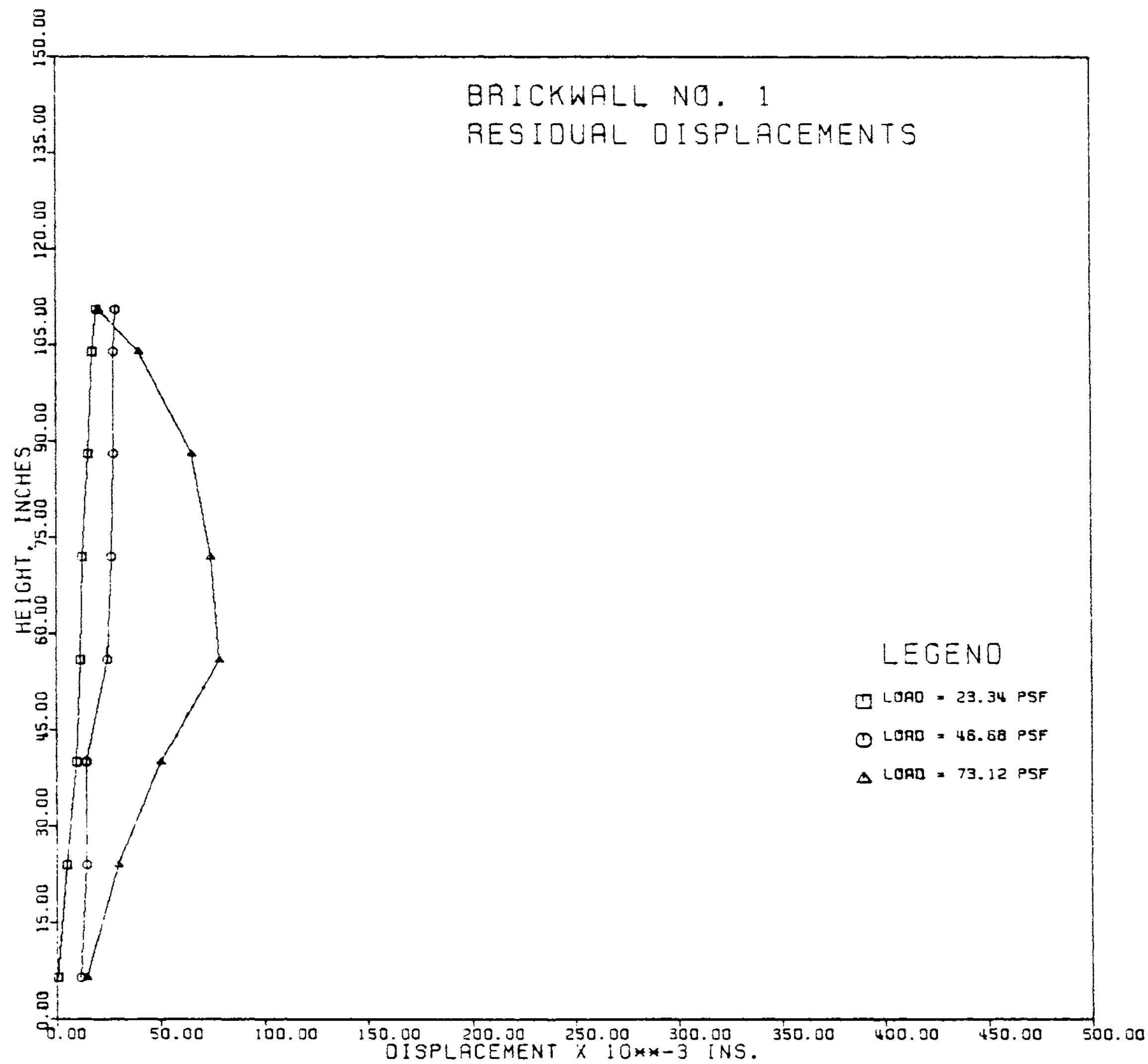

Figure C-7. Brickwall Residual Deflection for Wall No. 1 at Design Load, Twice Design Load and Three Times Design Load, Respectively.

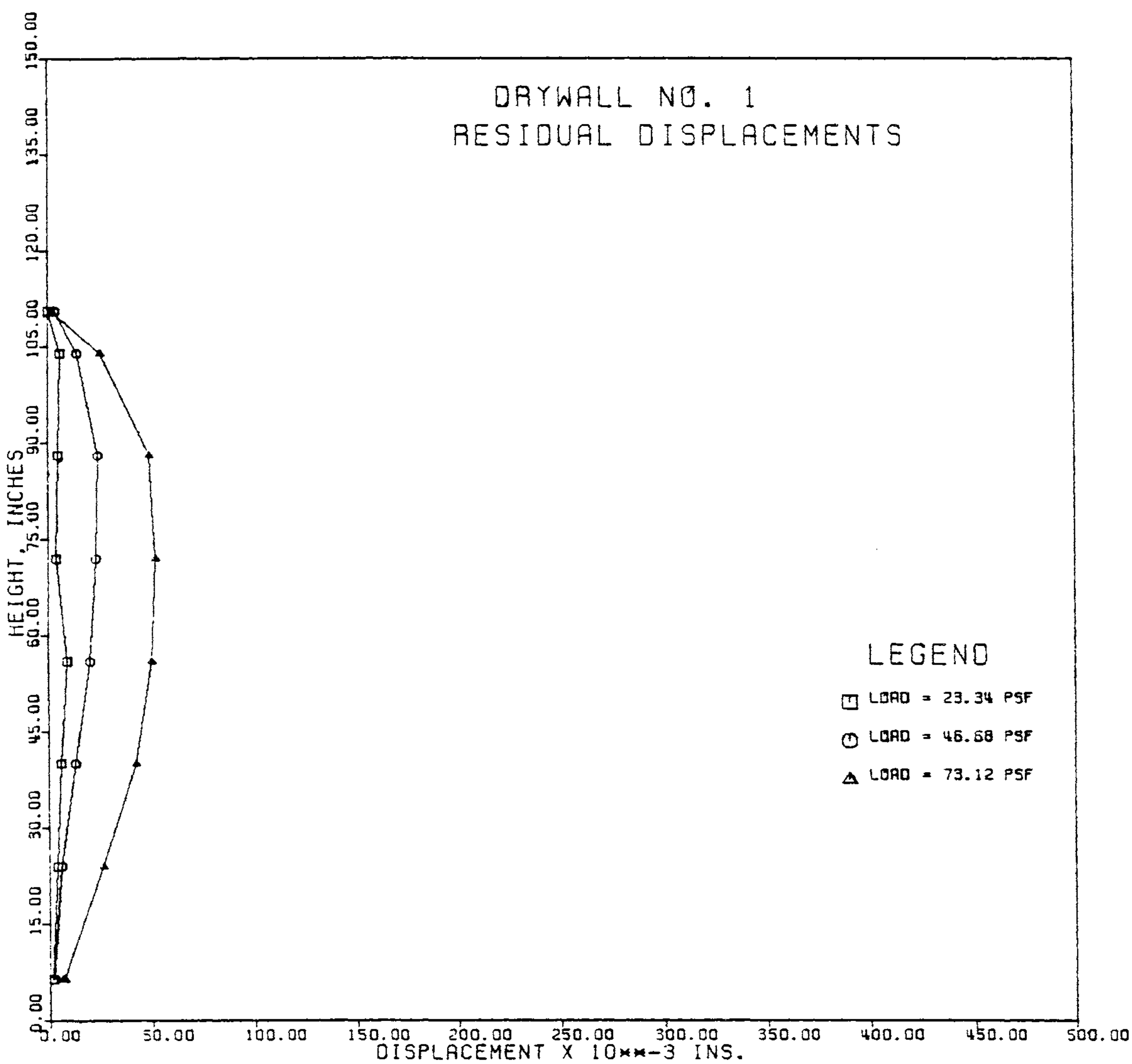

Figure C-8. Drywall Residual Deflection for Wall No. 1 at Design Load, Twice Design Load and Three Times Design Load, Respectively.

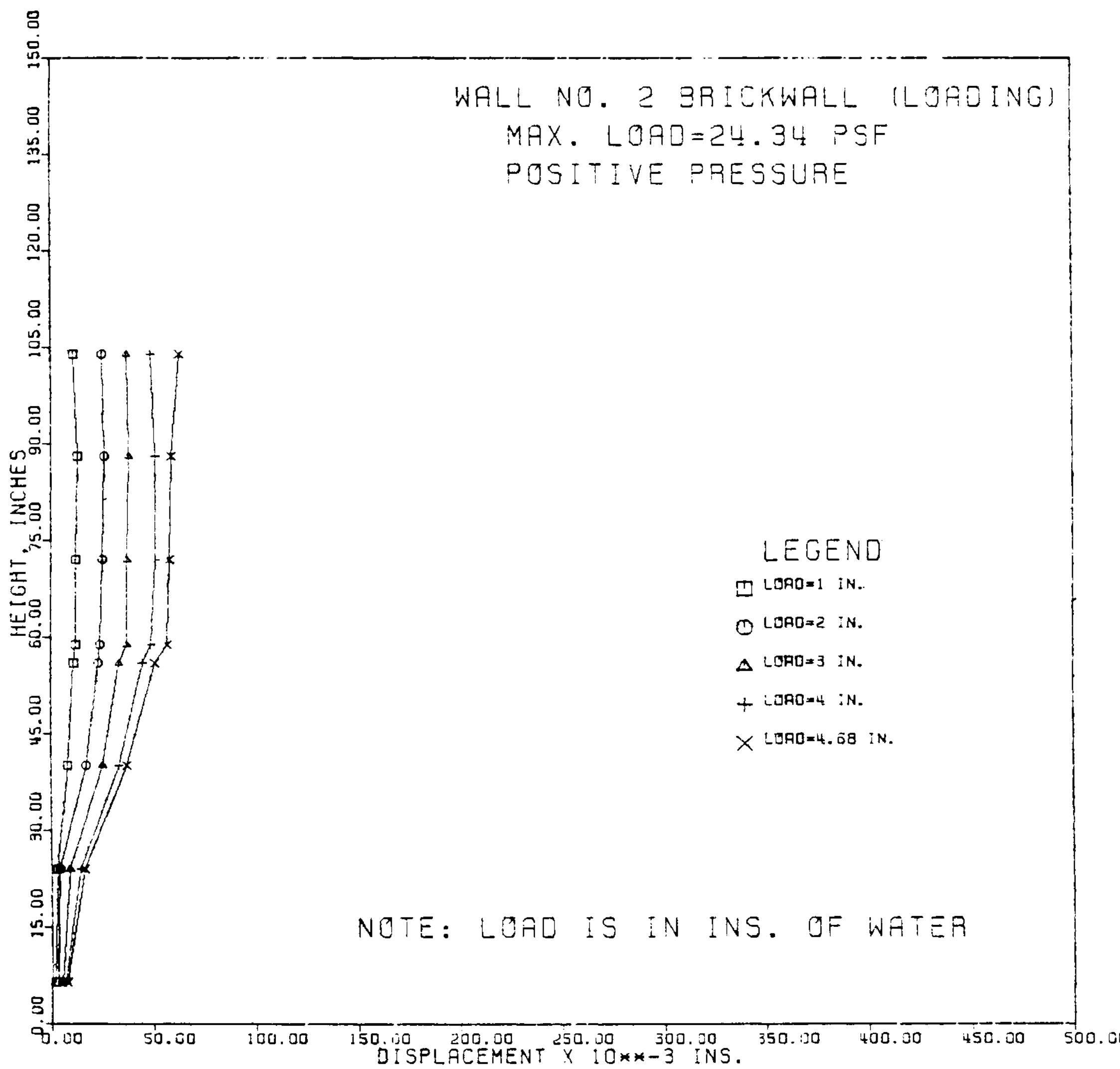

Figure C-9. Brickwall Lateral Deflection for Wall No. 2 at Design Load.

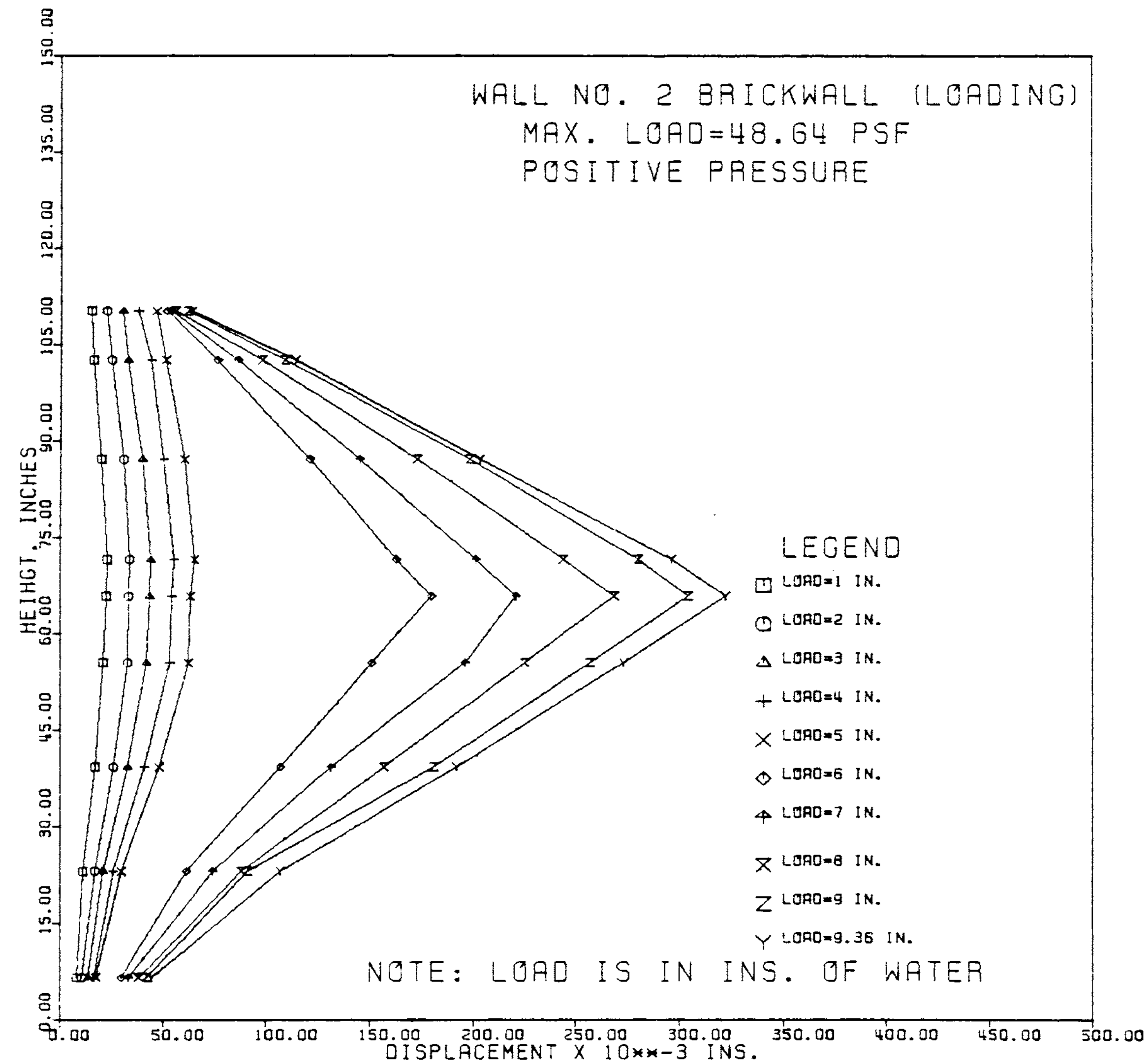

Figure C-10. Brickwall Lateral Deflection for Wall No. 2 at Twice Design Load.

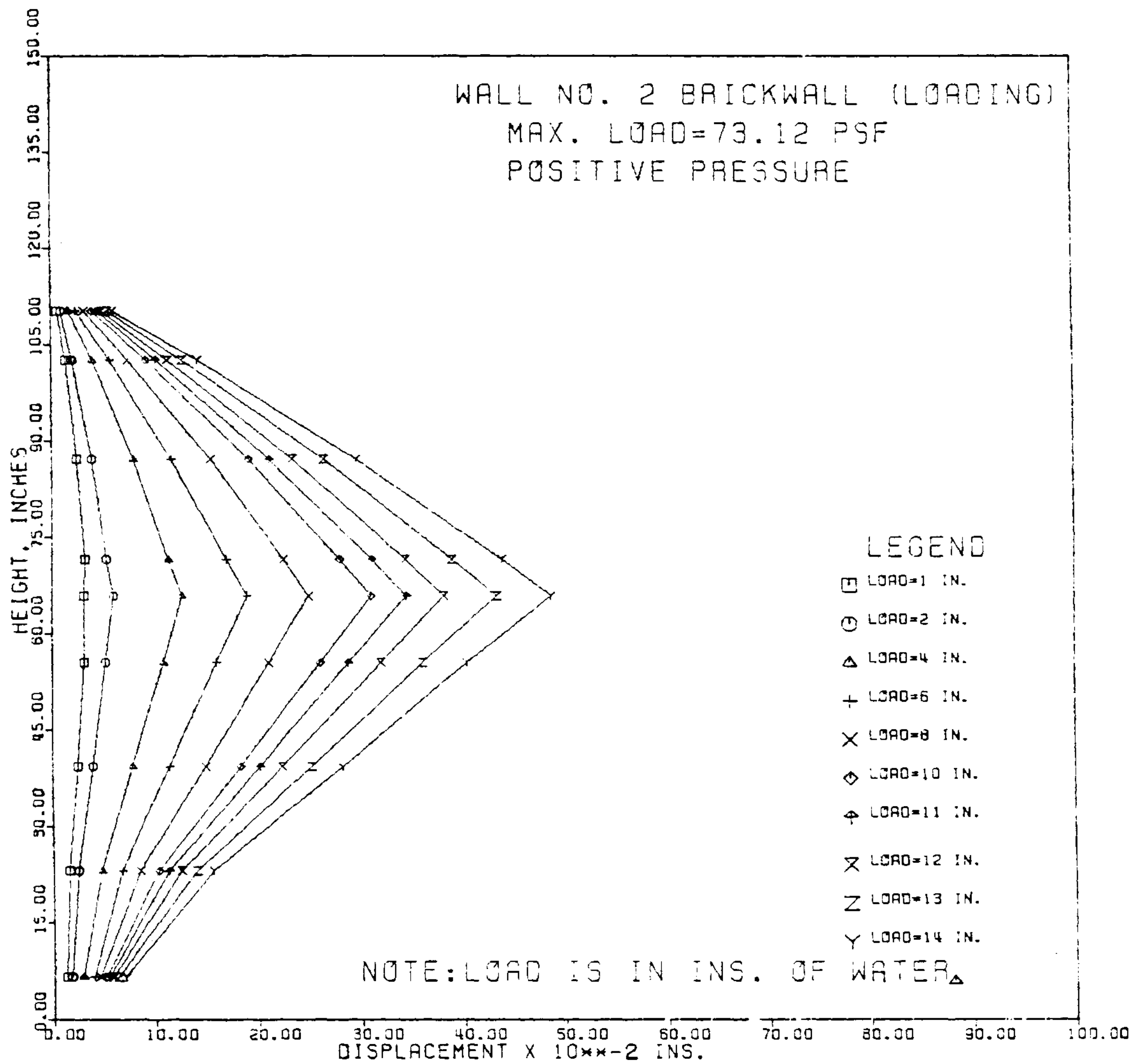

Figure C-11. Brickwall Lateral Deflection for Wall No. 2 at Three Times Design Load.

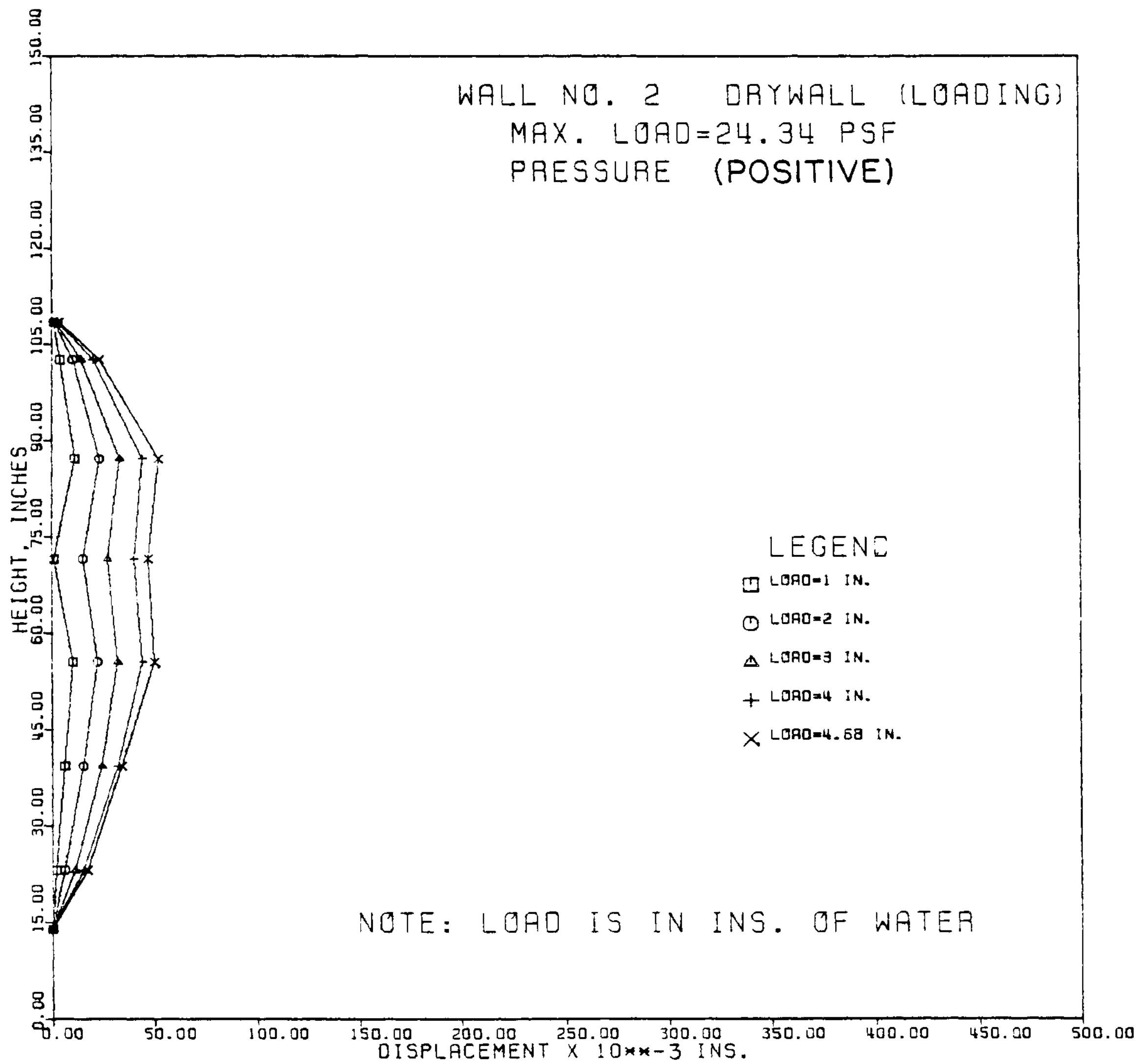

Figure C-12. Drywall Lateral Deflection for Wall No. 2 at Design Load.

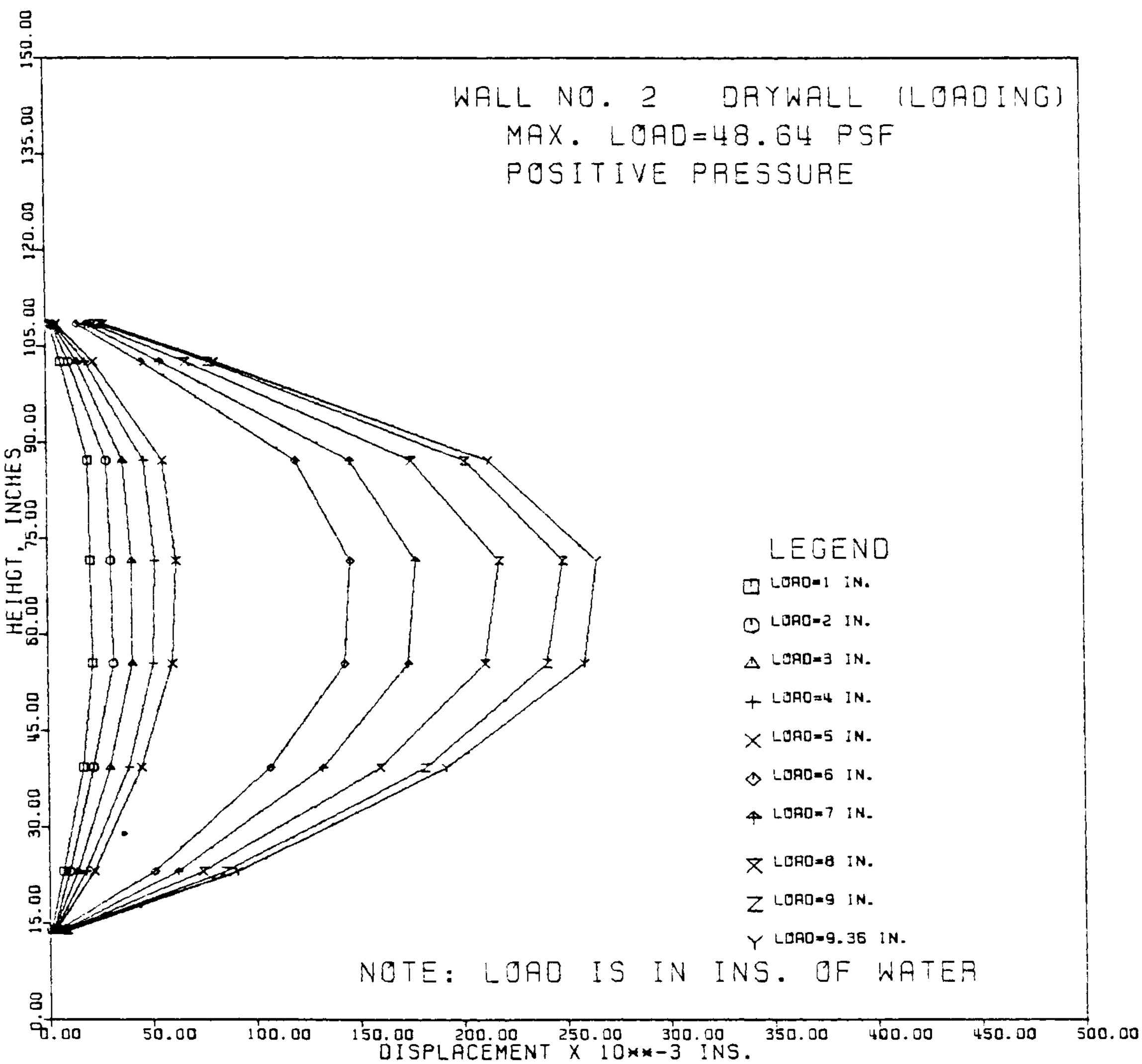

Figure C-13. Drywall Lateral Deflection for Wall No. 2 at Twice Design Load.

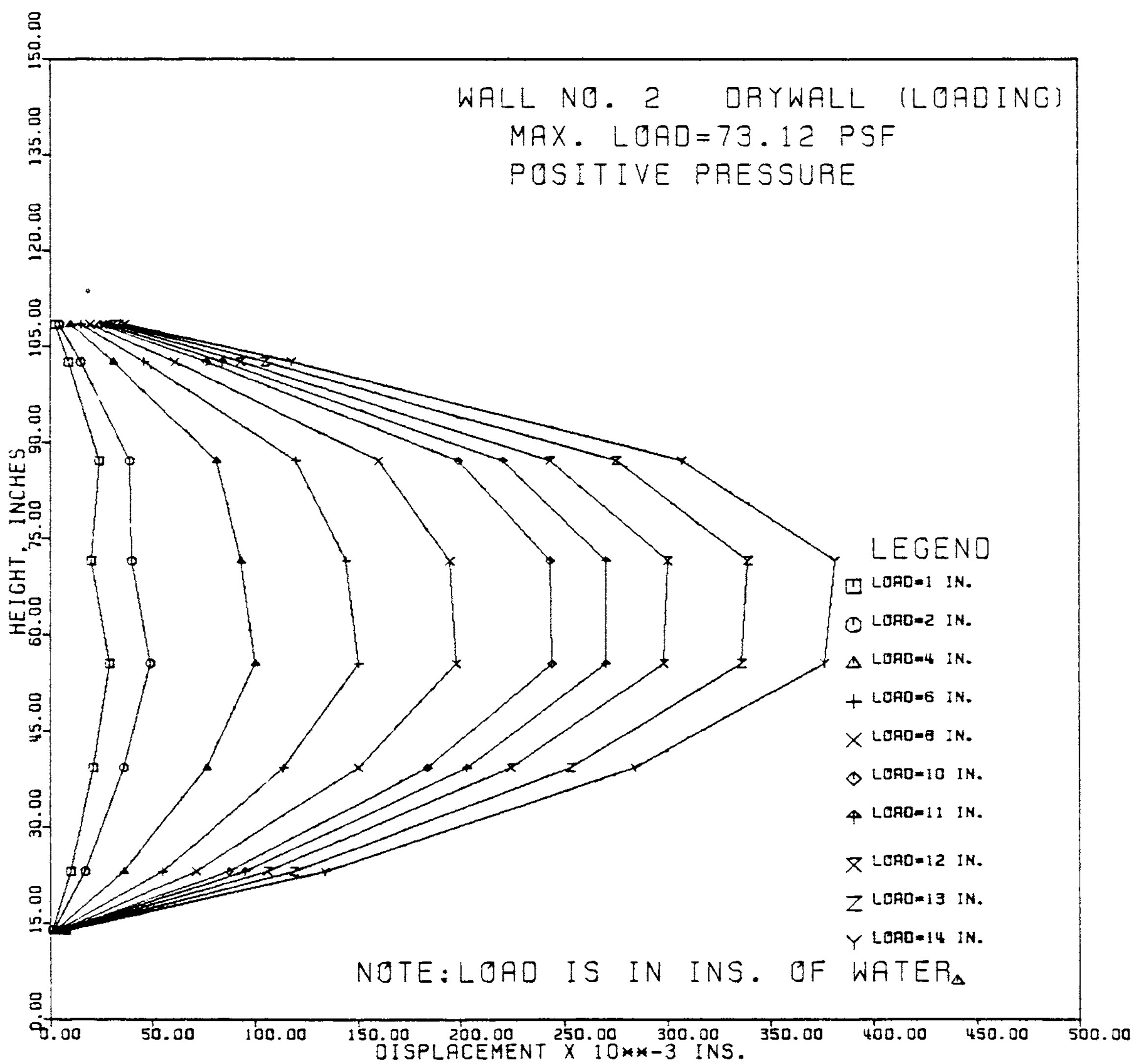

Figure C-14. Drywall Lateral Deflection for Wall No. 2 at Three Times Design Load.

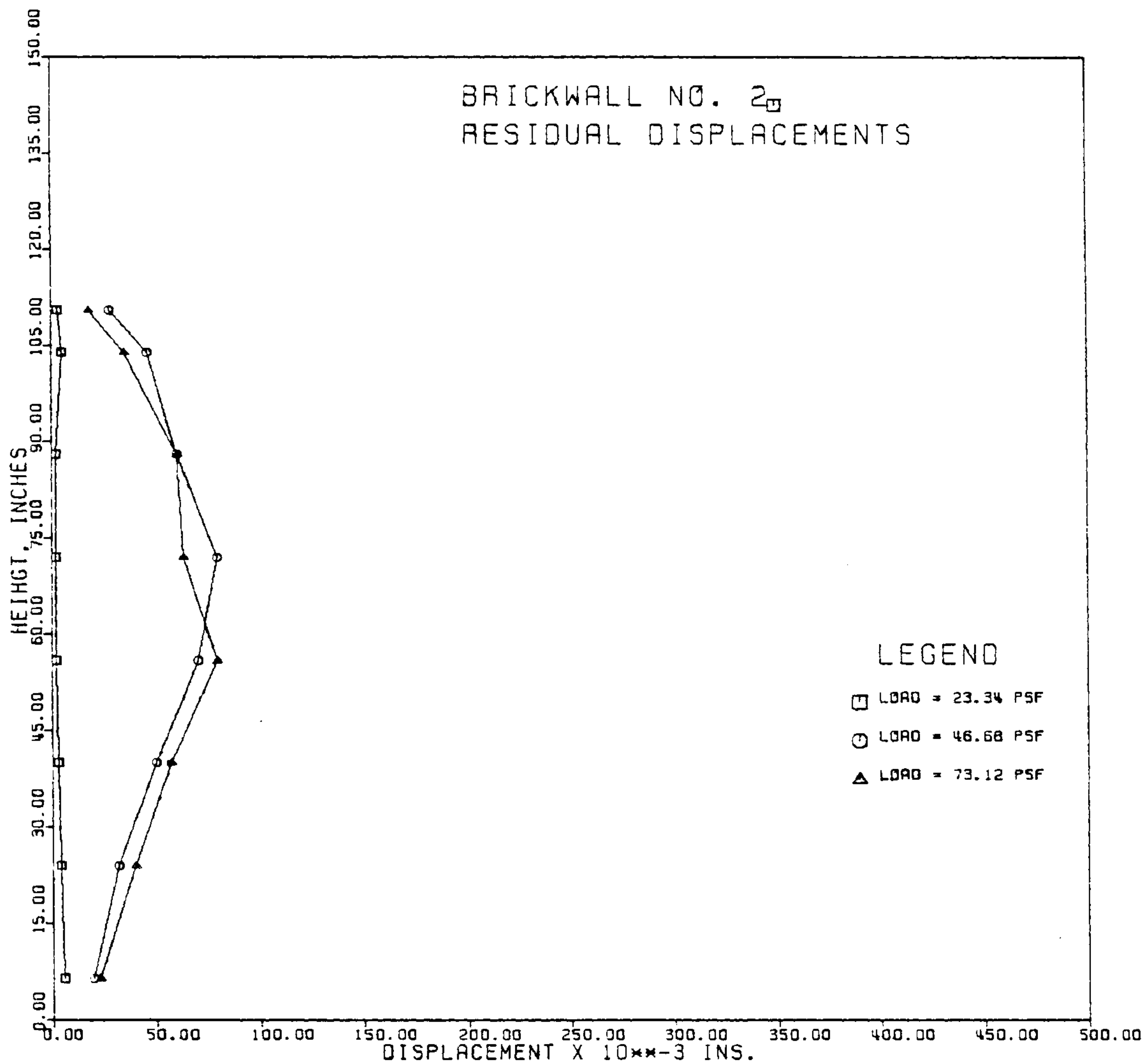

Figure C-15. Brickwall Residual Deflection for Wall No. 2 at Design Load, Twice Design Load and Three Times Design Load, Respectively.

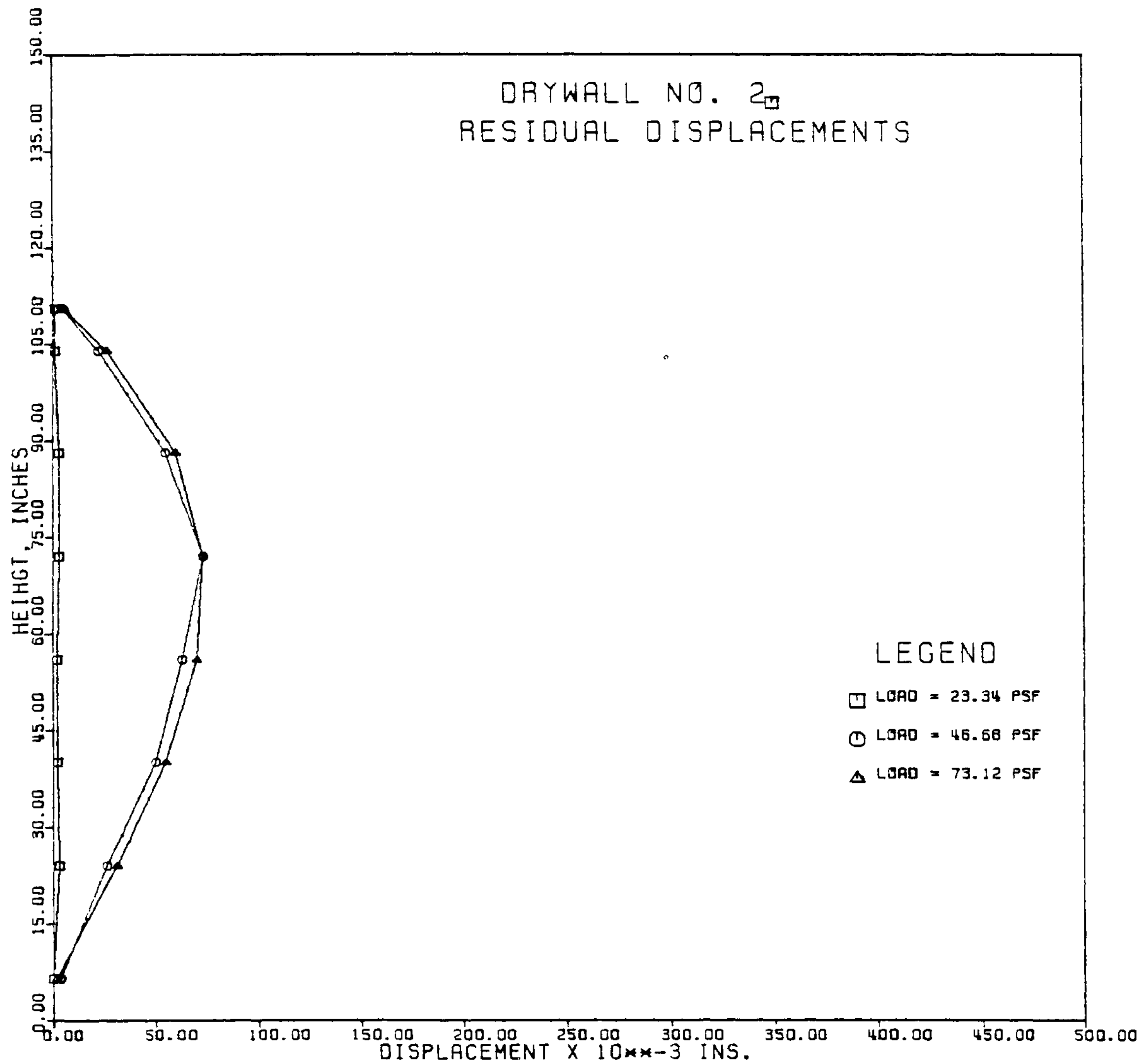

Figure C-16. Drywall Residual Deflection for Wall No. 2 at Design Load, Twice Design Load and Three Times Design Load, Respectively.

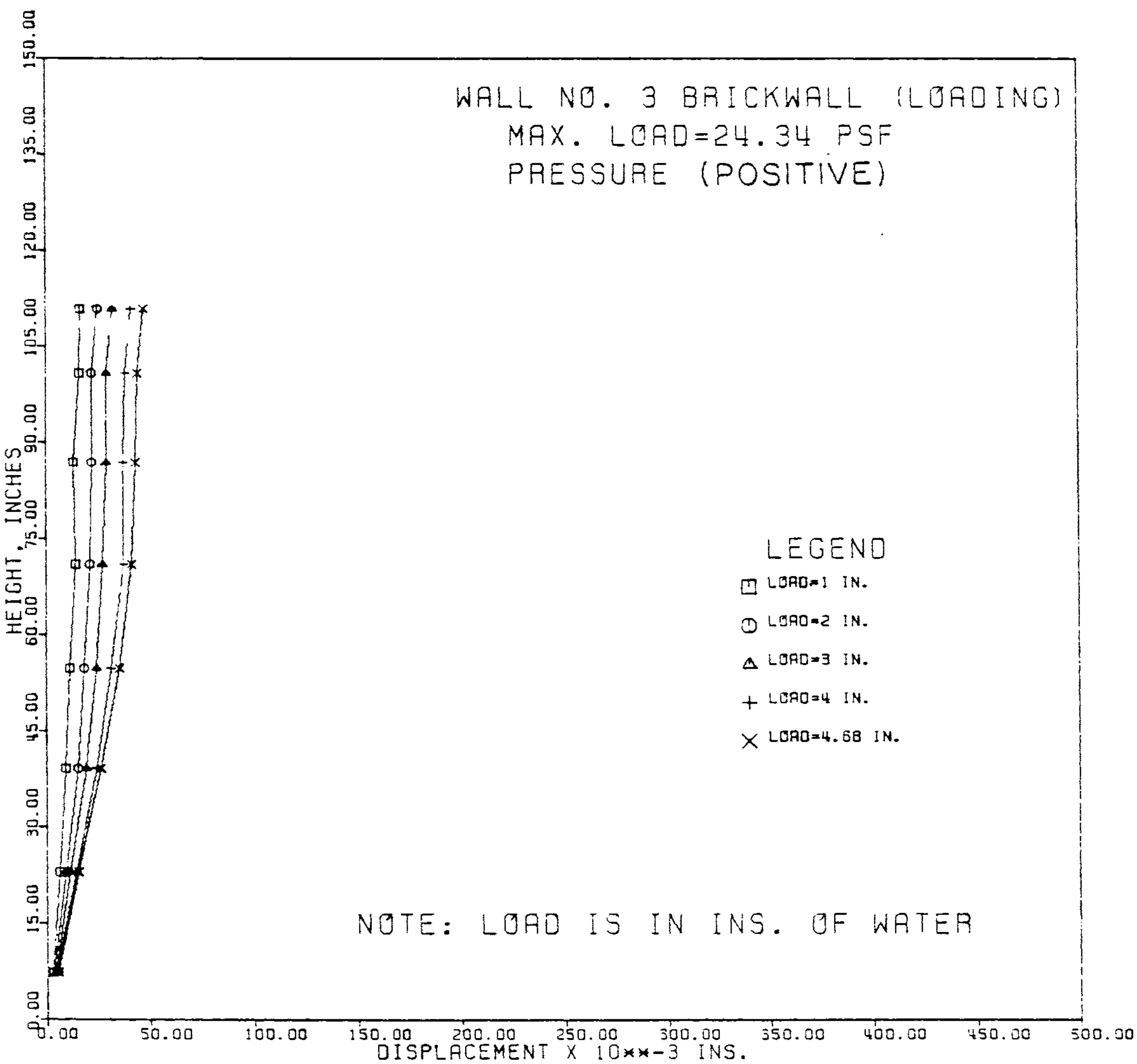

Figure C-17. Brickwall Lateral Deflection for Wall No. 3 at Design Load.

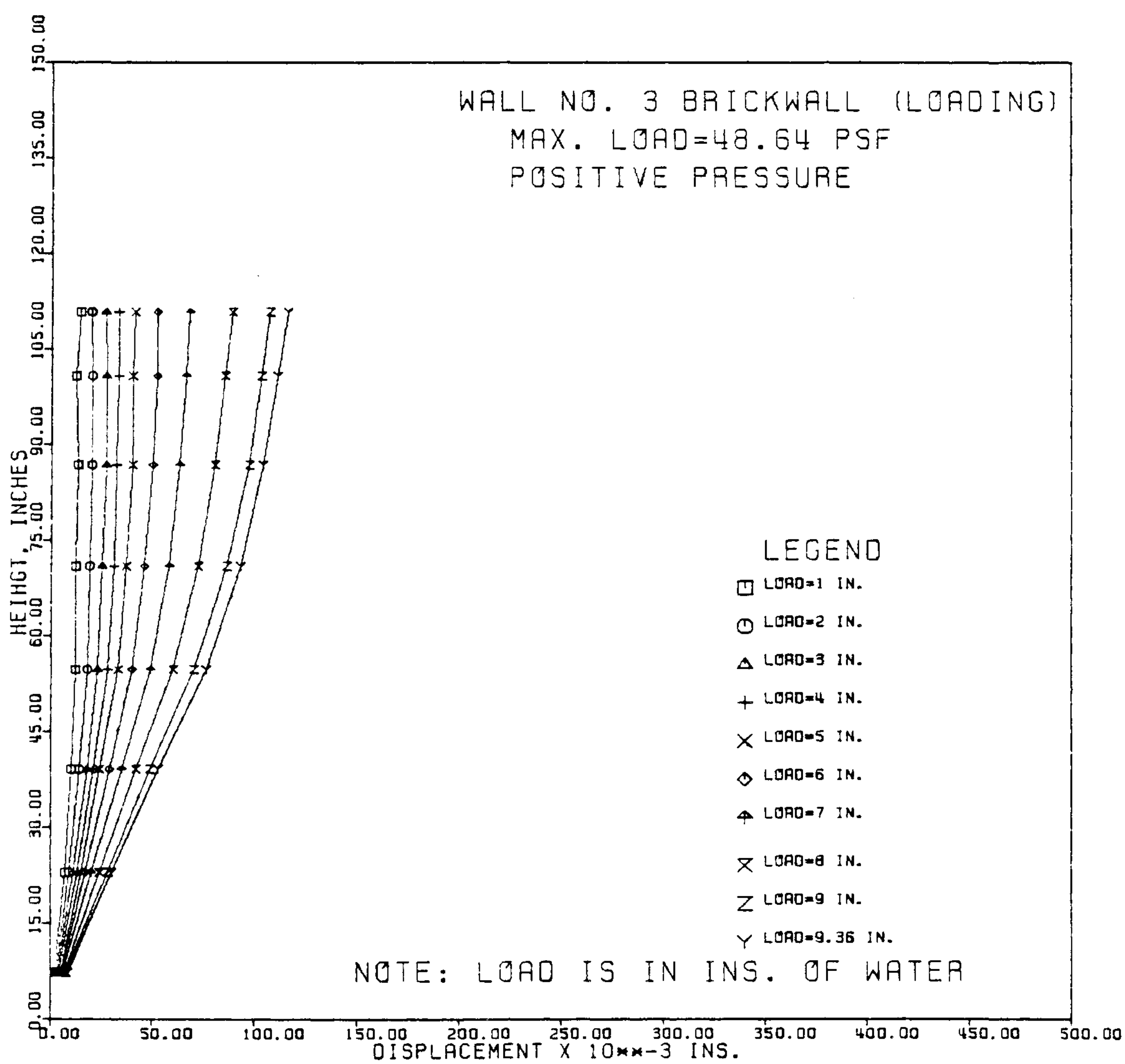

Figure C-18. Brickwall Lateral Deflection for Wall No. 3 at Twice Design Load.

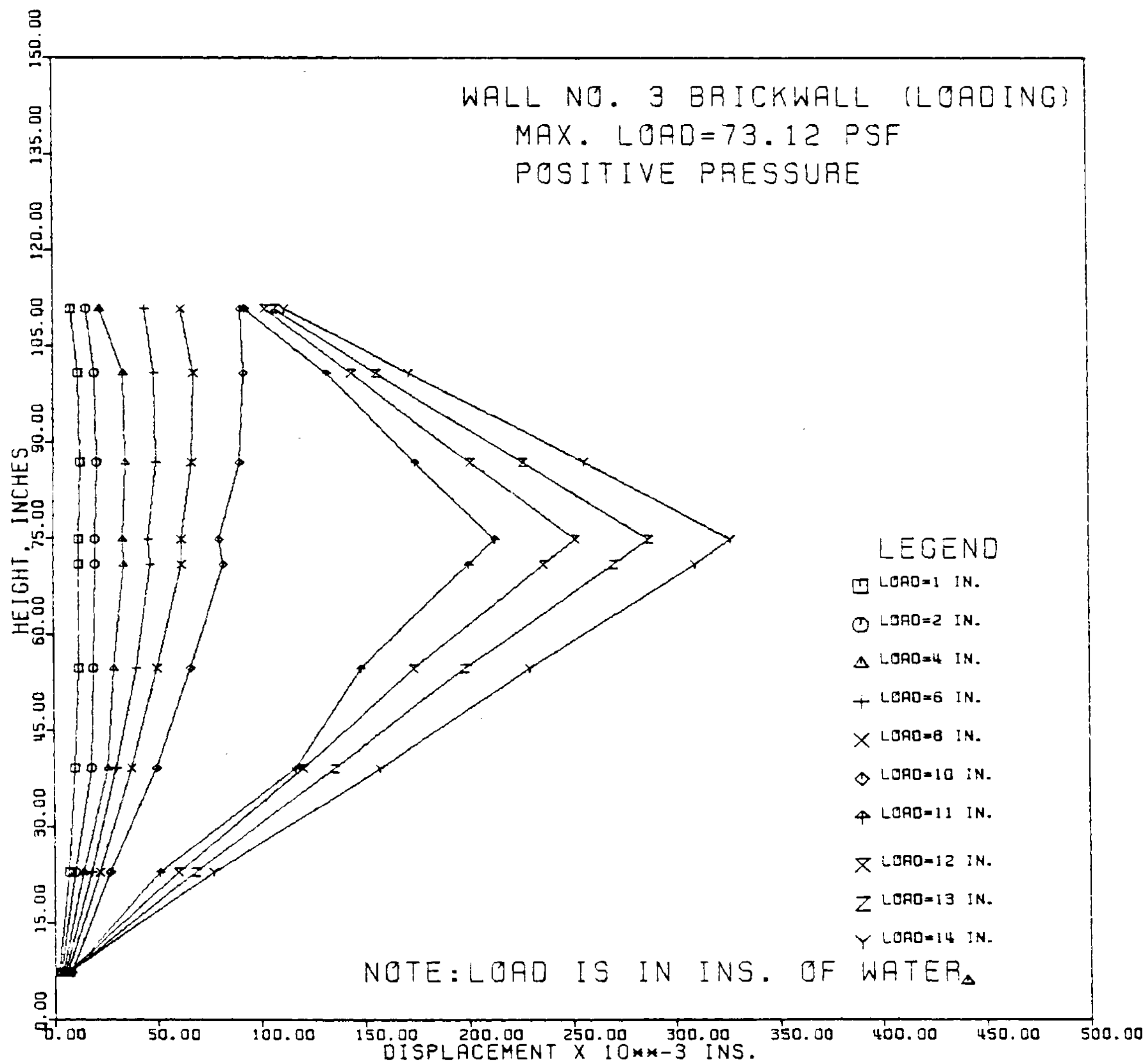

Figure C-19. Brickwall Lateral Deflection for Wall No. 3 at Three Times Design Load.

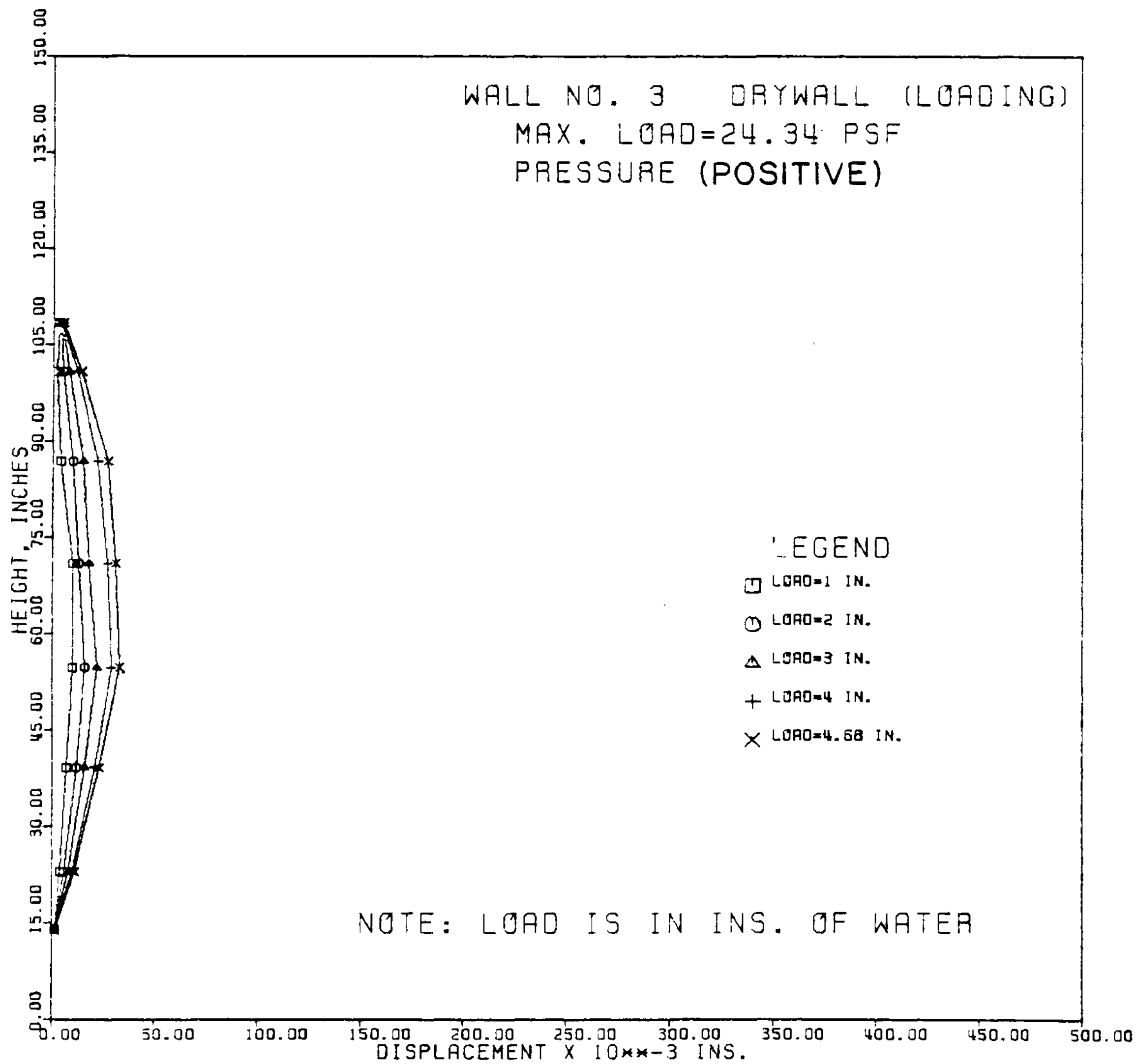

Figure C-20. Drywall Lateral Deflection for Wall No. 3 at Design Load.

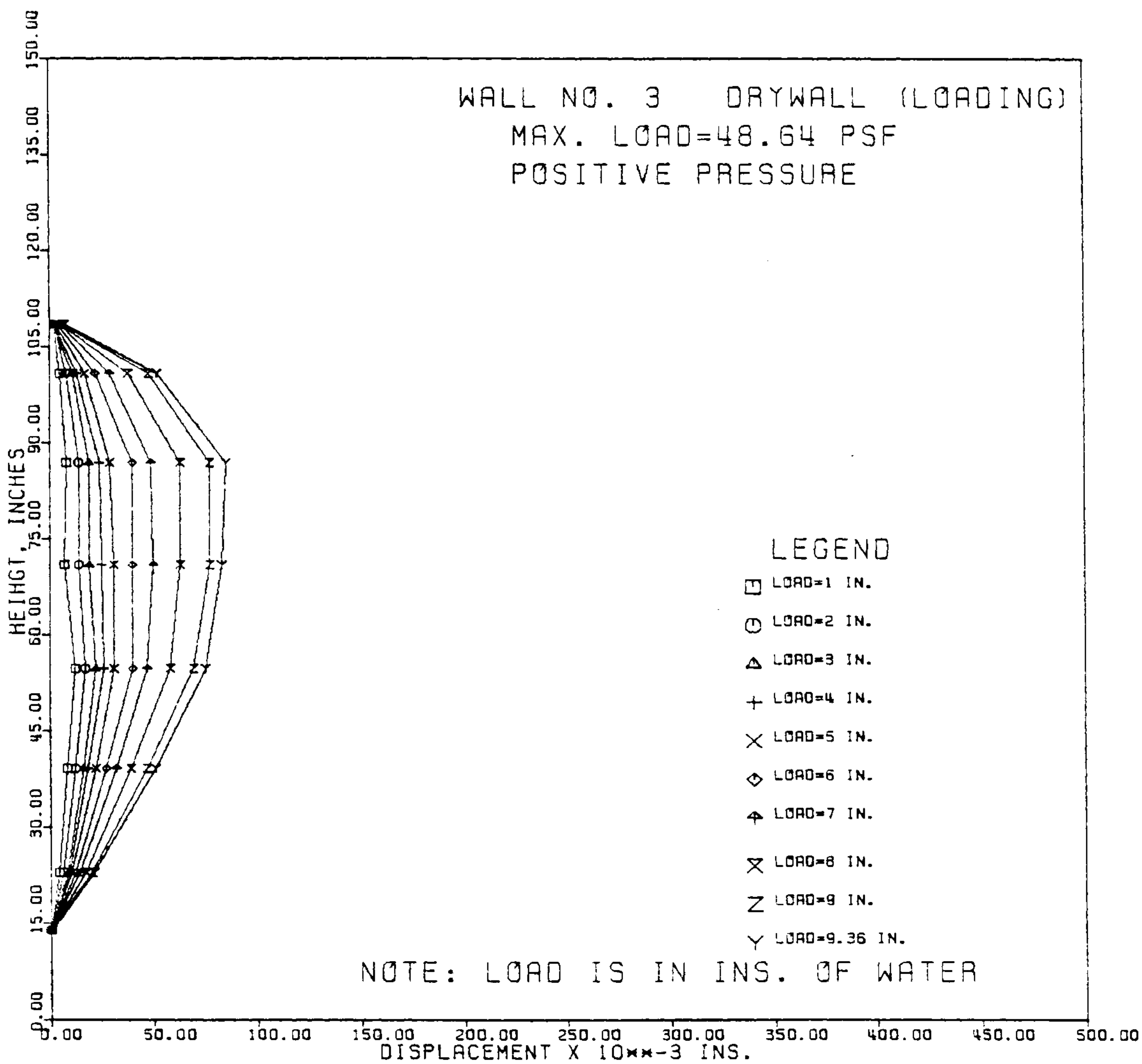

Figure C-21. Drywall Lateral Deflection for Wall No. 3 at Twice Design Load.

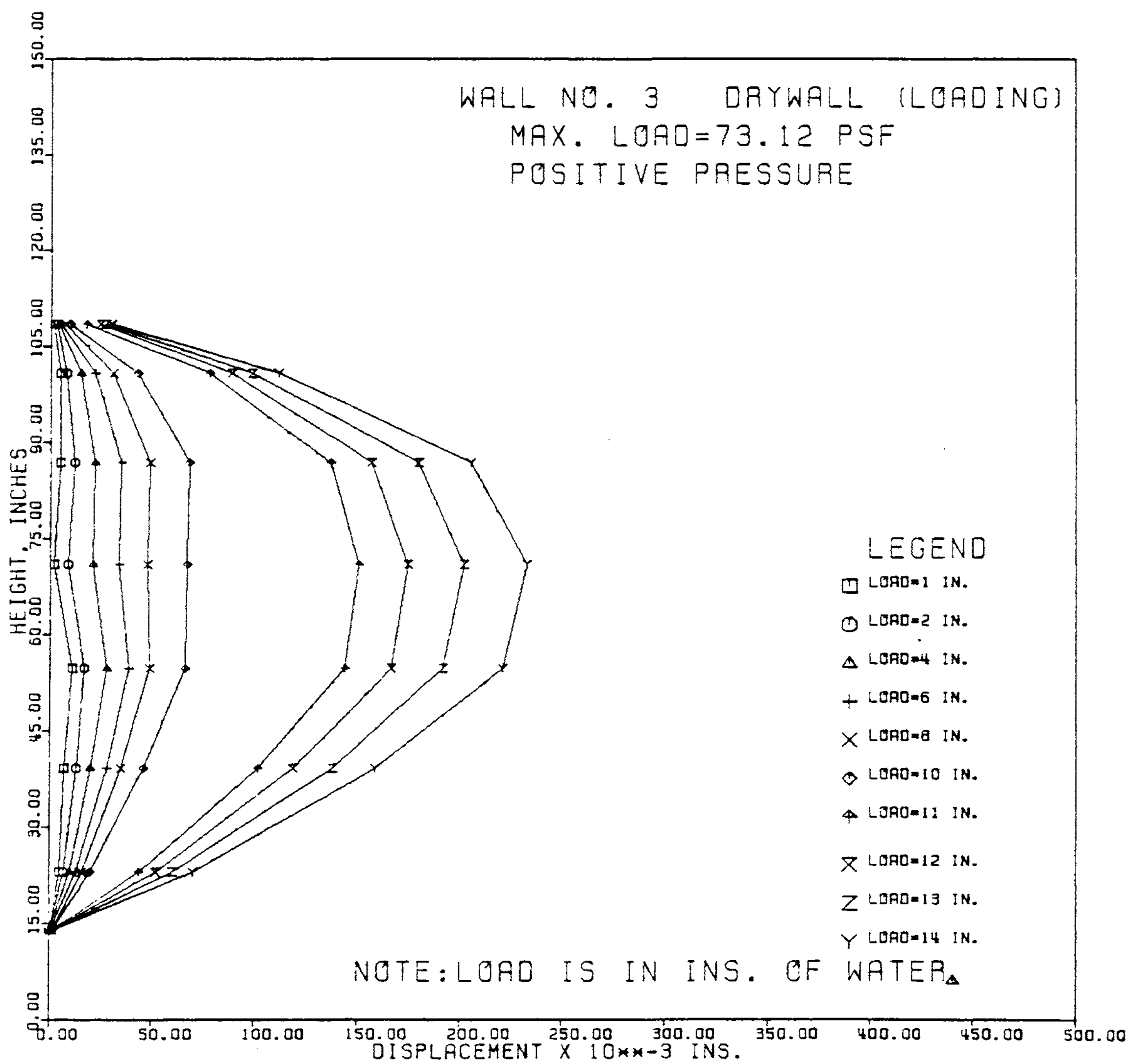

Figure C-22. Drywall Lateral Deflection for Wall No. 3 at Three Times Design Load.

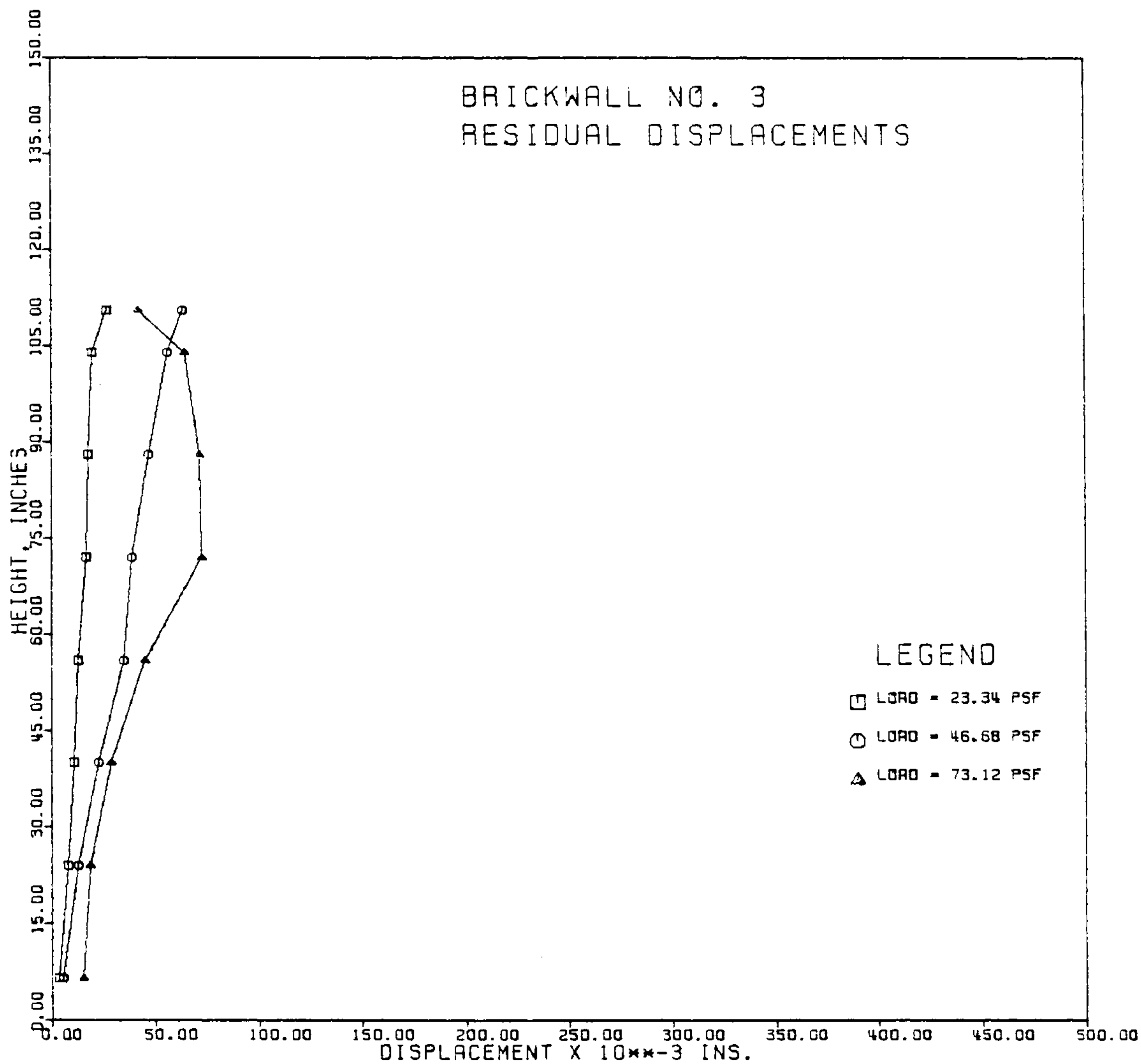

Figure C-23. Brickwall Residual Deflection for Wall No. 3 at Design Load, Twice Design Load and Three Times Design Load, Respectively.

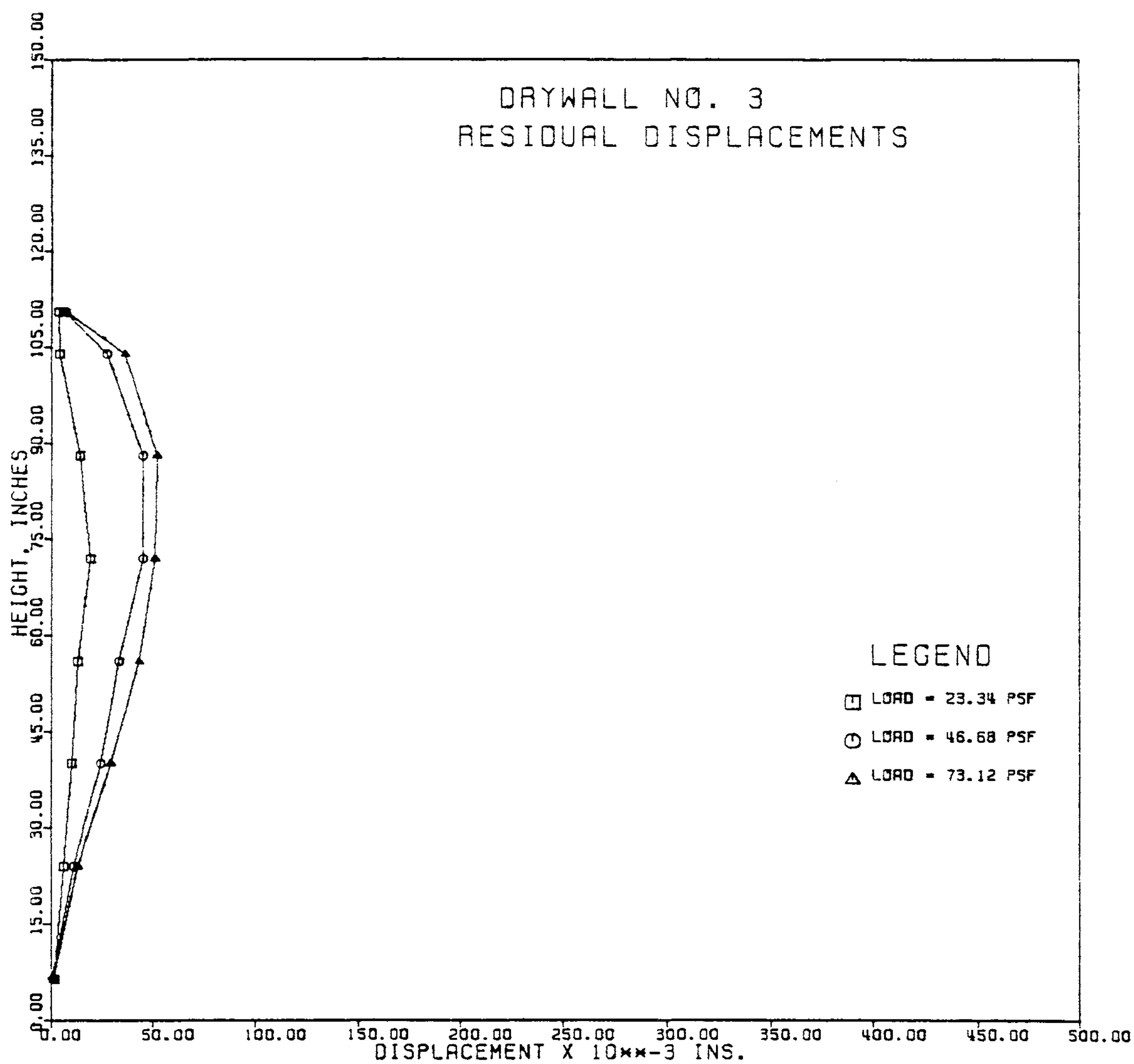

Figure C-24. Drywall Residual Deflection for Wall No. 3 at Design Load, Twice Design Load and Three Times Design Load, Respectively.

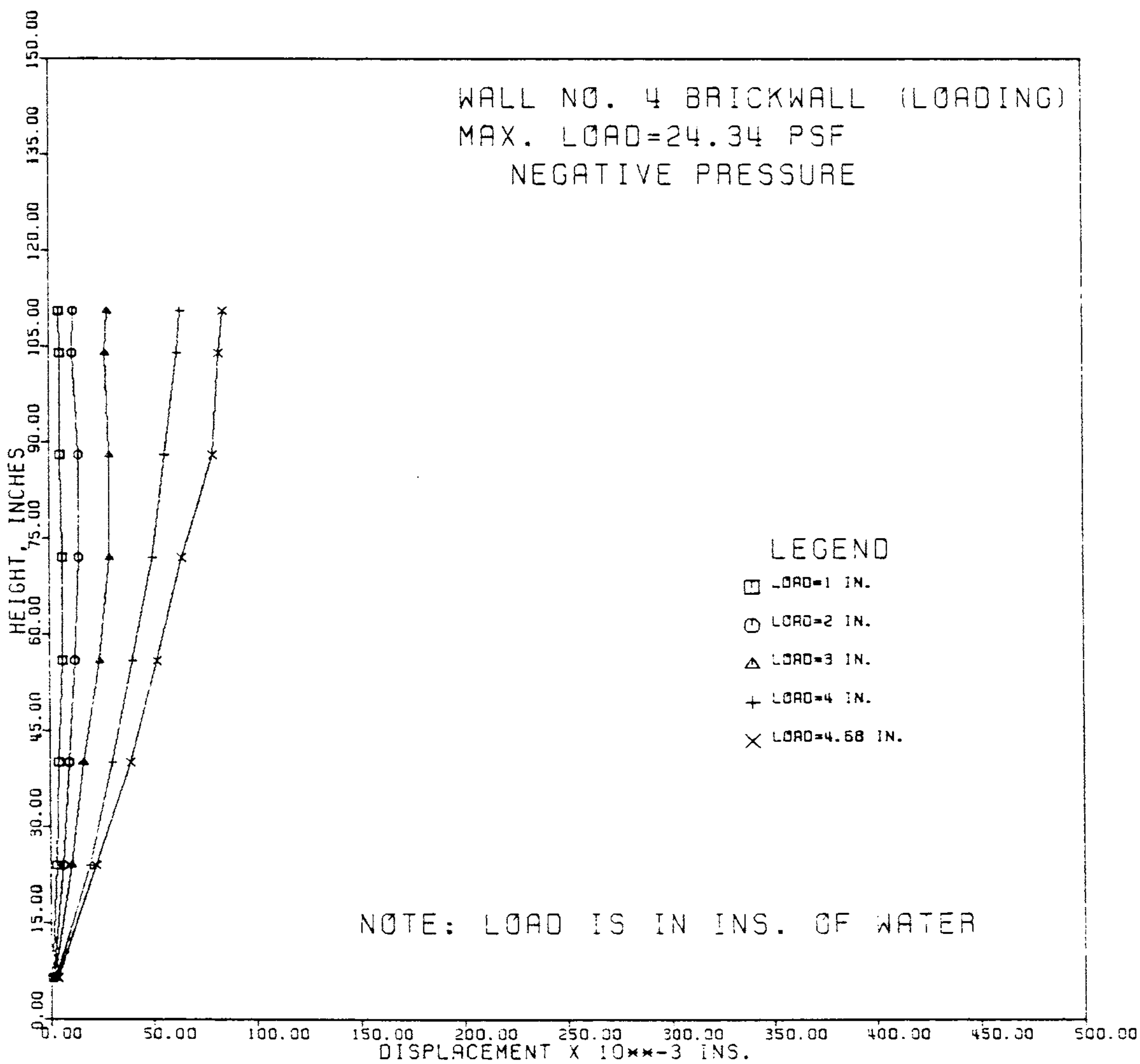

Figure C-25. Brickwall Lateral Deflection for Wall No. 4 at Design Load.

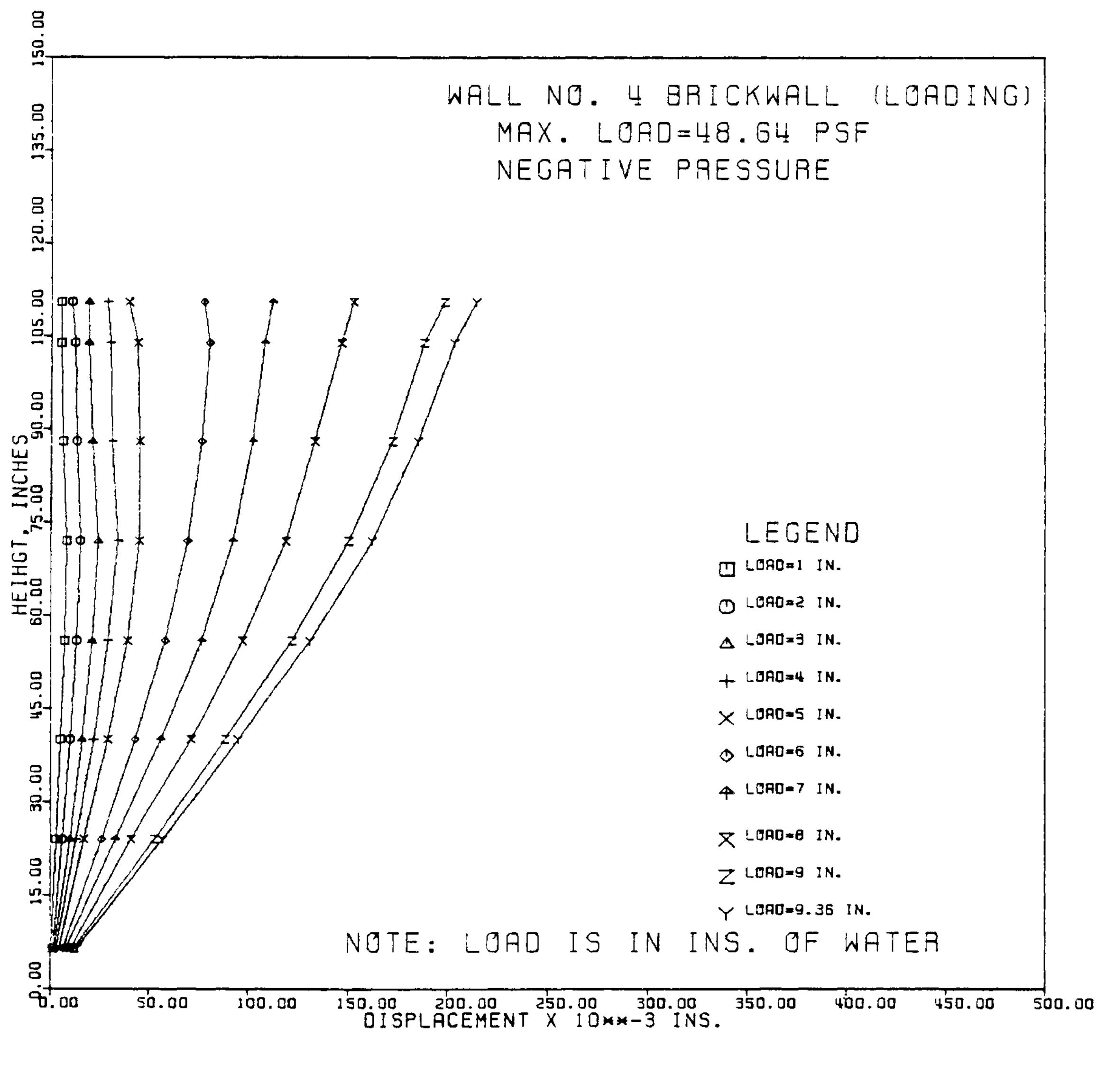

Figure C-26. Brickwall Lateral Deflection for Wall No. 4 at Twice Design Load.

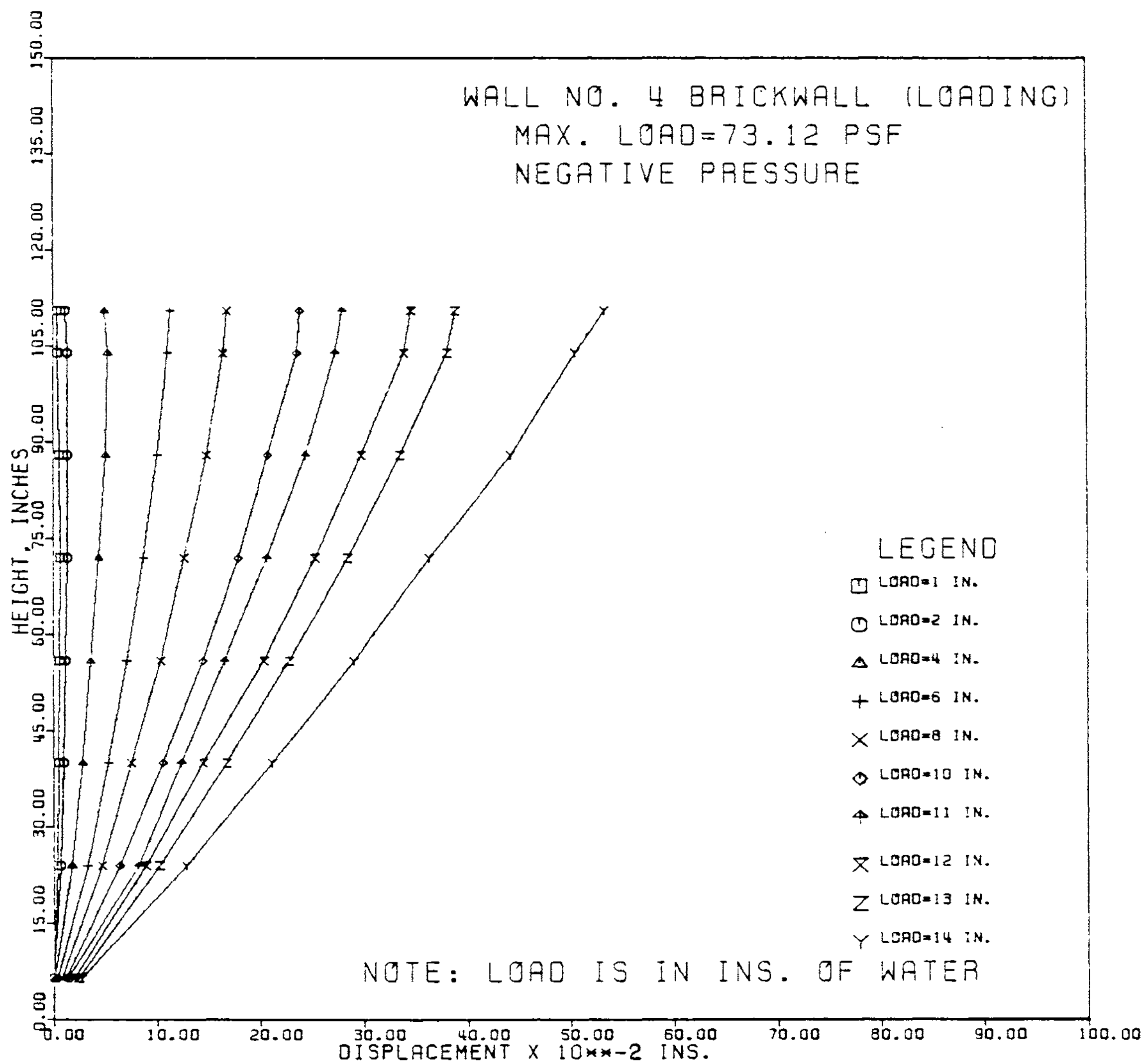

Figure C-27. Brickwall Lateral Deflection for Wall No. 4 at Three Times Design Load.

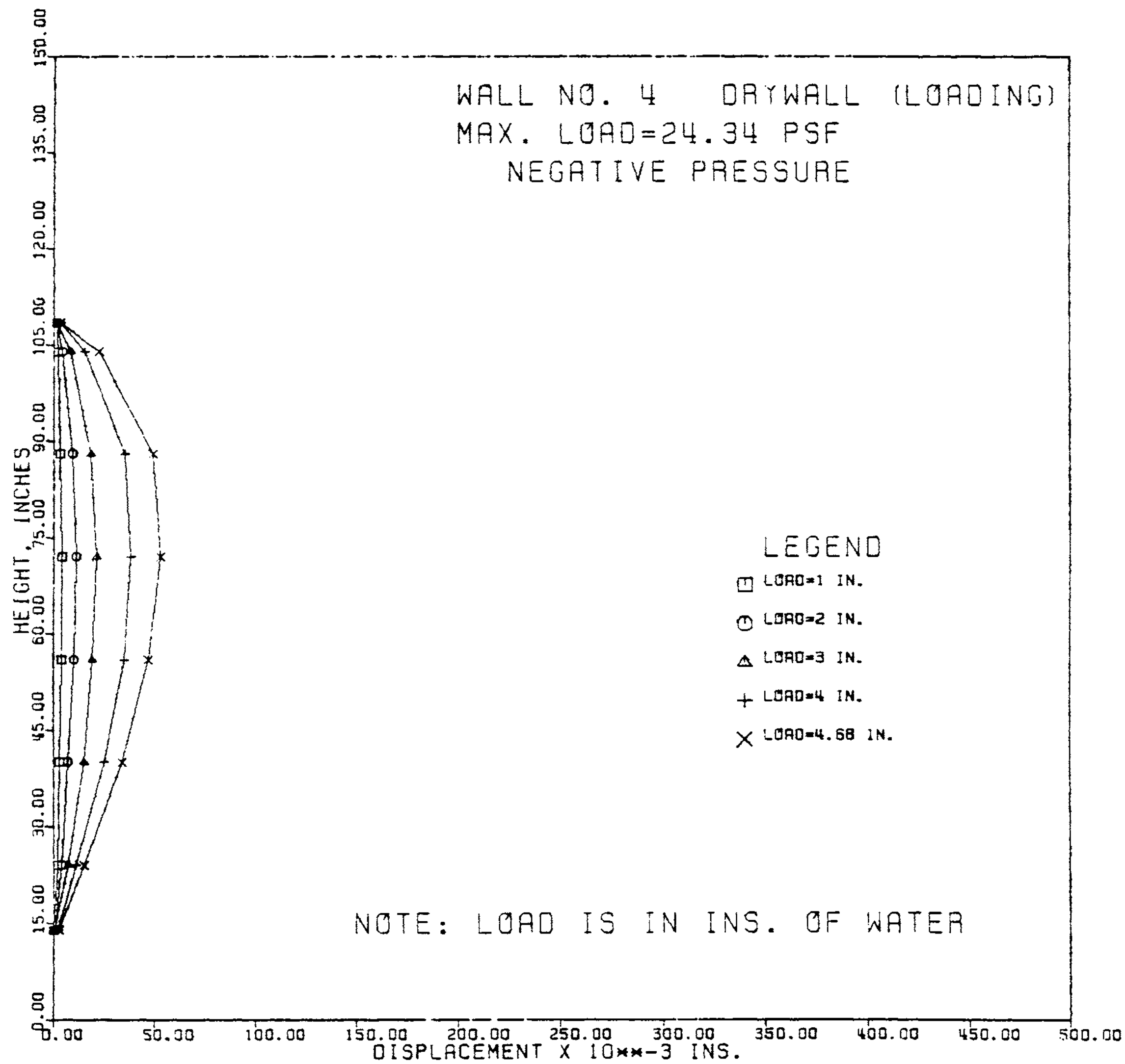

Figure C-28. Drywall Lateral Deflection for Wall No. 4 at Design Load.

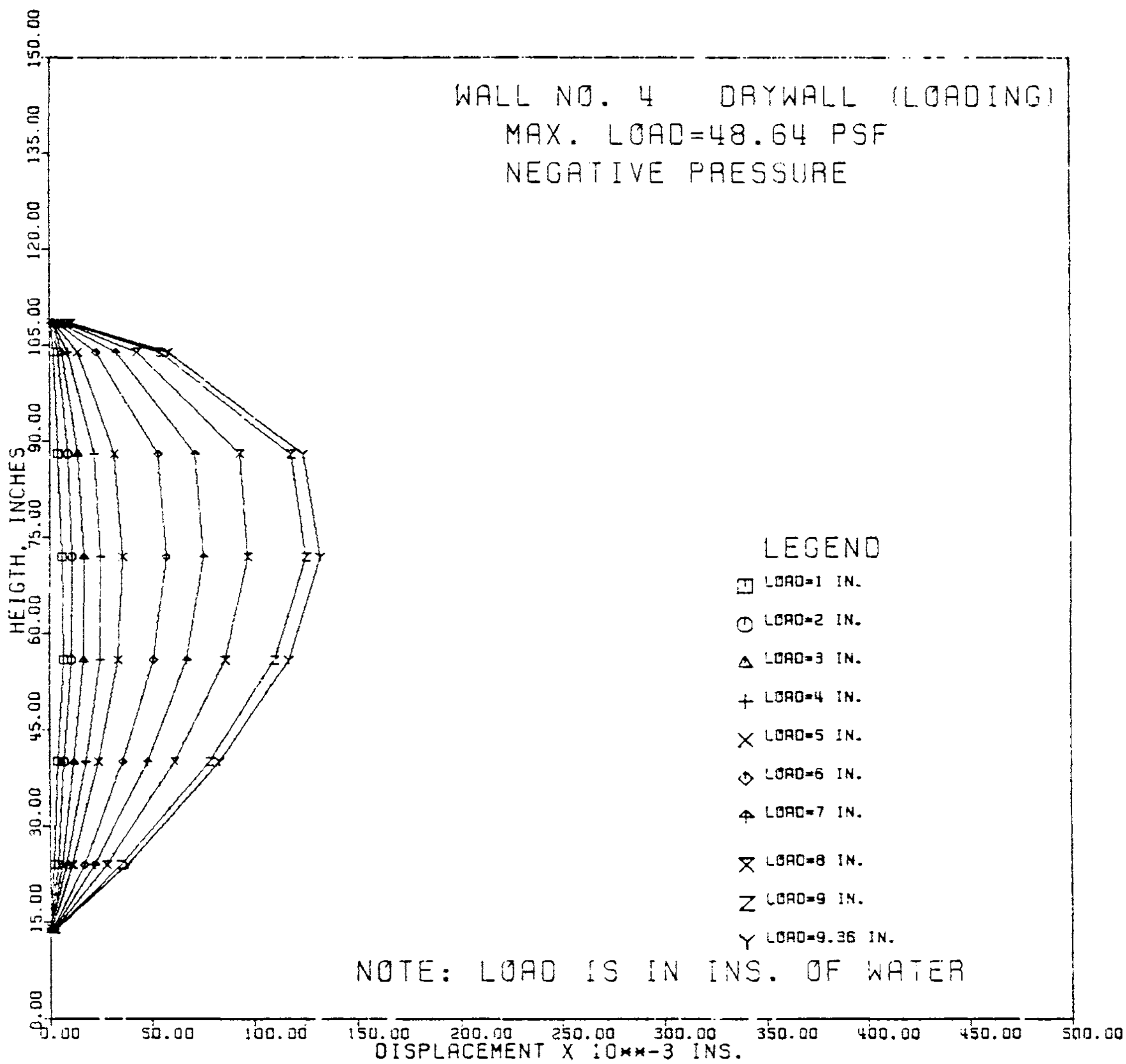

Figure C-29. Drywall Lateral Deflection for Wall No. 4 at Twice Design Load.

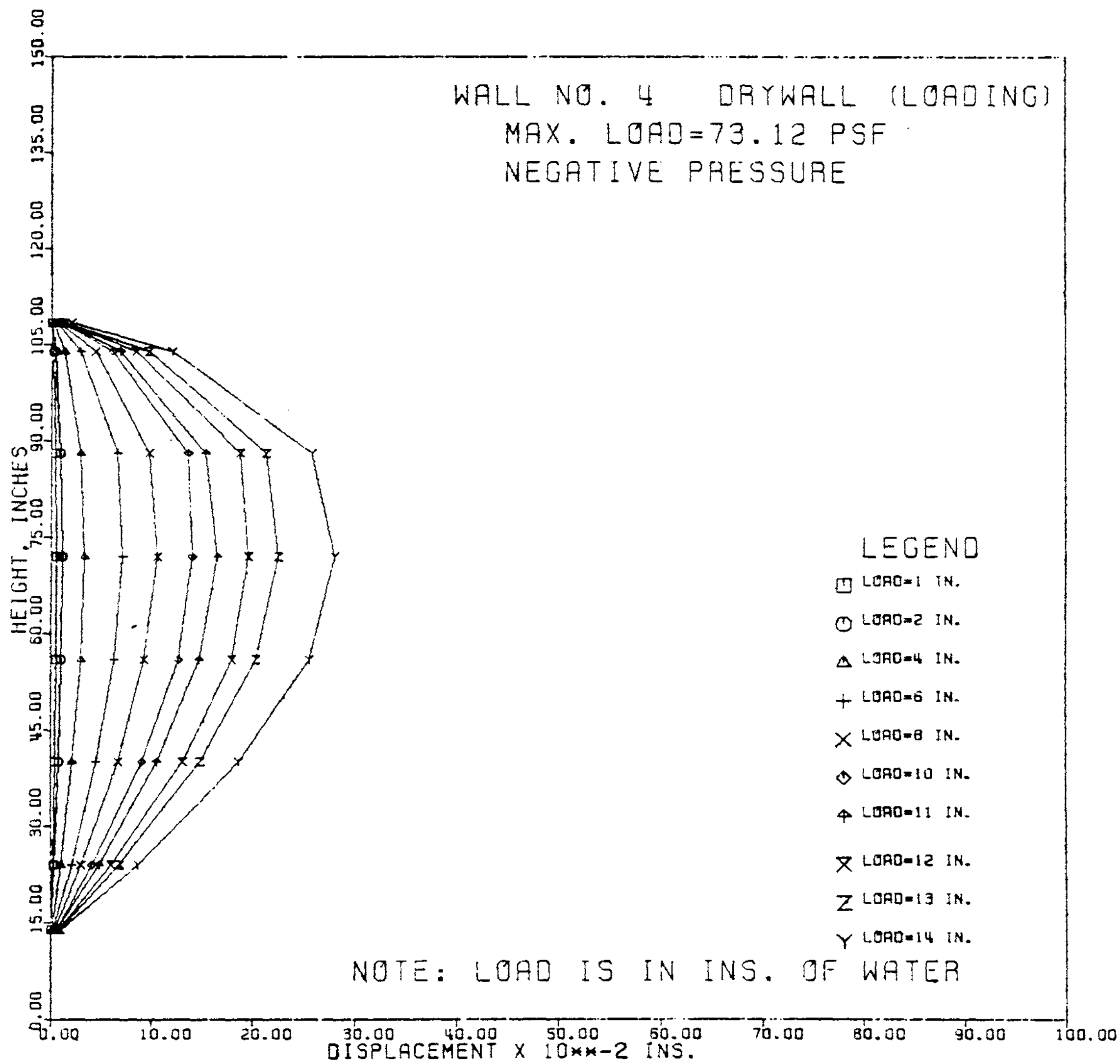

Figure C-30. Drywall Lateral Deflection for Wall No. 4 at Three Times Design Load.

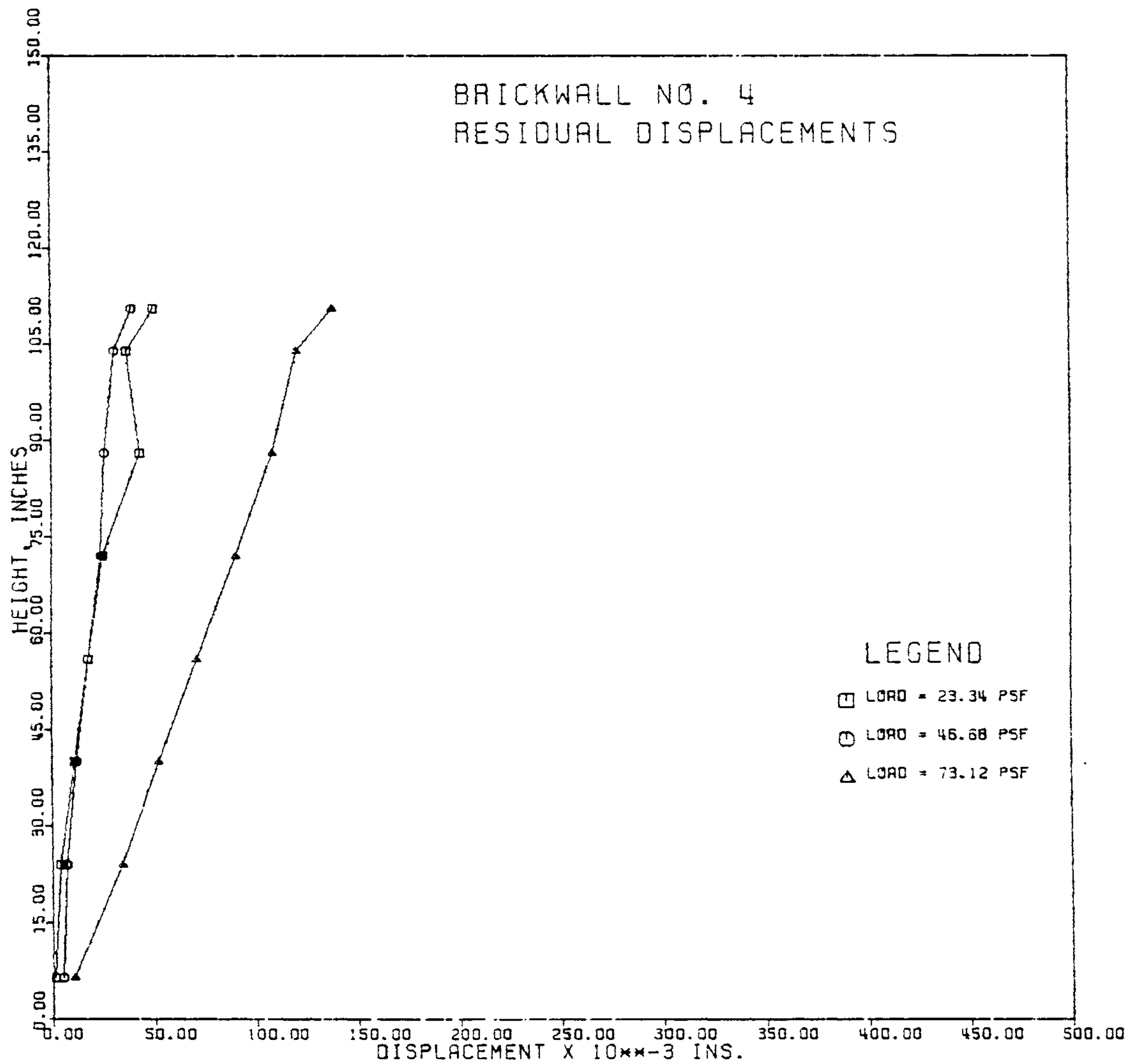

Figure C-31. Brickwall Residual Deflection for Wall No. 4 at Design Load, Twice Design Load and Three Times Design Load, Respectively.

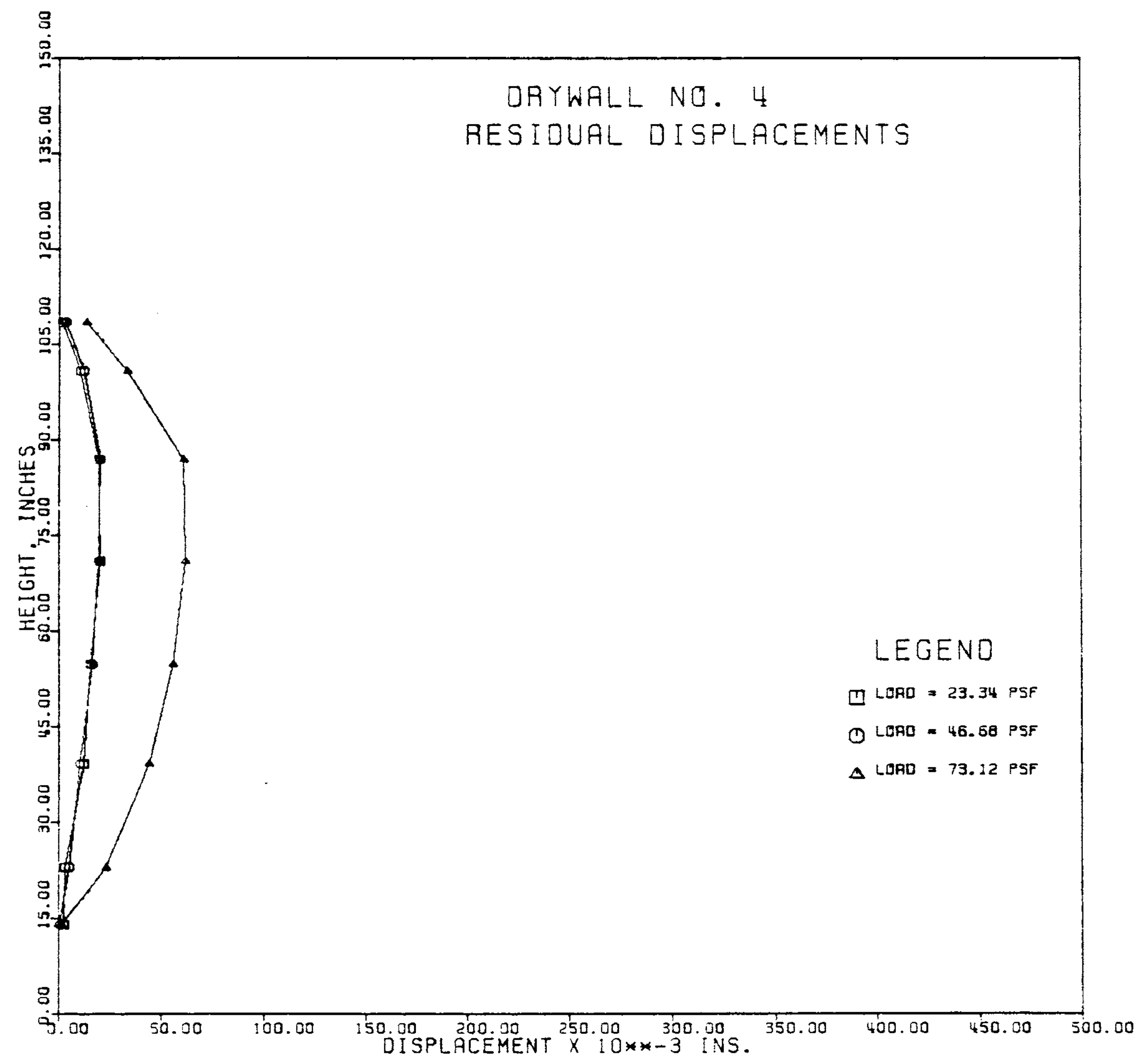

Figure C-32. Drywall Residual Deflection for Wall No. 4 at Design Load, Twice Design Load and Three Times Design Load, Respectively.

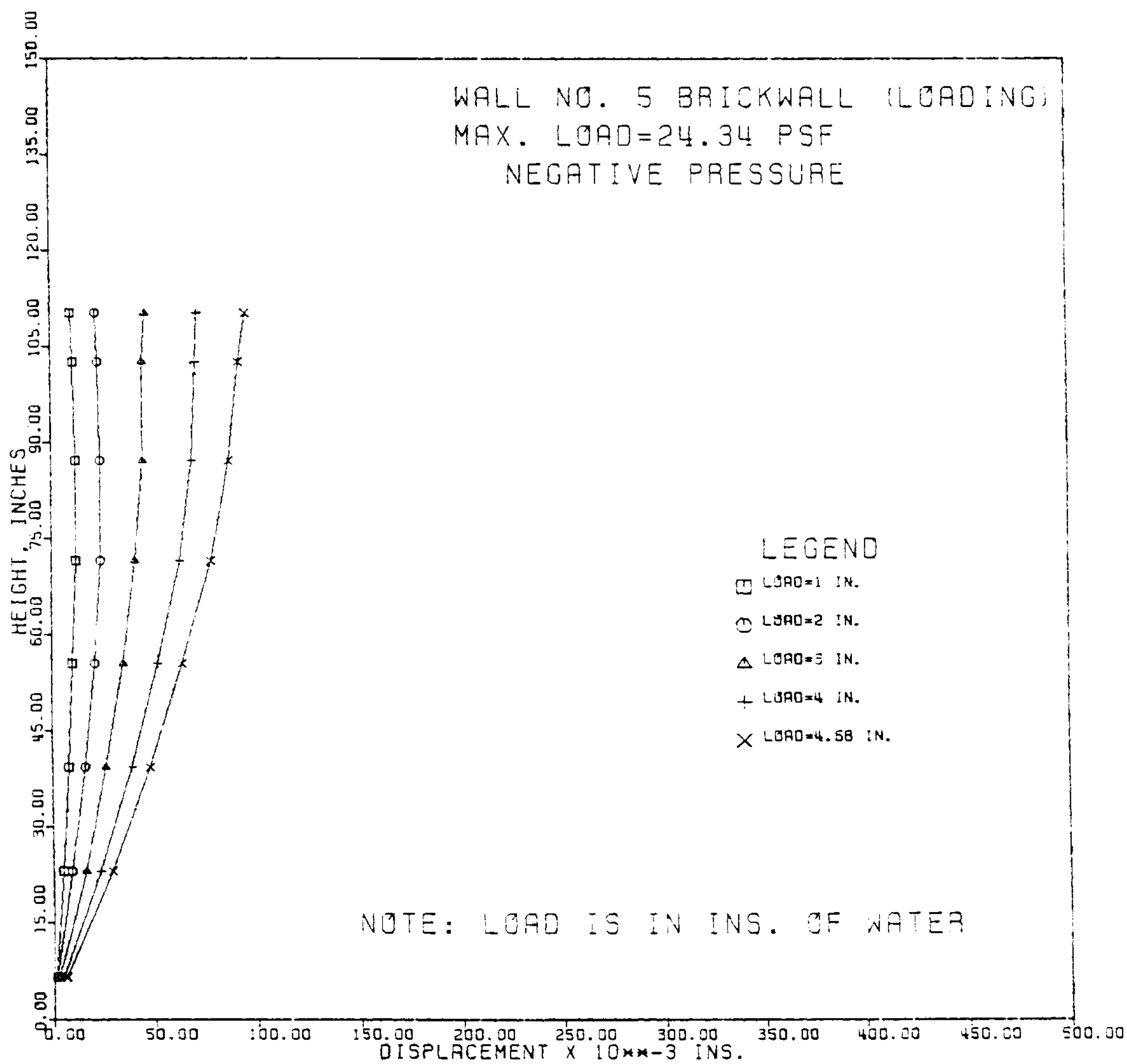

Figure C-33. Brickwall Lateral Deflection for Wall No. 5 at Design Load.

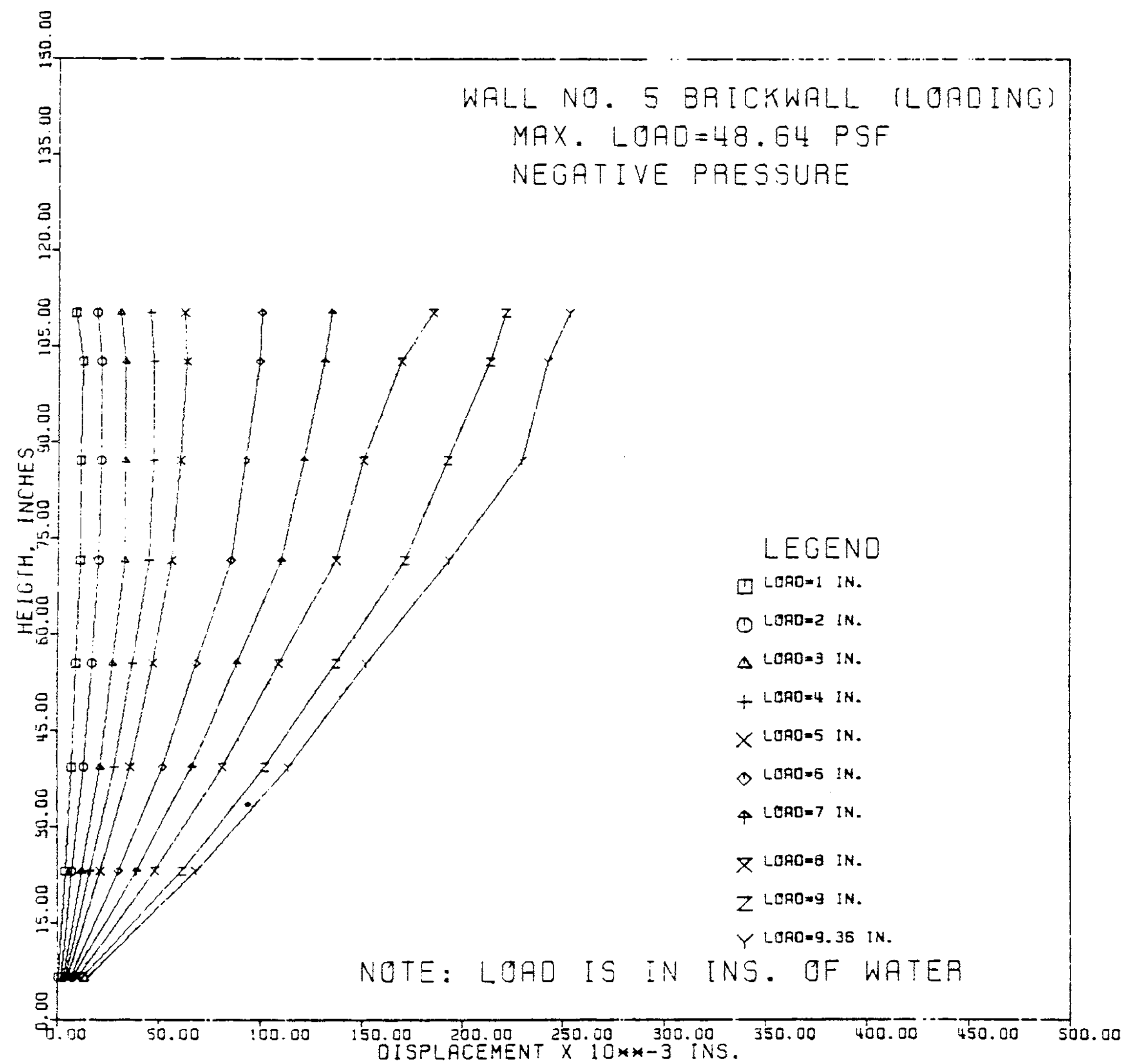

Figure C-34. Brickwall Lateral Deflection for Wall No. 5 at Twice Design Load.

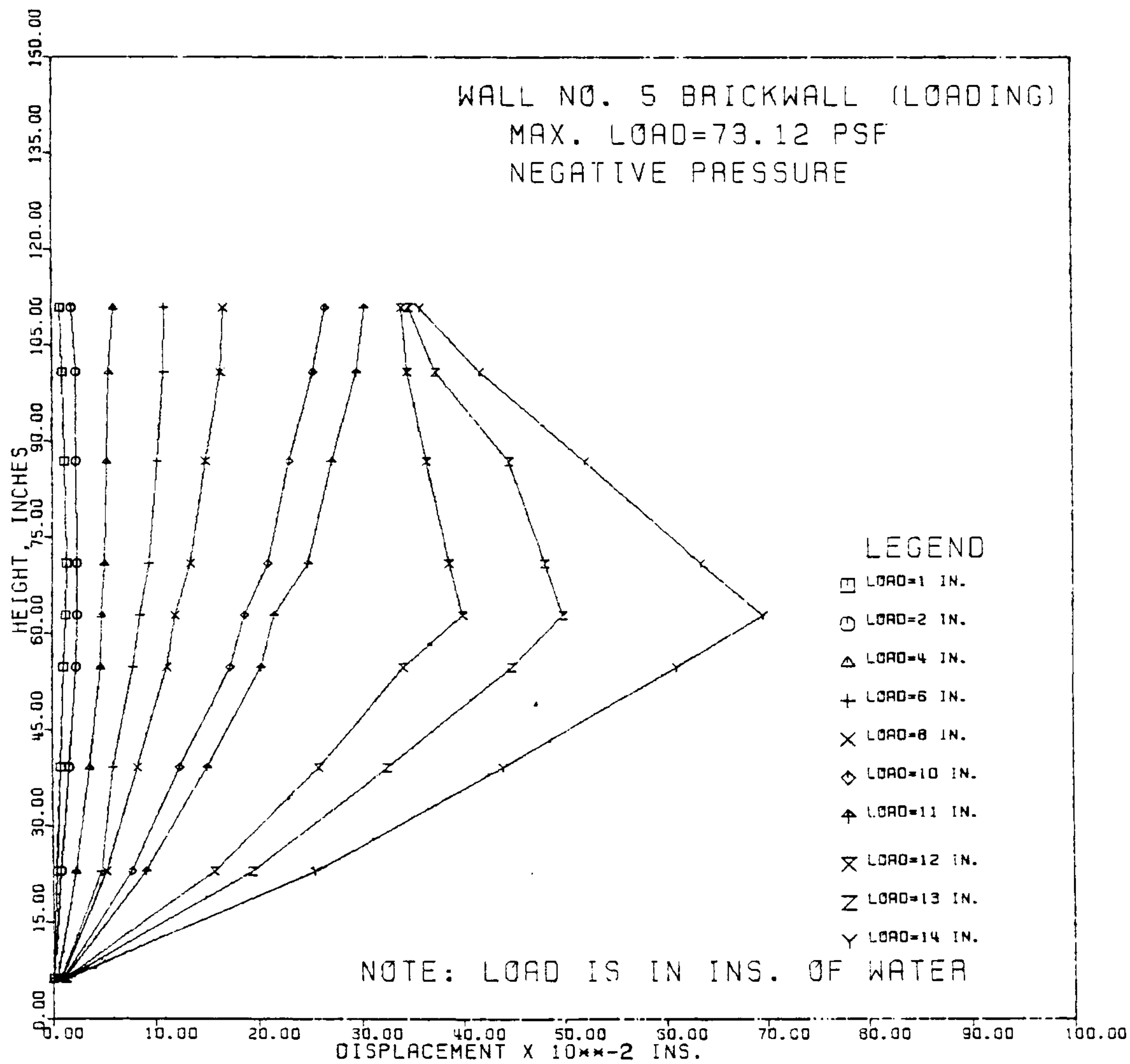

Figure C-35. Brickwall Lateral Deflection for Wall No. 5 at Three Times Design Load.

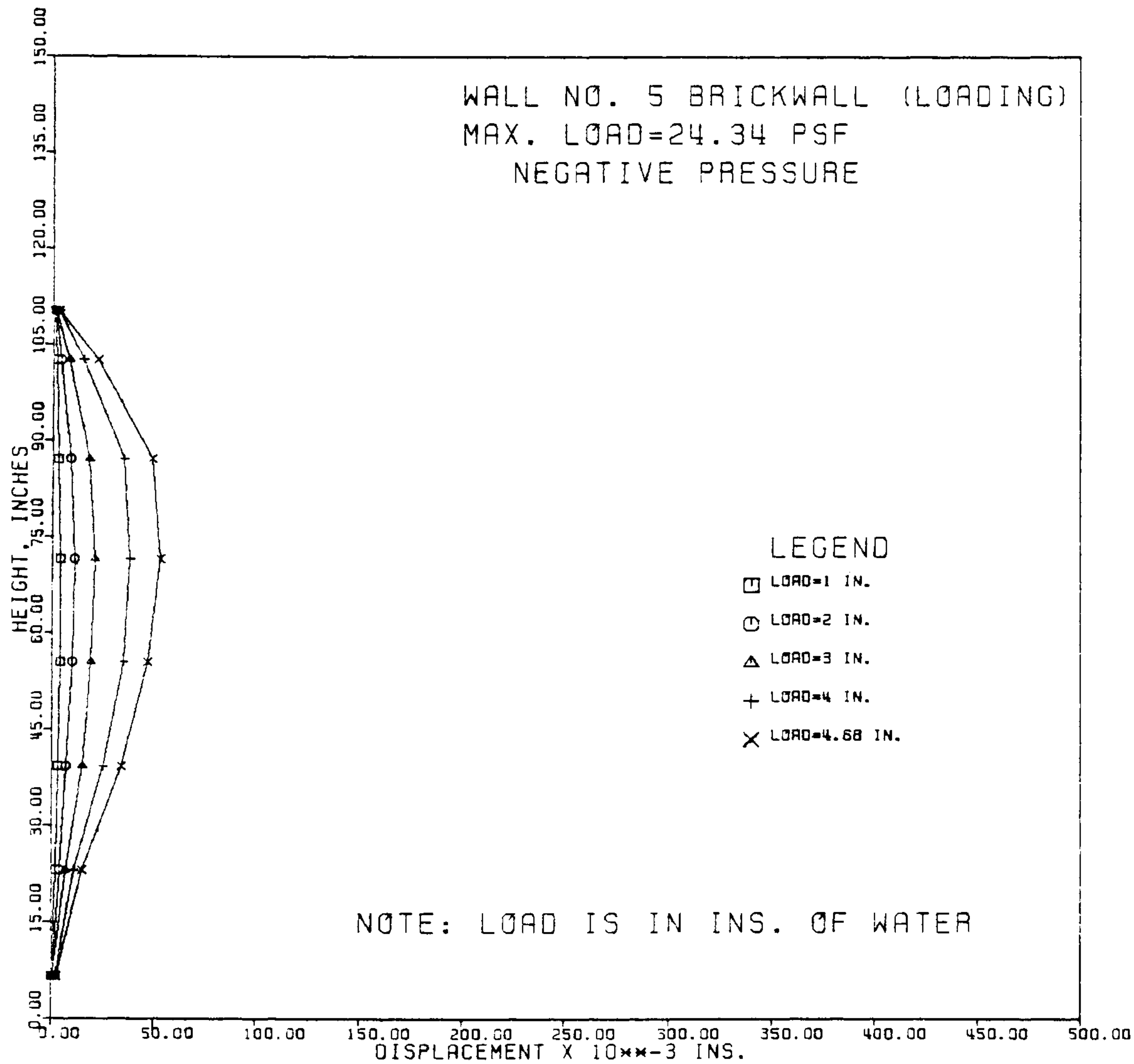

Figure C-36. Drywall Lateral Deflection for Wall No. 5 at Design Load.

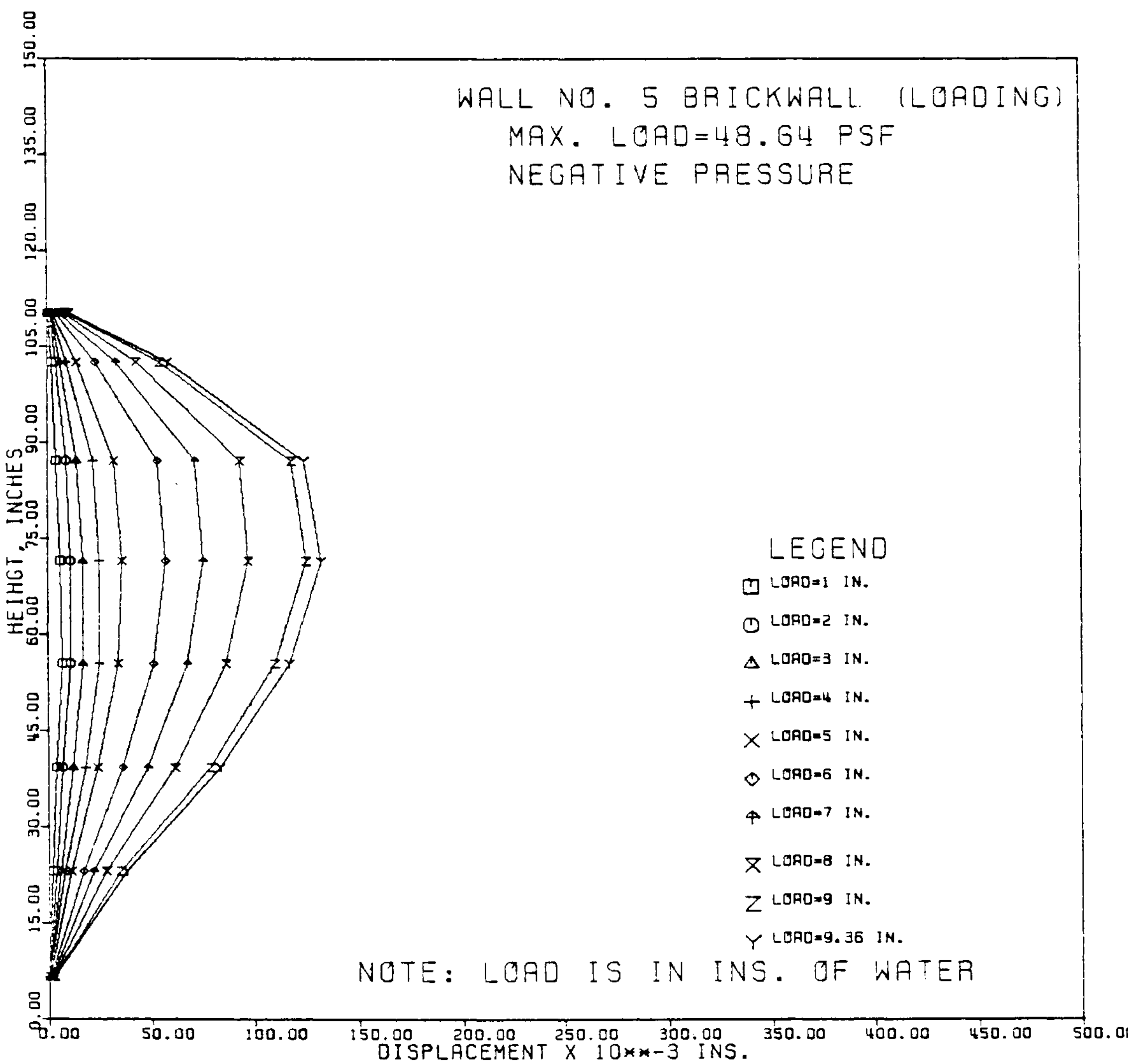

Figure C-37. Drywall Lateral Deflection for Wall No. 5 at Twice Design Load.

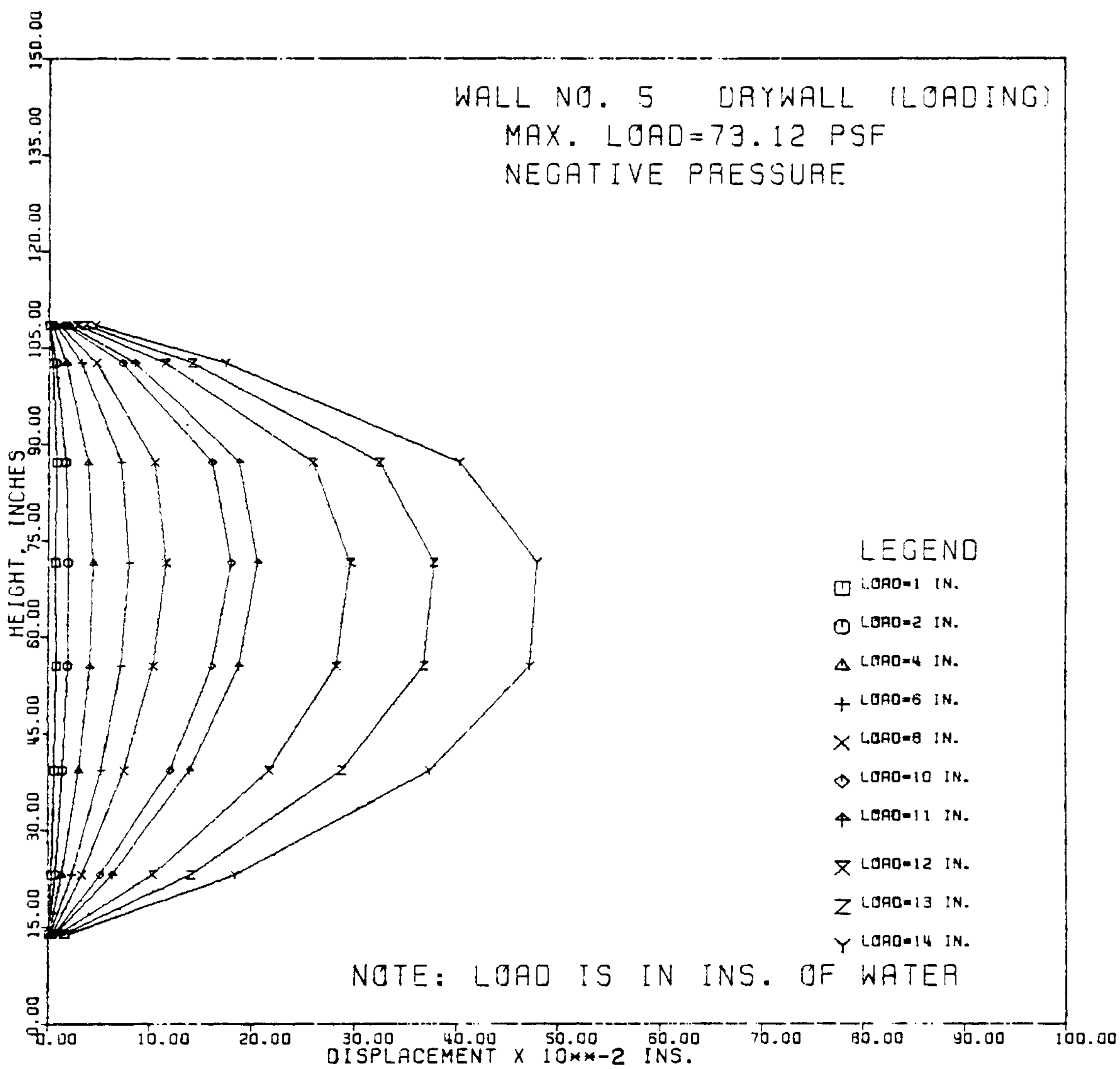

Figure C-38. Drywall Lateral Deflection for Wall No. 5 at Three Times Design Load.

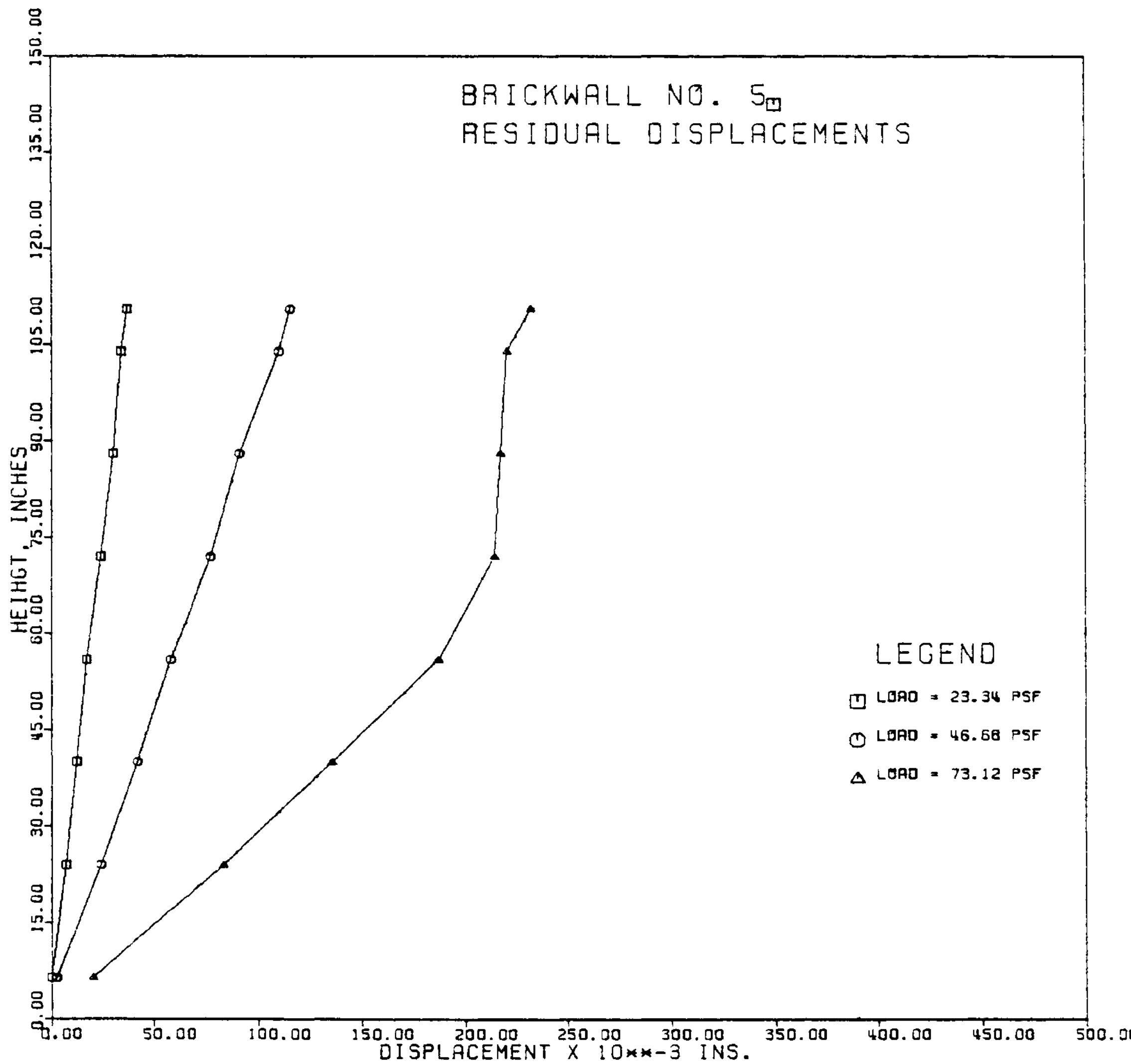

Figure C-39. Brickwall Residual Deflection for Wall No. 5 at Design Load, Twice Design Load and Three Times Design Load, Respectively.

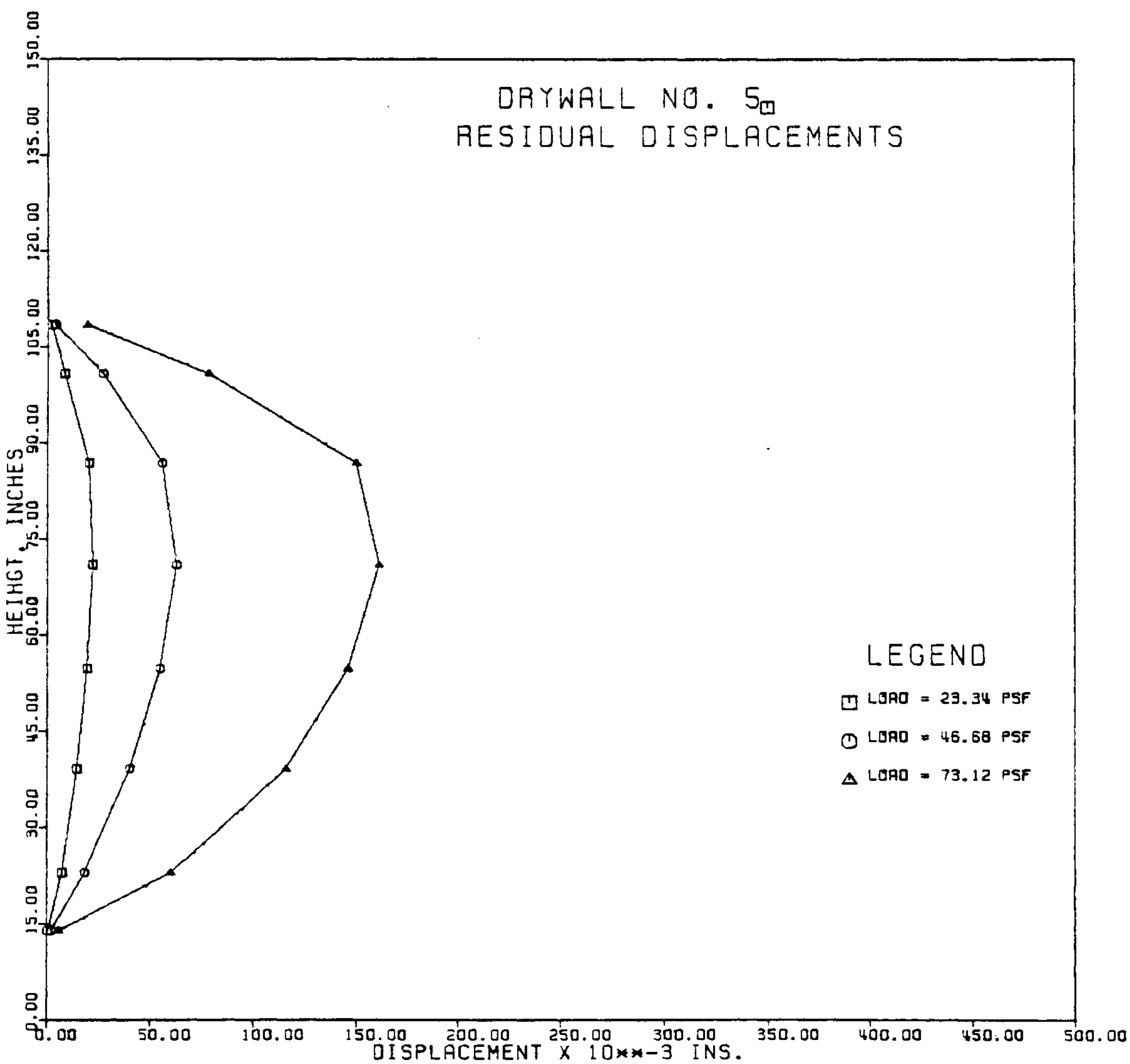

Figure C-40. Drywall Residual Deflection for Wall No. 5 at Design Load, Twice Design Load and Three Times Design Load, Respectively.

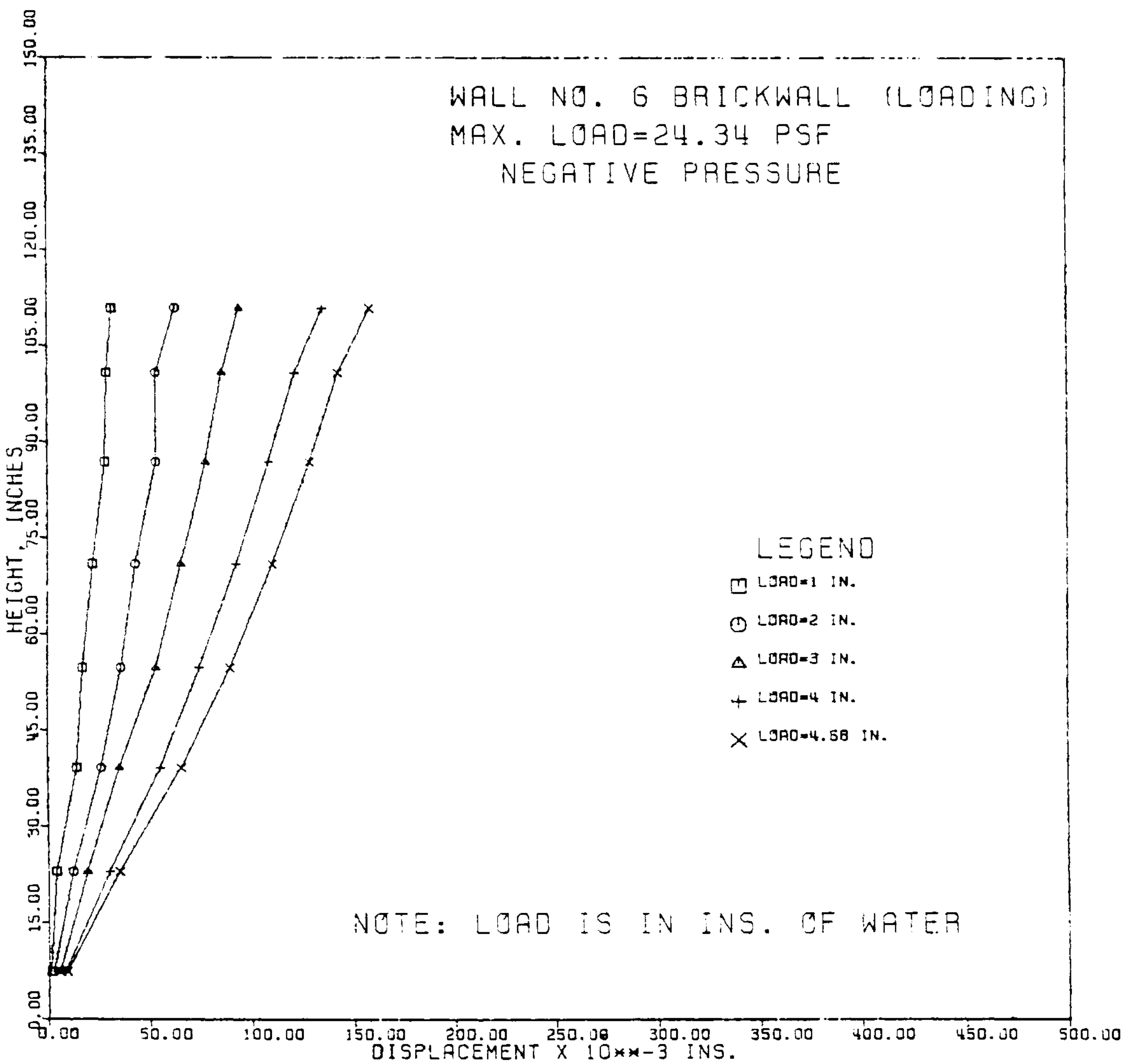

Figure C-41. Brickwall Lateral Deflection for Wall No. 6 at Design Load.

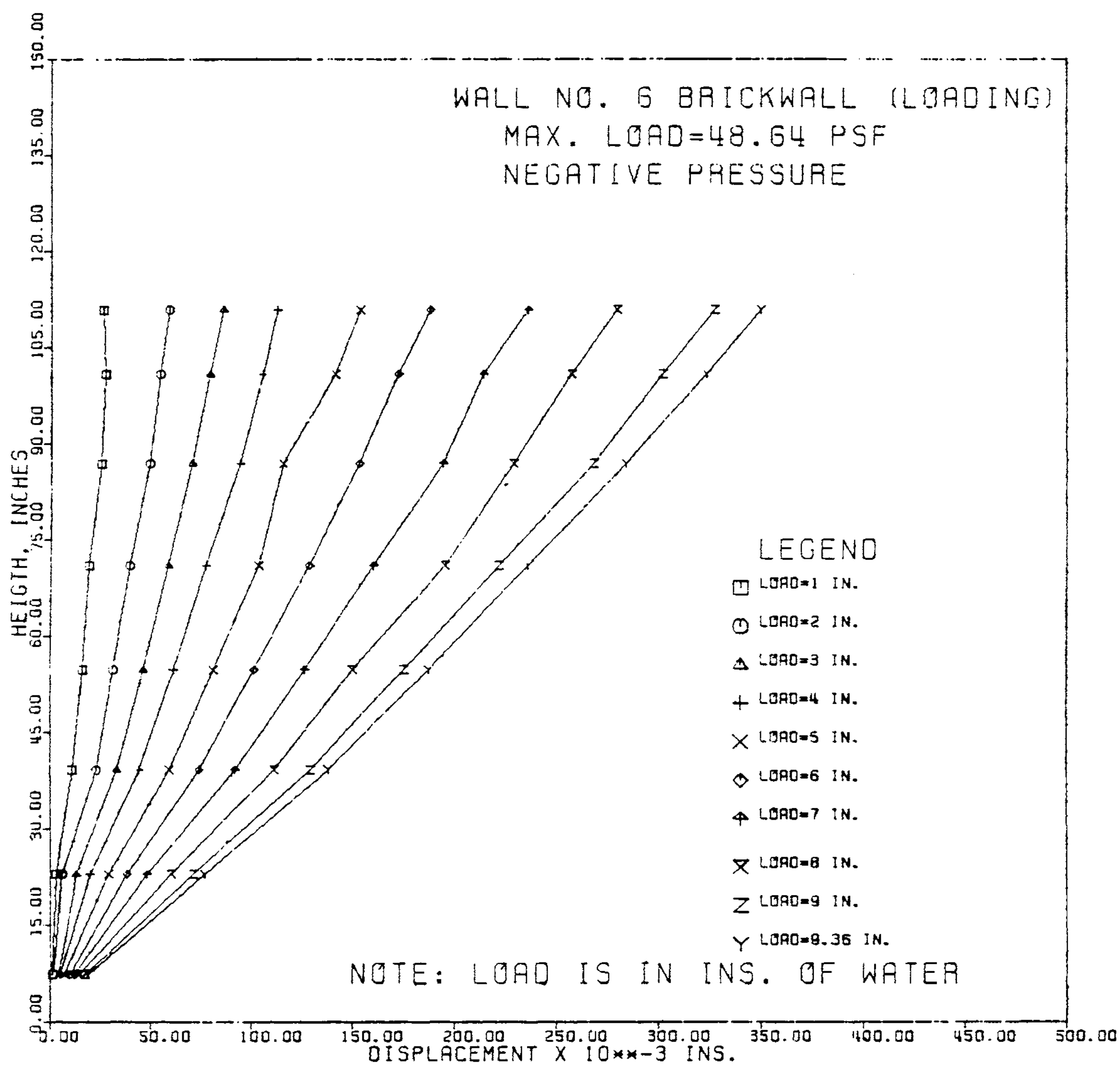

igure C-42. Brickwall Lateral Deflection for Wall No. 6 at Twice esign Load.

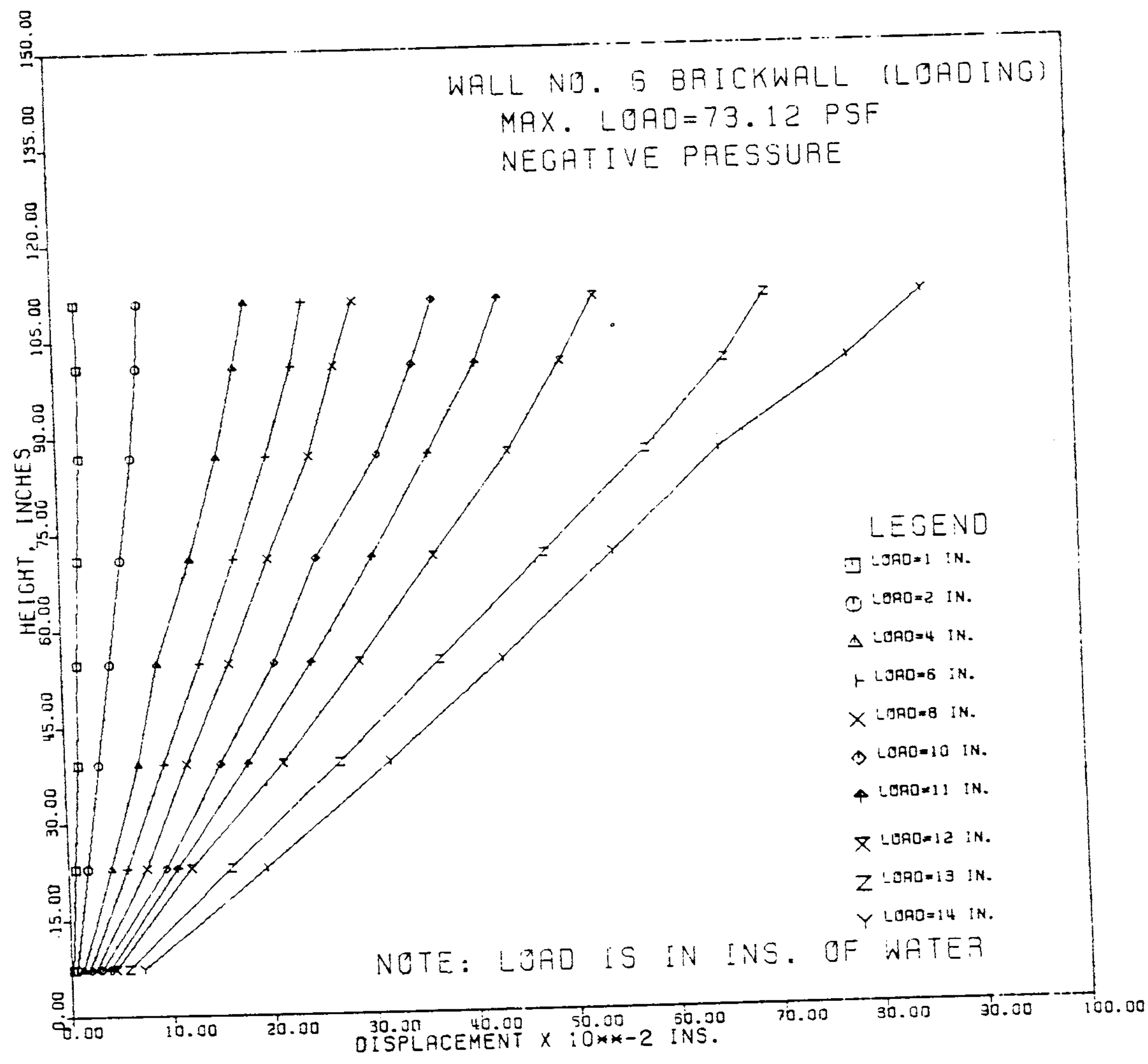

Figure C-43. Brickwall Lateral Deflection for Wall No. 6 at Three Times Design Load.

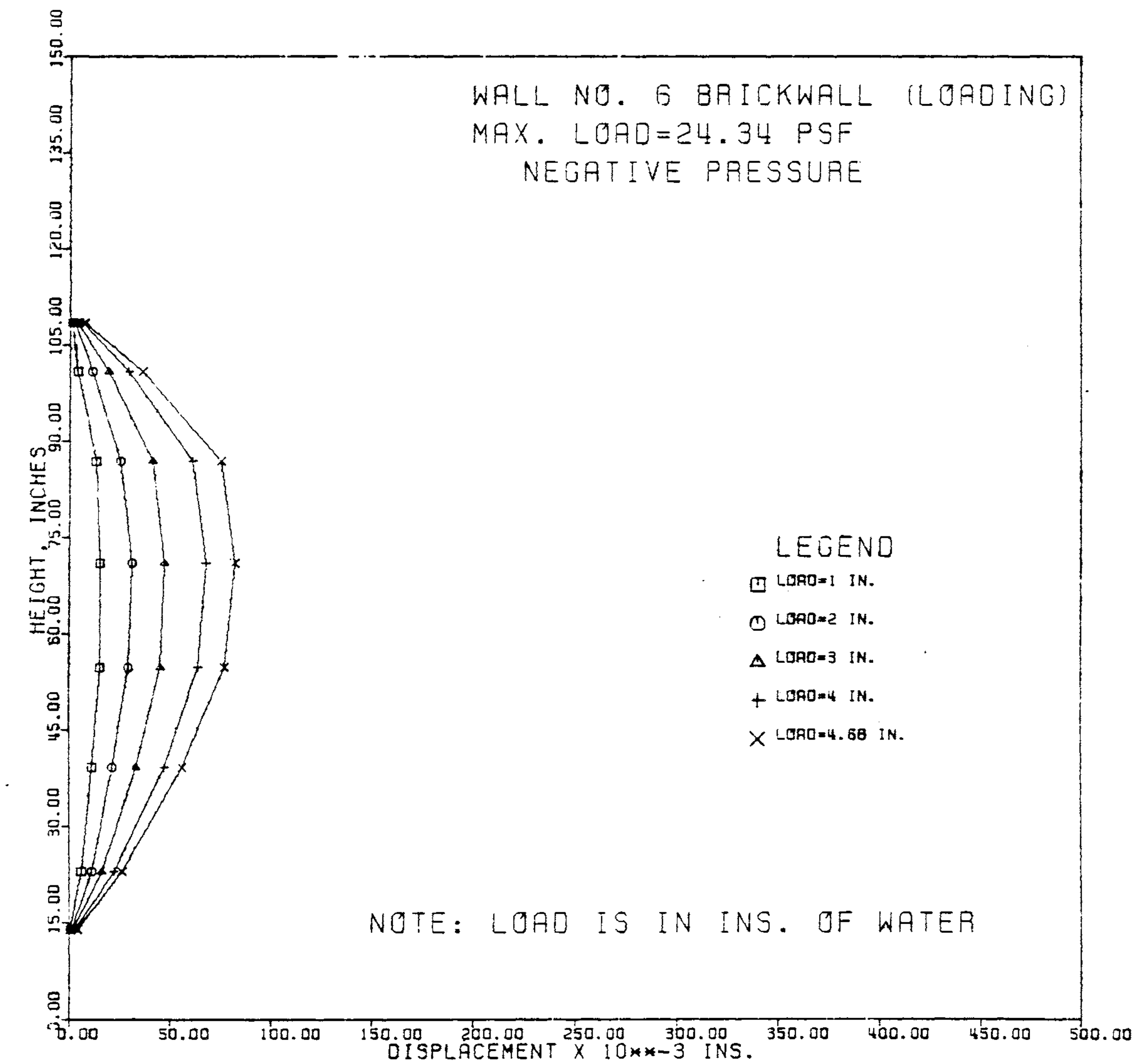

Figure C-44. Drywall Lateral Deflection for Wall No. 6 at Design Load.

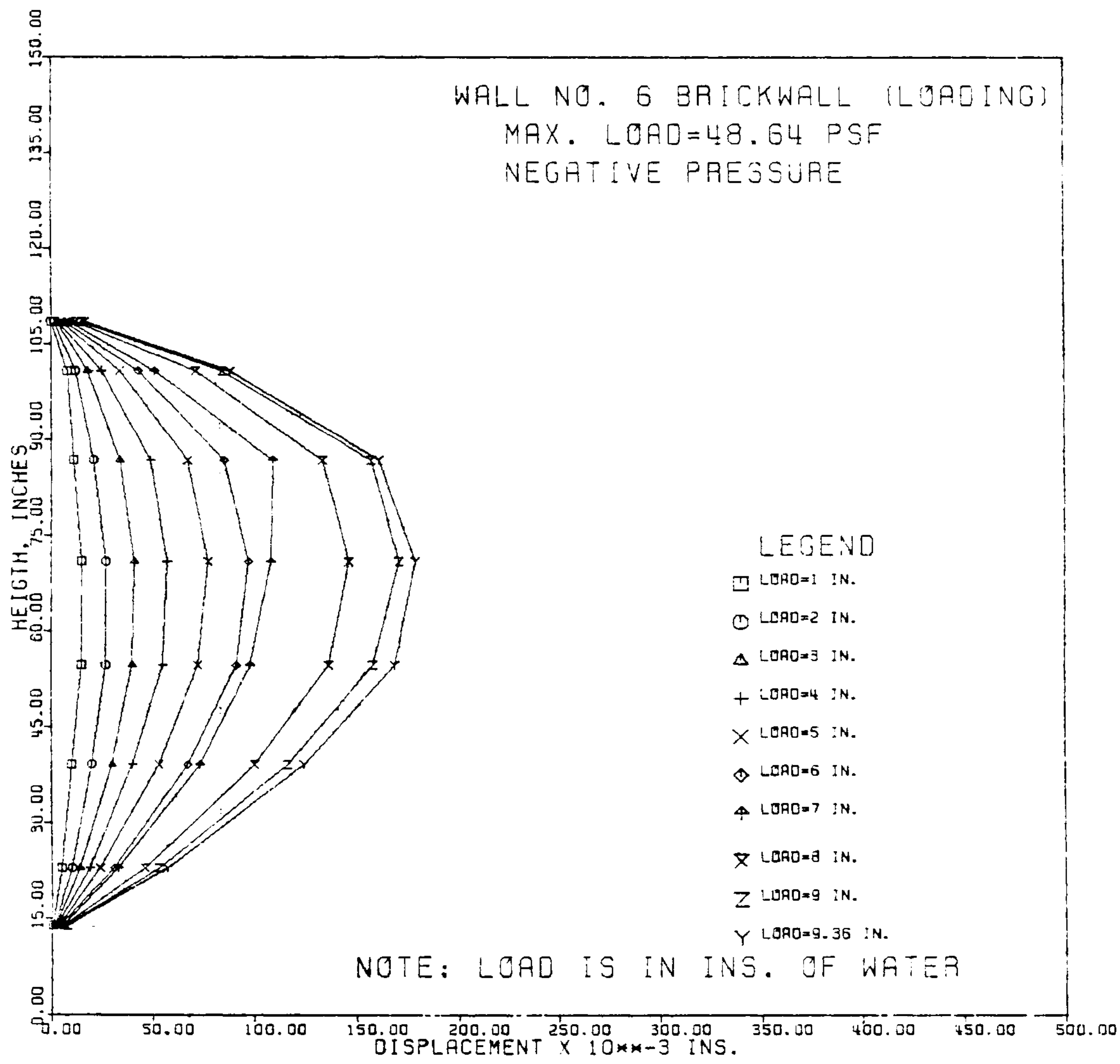

Figure C-45. Drywall Lateral Deflection for Wall No. 6 at Twice Design Load.

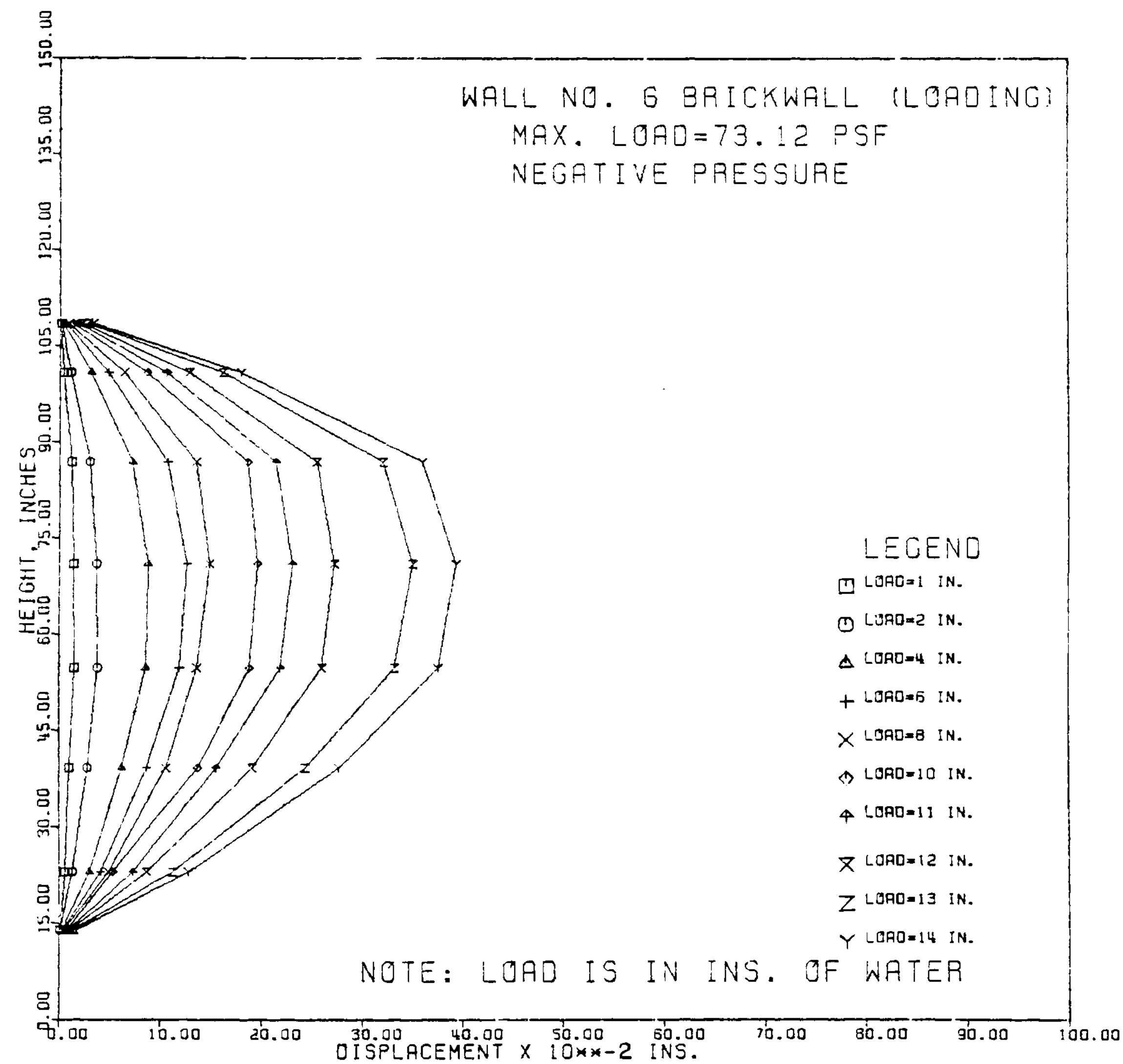

Figure C-46. Drywall Lateral Deflection for Wall No. 6 at Three Times Design Load.

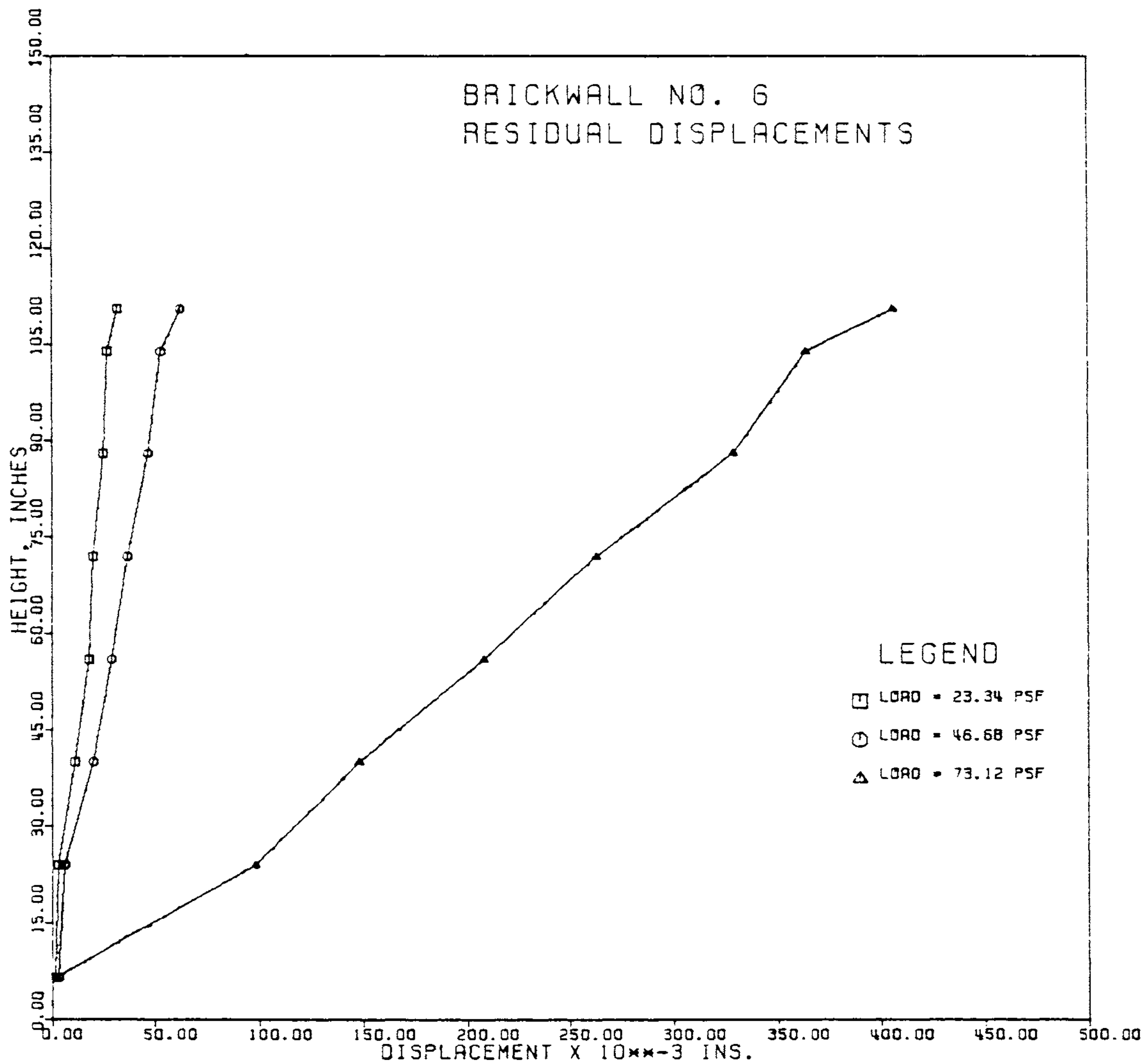

Figure C-47. Brickwall Residual Deflection for Wall No. 6 at Design Load, Twice Design Load and Three Times Design Load, Respectively.

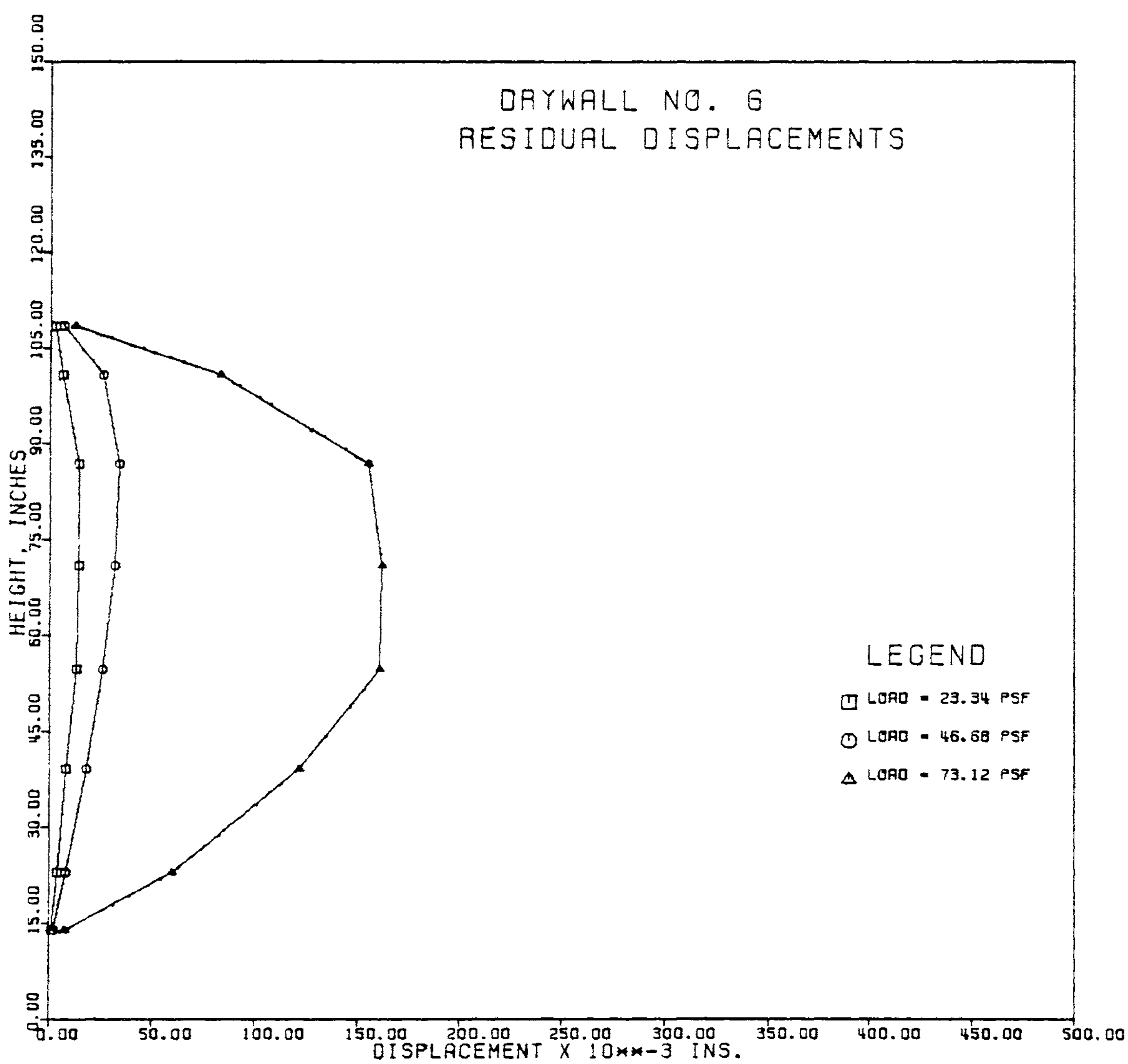

Figure C-48. Drywall Residual Deflection for Wall No. 6 at Design Load, Twice Design Load and Three Times Design Load, Respectively.

BIBLIOGRAPHY

1. Brick Veneer Panel and Curtain Walls, BIA Technical Notes on Brick Construction, 28B Revised, Brick Institute of America, McLean, VA, Jan./Feb. (1980).

2. Brown,R.H., and Elling,R.E.,"Lateral Load Distribution in Cavity Walls", Pre-prints of Papers presented at: 5th International Brick Masonry Conference, (1979).

3. "Compressive Strength of Masonry Prisms, ASTM E 447 - 79", American Society for Testing and Materials, Philadelphia, PA, (1979).

4. "Flexural Bond Strength of Masonry, ASTM E 518 - 79", American Society for Testing and Materials, Philadelphia, PA, 19103.

5. Brown,R.H. and Palm,B.D.,"Flexural Strength of Brick Masonry Using the Bond Wrench," Proceedings, Second North American Masonry Conference, College Park, MD, August, 1982.

6. "Mortar for Unit Masonry", ASTM C 270 - 78, American Society for Testing and Materials, Philadelphia, PA, (1978).

7. "Sampling and Testing Brick and Structural Clay Tiles", ASTM C 67 - 78, American Society for Testing and Materials, Philadelphia, PA, (1978).

8. "Conducting Strength Tests of Panels for Building Construction", ASTM E 72 - 68, American Society for Testing and Materials, Philadelphia, PA, 19103.

9. Recommended Practice for Engineered Brick Masonry, Brick Institute of America, McLean, VA, 1969, p. 1.

10. "Water Permeance of Masonry", ASTM E 514 - 79, American Society for Testing and Materials, Philadelphia, PA, (1979).

11. Davis, J. D. and Bose, D. K.,"Stress Distribution in Splitting Tests", Journal of the American Concrete Institute, No. 8 Proceedings v. 65, p. 662, (1968).

12. Inryco/Milcor Steel Framing Systems, Catalog 37-1, Inryco Inc., Baltimore, MD (1980).

13. Murphy, G.,Properties of Engineering Materials,

International Textbook Company, Scranton, PA, (1946).

14. Jastrzebski, Z. D., Damping Characteristics of Engineering Materials, John Wiley and Sons, Inc., New York (1976).

15. "ICES STRUDL II, vol. 1", Department of Civil Engineering, Massachusetts Institute of Technology, Cambridge, MA, (1968).

16. USG Curtain Wall Systems, SA-805, United States Gypsum, Chicago, Illinois, (1979).